AD-A139 778 UNIPOLAR ELECTRIC MACHINES WITH LIQUID-METAL CURRENT PICKUP(U) FOREIGN TECHNOLOGY DIV WRIGHT-PATTERSON AFB OH A I BETTINOV ET AL. 08 MAR 84 FTD-ID(RS)T-1205-83 1/6

UNCLASSIFIED F/G 9/3 NL

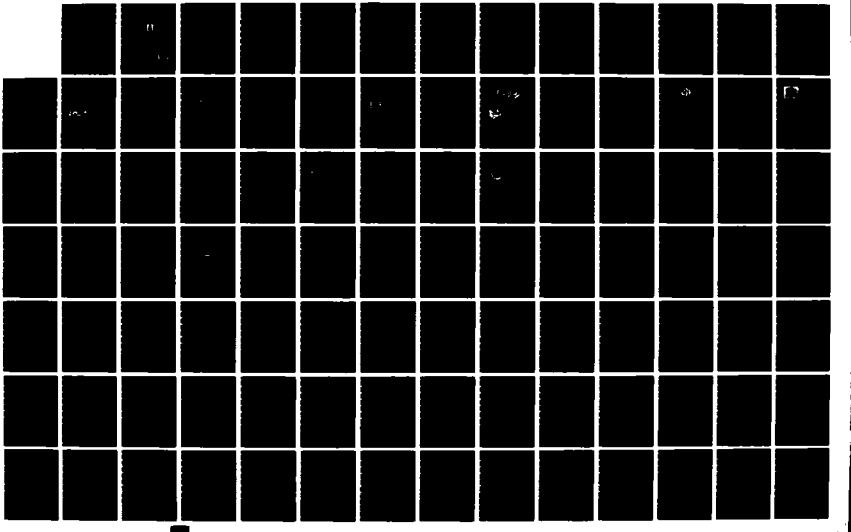

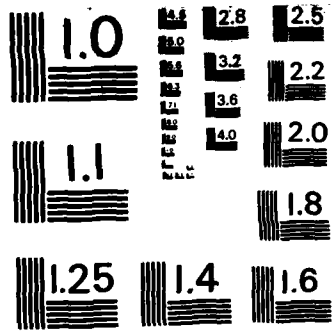

MICROCOPY RESOLUTION TEST CHART
NATIONAL BUREAU OF STANDARDS-1963-A

FTD-ID(RS)T-1205-83

AD A139778

FOREIGN TECHNOLOGY DIVISION

UNIPOLAR ELECTRIC MACHINES WITH LIQUID-METAL CURRENT PICKUP

by

A. I. Bertinov, B. L. Aliyevskiy, S. R. Troitsky

DTIC FILE COPY

DTIC ELECTE S D APR 5 1984 D

Approved for public release; distribution unlimited.

84 04 05 026

UNEDITED MACHINE TRANSLATION

FTD-ID(RS)T-1205-83 8 March 1984

MICROFICHE NR: FTD-84-C-000261

UNIPOLAR ELECTRIC MACHINES WITH LIQUID-METAL CURRENT PICKUP

By: A. I. Bertinov, B. L. Aliyevskiy, S. R. Troitsky

English pages: 521

Source: Unipolyarnyye Elektricheskiye Mashiny s Zhidko-metallicheskim Tokos"yemom, Energiya, Moscow-Leningrad, 1966, pp. 1-311

Country of origin: USSR
This document is a machine translation.
Requester: FTD/TQTD
Approved for public release; distribution unlimited.

Accession For
NTIS GRA&I [X]
DTIC TAB [ ]
Unannounced [ ]
Justification
By
Distribution/
Availability Codes
Dist | Avail and/or Special
A/1

THIS TRANSLATION IS A RENDITION OF THE ORIGINAL FOREIGN TEXT WITHOUT ANY ANALYTICAL OR EDITORIAL COMMENT. STATEMENTS OR THEORIES ADVOCATED OR IMPLIED ARE THOSE OF THE SOURCE AND DO NOT NECESSARILY REFLECT THE POSITION OR OPINION OF THE FOREIGN TECHNOLOGY DIVISION.

PREPARED BY:

TRANSLATION DIVISION
FOREIGN TECHNOLOGY DIVISION
WP-AFB, OHIO.

DTIC COPY INSPECTED

Table of Contents

U.S. Board on Geographic Names Transliteration System ii

Preface 4

Chapter I. Survey of Contemporary State and Classification of Unipolar Electrical Machines 7

Chapter II. Electromagnetic Field of Acyclic Machines 62

Chapter III. Magnetic Leakage and Special Features of the Calculation of the Magnetic Circuit of Unipolar Machines with Idling 91

Chapter IV. Armature Reaction in Acyclic Machines with Liquid-Metal Current Pickup 131

Chapter V. Liquid-Metal Slide Contact of Homodynamo 179

Chapter VI. Fundamental Questions of the Calculation of Acyclic Machines 226

Chapter VII. Comparison of Different Acyclic Machines 272

Chapter VIII. Motor Mode of Unipolar Electrical Machine 301

Chapter IX. Bases of Theory and Calculation of Nonpolar Dynamos without Ferromagnetic Circuit 385

Chapter X. Experimental Study of Acyclic Machines with Liquid-Metal Current Pickup 420

Appendix 459

References 516

U. S. BOARD ON GEOGRAPHIC NAMES TRANSLITERATION SYSTEM

Block	Italic	Transliteration	Block	Italic	Transliteration
А а	*А а*	A, a	Р р	*Р р*	R, r
Б б	*Б б*	B, b	С с	*С с*	S, s
В в	*В в*	V, v	Т т	*Т т*	T, t
Г г	*Г г*	G, g	У у	*У у*	U, u
Д д	*Д д*	D, d	Ф ф	*Ф ф*	F, f
Е е	*Е е*	Ye, ye; E, e*	Х х	*Х х*	Kh, kh
Ж ж	*Ж ж*	Zh, zh	Ц ц	*Ц ц*	Ts, ts
З з	*З з*	Z, z	Ч ч	*Ч ч*	Ch, ch
И и	*И и*	I, i	Ш ш	*Ш ш*	Sh, sh
Й й	*Й й*	Y, y	Щ щ	*Щ щ*	Shch, shch
К к	*К к*	K, k	Ъ ъ	*Ъ ъ*	"
Л л	*Л л*	L, l	Ы ы	*Ы ы*	Y, y
М м	*М м*	M, m	Ь ь	*Ь ь*	'
Н н	*Н н*	N, n	Э э	*Э э*	E, e
О о	*О о*	O, o	Ю ю	*Ю ю*	Yu, yu
П п	*П п*	P, p	Я я	*Я я*	Ya, ya

*ye initially, after vowels, and after ъ, ь; e elsewhere.
When written as ё in Russian, transliterate as yё or ё.

RUSSIAN AND ENGLISH TRIGONOMETRIC FUNCTIONS

Russian	English	Russian	English	Russian	English
sin	sin	sh	sinh	arc sh	$\sinh^{-1}$
cos	cos	ch	cosh	arc ch	$\cosh^{-1}$
tg	tan	th	tanh	arc th	$\tanh^{-1}$
ctg	cot	cth	coth	arc cth	$\coth^{-1}$
sec	sec	sch	sech	arc sch	sech^{-1}
cosec	csc	csch	csch	arc csch	csch^{-1}

Russian	English
rot	curl
lg	log

GRAPHICS DISCLAIMER

All figures, graphics, tables, equations, etc. merged into this translation were extracted from the best quality copy available.

UNIPOLAR ELECTRIC MACHINES WITH LIQUID-METAL CURRENT PICKUP.

A. I. Bertinov, B. L. Aliyevskiy, S. R. Troitsky.

Pages 2-3.

No Typing.

Page 4.

In the book the research in the region of the unipolar electrical machines with the liquid-metal current pickup, which obtained wide acceptance in the series/row of new areas of technology, is generalized in recent years. Classification, principles of theory, calculation methods and comparison of different types of acyclic machines, are given, results of tests, examples of calculation are given.

The book is intended for the engineers and scientific workers, who develop/process and who use the electrical machines and other devices/equipment of the high values of direct current, and also for the students and graduate students, who specialize in the electrical machines. It can be useful for the workers of electrochemical industry, for experimental physicists and power engineers, who deal concerning the liquid-metal heat-transfer agents.

Page 5.

Preface.

Acyclic machines with the liquid-metal current pickup in recent years began to receive wide acceptance in different regions of technology and scientific research. In spite of the fact that these machines passed the large way of historical development, their theory and methods of design are up to now worked out insufficiently. Numerous periodical articles are dedicated in essence to the description of the separate types of acyclic machines, created in different countries. The use/application of liquid-metal current pickup made it possible to considerably improve the characteristics of acyclic machines, stipulated the large progress in their construction/design, revealed the new possibilities of technical use.

While in the Soviet, so in the foreign literature is absent any complete research in the region of acyclic machines. In this book the attempt to complete the existing gap/spacing is done.

The book contains the bases of theory, calculation and experimental study of different acyclic machines with the liquid-metal contacts: cylindrical and disk, with the hollow rotor,

machines without the ferromagnetic circuit, the unipolar electric motors. Are examined questions of the classification of acyclic machines, their electromagnetic field, calculation of magnetic circuit taking into account the leakage fluxes, armature reaction and its compensation, determination of main sizes/dimensions, comparison of the varieties of acyclic machines indicated.

Page 6.

Results of experimental research and examples of calculation are given. The large part of the materials is original and reflects independent research of the authors.

The book is written on the basis of the results of the scientific research work, conducted by the authors over a number of years in the Moscow Aviation Institute named Sergo Ordzhonikidze.

The work on the book was distributed as follows: Chapter 6 was written by the authors together; Chapters 1-4 and 9 were written by Cand. of tech. sciences B. L. Aliyevskiy; chapters 5, 7 and 10 were written together by the doctor of tech. sciences, Prof. A. I. Bertinov and B. L. Aliyevskiy; chapter 8 was written by eng. S. R. Troitsky. B. L. Aliyevskiy and S. R. Troitsky wrote appendix. The general/common/total editing of the book was led by Prof. A. I.

Bertinov.

The book is the first experiment of the generalization of works on acyclic machines. The authors with the appreciation will take all critical observations, which request to send to an address: Moscow Zh-114, Shlyuzovaya nab., d. 10, publishing house "Energiya".

The authors express their gratitude to the reviewer of the book of Cand. of tech. sciences, docent V. I. Radin for the useful observations.

Chapter One.

SURVEY OF CONTEMPORARY STATE AND CLASSIFICATION OF UNIPOLAR ELECTRICAL MACHINES.

1.1. Development and the application of acyclic machines..

First electrical acyclic machines (UM) of direct current, which are simplest electric motor and generator, were constructed by P. Barlow (1824) and M. Faraday (1831) [1-3].

Schematically these machines are shown in Fig. 1-1 and 8-1. In the 80's of past century A. Forbst worked out double-disk UM with electromagnetic excitation [4]. Then non-polar dynamo (UG) with hollow rotor [5] proposed A. Ler.

In detail the history of the first development period of UM is presented in the dissertation work of B. I. Ugrimov (1910), made under Prof. E. Arnold's management/manual [6].

The first industrial standards of UG were constructed according

to the projects of J. Neggerat (1904), B. Ugrimov (1908) and B. Lyamm (1912). The device/equipment of these machines is described in [6-8].

Development of UM followed the path of improvement of UG, and only in the latter/last 20 years are noted attempts at the development of unipolar electric motors (UD) and special forms of UM, in particular unipolar converters (UP).

In 1934 the firm Westinghouse constructed UG with the power of 1125 kW on 150 kA, 7.5 V for welding large-diameter the steel tubes according to the impedance method. This generator (Fig. 1-2) was operated for 25 years [9]. On the international exhibition in 1937 in Paris was demonstrated the compensated UM of A. Puarson with the massive cylindrical armature (Fig. 1-3), intended for purposes of electrolysis [10].

Page 8.

Development of UM in the USSR is connected with the names of the engineers I. P. Ivanov and B. V. Kostin, on projects of which at the Yaroslavl Electrical Machinery Plant (YaEMZ) were made UG for electrolytic industry [10]. In 1939 the department of physical sciences of the AS USSR together with Glavelektroprom at YaEMZ convoked conference on UM (and to the use/application of permanent

magnets in the electric machine construction) with the participation of the most visible scientist-electricians: the academicians K. I. Shenfer, V. F. Mitkevich, M. P. Kostenko, V. S. Kulebakin, the corresponding members G. N. Petrov, A. N. Larionov et al. In its solutions the conference noted the need for setting scientific research works in the region of UG. The facts of the military years of 1941-1945 stirred their timely realization.

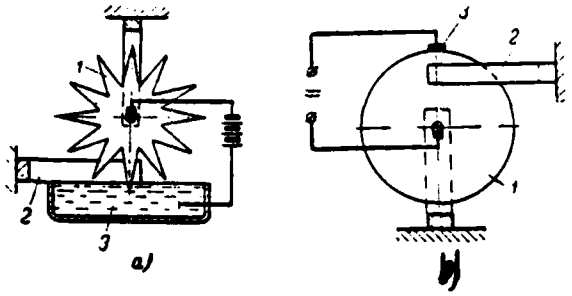

Fig. 1-1. First unipolar electrical machines. a) P. Barlow's engine; b) M. Faraday's generator; 1 - armature; 2 - inductor; 3 - current pickup (mercury cells or solid brush).

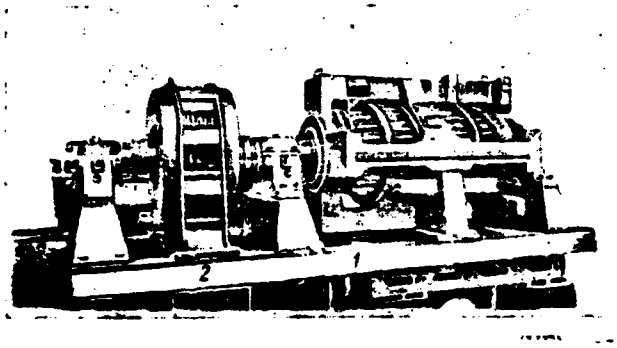

Fig. 1-2.

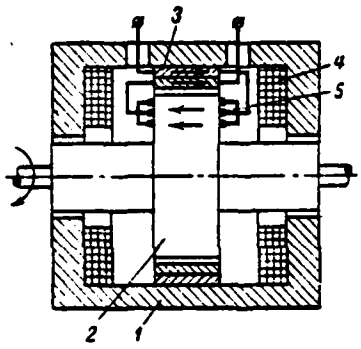

Fig. 1-3.

Fig. 1-2. The general view of homopolar generator (UG) for the electric welding of firm Westinghouse on 150 kA, 7.5 V. 1 - generator; 2 - electric servomotor.

Fig. 1-3. Diagram of compensated UG of A. Puarson for the electrolysis. 1 - stator; 2 - rotor with the expansion; 3 - pole face winding; 4 - excitation winding; 5 - brush end-type current pickup.

Page 9.

The successes in the development of the collector (bipolar) machines of direct current made irrational the use/application of UM with the voltages/stresses 110 V and above. Up to Thirties it was approximately/exemplarily considered that UM are not of practical use [4]. However, with the low voltage and the high currents they compete with the commutator machines according to the weight and energy indices.

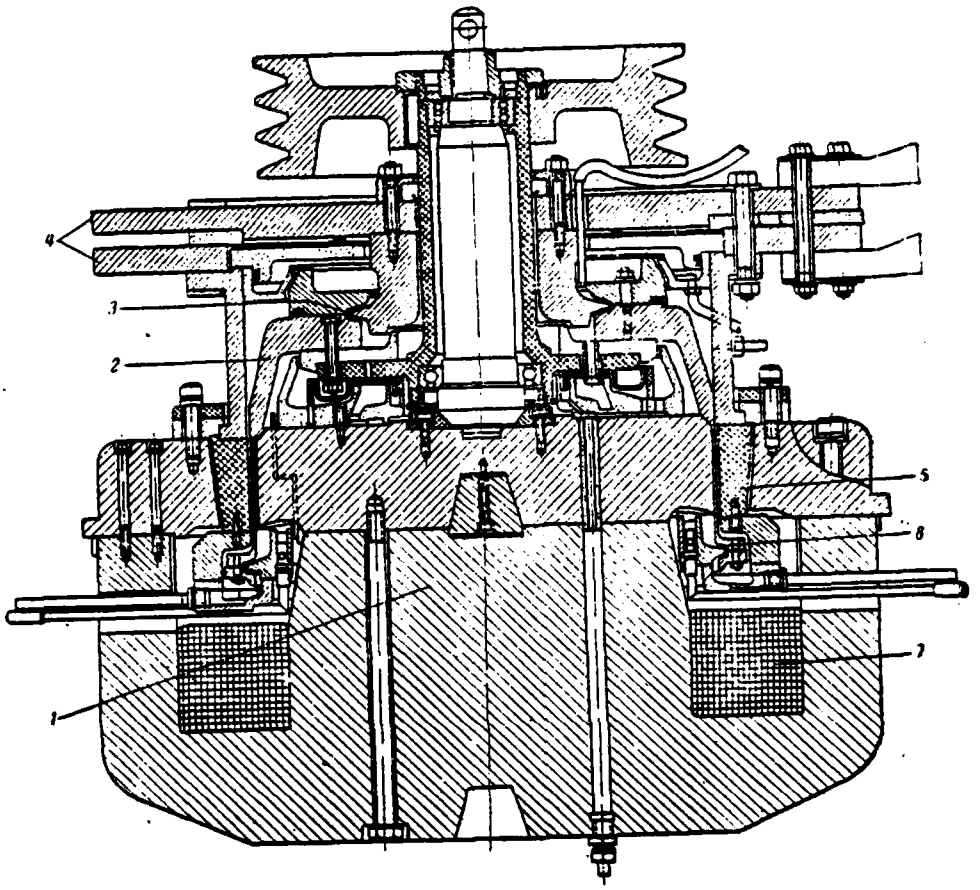

Fig. 1-4. Construction/design of UG of D. Watt for the feed of electromagnetic pumps. 1 - stator; 2 - hollow bell-shaped copper rotor; 3 - semitoroidal type upper mercury slit ring terminal; 4 - leading-out busbars; 5 - compensative "winding" from the ferromagnetic material; 6 - lower mercury contact; 7 - field coil.

In recent decade UM survive the period of lift. Is explained this by the development of the new regions of technology and scientific research - atomic power engineering, the charged particle accelerators, physics of plasma, and also by the successes in the region of liquid-metal heat-transfer agents. The study of the properties of liquid metals and alloys made it possible to use them in the slide contact of current-tap apparatus of UM. This stipulated the considerable progress in the construction/design of machines, it widened the sphere of their use/application, since during the liquid-metal current pickup are most noticeable advantages of UM over commutator machines with the high currents.

Non-polars dynamo found use as the supplies of power of the electromagnetic conduction pumps, moving liquid metal in the heat transfer systems of atomic reactors [11, 12], for the feed of the electromagnets of accelerators during the creation of strong magnetic fields [13].

Electromagnetic pumps are the ideal users of electric power of UG of direct current with the significant magnitude of current and the low voltage. Fig. 1-4 and 1-5 show the examples to construction/design of UG for the feed of pumps [14, 15]. UG are used also during the electrolysis for obtaining of aluminum and chlorine, where for the feed of electrolytic lines is required current 150 kA,

respectively with voltage/stress 400 and 134 V. In this case the aggregate/unit of six UG, mounted on the shaft of steam turbine (Fig. 1-6), is applied. Each of UG, constructed by firm General Electric, gives current 150 kA with 67 V.

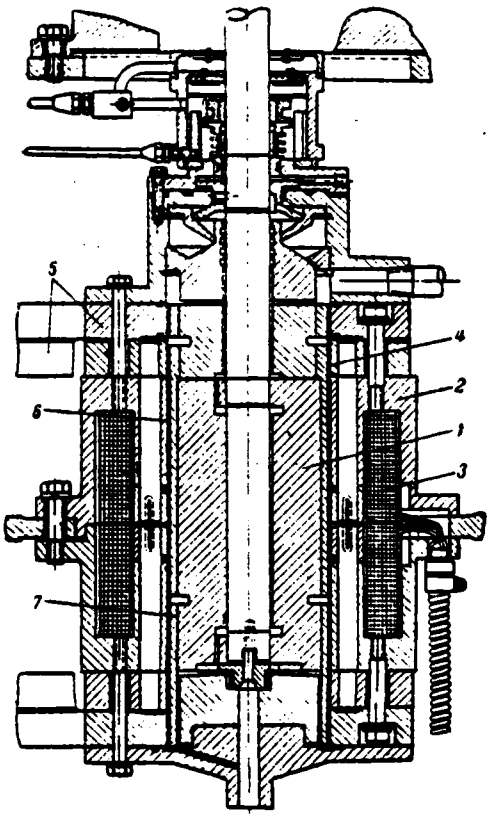

Fig. 1-5. Construction/design of UG with sodium-potassium contact for the feed of electromagnetic pumps. 1 - rotor; 2 - stator; 3 - field coil; 4 - liquid metal of contact; 5 - current tap; 6 - compensative busbar; 7 - contact cylinder (Cu).

Page 11.

During the operation for obtaining aluminum all six UG are connected electrically consecutively/serially, for obtaining chlorine they are connected in series in pairs. Fig. 1-7 shows the

device/equipment of UG of firm General Electric.

Group of four similar UG (Fig. 1-8b) is applied by USAF [United States Air Force] for the feed of the inductive coil of arc wind tunnel. Generators are combined on the diagram, given in Fig. 1-8a, which provides the power of 100000 kW and current 1100 kA with the voltage/stress 90 V (each generator it gives 550 kA with 45 V in the impulse/momentum/pulse. With the help of the arc discharge of coil in the tube obtain air-stream velocities more than 20 numbers of Mach for model test of rockets and space vehicles [16-18].

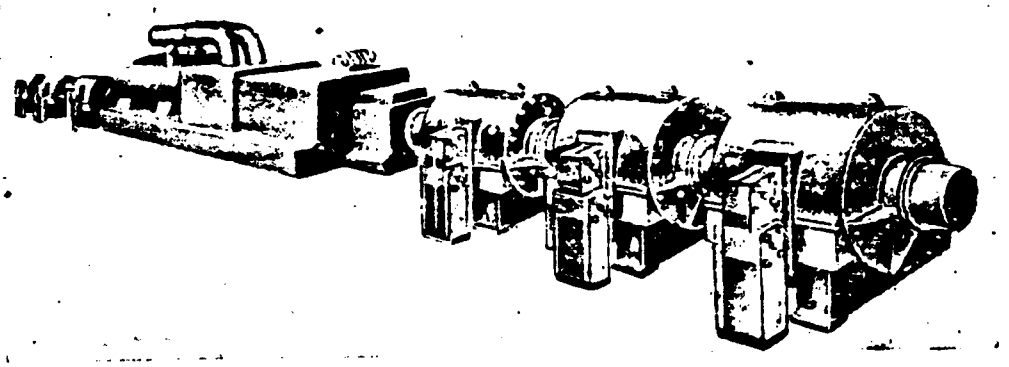

Fig. 1-6. The general view of aggregate/unit of six UG with the steam turbine for the feed of the line of electrolytic baths (general/common/total voltage/stress 400 V, current 150000 A).

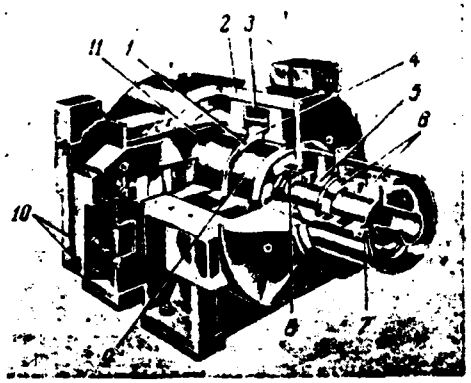

Fig. 1-7. Device/equipment of UG of firm General Electric of Company with the power of 10 MW, 67 V, 150 kA. 1 - movable electrode of the sodium-potassium current pickup; 2 - stator; 3 - field coil; 4 - stationary electrode of current pickup; 5 - main bearing; 6 - thrust bearing; 7 - elastic coupling; 8 - multiplexing; 9 - rotor; 10, 11 - discharge busbars, cooled by sodium-potassium alloy (NaK).

Fig. 1-9 presents UG of firm Allis Chalmers on 1800 kW, by 60 kA with the voltage/stress 30 V, utilized for the guarantee with electric power of different physical research.

Giant four-disk UG with the frame magnetic system is constructed in 1956-1962 in the physical institute of Australian national university (Canberra), under M. Olifant's management/manual [19-21]. Non-polar dynamo in the impulse/momentum/pulse develops power $1.44 \cdot 10^4$ kW and gives current $1.8 \cdot 10^4$ a with the voltage/stress 800 V, this generator is intended for the feed of proton accelerator on 10 GeV. The schematic of the construction/design of this machine is given in Fig. 1-10.

Fig. 1-11 shows the device/equipment of UG of highest technical school Graz (Austria), intended for the research targets.

Some fundamental technical data of foreign and Soviet UG are given in Table 1-1.

From Table 1-1 it is evident that propagation received the generators over a wide range of power, moreover are used UM of the different construction/design: with the cylindrical massive and

hollow rotors, with the disk rotors, without the ferromagnetic circuit of inductor. All generators, released in recent years, have liquid-metal current pickup and are implemented without the windings on the rotor.

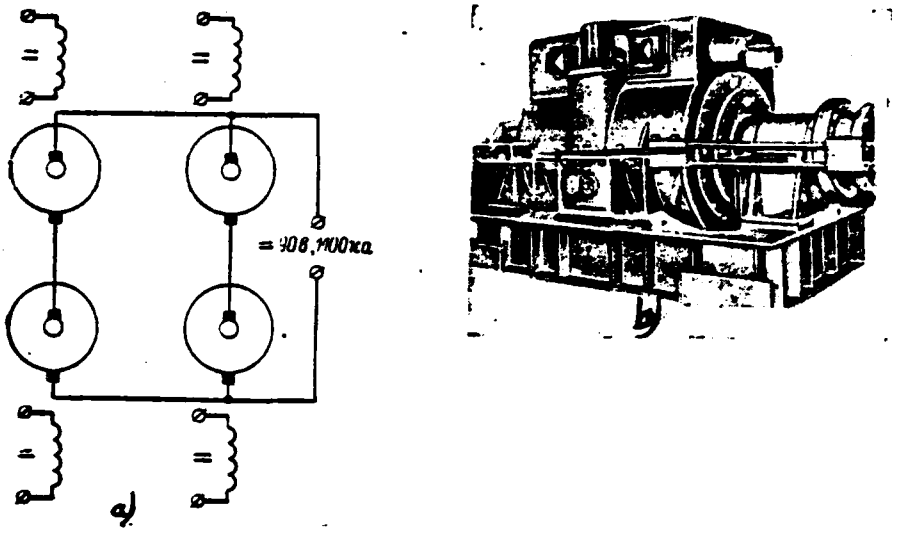

Fig. 1-8. Generators for the feed of the arc wind tunnel of the USAF. a) the diagram of connection of the group of four UG; b) appearance of UG.

Page 13.

Besides those indicated in table 1-1, in different research centers and at universities of the USA, according to the data [13], is operated the series/row of UG to the currents $30 \cdot 10^3$-$1.5 \cdot 10^4$ a (more than 10^4 a - in the impulse/momentum/pulse).

Homopolar generator with the mercury high-speed/high-velocity contact in 1906-1910 was worked out and investigated by Prof. B. I. Ugrimov, moreover the speed, achieved/reached by it in the slide

contact, which comprises more than 300 m/s, was not exceeded, until now. However, the knife contact proposed by B. I. Ugrimov was not suitable for the continuous operation due to the high consumption of mercury from the evaporation on the knife (on the order of 14 g/h) and it was not adapted for the transmission of high currents [10].

Mercury contact for UM in the USSR is investigated by Yu. Yu. Kaunas [22], by whom the recommendations for calculating the optimum sizes/dimensions of circular type contact are given.

Since 1959 in the Moscow Aviation Institute of name Sergo Ordzhonikidze is conducted the research of UM, as a result of which are worked out the principles of theory and calculation procedure of UM of different types and is constructed experimental UG with the mercury contacts for the current 4000 a.

General view of experimental UG, prepared in MAI, is given in Fig. 1-12.

High-speed UM because of the absence of commutation difficulties can be used in the reversible electric drive. It is proposed to use a gyroeffect of rotor UG for the stabilization of attitude of the axis of ship or submarine, electrical energy of generator is intended for the feed of onboard users, charging of storage batteries [23].

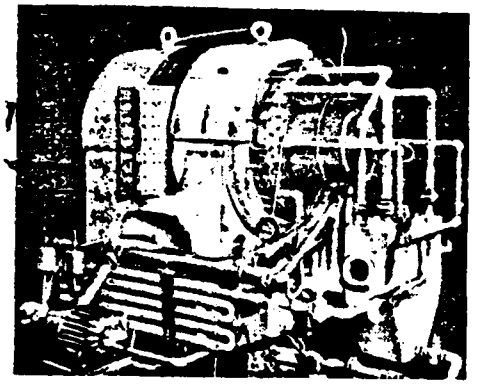

Fig. 1-9. The general view of UG of firm Allis Chalmers for the feed of electrophysical equipment with a power of 1800 kW, 30 V, 60 kA with sodium-potassium current pickup.

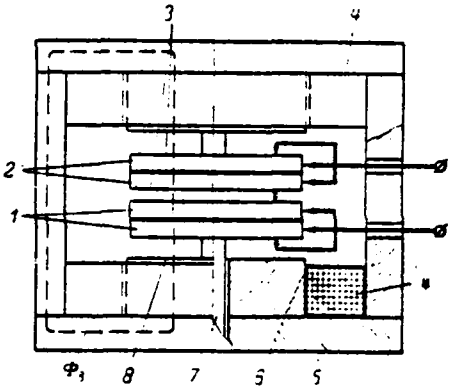

Fig. 1-10. Diagram of construction/design pulse UG of the institute of physics of Australian national university. 1 - disks of lower rotor; 2 - disks of upper rotor; 3 - insulation spacers; 4 - field coil; 5 - frame magnetic circuit of stator; 6 - liquid-metal (NaK) jet-edge contacts; 7 - rotor shaft; 8 - pole of stator; ▬ flow of excitation (diameter of rotor disks ≈3.6 m, the distance between the poles ≈1.56 m).

Pages 14-17.

Table 1-1. Basic data of some homopolar generators (using the published materials).

Конструктор, страна, фирма, год выпуска	Конструкция якоря генератора	Мощность, ток, напряжение, скорость вращения, к. п. д.	Тип токосъема, скорость в контакте	Режим работы генератора	Назначение, литературный источник
Неггерат, США, Дженерал Электрик, 1904	Цилиндрический со стержневой обмоткой	300 кат; 600 а; 500 в; 3 000 об/мин	Щеточный	Длительный	Для электролиза, [Л. 5]
Угримов, Россия, 1908	Дисковый	60 кат; 150 а; 40 55 в; 6 000/8 000 об/мин; 80%	Жидкометаллический ртутный 220/300 м/сек	Длительный	Для питания ламп накаливания, [Л. 6]
Лямм, США, Вестингауз, 1912	Цилиндрический со стержневой обмоткой	2 000 кат; 700 а; 260 в; 1 200 об/мин	Щеточный, щетки из набора медных пластин, 67 м/сек	Длительный	Общего применения, [Л. 4]
Вестингауз, США, 1934	Цилиндрический со стержневой обмоткой	1 130 кат; 150·10³ а; 7,5 в; 514 об/мин; 75%	Щеточный с угольными щетками	Длительный	Для сварки труб, [Л. 9]
Пуарсон, Франция, 1937	Цилиндрический массивный с расширением	700 кат; 50·10³ а; 14 в; 750 об/мин; 93%	Щеточный с торцовым расположением щеток	Длительный	Для электролиза, [Л. 10]
Иванов, СССР, ЯЭМЗ, 1933—1939	Цилиндрический массивный гладкий	60 кат; 6/12 в; 5 000/10 000 а	Щеточный	Длительный	Для электролиза, [Л. 1]
Костин, СССР, ЯЭМЗ, 1939	Цилиндрический массивный с расширением	7,5 кат; 2 500 а; 3 в; 4 000 об/мин	Щеточный	Длительный	Для электролиза, [Л. 10]
Мозжерин, СССР, ИЭИ, 1939	Цилиндрический полый	16,5 кат; 15 400 а; 10,7 в	Щеточный	Длительный	Экспериментальный, [Л. 56]
США, 1949	Цилиндрический со стержневой обмоткой	400 кат; 21·10³ а; 18,7 в	Щеточный	Длительный	Для питания синхроциклотрона, [Л. 91]
Штроу и Шредер, США, 1951	Дисковый (без ферромагнитного индуктора)	162 кат; 65·10³ а; 16 000 об/мин	Жидкометаллический ртутный, 120 м/сек	Импульсный	Для питания бетатрона, [Л. 95]
Каунас, СССР, КПИ, 1954	Цилиндрический массивный гладкий	2 кат; 2 000 а; 1 в	Жидкометаллический ртутный, 30 м/сек	Длительный	Экспериментальный, [Л. 22]

Конструктор, страна, фирма, год выпуска	Конструкция опора генератора	Мощность, ток, напряжение, скорость вращения, к. п. д.	Тип топологии, скорость в контакте	Режим работы генератора	Назначение, литературный источник
Ватт, США, 1966	Цилиндрический полый	10 кат; 4 000/16 000 а; 0,625/2,5 в; 780/935 об/мин; 90%	Жидкометаллический ртутный, 18 м/сек	Длительный	Для питания электромагнитного насоса. [Л. 48]
Дженерал Электрик Компани, США, 1968	Цилиндрический массивный гладкий	а) $25 \cdot 10^3$ кат; $550 \cdot 10^3$ а; 45 в; 1 800 об/мин; 98%	Жидкометаллический на основе эвтетики NaK, 150 м/сек	Импульсный	Для питания дуговой аэродинамической трубы. [Л. 16]
		б) $10 \cdot 10^3$ кат; $150 \cdot 10^3$ а; 67 в; 3 600 об/мин; 98%		Длительный	Для электролиза при получении алюминия и хлора. [Л. 17]
СССР, ИЭФА, 1969	Цилиндрический полый	9 кат; $8 \cdot 10^3$ а; 1,5 в; 1 500 об/мин; 81%	Жидкометаллический ртутный, 20 м/сек	Длительный	Для экспериментального стенда. [Л. 129]
Аллис Чалмерс, США, 1960	Цилиндрический массивный гладкий	1 800 кат; $60 \cdot 10^3$ а; 30 в	Жидкометаллический на основе NaK	Длительный	Для термоядерных исследований. [Л. 11]
Клаудя, Австрия, 1961	Дисковый конический	200 кат; $20 \cdot 10^3$ а; 10 в; 9 000 об/мин; 82%	Жидкометаллический ртутный, 125 м/сек	Длительный	Экспериментальный. [Л. 96]
Пулен, Франция, 1961	Цилиндрический с погружением в контактную жидкость	2,1 кат; 3 000 а; 0,7 в; 8 000 об/мин; 60%	Жидкометаллический на основе ртутно-индиевого сплава, 21 м/сек	Длительный	Экспериментальный. [Л. 46]
Олифант и др., Австралия, 1962	Дисковый (с четырьмя дисками)	$1,3 \cdot 10^3$ кат; $1,6 \cdot 10^3$ а; 800 в; 900 об/мин	Жидкометаллический на основе NaK, 165 м/сек	Импульсный	Для питания синхроциклотрона и исследований по физике плазмы. [Л. 20]
Франция, 1962	Цилиндрический полый (без ферромагнитного индуктора)	100 кат; $300 \cdot 10^3$ а	Жидкометаллический	Импульсный	Для получения сильных полей (до 10 тл). [Л. 122]
СССР, МАИ, 1968	Цилиндрический массивный гладкий	3,4—10 кат; 4 000 а; 0,84—2,5 в; 3 000—9 000 об/мин; 87—78%	Жидкометаллический ртутный, 19—57 м/сек	Длительный	Экспериментальный. [Л. 67]

Key: (1). Designer, country, firm, the year of issue. (2). Neggerat, USA, General Electric, 1904. (3). Ugrimov, Russia, 1908. (4). Lyamm, USA, Westinghouse, 1912. (5). Westinghouse, USA, 1934. (6). Puarson, France, 1937. (7). Ivanov, USSR, YaEMZ, 1933-1939. (8). Kostin, USSR, YaEMZ, 1939. (9). Mozzherin, USSR, IEI, 1939. (10). USA, 1949. (11). Schtrou and Schroeder, USA, 1951. (12). Kaunas, USSR, KPI, 1954. (13). Watt, USA, 1956. (14). General Electric Company, USA, 1958. (15). USSR, IEFA, 1959. (16). Allis Chalmers, USA, 1960. (17). Klaudi, Austria, 1961. (18). Pulen, France, 1961. (19). Olifant, etc., Australia, 1962. (20). France, 1962. (21). USSR, MAI, 1963. (22). Construction/design of generator armature. (23). Cylindrical with bar winding. (24). Disk. (25). Cylindrical massive with the expansion. (26). Cylindrical massive flat. (27). Cylindrical hollow. (28). Disk (without the ferromagnetic inductor). (29). Disk conical. (30). Cylindrical with the insertion/immersion into the contact liquid. (31). Disk (with four disks). (32). Cylindrical hollow (without the ferromagnetic inductor). (32a). Power, current is voltage/stress, the speed of rotation, efficiency. (33). kW. (34). in. (35). r/min. (36). Type of current pickup, the speed in the contact. (37). Brush. (38). Liquid-metal mercury. (39). m/s. (40). Brush, brush from the set of copper plates. (41). Brush with the motor carbons. (42). Brush with the end-type location of brushes. (43). Liquid-metal mercury. (44). Liquid-metal on the base of

eutectic NaK. (45). Liquid-metal on base of NaK. (46). Liquid-metal on the base of mercury-indium alloy. (47). Liquid-metal. (48). Mode/conditions of the work of generator. (49). Prolonged. (50). Pulse. (51). Designation/purpose, literary source. (52). For the electrolysis. (53). For the feed of incandescent lamps. (54). Overall use/application. (55). For tube welding. (56). Experimental. (57). For the feed of synchrocyclotron. (58). For the feed of betatron. (59). For the feed of electromagnetic pump. (60). For the feed of arc wind tunnel. (61). For the electrolysis in obtaining of aluminum and chlorine. (62). For the test bench. (63). For the thermonuclear research. (64). For the feed of synchrocyclotron eand research in physics of plasma. (65). For obtaining the strong fields (to 10 T).

Page 18.

Some questions of use/application of UM are examined in survey works [24-26], and also in [128].

To unipolar electric motor was up to now devoted insignificant number of works. Articles [27, 28] are known only. Between those UD can find use in the special devices/equipment, for example, for the drive of hydraulic pumps with the pumping over of liquid metals [29].

From the special-purpose UM it is possible to note those

invented in the USSR: UG of alternating current [30], UG of periodic impulses/momenta/pulses for electrosparking [31], unipolar-one-armature converters of alternating current into constant [32], unipolar amplidyne [33], unipolar pulse generator of arbitrary form [34], etc.

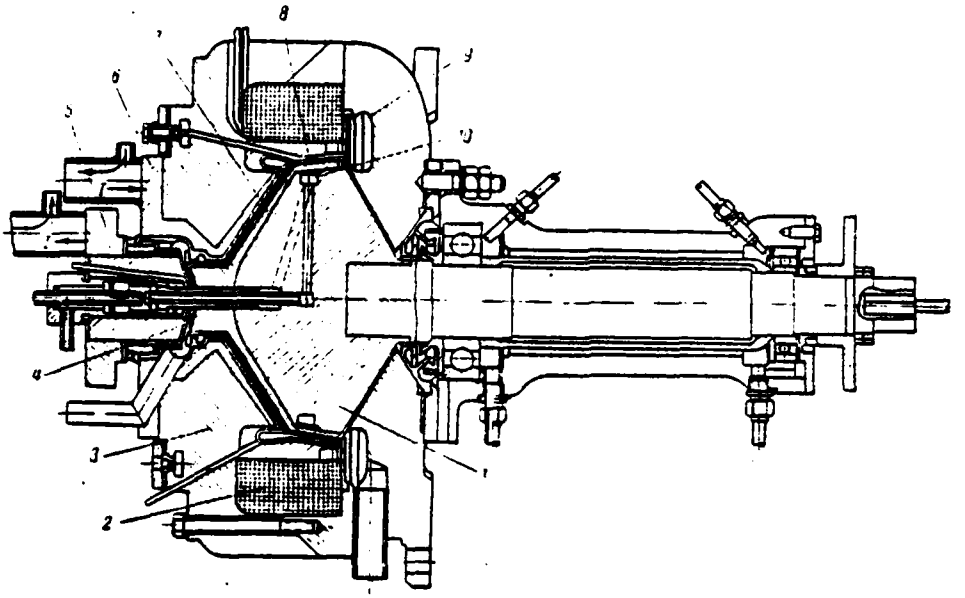

Fig. 1-11. Device/equipment of UG of highest technical school (Graz, Austria). 1 - magnetic circuit of rotor; 2 - excitation winding; 3 - magnetic circuit of stator; 4 - mercury central contact; 5 - current changing busbar; 6 - compensative current-deflecting copper busbar; 7 - copper conductor of rotor; 8 - shaped slit ring terminal; 9 - channel for the collection of mercury; 10 - cooling water channel of rotor.

Let us note that to UM of alternating current and unipolar-single-armature converter abroad were given out patents [35 and 36] are considerably later than their invention in the USSR.

Unipolar micromachines are applied as tachogenerators [37, 38], the sensors of slip during testing of induction machines [39], in the electrical measuring technology during the determination of one resistor/resistance [40]. Are known also unipolar electromagnetic couplings [41], converters of turning moment [42], electromechanical storage batteries/accumulators [43] and other forms of special UM. In more detail in this book they are not examined also for the familiarization with them one should be converted to the literature indicated.

1.2. Fundamental requirements for non-polars dynamo of low voltage.

The requirements, presented by the main groups of users to the electric power sources of large values of the direct current of low voltage, are reduced in essence to the following.

Conduction pumps need current 10^3-10^5 with the voltage/stress 0.5-3 V. For decreasing the losses in the supplying busbars the power supply must be established/installed as near as possible to the pump. The transported metal can have high temperature and possess radioactivity; therefore of the source efficiency during the increased heatings and resistance to possible radioactive irradiation is required. It must have prolonged service life, a sufficient reliability, to be simple by the construction/design and in the operation and to have low cost/value.

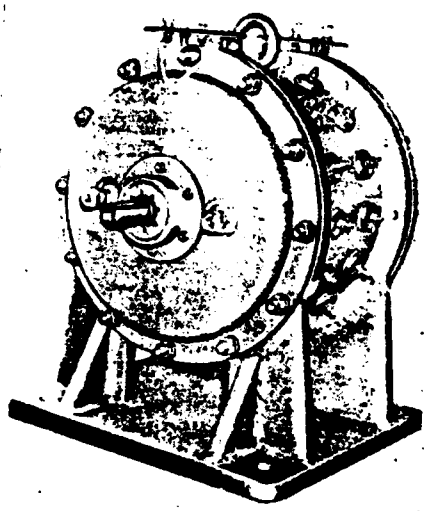

Fig. 1-12. The general view of generator MAI (overall dimensions 355×320×385 mm).

Page 20.

For the movable objects are necessary small over-all payload ratio (to the unit of power) and the overall sizes.

For the magnet windings of accelerators and installations for the creation of strong magnetic fields are required the currents to 10^{4} A with the voltage/stress from ones to 10-100 V. By the special features/peculiarities of power supply must large overload capacity, operating speed, possibility reserve and give up during the short time interval considerable energy.

Electrolytic baths and lines consume currents 10^3-10^5 A with the voltage/stress from 6-12 to 100 V. The requirements of the absence of the pulsations of voltage/stress, the ease of a change in the polarity, the minimum one-time expenditures during the construction of installations, buildings, current inputs, efficiency/cost-effectiveness and operations are specific.

Rectifying installations, all possible straight/direct converters of different forms of energy can serve as the fundamental types of the sources of high currents into the electrical [44], the batteries of chemical elements, dynamo generators (collector and unipolar).

The sources, which directly convert thermal, nuclear, solar energy, into the electrical, are at present developed insufficiently. Chemical sources are bulky and way. Commutator machines of low voltage with the high currents possess a number of deficiencies/lacks. The uses/applications of special transformers require rectifying installations, ripple filters, have run-aways characteristic; their advantage consists in the absence of movable electrical contacts.

Unipolar direct-current generators satisfy the majority of the requirements indicated. According to the data [45] their cost/value lower than cost/value of the corresponding rectifying installations for the electrolysis to 25%. Furthermore, UG are free from the pulsations of voltage/stress. The absence of insulation and windings on the armature determines their resistance to overloadings. The solid rotors of generators are used as the flywheels, which reserve the kinetic energy, converted into the energy of the impulse/momentum/pulse of electric current with the feed of accelerators.

Page 21.

Advantages of UG over the appropriate bipolar machines are: the absence of collector/receptacle from the copper plates, the possibility of applying the liquid-metal current pickup, which allows/assumes high ones current density and the relative rate in the contact and ensuring reliable work with the high currents, double use of active materials simultaneously as conductors and magnetic circuits and smaller over-all payload ratio with the low voltages, greater efficiency as a result of the absence of the losses into steel to hysteresis and eddy currents and of decrease in the mechanical and electrical losses in the liquid-metal contact of current-tap apparatus, simplicity of construction/design as a result

of a small quantity of parts, high heat resistance and life, a savings of nonferrous metal (copper), the smaller cost/value of machine and easy servicing.

Collector generators cannot satisfactorily work with the voltage/stress 0.5-1 V, since a voltage drop across their brushes has the same order. Acyclic machines with the liquid-metal current pickup recommended well themselves with these voltages/stresses. The improvement of liquid-metal contact and the use/application of new magnetic materials open/disclose further paths to an improvement in the parameters of UM.

Use of UG of low voltage with the high currents is extremely urgent. In particular, UG are the most adequate/approaching supply of power of the pumps of direct current, which obtained propagation in practice, at present. In spite of the available traditions in the development of UG, their practical possibilities are mastered by our technology insufficiently. Meanwhile is of undoubted interest the use of these generators in the regions of industry and scientific research indicated.

The use/application of UD is promising in connection with the development of the thermoelectric generators, which give the low voltage of feed [46].

1.3. Short survey/coverage of literature on the study of non-polars dynamo.

Considerable experimental design work in the region of UG at present is mainly done in the USA. However, judging by the published literature, designing-theoretical and experimental research of UM abroad lags behind the development of their constructions/designs. Are selected only the works of D. Vatt [14, 47, 48], dedicated to the research of UG with the hollow rotor and the liquid contact, and the works of P. Klaudi [49, 50] on the basis of the theory of liquid-metal contact and some laws governing the calculation of machines.

Page 22.

Article [51] is dedicated to the calculation of the fundamental parameters of armature UG with the winding on the rotor. Experimental research of the contact properties of mercury-indium alloy in connection with current pickup of UM is stated in works [46, 52].

The series/row of theoretical questions is more fully investigated by Soviet scientists. In B. I. Ugrimov's dissertation

[6] are given the theory and calculation of knife liquid-metal contact for for the disk UM and are given the results of experiments with the contact with the electrodes of various forms. Ye. G. Komar's article [53] is dedicated to calculation of cylindrical UM with the rod at the armature. cylindrical machines with the brush current pickup they are investigated in the work of I. P. Ivanov and B. V. Kostin [10, 54]. In article [54] some calculated relationships/ratios of the generator, which has rotor with the expansion, are given. The dissertation work of Yu. Yu. Kaunas [22] is dedicated to the research of hydrodynamics of circular mercury contact for UG. Work gives expressions for sizing of contact and power losses in the current pickup. In the works of V. G. Mozzherin [55-57] is given study of generator with the hollow nonmagnetic cylindrical rotor and the "ray" magnetic system of inductor. In articles [55, 56] are presented the elements of the calculation of generator and is made more precise "machine constant" Arnold by the introduction of the coefficients, which characterize the use of a contact surface of current pickup.

The phenomenon of armature reaction UG is partially investigated by B. S. Khlusevich [58]; however, the method proposed by them of the graph-analytic account of the demagnetizing effect of mag. force of armature is bulky and little suitable in the engineering practice. In the work of B. S. Khlusevich is carried out also the first theoretical studies of UM of alternating current [59]. The number of

questions of theory and calculation of UG is illuminated in [128]. Non-polars dynamo of periodic impulses/momenta/pulses are examined in the book of A. L. Lifshitz and I. S. Rogachev [31].

Works in the region of UM are conducted in different countries (USSR, Poland, Rumania, Hungary, USA, France, Australia, FRG, Austria, Japan, etc.), about which the vast patent and periodical literature of recent years testifies. In spite of a large number of published works on UM, systematic studies according to theory and calculation of different forms of UM, including UG, is absent. The majority of articles carries descriptive character. Existing knowledges are incomplete, in separate questions imprecise and contradictory, sometimes erroneous. In particular, Zh. Pulen [46] considers that the demagnetizing effect of mag. force of armature in UG is insignificant. However, our calculational-theoretical and experimental research showed that with the high currents, characteristic UM, the armature reaction is exhibited very strongly, especially in the solid rotor.

Page 23.

One of the associated factors, which influenced the delay of development and use/application of UM, was the absence of the engineering methodologies of their calculation taking into account

the armature reaction, magnetic leakage, distribution of electromagnetic field. Up to now was not also carried out classification of UM. The need of solving some of these tasks was noted even at the Yaroslavl conference in 1939 [10]. Since 1959 in the MAI is conducted the work, dedicated to theory, to calculation, to the creation of experimental models and to experimental research of UM with the liquid-metal current pickup. Fundamental tasks in the process of performing this work they were: the development of common classification of UM and more detailed classification UG, research of the distribution of magnetic induction and current density in the armature of UM and proof and the refinement of the fundamental calculated relationships/ratios of machines, the development of theory, methods of quantitative account and compensation for armature reaction, and also its experimental research in the models and the samples/specimens of UM, the calculation of magnetic circuit taking into account leakage fluxes; research of the work of liquid-metal current pickup of UM, the comparison of the fundamental parameters of different types of UM, the experimental study of the steady-state and nonstationary systems of the work of generator with the liquid contacts. Furthermore, were examined questions of unbalanced magnetic pull into UM of different construction/design. Are obtained the systematized engineering methods of calculation (taking into account the indicated factors) cylindrical UM with the massive and hollow rotors and disk UM of direct current, and are also given the bases of

calculation of UG without the ferromagnetic circuit. The fundamental results of research are presented in [60-68].

1.4. Induction of emf in acyclic machine. Determination is mind. Some electromagnetic paradoxes.

Cylindrical or disc armature of UM (generator) revolves in the magnetic field of constant/invariable polarity (Fig. 1-13). As is known, induced emf.

$$e=-\frac{d\Psi}{dt}=-w\frac{d\Phi}{dt}.$$

In the general case the magnetic flux $\Phi=\Phi(t, \varphi)$, engaged with the duct/contour, formed by the elementary conductor of armature and by external circuit, is the function of time t and angle of rotation of rotor φ.

Page 24.

In acyclic machine of direct current with steady-state flow regime in the time is constant/invariable; therefore

$$\frac{d\Phi}{dt}=\frac{\partial\Phi}{\partial t}+\frac{\partial\Phi}{\partial\varphi}\frac{d\varphi}{dt}=\omega\frac{\partial\Phi}{\partial\varphi},$$

where

$$\omega=\frac{d\varphi}{dt}.$$

Taking into account that a number of armature "turns" w=1, and

lowering minus sign, we obtain:

$$e = \omega \frac{\partial \Phi}{\partial \varphi}.$$

For the cylindrical machine

$$\Phi_{ц} = \int_0^{2\pi} B_{з}(\varphi) \frac{Dl}{2} d\varphi;$$

for the disk

$$\Phi_{д} = \int_0^{2\pi} B_{з}(\varphi) \frac{D^2 - D_{п}^2}{8 \cos \alpha} d\varphi.$$

With the constant/invariable in the limits of the pole of magnetic induction in worker [redacted] = const we have respectively:

$$e_{ц} = \frac{\omega}{2} B_{з} Dl = \pi n B_{з} Dl = B_{з} lv = \Phi_{ц} n; \qquad (1\text{-}1)$$

$$e_{д} = \frac{\omega}{8} B_{з} \frac{D^2 - D_{п}^2}{\cos \alpha} = \frac{\pi n}{4} B_{з} \frac{D^2 - D_{п}^2}{\cos \alpha} = \Phi_{д} n. \qquad (1\text{-}2)$$

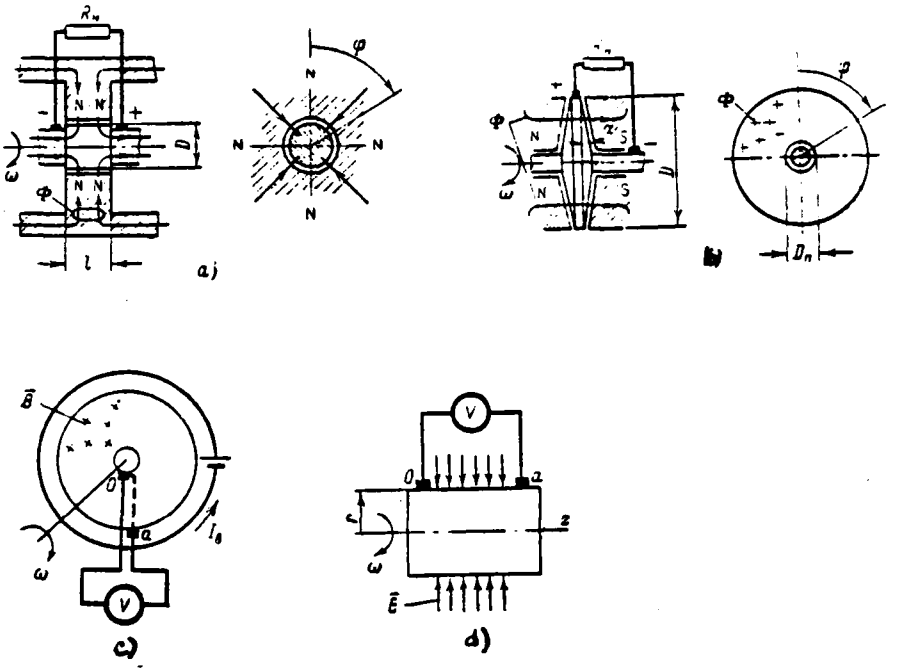

Fig. 1-13. To the induction of emf in acyclic machines. a, d) cylindrical; b, c) disk.

Page 25.

In expressions (1-1) and (1-2) it is marked: D, D_a, l, α - geometric dimensions of UM in accordance with Fig. 1-13a, b; n, r/s, and v - rotational speed and the linear velocity of the surface of armature [1].

FOOTNOTE [1]. In this book the international sistem of the units of the measurements SI (GOST 9867-61) everywhere is provided. ENDFOOTNOTE.

Upon the inclusion/connection of load current UG

$$I_я = \frac{e_н}{R_н + R_я} = \frac{U}{R_н},$$

where $e_н, U$ - emf with the load and voltage/stress of UG;

$R_н, R_я$ - resistance/resistor of load and circuit of armature of UG.

Direction of flow coincides with the direction of emf and is not changed during the rotation of armature. Therefore in contrast to the commutator machines (bipolar, heteropolar), in which the periodic commutation of current occurs, UM have the second name - acyclic.

The operating principle of acyclic machine is described in [7, 8]. It can be also clarified with the help of the following model. Let us visualize the fabric of railroad, is normal to which directed uniform magnetic field with the constant induction B.

Generator mode.

Perpendicular to rails the conducting rod is placed and we will move it along the fabric (on coordinate x) with a constant velocity v. In the beginning of reading (x=0) between the rails the voltmeter is included/connected. Then the electrical circuit, which consists of

the conducting rod, rails and voltmeter, forms closed the single-turn changing duct/contour, in which between the rails and the rod there are sliding contacts.

Page 26.

If the distance between the rails is equal to l, then during the motion of rod and the intersection with it of unit magnetic flux of field in it will be directed emf, which will measure the voltmeter, by the value

$$e = w\frac{d\Phi}{dt} = w\frac{d}{dt}BS(x) = B\frac{d}{dt}lx = Blv;\ v = \frac{dx}{dt},$$

where S(x)=lx=var - area of the changing duct/contour;

w=1 - number of turns of duct/contour.

Motoring.

If we to the rails conduct to conduct the direct current I from the independent source, then the conducting rod will be moved along x with a velocity v under the action of the electromagnetic force, whose value $T_э = BlI$.

From that presented the definition escape/ensues: the collectorless machine, in which the direction of emf, induced in the

conductors of armature, and current they remain constant/invariable relative to these conductors, is called the unipolar (homopolar, acyclic) machine of direct current.

With UM some electromagnetic paradoxes are connected. Let us consider the machine, depicted in Fig. 1-13c. Considering that the disk of armature and energizing circuit are located in one plane and after selecting the duct/contour of the integration 0Va0, let us compute emf according to Stokes's theorem [69]:

$$e = \oint_l \mathbf{E}\, d\mathbf{l} = \iint_s \operatorname{rot} \mathbf{E}\, d\mathbf{s} = 0. \qquad (1\text{-}3)$$

Actually/really, in the stationary magnetic field B, caused by direct field current $I_в$, on the basis of the generalized expression of intensity/strength E of electric field and second equation of Maxwell in the system of cylindrical coordinates r, φ, z curl

$$\operatorname{rot} \mathbf{E} = -\frac{d\mathbf{B}}{dt} + [\bar{\omega}\mathbf{B}] = 0,$$

where B=B(t, r, φ);

$$\frac{d\mathbf{B}}{dt} = \frac{\partial \mathbf{B}}{\partial t} + \frac{\partial \mathbf{B}}{\partial r}\frac{dr}{dt} + \frac{\partial \mathbf{B}}{\partial \varphi}\frac{d\varphi}{dt} = 0,$$

since ∂B/∂t=0, ∂r/dt=0 and as a result of the symmetry ∂B/∂φ=0; [ωB] =0, since in the plane of drawing (z=0) vectors $\mathcal{B}=$ [illegible] and $\bar{\omega}$ - have the identical direction (they are collinear).

According to data of the experiment of emf, on the brushes 0 a during the rotation of the disk

$$\mathscr{E}=\int_{r_0}^{r_a}\omega B_z(r)\,r\,dr\neq 0.$$

Contradiction is explained by the fact that to the changing duct/contour they are not applied the theorem of Stokes and equation of Maxwell, whereas part a0 duct/contour of integration 0Va0 is variable/alternating/variable. For physical reasons the onset of emf can be explained by the action of field E*= [vB] to the revolving with the disk electrons. Under the action of this field the electric current, which creates charges on the circles/circumferences of current pickups, appears. Field E* in the disk of armature is compensated by the field of charges; therefore the circulation of field ducts/contours 0Va0 (one part of which is located in the moving/driving disk, and another is motionless) is different from zero.

On the basis of expression (1-3) during the contour integration 0Va0 for the cylindrical UM (Fig. 1-13d) of emf e=0. However, experiment shows that with different cases of relative motion of armature, source of field and circuit with the voltmeter (observer) of emf of armature $e=\int_{z_0}^{z_a}\omega B_r(z)\,r\,dz\neq 0$ (Table 1-2).

This contradiction can be explained similarly to previous. Table 1-2 shows that in the cases of 2 and 6 unalterable/invariable ducts/contours e=0.

Table 1-2. Different cases of relative motion.

(1) Скорость вращения			(2) Электродвижущая сила, измеренная вольтметром
(3) цилиндра	(4) источника поля	(5) цепи с вольтметром	
ω_1	0	0	e
0	ω_1	0	0
0	ω_1	ω_1	e
ω_1	ω_1	0	e
0	0	ω_1	e
ω_1	0	ω_1	0

Key: (1). Rotational speed. (2). Electromotive force, measured by voltmeter. (3). cylinder. (4). the source of field. (5). circuit with the voltmeter.

Page 28.

The principle of the impossibility of prolonged obtaining by constant emf without the use/application of slide contacts is confirmed thus. In the works of K. I. Shenfer [10], V. F. Mitkevich [70] are criticized some stressed-skin constructions of the electrical machines, incorrectly carried to UM. In them is violated the principle indicated, and they either are inefficient or they are the machines of alternating current. In particular, an increase in the voltage/stress of UM due to an increase in the number of the "turns" of armature is possible only with the fulfillment of series

connection of conductors with the help of the slide contacts (according to the type of the machine of Neggerat).

In order not to encounter similar paradoxes in the examination of UM (and by some paradoxes in other electromagnetic phenomena), P. Mun and D. E. Spencer proposed during the solution of such problems of using the equation of "new electrodynamics" [71], which gives the results, which coincide with experiment.

Matter in UM concerning the armature in the form of the revolving cylindrical permanent magnet, magnetized along the longitudinal axis, is more complicated. For a strict proof of the reason for the onset of emf, and also for the definition, what part of the circuit of armature (movable or motionless) is the source of emf, it is proposed to examine phenomena with the help of the theory of relativity [72, 73]. However, as shown in [70], the onset of emf can be explained, on the basis of the Faraday representations about the lines of magnetic induction, if we use the concept of the changing duct/contour and the principle of continuity of magnetic flux.

In acyclic machines the following curious phenomena are observed. As shown below (see Chapter 2), during the rotation of massive cylindrical or disc armature in the stationary axisymmetric

magnetic field in the armature core the eddy currents do not appear. In the general case according to the equations of the electrodynamics of continuous media they must appear. Thus, armature of UM presents exception/elimination from the rule. The resulting magnetic field with the load of UM to a certain extent is similar to the field of the system of rectilinear and circular currents, by the specific form of those oriented. As showed I. Ye. Tamm [72], if the relation of these currents represents an irrational number, the lines of the magnetic induction of the resulting field will be multipoint open and "tightly" they will fill the surface of torus/Torr (or certain space). This contradicts physical representation about the lines of magnetic induction, which are subordinated to the equation of continuity div B=0. V. F. Mitkevich [70] finds the explanation of this contradiction in the fact that according to quantum representations the value of the relation of currents, apparently, cannot be expressed by an irrational number.

1.5. The classification of electrical unipolar ones it is machine.

In connection with the propagation of different forms of UM and an increase in the number of their new modifications appears the need of conducting the general/common/total classification of these machines. The worked out classification on the series/row of fundamental signs/criteria is given in table 1-3.

Capacitive UM of high voltage represent the completely special region of electromechanical devices/equipment [75].

Acyclic machines of alternating current with the uniform working gap are characterized by the field of exictation changing in the time. The laws of a change in this field and voltage/stress on the armature of machine are determined by frequency and form of the voltage/stress, applied to the excitation winding. The current frequency of the armature of these UM does not depend on the rotational speed. Magnetic system is implemented with the radial blending. At the armature bar winding is placed. The slide contact of current pickup, which is located within the machine, cannot be implemented by circular liquid-metal to avoid damping field of exictation by the short-circuited duct/contour. As an example UM of alternating current with the periodically changing in the value working gap serve the generators of unipolar impulses/momenta/pulses [31]. The armature of machine has bar winding, at the pole of stator the teeth and pockets are alternated.

Pulse frequency is determined by a number of teeth of inductor and by the speed of rotation of machine. Special UM with the brushes, which have rotary or reciprocating displacement/movement over the

surface of armature, are intended for pulsing of the current of various forms [34], form and pulse frequency depend on the law of the motion of brushes.

Different driving circuits of UM are shown in Fig. 1-4. During the combined excitation (Fig. 1-14c) basic part of the magnetic flux depends on permanent magnet, the winding of separate excitation is managing. Similar UM are proposed in [76].

Rotary UM usually have solid metallic armature. For example, unipolar-single-armature converters UOYaP are exception, where the rotor of generator can present the layer of liquid metal. The progressive/forward UM include according to the operating principle conductor liquid-metal pumps and flow gauges and conductor magnetogasdynamic generators and accelerators.

Table 1-3. General/common/total classification of acyclic machines.

(1) Признак	(2) Тип машин
(3) Вид поля	(a) Индуктивные УМ (b) Емкостные УМ
(4) Род тока	(a) Постоянного тока (b) Переменного тока 1) с равномерным рабочим зазором 2) с изменяющимся по величине зазором 3) с движущимися щетками
(5) Схема возбуждения	(a) С независимым возбуждением (b) С самовозбуждением 1) параллельным 2) последовательным 3) смешанным 4) от постоянных магнитов (УМЭМ) (c) С комбинированным возбуждением
(6) Тип якоря	(a) С твердым металлическим якорем (b) С жидкостным проводящим якорем (c) С газообразным ионизированным якорем
(7) Движение якоря	(a) Вращательные УМ (b) Поступательные УМ
(8) Характер использования	(a) Генераторы 1) с ферромагнитным магнитопроводом 2) без ферромагнитного магнитопровода (b) Электродвигатели (c) Специальные УМ 1) одноякорные преобразователи (УОЯП) 2) электромашинные усилители (УЭМУ) 3) электромагнитные муфты (УЭМ) 4) преобразователи вращающего момента 5) униполярные микромашины (тахогенераторы, датчики скольжения)

Key: (1). Sign/criterion. (2). Type of machines. (3). Form of field. (a). Inductive UM. (b). Capacitive UM. (4). Kind of current. (a).

Direct current. (b). Alternating current. 1). with the uniform working gap. 2). with the changing in air-gap clearance. 3). with the moving/driving brushes. (5). Driving circuit. (a). With separate excitation. (b). With the self-excitation. 1). parallel. 2). consecutive. 3). mixed. 4). from the permanent magnets (UMEM). (c). With the combined excitation. (6). Type of armature. (a). With the solid metallic armature. (b). With the liquid conducting armature. (c). With the vapor ionized armature. (7). Motion of armature. (a). Rotary UM. (b). Progressive/forward UM. (8). Character of use. (a). Generators. 1). with the ferromagnetic circuit. 2). without the ferromagnetic magnetooccasion. (b). Electric motors. (c). Special UM. 1). single-armature converters (UOYaP). 2). amplidynes UEMU). 3). electromagnetic couplings (UEM). 4). the converters of turning moment. 5). unipolar micromachines (tachogenerators, the sensors of slip).

Page 31.

The role of armature in them plays moving liquid metal or ionized conducting gas (plasma). Subsequently these forms of UM in this work are not examined, just as special UM. The subsequent chapters are dedicated to the examination of inductive UM of direct current with the electromagnetic excitation.

The diagram of the more detailed classification of UG of direct current with the ferromagnetic circuit of inductor is represented in Fig. 1-15. With the fundamental signs/criteria of classification they are selected: 1) the structural/design type of rotor (armature), 2) a number of polar extensions, 3) the presence of devices/equipment for the compensation for armature reaction, 4) the type of current pickup.

Varieties of UG, which correspond to this classification, are schematically represented in Fig. 1-15. Figures 1-15e and f demonstrate machines with the complete utilization of active length of cylindrical armature.

The rotor of bipolar machine, shown in Fig. 1-15e, is divided to two parts by insulation spacer. These parts of the rotor, which are located under unlike poles, can be connected in series with the help of the slide contacts for the complete voltage of the generator.

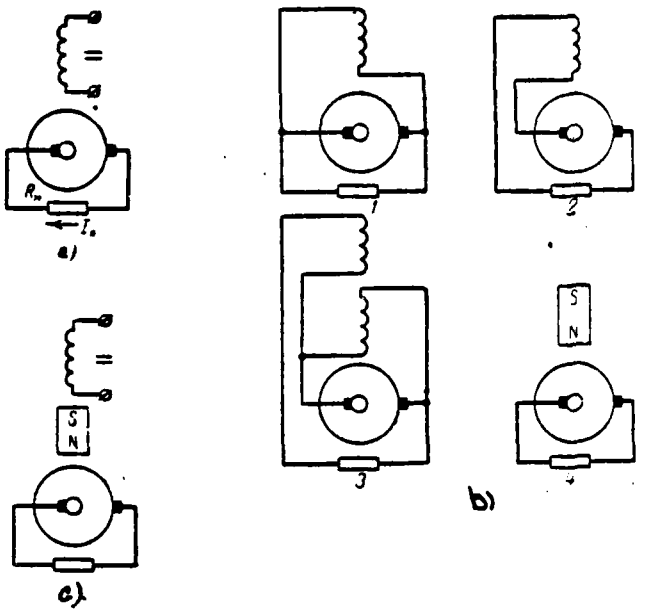

Fig. 1-14. Driving circuits of UM. a) with separate excitation; b) with the self-excitation; 1 - parallel; 2 - consecutive; 3 - mixed; 4 - from the permanent magnet; c) with the combined excitation.

Pages 32-33.

The complete utilization of active length of armature UG (Fig. 1-15f) is achieved/reached by the installation of further third current pickup without the distribution of rotor by separator. With the doubly smaller (half) voltage/stress and at the identical power this machine has doubly larger current in comparison with UG, represented in Fig. 1-15e. Generators with the complete utilization of active

length of armature have smaller over-all payload ratio than UG with the half use. However, in practice the latter as a result of their higher reliability due to a smaller number of slide contacts and simplicity of construction/design frequently are applied.

The rotor expansion of generator (Fig. 1-15b) during the brush current pickup can be used for the end-type installation of brushes, which decreases their vibration in comparison with the same during the radial installation. Faces of rotor expansion are equipotential. Hollow rotor of generator (fig. 1-15c) can be fulfilled both of the magnetic material and nonmagnetic (copper). The latter allows/assumes higher current density, but considerably increases nonmagnetic gap/interval in the machine. The selection of the material of rotor depends on the required parameters of UG.

Disk UG with the magnetic armature have the essential deficiency/lack, which consists in strong unbalanced magnetic pull of rotor to the pole of stator with the inequality of gaps along both sides of disk and asymmetry of leakage fluxes. This fact complicates the construction/design of the bearing units of machine. For eliminating the one-sided attraction the use/application of nonmagnetic disks is expedient. Armature disks can be implemented by flat/plane ones (equal thickness), with the hyperbolic profile/airfoil (uniformly strong) at the high peripheral speed and

conical. The latter are little inferior on the strength to hyperbolic, but are more simple on technology productions. They ensure more uniform current distribution in the armature, than flat/plane disks. During the bilateral current pickup on the shaft of UG of the disk type (Fig. 1-15j) is reduced the diameter of shaft and increases the active radial length of armature, which contributes to obtaining by larger emf. However, the appearance of further on movable contact decreases reliability and complicates the construction/design of machine in comparison with UG, which have one-sided current pickup on the shaft (Fig. 1-15i).

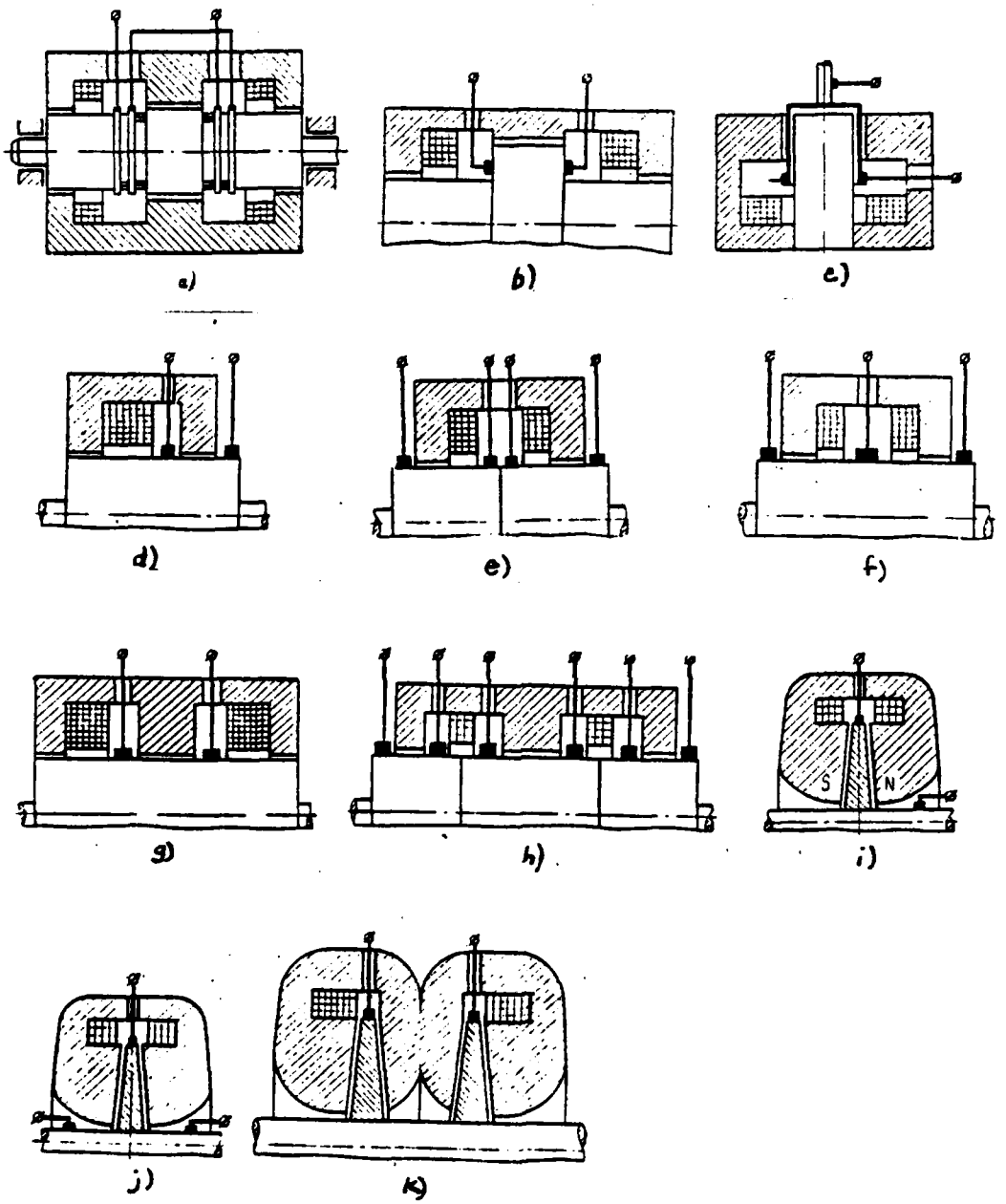
a)
b)
c)
d)
e)
f)
g)
h)
i)
S
N
j)
k)

Fig. 1-15. Design concepts of UG of direct current. Cylindrical UG: a) with bar winding on the rotor; b) with the rotor expansion; c) with the hollow rotor; d) two-pole with half use; e) two-pole with the complete utilization and the total voltage; f) the same with the half voltage/stress; g) multiline (2p=4) with the half use; h) the same with the complete utilization; disk UG with the conical rotors: i) two-pole with the one-sided current pickup on the shaft; j) the same with the bilateral current pickup; k) multipole (2p=4) with series connection of armatures.

Page 34.

The compensative and collector shoe gears of different types of UG are examined below (see Chapter 4 and 5).

On the series/row of unspecific for UM structural/design machines [77].

Unipolar engines are examined in Chapter 8.

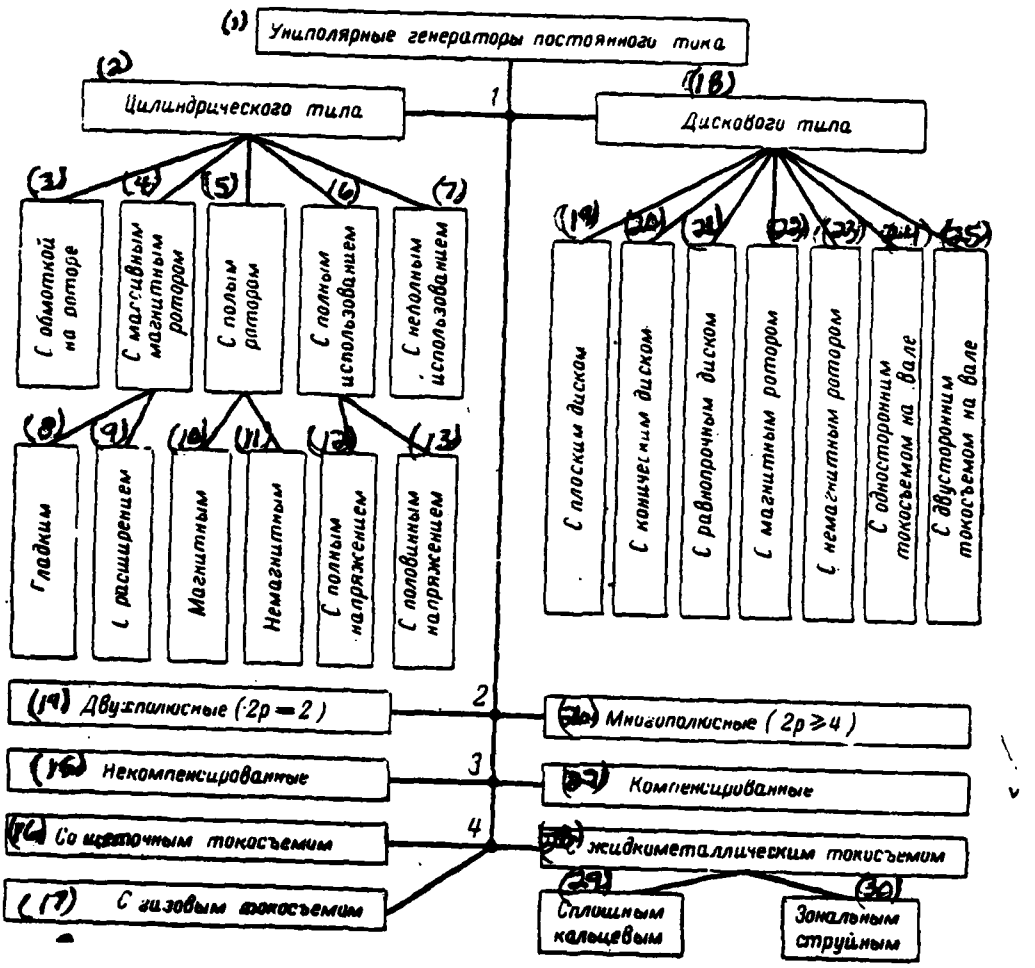

Fig. 1-16. Schematic of the classification of unipolar electric generators. 1 - according to the structural/design type of rotor; 2 - according to a number of poles; 3 - on the presence of compensators; 4 - according to the type of current-tap apparatus.

Key: (1). Unipolar direct-current generator. (2). Cylindrical type. (3). With the winding but rotor. (4). With the massive magnetic

rotor. (5). With the complete rotor. (6). With the complete utilization. (7). With the incomplete use. (8). Flat. (9). With the expansion. (10). Magnetic. (11). Nonmagnetic. (12). With the total voltage. (13). With the half voltage/stress. (14). Two-pole (2p=2). (15). Not compensated. (16). With the brush current pickup. (17). With the gas current pickup. (18). Disk type. (19). With the flat/plane disk. (20). With the conical disk. (21). With the uniformly strong. (22). With the magnetic rotor. (23). With the nonmagnetic rotor. (24). With the one-sided current pickup on the shaft. (25). With the bilateral current pickup on the shaft. (26). Multipole. (27). Compensated. (28). With the liquid-metal current pickup. (29). By continuous annular. (30). By zonal jet-edge.

Page 35.

Chapter Two.

ELECTROMAGNETIC FIELD OF ACYCLIC MACHINES.

2.1. Formulation of the problems.

Electromagnetic field of acyclic machines (UM) of direct current, that work in the steady-state mode/conditions, constantly/invariably in the time has complicated spatial distribution. This distribution it is necessary to know for studying of the occurring in the machines electromagnetic processes and refinement of questions of calculation and construction of UM. The designing-theoretical study of electromagnetic field of UM consists of the following: in the limits of the assumptions adopted to find the mathematically strict solution of the tasks about the distribution of the magnetic induction B in the magnetic circuit with the idling and the current densities j in the armature with the load of machines. Since during the solution of the problems the assumption will serve as fundamental assumption about the independence of

magnetic permeability from the intensity/strength of the resulting magnetic field, the appearing with the load tangentially directed field of transverse armature reaction will not change in the value the longitudinal field of exictation, which does not have azimuth component. The effect of the magnetic field of armature, which is manifested in the decrease of magnetic permeability of the material of magnetic circuit and weakening of the flow of excitation due to the saturation, is considered below (see Chapter 4) approximation methods.

Let us consider cylindrical UM with the flat massive ferromagnetic rotor and disk UM with the conical rotor. Let us take in this case some assumptions, which facilitate the solution of problems.

These assumptions are enumerated below.

Page 36.

1. The material of magnetic circuit is isotropic. Magnetic permeability is constant (μ_a=const) and limited, but considerably exceeds the permeability of vacuum; the specific electrical conductivity of armature is constant (γ=const) and limited (i.e. let us disregard saturation and consider heating the sections of armature

uniform).

2. Hysteresis effects are absent, the vectors of induction B and intensity/strength H of magnetic field lie/rest on one straight line and coincide in the direction (steady-load condition).

3. Cylindrical UM has uniform in the limits of pole magnetic field in air gaps (edge effects let us disregard). Magnetic circuit is limited by cylindrical surfaces with the circular foundations on faces, the magnetic circuit of machine is symmetrical relative to the spin axis of rotor and plane of its equator. All sizes/dimensions of magnetic circuit are known, let us conditionally divide magnetic circuit in the cylindrical (continuous or hollow) calculated sections, moreover on some of them we approximately consider field uniform.

4. The surface of the pole of disk UM, converted to air gaps, equipotential; magnetic circuit is symmetrical relative to the spin axis of rotor. We approximately consider direction of flow in the disk of armature radial.

5. Current pickup of continuous, circular on the base liquid-metal contact (current distribution in the armature UM axisymmetric). Currents, caused by Hall emf, let us disregard in view

of their very low value.

The tasks indicated can be investigated on the basis of the solution of the system of equations of the electrodynamics of continuous media, which taking into account the motion of rotor UM in the magnetic field is reduced to the form

$$\text{rot } \mathbf{H} = \text{rot } \frac{1}{\mu_a} \mathbf{B} = \mathbf{j}; \tag{2-1}$$

$$\text{rot } \mathbf{E} = -\frac{\partial \mathbf{B}}{\partial t} + \text{rot } [\mathbf{vB}]; \tag{2-2}$$

$$\text{div } \mathbf{B} = 0; \tag{2-3}$$

$$\mathbf{E} = \frac{1}{\gamma} \mathbf{j}, \tag{2-4}$$

where $\mathbf{E}=[\mathbf{vB}]-\nabla U^e-\frac{\partial \mathbf{A}}{\partial t}$ — generalized expression of electric intensity [78], introduced by D. Maxwell;

A - vector potential of electromagnetic field (rot A=B);

U^e — scalar potential of electric field;

v - vector of the linear rate of the points of rotor.

Page 37.

Let us show that with the idling UM current in the rotor is absent. Actually/really external circuit is opened and the component does not pass current, caused by a potential difference, through the

rotor. From equations (2-2) (2-3) it follows that during the rotation of the solid rotor of cylindrical UM in the stationary magnetic field

$$\operatorname{rot}[\mathbf{vB}] = (\mathbf{B}\nabla)\,\mathbf{v} - (\mathbf{v}\nabla)\,\mathbf{B} + \mathbf{v}\nabla\mathbf{B} - \mathbf{B}\nabla\mathbf{v} = [\bar{\omega}\mathbf{B}] - (\mathbf{v}\nabla)\,\mathbf{B};$$
$$\operatorname{rot}\mathbf{E} = -\frac{d\mathbf{B}}{dt} + [\bar{\omega}\mathbf{B}], \qquad (2\text{-}5)$$

moreover with the meridional symmetry in the system of cylindrical coordinates r, φ, z the "substantial" derivative dB/dt=0, since $\partial B/\partial t=0$ and $\partial B/\partial\varphi=0$. On the basis (2-4) and (2-5) in any cross section z=const on each circle/circumference r=const of the revolving cylinder

$$\int_{\varphi=0}^{2\pi} \operatorname{rot}\mathbf{j}\,d\varphi = 0,$$

since vectors [ωB] form the locked equilateral polygons. Consequently, eddy currents are absent. However, in the general case of rotating the massive conductor in the magnetic field in it the eddy currents appear, UM are exception/elimination from the rule. This is explained by the fact that expression (B∇)v= [ωB] considers a change in orientation B with respect to the revolving rotor, and in UM vectors B are symmetrical relative to rotational axis. More simply is matter concerning the revolving disc armature UM. Since the angular velocity vectors ω and induction B are collinear, rot j=0. On the magnetic circuit of stator the currents also do not pass cylindrical and disk machines. Thus, with the idling UM j=0.

2.2. Magnetic field in the magnetic circuit with the idling of cylindrical machine.

Let us introduce the scalar potential of magnetic field $U^{м}$. On the basis of relationship/ratio [69]

$$\text{rot grad } U^{м}=0$$

and equations (2-1) (2-3) taking into account the adopted assumptions we have

$$\mathbf{B}=-\text{grad}\,U^{м}=-\nabla U^{м};\ \text{div}\,\mathbf{B}=-\nabla^2 U^{м}=0,$$

or in coordinates r, φ, z

$$\nabla U^{м}=\frac{1}{r}\frac{\partial}{\partial r}\left(r\frac{\partial U^{м}}{\partial r}\right)+\frac{1}{r^2}\frac{\partial^2 U^{м}}{\partial \varphi^2}+\frac{\partial^2 U^{м}}{\partial z^2}=0$$

With meridional symmetry $\partial U^{м}/\partial\varphi=0$, $\partial^2 U^{м}/\partial\varphi^2=0$, consequently,

$$\Delta U^{м}=\frac{\partial^2 U^{м}}{\partial r^2}+\frac{1}{r}\frac{\partial U^{м}}{\partial r}+\frac{\partial^2 U^{м}}{\partial z^2}=0. \qquad (2\text{-}6)$$

For solving the obtained equation of Laplace (2-6) the assignment of boundary conditions is necessary. Let us consider two-pole cylindrical UM (Fig. 2-1a). Magnetic circuit is conditionally divided in four sections: 1 - rotor; 2, 4 - poles of stator; 3 - framework of stator. Multipole ($2p\geqslant 4$) cylindrical machines are obtained from the region, shown in Fig. 2-1, with the appropriate p-multiple addition of similar two-pole regions. According to the adopted assumptions magnetic induction in working gap B_δ is considered constant/invariable that it is correct, since usually axial gap length composes approximately/exemplarily half of a radius of rotor UM, i.e., $l\approx 0{,}5R$, and $\delta<<R$.

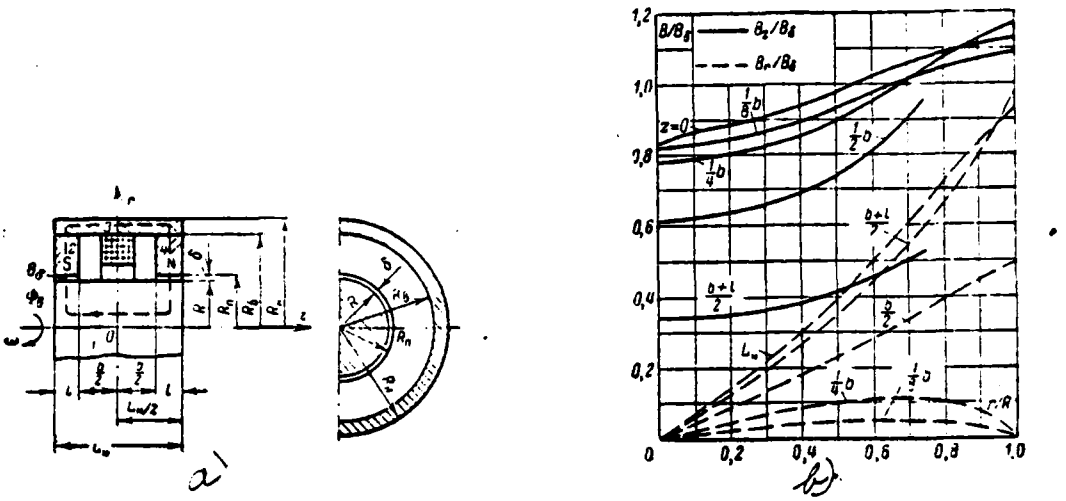

Fig. 2-1. Two-pole cylindrical is UM. a) the designation of calculated sections and geometric dimensions; b) the distribution curves of magnetic induction in the rotor, calculated by ETsVM [digital computer] "Ural".

Page 39.

We accept magnetic field in the poles when $R_п \leqslant r \leqslant R_в$ radial, and problem for sections 2 and 4 is solved elementarily:

$$\mathbf{B} = B_r \mathbf{e}_r; \quad \Phi_в = B_r S(r) = 2\pi B_r l r = 2\pi B_δ R_п l = 2\pi B_{R_в} R_в l;$$

$$B_r = B_δ \frac{R_п}{r} = B_{R_в} \frac{R_в}{r},$$

moreover

$$B_{R_в} = B_δ \frac{R_п}{R_в}; \quad S(r) = 2\pi l r.$$

Boundary conditions for section 1 (rotor) let us register, by taking into account the adopted assumptions and by using the property

of the magnetic potential:

$$-\frac{\partial U^{м}}{\partial n}=B_n,$$

where n - direction of external normal to the surface, which consists the region in question; B_n — magnetic induction in the direction of standard/normal.

a). On faces of the rotor:

$$\left.\frac{\partial U^{м}}{\partial z}\right|_{z=\pm\frac{L_{м}}{2}}=0.$$

b). On the lateral surface:

$$\left.\frac{\partial U^{м}}{\partial r}\right|_{r=R}=f(z),$$

moreover function f(z)≠0 only in the limits of gaps under the poles (at the length l), which are located on the distances +-(b/2) from the equatorial plane (z=0). Since here $B_n=B_\delta$,

$$f(z)=-B_\delta.$$

Page 40.

c). Further condition, necessary for determining the arbitrary constant in the solution of the problem of Neumann:

$$\left.U^{м}\right|_{z=0}=0,$$

Boundary conditions for section 3 (framework of stator).

a). On faces of the hollow cylinder:

$$\left.\frac{\partial U^{м}}{\partial z}\right|_{z=\pm\frac{L_{м}}{2}}=0.$$

b). On the internal lateral surface:

$$\left.\frac{\partial U^{м}}{\partial r}\right|_{r=R_{в}}=\varphi(z),$$

moreover $\varphi(z)\neq 0$ only in the limits of length l, where

$$\varphi(z)=-B_{Rв}.$$

c). On the external lateral surface:

$$\left.\frac{\partial U^{м}}{\partial r}\right|_{r=R_{м}}=0.$$

Equation (2-6) with the assigned boundary conditions we integrate by Fourier-Lame method separation of variables (to method of particular solutions) [79]. Solvability condition of stated problem it is:

$$\oint_{s}\frac{\partial U^{м}}{\partial n}ds=0,$$

i.e. the equality of the entering and outgoing magnetic fluxes.

Page 41.

The solution of task for section 1, the describing distribution of the components of magnetic induction in the rotor, take the form:

$$B_r(r, z) = -\frac{\partial U^м}{\partial r} = \sum_{m=0}^{\infty} A_m I_1(\varphi_m r)\cos[\varphi_m(z+0{,}5L_п)]; \qquad (2\text{-}7)$$

$$B_z(r, z) = -\frac{\partial U^м}{\partial z} = -\sum_{m=0}^{\infty} A_m I_0(\varphi_m r)\sin[\varphi_m(z+0{,}5L_п)], \qquad (2\text{-}8)$$

where

$$A_m = \frac{8B_з}{L_п\varphi_m I_1(\varphi_m R)}\sin(0{,}5\varphi_m l)\cos[0{,}5\varphi_m(2L_п - l)];$$

$$\varphi_m = \frac{2m+1}{L_п}\pi;$$

$I_0(\varphi_m r)$, $I_1(\varphi_m r)$ — the modified functions of Bessel of the first order.

We will obtain by the method of solution of equation (2-6) for section 3:

$$B_r(r, z) = \sum_{m=0}^{\infty} C_m[I_1(\varphi_m r) + MK_1(\varphi_m r)]\cos[\varphi_m(z+0{,}5L_п)];$$

$$B_z(r, z) = -\sum_{m=0}^{\infty} C_m[I_0(\varphi_m r) + MK_0(\varphi_m r)]\sin[\varphi_m(z+0{,}5L_п)],$$

where

$$C_m = \frac{8B_{Rп}}{L_п\varphi_m[I_1(\varphi_m R_п) + MK_1(\varphi_m R_п)]}\sin(0{,}5\varphi_m l)\cos[0{,}5\varphi_m(2L_п - l)];$$

$$M = -\frac{I_1(\varphi_m R_п)}{K_1(\varphi_m R_п)};$$

$K_0(\varphi_m r)$, $K_1(\varphi_m r)$ — the modified functions of Bessel of the second order (MacDonald's function).

Especially important practical value have derived calculation formulas (2-7) and (2-8) for the components of magnetic induction in the rotor. The calculations [1] of the values of induction conducted

with the characteristic for UM relationships/ratios of the geometric dimensions:

$$l \cong 0{,}5R \text{ и } L_{\text{п}} \cong 4l = 2R = D$$

it showed that the distribution of magnetic flow in the middle part of the rotor is close to axial-uniform.

FOOTNOTE [1]. In the computer "Urals". ENDFOOTNOTE.

The results of calculation are given in the form of curves in Fig. 2-1b. They are used for proof and construction of engineering calculation procedure cylindrical type UM: magnetic induction in the rotor is taken as the approximately equal to

$$B_{\text{р}} \cong \frac{\Phi_{\text{в}}}{\pi R^2} \cong \frac{2B_{\text{в}}l}{R}.$$

Experiments to the electrolytic model (see Chapter 10) confirmed the obtained output.

2.3. The magnetic field of disk acyclic machine.

The magnetic circuit of the stator of disk machine has, as a rule, complicated bounding surface (Fig. 2-2). During the layout of the configurations of outer duct are guided by the considerations of the greatest "quality" [80] the magnetic circuits, which

characterizes the relationship/ratio between necessary magnetizing force and volume of magnetic circuit and given ones by magnetic flux and length of its path. Most economical with the use of a material of magnetic circuit and material of excitation winding are systems with the even distribution of magnetic induction in the cross sections of magnetic circuit along the length the path of magnetic flux. Thus, one should approach the retention/preservation/maintaining of constant quantity of the cross-sectional area of the magnetic circuit of disk UM. In this case magnetic flux distribution in the stator approaches uniform. Precise analytical expressions for components B_r (r, z) and B_z(r, z) magnetic induction with the network circuits of bounding surfaces to obtain is very difficult. In detail this question here is not examined, since its practical value for developing the engineering methods of calculation of disk UM is small.

In the disk UM with the ferromagnetic rotors the distribution of gap density is close to the uniform. Field distribution along air gap of UM with the nonmagnetic conical disk and taking into account the adopted assumptions is described by the function

$$B_\delta(r)=\frac{\mu_0 F_\delta}{2\alpha\rho_1}=\frac{\mu_0 F_\delta}{2\alpha(\rho-r)}, \qquad (2\text{-}9)$$

where $F_\delta=\text{const}$ — drop in the magnetic potential in the interpolar space; $\delta(r)=2\alpha(\rho-r)$ - the law of a change in the length of the line of magnetic induction between the poles of UM on the assumption that

the lines have a form of circular arcs with the centers at the points

$$|\pm r| = \rho = \frac{1}{2}(D + c\,\mathrm{ctg}\,\alpha);$$

D=2R, c, α - geometric dimensions in accordance with Fig. 2-2b.

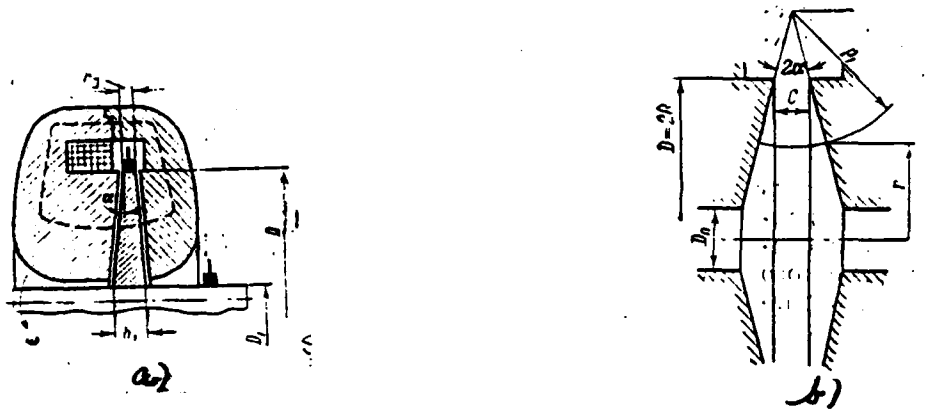

Fig. 2-2. Disk UM. a) the form of magnetic circuit and the designation of the sizes/dimensions of machine; b) illustration to the calculation of the magnetic field of machine with the conical nonmagnetic armature.

Page 43.

Expression (2-9) is used for the refined calculation of emf of the armature

$$e = \omega \int_{0,5D_{\text{п}}}^{0,5D} B_{\delta}(r)\, r\, dr = \frac{\omega \mu_0 F_{\delta}}{2\alpha}\left(\rho \ln \frac{2\rho - D_{\text{п}}}{2\rho - D} - \frac{D - D_{\text{п}}}{2}\right). \quad (2\text{-}10)$$

Usually the value of angle a is the units of degrees, in this case induction in the gap it is possible to approximately consider independent variable from r:

$$B_{\delta} \cong \frac{\mu_0 F_{\delta}}{l_{\text{ср}}};\ l_{\text{ср}} = \frac{1}{2}(D - D_{\text{п}}) - c \operatorname{ctg} \alpha$$

and to compute emf according to the expression, accepted in the

engineering methodology,

$$e = \int_{0,5D_a}^{0,5D} \frac{\omega B_\delta}{\cos\alpha} r\,dr = \frac{\omega}{8\cos\alpha} B_\delta (D^2 - D_a^2). \qquad (2\text{-}11)$$

2.4. Distribution of electric current in the armature of cylindrical machine.

According to adopted assumptions $\mu_a = \text{const}$ and $\gamma = \text{const}$ a question about density distribution of current in the ferromagnetic cylinder of rotor UM is considered as linear task. We will use artificial reception/procedure, after using for facilitating the calculation the theorem of Helmholtz-Tevenen about the equivalent source of voltage of the theory of linear electrical circuits [81] to non-polar dynamo. Current distribution in the armature of loaded UM is determined according to the principle of the superposition of the currents of two modes/conditions: idling with the spatial distribution by the space of the rotor UG of emf of rotation, caused by product [vB], and load mode/conditions with passive internal circuit UG and by the outlying to the clamps equivalent voltage source. Current distribution in the armature with the idling of machine with the symmetrical magnetic system is already found earlier: j=0.

Page 44.

Thus, task is reduced to the finding in tube domain of the

current distribution, which satisfies on the basis (2-4) the equation

$$\frac{1}{\gamma}\mathbf{j} = -\nabla U^e = -\operatorname{grad} U^e. \qquad (2\text{-}12)$$

Taking into account (2-12), the known [69] relationship/ratio div rot H=0 and equation (2-1), we find with the assumptions, accepted above:

$$\Delta U^e = \frac{\partial^2 U^e}{\partial r^2} + \frac{1}{r}\frac{\partial U^e}{\partial r} + \frac{\partial^2 U^e}{\partial z^2} = 0. \qquad (2\text{-}13)$$

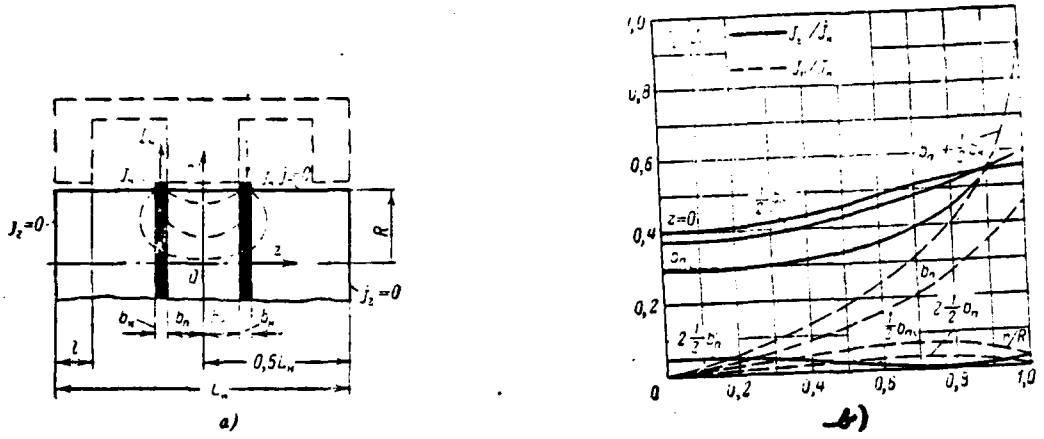

Fig. 2-3. Cylindrical UM. a) the designation of the sizes/dimensions of machine; b) the curves of density distribution of current in the cylindrical armature, calculated by ETsVM "Ural".

Page 45.

On the basis (2-12) let us register the boundary conditions of the second boundary-value problem (Neumann's task for the region, indicated in Fig. 2-3a.

a). On faces of the cylinder:

$$\left.\frac{\partial U^*}{\partial z}\right|_{z=\pm\frac{L_n}{2}}=0.$$

b). On the lateral surface:

$$\left.\frac{\partial U^*}{\partial r}\right|_{r=R}=f(z),$$

moreover $f(z) \neq 0$ only within the limits of circular current pickups with width $b_к$, that are located at a distance $\pm b_п$ from equator ($z=0$). Usually in UM $b_к \ll 0{,}5L_ц$, therefore current density in the contact we accept constant:

$$j_к = \frac{I_п}{2\pi R b_к}.$$

Thus, in the zone of current pickups $f(z) = -\frac{1}{\gamma} j_к$.

c). Further condition at the equator:

$$U^e|_{z=0} = 0.$$

Integrating the equation of Laplace for the scalar electric potential (2-13) for Fourier-Lame method, we obtain the solution of stated problem in the form of the expressions, which describe the distribution of the components of current density in the function of the coordinates of the points of the rotor:

$$j_r(r, z) = -\gamma \frac{\partial U^e}{\partial r} = \sum_{m=0}^{\infty} D_m I_1(\varphi_m r) \cos[\varphi_m (z + 0{,}5L_ц)]; \quad (2\text{-}14)$$

$$j_z(r, z) = -\gamma \frac{\partial U^e}{\partial z} = -\sum_{m=0}^{\infty} D_m I_0(\varphi_m r) \sin[\varphi_m (z + 0{,}5L_ц)], \quad (2\text{-}15)$$

where

$$D_m = \frac{8 j_к}{L_ц \varphi_m I_1(\varphi_m R)} \sin(0{,}5\varphi_m b_к) \cos[0{,}5\varphi_m (2b_п + b_к + L_ц)];$$

$$\varphi_m = \frac{2m+1}{L_ц}\pi;$$

$I_0(\varphi_m r)$, $I_1(\varphi_m r)$ — the modified functions of Bessel of the first order.

Azimuth component $j_\varphi = 0$, since $\partial U^e/\partial\varphi = 0$. Resulting current density at each point of the armature

$$j(r, z) = \sqrt{j_r^2(r, z) + j_z^2(r, z)}. \qquad (2\text{-}16)$$

The results of the calculations [1] of the values of current density conducted according to the derived formulas are represented in Fig. 2-3b in the form of curves.

FOOTNOTE [1]. In the computer "Ural". ENDFOOTNOTE.

Page 46.

They show that with the characteristic for UM relationships/ratios of the geometric dimensions

$$b_к \approx \frac{L_я}{12} + \frac{L_я}{16};\ b_м \approx \frac{L_я}{8};\ R \approx \frac{L_я}{4}$$

the current distribution in the zone between the current pickups is close to axial-uniform. On the base of the obtained solutions it is possible to justify engineering calculation procedure UM, after taking approximately current density in the armature

$$j_p \approx \frac{I_я}{\pi R^2} = \frac{2b_к j_к}{R}.$$

This expression is used also upon consideration of the demagnetizing effect of magnetizing force of armature.

Experiments to electrolytic model confirmed the obtained output (see Chapter 10).

2.5. Electrical losses and the resistor/resistance of cylindrical armature.

Electrical power losses are caused by the passage of direct current in the armature.

During the uniform current distribution between the axes of circular current pickup the resistor/resistance of armature is determined by expression (Fig. 2-3a)

$$R_{\text{я.р}} = \frac{L}{\gamma S} = \frac{2b_{\text{п}} + b_{\text{к}}}{\gamma \pi R^2},$$

where $2b_{\text{п}}+b_{\text{к}}$ — distance between the middles of the contact surfaces of current pickup on the generatrix of armature (lengths of conductor); S - the cross section of armature (section of conductor).

Electrical losses in the armature

$$p_{\text{э.р}} = R_{\text{я.р}} I_{\text{я}}^2 = 4\pi (b_{\text{к}} j_{\text{к}})^2 \frac{2b_{\text{п}} + b_{\text{к}}}{\gamma}.$$

However, as it was shown above, current in the space of armature is distributed unevenly and, therefore, resulting expressions for determination $R_{\text{я}}$ and $p_{\text{э}}$ are not precise.

For the purpose of the refinement of the calculation of electrical losses and resistor/resistance of armature we will use the previously obtained expressions for the components of current density on coordinates r and z.

Electrical losses in the element of volume of armature can be represented by the expression

$$dp_э = \mathbf{E}\mathbf{j}dV = \frac{1}{\gamma} j^2(r, z)\, dV,$$

where j(r, z) - the resulting current density at each point of armature. Electrical losses in entire space of the armature

$$p_э = \iiint_V dp_э = \frac{1}{\gamma} \iiint_V j^2(r, z)\, dV.$$

After expressing the element of volume of armature in cylindrical coordinates dV=r dr dφdz and after taking into account (2-16), we will obtain:

$$p_э = \frac{1}{\gamma}\left[\int_0^R \int_0^{2\pi} \int_0^{L_д} j_r^2(r, z)\, r\, dr\, d\varphi\, dz + \int_0^R \int_0^{2\pi} \int_0^{L_д} j_z^2(r, z)\, r\, dr\, d\varphi\, dz\right].$$

Substituting into the latter/last expression of the value of the components of current density from (2-14) and (2-15), after integration and series/row of conversions we obtain:

$$p_э = \frac{64}{\pi^2} \frac{j_к^2}{\gamma} RL_д^2 \sum_{m=0}^{\infty} G_m \frac{I_0(\varphi_m R)}{I_1(\varphi_m R)}, \qquad (2\text{-}17)$$

where $\varphi_m = \frac{2m+1}{L_д}\pi$;

$$G_m = \left(\frac{\pi}{L_д \varphi_m}\right)^3 \sin^2\left(\varphi_m \frac{b_к}{2}\right) \cos^2\left[\frac{\varphi_m}{2}(2b_д + b_к + L_д)\right].$$

During conclusion/output (2-17) are taken into consideration the orthogonality of functions $\sin[\varphi_m(z+0{,}5L_{\text{н}})]$ and $\cos[\varphi_m(z+0{,}5L_{\text{н}})]$ on $[0,\ L_{\text{н}}/2]$, and also the relationship/ratio between the modified functions of Bessel

$$I_2(\varphi_m r) = I_0(\varphi_m r) - \frac{2}{r\varphi_m} I_1(\varphi_m r).$$

Page 48.

The refined value of the electrical resistance of the armature

$$R_{\text{я}} = \frac{p_0}{I_{\text{я}}^2} = \frac{p_0}{(2\pi R b_{\text{к}} j_{\text{к}})^2} = k_R R_{\text{я.р}}, \qquad (2\text{-}18)$$

where $k_R = \frac{p_0}{p_{0.g}} = \frac{R_{\text{я}}}{R_{\text{я.р}}} > 1$ — coefficient, which considers the increase of losses and resistor/resistance as a result of the nonuniform current distribution according to the volume of armature.

After substituting (2-17) in (2-18), we will obtain the expression of variation factor

$$k_R = \frac{16}{\pi^2} \frac{RL_{\text{н}}^2}{(2b_{\text{н}} + b_{\text{к}})\, b_{\text{к}}^2} \sum_{m=0}^{\infty} G_m \frac{I_0(\varphi_m R)}{I_1(\varphi_m R)}. \qquad (2\text{-}19)$$

in general form. Let us take $b_{\text{н}} \approx L_{\text{н}}/8$, $b_{\text{к}} \approx L_{\text{н}}/12$ ($b_{\text{к}}$ - width of movable electrode in the zone of pressing on the surface of rotor, but not the width of the moistened by liquid metal surface of current pickup).

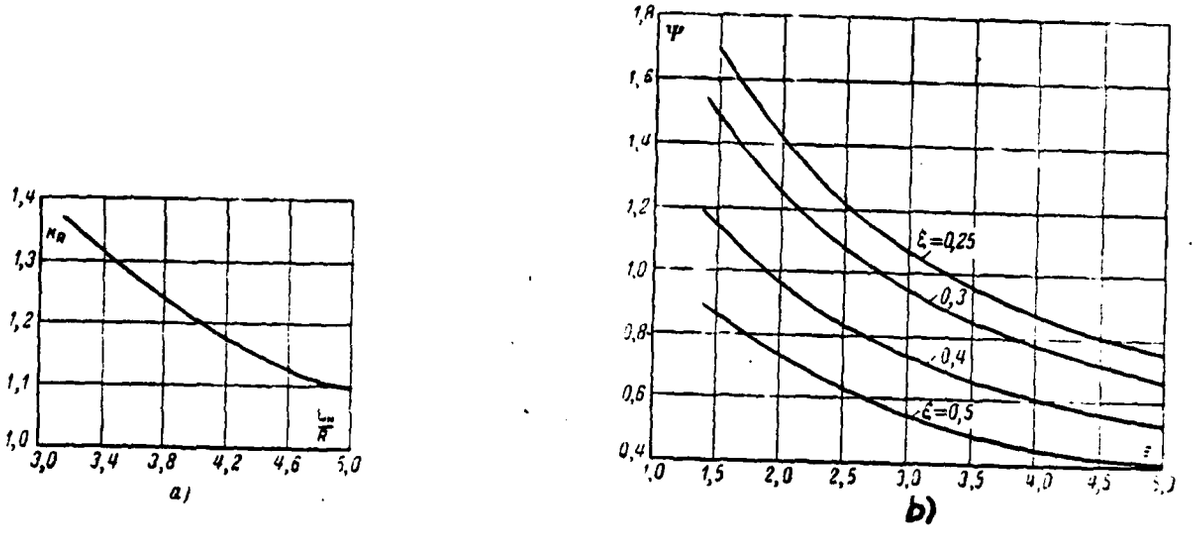

Fig. 2-4. On the calculation of the electrical resistance of armature UM. a) cylindrical; b) disk.

Page 49.

In this case

$$k_R \approx 2{,}23 \frac{R}{L_a} \sum_{m=0}^{\infty} G_m \frac{I_0(\varphi_m R)}{I_1(\varphi_m R)} = f\left(\frac{L_a}{R}\right), \qquad (2\text{-}20)$$

where

$$G_m = \frac{1}{(2m+1)^3} \sin\left(\frac{2m+1}{24}\pi\right) \cos^2\left[\frac{2(2m+1)}{3}\pi\right].$$

Expressions (2-19) and (2-20) make it possible to produce the calculation of coefficient k_R, utilized during the determination of electrical resistance $R_я$, and also drops in voltage $\Delta U_я = I_я R_я$ and losses in armature $I_я^2 R_я$.

For convenience in the calculations Fig. 2-4a gives the values of coefficient $k_R=f(L_н/R)$ with a change in the ratio of a radius of rotor to its length in in practice possible range $L_н/R\cong 3,5—5$. Values are obtained during the approximate computation according to formula (2-20), moreover relationships/ratios $b_п/L_н$ and $b_к/L_н$ remained constant/invariable. Let us note that with an increase in relation $L_н/R$ value k_R approaches one. For example, when $L_н/R\cong 10$ $k_R\approx 1,05$. With the decrease of relation $L_н/R$ coefficient k_R grows; for $L_н/R\cong 2$ $k_R\approx 1,73$.

Usually in UM of the construction/design (during the four-terminal performance) in question they choose $L_н/R\cong 4$; in this case $k_R\approx 1,2$.

The values of the Bessel functions were determined from [82], where they were tabulated.

2.6. Density distribution of current and the electrical resistance of the armature of disk machine.

The thickness of disc armature of UM is relatively small; therefore according to the adopted assumption it is possible to count current density in the disk

$$j(r)=j_r(r)=\frac{I_н}{S(r)}=\frac{I_н}{2\pi r b(r)}, \qquad (2\text{-}21)$$

where S(r) and b(r) - the sectional area of disk, normal to a radius,

and its thickness on the circle/circumference of radius r.

In the flat/plane disk the current density is reduced from the center to the periphery, since $b(r)=b_д=\text{const}$, and S(r) in this case grows.

In the conical disk (Fig. 2-2a) the thickness and the section of disk on the circle/circumference of radius r comprise respectively:

$$b(r)=b_D+(D-2r)\operatorname{tg}\alpha$$

and

$$S(r)=2\pi r[b_D+(D-2r)\operatorname{tg}\alpha],$$

where b_D — thickness of disk with r=0.5D.

Page 50.

It is easy to establish that the sectional area of the conical disk S(r) has a maximum on the height/altitude of disk, and current density has a minimum, which is determined by differentiation (2-21) respectively. ¶ Current density on the height/altitude of conical disk reaches the minimum value with

$$r=r_m=0{,}5R\left(1+\frac{b_D}{D\operatorname{tg}\alpha}\right),$$

the code

$$b(r)=b_m=0{,}5b_D\left(1+\frac{D\operatorname{tg}\alpha}{b_D}\right)$$

and

$$S(r)=S_{\text{макс}}=\frac{1}{4}S_D\left[2+\frac{b_D}{D\operatorname{tg}\alpha}+\frac{D\operatorname{tg}\alpha}{b_D}\right],$$

and it is equal to

$$j_{\text{мин}} = \frac{I_\text{п}}{S_D} 4 \left[2 + \frac{b_D}{D \operatorname{tg} \alpha} + \frac{D \operatorname{tg} \alpha}{b_D}\right]^{-1} = j_D \varphi \left(\frac{b_D}{D \operatorname{tg} \alpha}\right).$$

The analysis of latter/last expression shows that if

$$b_D / D \operatorname{tg} \alpha = 1,$$

then

$$\varphi \left(\frac{b_D}{D \operatorname{tg} \alpha}\right) = 1,$$

and current density has the minimum value

$$j_{\text{мин}} = j_D = \frac{I_\text{п}}{\pi D b_D} \quad \text{where} \quad r_m = R,\ b_m = b_D \text{ и } S_{\text{макс}} = S_D = \pi D b_D.$$

In this case the current density grows from the periphery to the center of disk.

When $\frac{b_D}{D \operatorname{tg} \alpha} \neq 1$ the current density is minimum on the circle with a radius of $r_m = 0{,}5R\left(1 + \frac{b_D}{D \operatorname{tg} \alpha}\right)$, growing to center and periphery of disk.

Degree of irregularity of current density on the height/altitude of disk can be determined, using the expression

$$\frac{j_r(r)}{j_{\text{мин}}} = \frac{2 + \frac{b_D}{D \operatorname{tg} \alpha} + \frac{D \operatorname{tg} \alpha}{b_D}}{4\overset{*}{r}\left[1 + \frac{D \operatorname{tg} \alpha}{b_D}(1 - \overset{*}{r})\right]} = f\left(\frac{b_D}{D \operatorname{tg} \alpha}\right) \text{ on } \overset{*}{r},$$

where r=r/R=2r/D.

Page 51.

The electrical resistance of the conical disk of armature UM

$$R_{\text{я}} = \int_{R_1}^{R} \frac{dr}{2\pi r b(r)\gamma} = \frac{\Psi(\epsilon, \xi)}{\gamma b_D}, \qquad (2\text{-}22)$$

where $\Psi(\epsilon, \xi) = (1-\xi)/(2\pi(\epsilon-\xi))\ln(\epsilon/\xi)$ - the function, whose values depending on the value of coefficients

$$\epsilon = \frac{b_1}{b_D} \quad \text{and} \quad \xi = \frac{D_1}{D} = \frac{R_1}{R}$$

are given for convenience in the calculation in Fig. 2-4b;

D_1 and b_1 - diameter of the current carrying shaft of UM and the thickness of disk with $r=R_1=D_1/2$.

Formula (2-22) is general/common/total: with $\epsilon=1$ it is suitable for calculating the electrical resistance of the disk of equal thickness ($b_{\text{я}}$).

A voltage drop and electrical losses in the disc armature of UM, correspondingly, will be:

$$\Delta U_{\text{я}} = R_{\text{я}} I_{\text{я}} \text{ и } p_{\text{э}} = R_{\text{я}} I_{\text{я}}^2.$$

2.7. Electromagnetic turning moments

Turning moment is formed by cumulative effect of forces of periphery $dT_э=[jB]dV$, applied to the elementary conductors of rotor.

For the disk UM with the rotor of constant thickness $b_я$ element of volume $dV=2\pi r\,dr b_я$, current density and the induction

$$j=\frac{I_я}{2\pi r b_я};\quad B=\frac{4\Phi_б}{\pi(D^2-D_я^2)},$$

where $\Phi_б$ — magnetic flux, which penetrates disk.

Integrating elementary moments/torques $dM_э=rdT_э$ in the limits of pole, we find electromagnetic turning moment:

$$M_э=\int_{D_я/2}^{D/2}\frac{4I_я\Phi_б r\,dr}{\pi(D^2-D_я^2)}=\frac{I_я\Phi_б}{2\pi}.$$

Page 52.

With a number of poles of disk machine 2p we have:

$$M_э=\frac{1}{2\pi}p\Phi_б I_я,\ \text{N·m},\qquad(2\text{-}23)$$

moreover $I_я$ is expressed in the amperes; $\Phi_б$ — in the webers; p is equal to a number of disks.

For UM with the hollow cylindrical rotor of the relatively small

thickness

$$j=\frac{4I_n}{\pi(D^2-D_1^2)};\quad B=\frac{\Phi_\delta}{2\pi rl},$$

where D and D_1 - external and inner diameters of the rotor, according to cross section of which uniform current distribution is accepted; Φ_δ and l - radial magnetic flux and the axial length of rotor, which corresponds to one pole pair. In this case M_n is expressed by the formula, analogous (2-23).

For UM with the massive cylindrical rotor product [jB] is expressed by complex function. Accepting in accordance with the engineering procedure of calculation $j=4I_n/\pi D^2$ and assuming/setting conditionally $B\cong\Phi_\delta/2\pi rl$, we also obtain a similar (2-23) formula.

Thus, expression for electromagnetic turning moment UG is identical with the same for the collector direct-current generators [7] with the number of conductors of armature, equal to one.

In more detail a question about the electromagnetic moments is examined in chapter 8, where on the base of the formulas of moments/torques is constructed calculation UD.

Page 53.

Chapter Three.

MAGNETIC LEAKAGE AND SPECIAL FEATURES OF THE CALCULATION OF THE MAGNETIC CIRCUIT OF UNIPOLAR MACHINES WITH IDLING.

3.1. Equivalent replacement schemes of the magnetic circuit of cylindrical ones mind with the solid rotor.

Let us consider two-pole UM[unipolar machine], the conditional location of magnetic fluxes in which is represented in Fig. 3-1a. In the general case, besides the flow of mutual induction Φ_{δ} passing through working gaps, are leakage fluxes in the field coil $\Phi_{\sigma 1}$, $\Phi_{\sigma 2}$ and between the external surfaces of magnetic circuit $\Phi_{\sigma 3}$. Flow $\Phi_{\sigma 2}$, engaged with all turns of excitation winding, is created by its complete n. s. [magnetizing force]. The magnetizing force, which creates flow $\Phi_{\sigma 1}$, is changed for separate field tubes in the dependence on a radius of the layer of the turns of coil. In the particular case during the location of current pickups of UM shown in Fig. 3-1b, Ψ_{σ} is not

leakage flux. It induces in the end-type part of the armature supplementary emf, which coincides in the direction with fundamental emf of pole.

The location of leakage fluxes in the multipole cylindrical UM is shown in Fig. 3-1c, d. The presence of flow Φ_{s3} leads to certain magnetic asymmetry of extreme and average/mean poles. For average/mean poles Φ_{s3} it is useful flow. In the UM with even number of pole pairs (p=2, 4, 6 ...) flow Φ_{s3} will be more than that in the UM with the odd number of pole pairs (p=1, 3, 5 ...), since in the first case, other conditions being equal, this flow meets with smaller reluctance on its path.

Page 54.

The structure of the equivalent replacement schemes of magnetic circuit, which corresponds to magnetic flux distribution accepted, it is shown in Fig. 3-2a, b. Here Λ_1 and Λ_2 are the given permeance of scattering respectively for flows Φ_{s1} and Φ_{s2}, that correspond to one pole pair; Λ_3 and Λ_4 — given permeance of scattering for flow Φ_{s3} and permeance of working gap, that correspond to one pole. During the construction of diagrams it is conditionally accepted that n. s. of excitation during the assigned mode of operation F_δ is concentrated on the stator in the plane of the symmetry of the pole pair, which

AD-A139 778 UNIPOLAR ELECTRIC MACHINES WITH LIQUID-METAL CURRENT PICKUP(U) FOREIGN TECHNOLOGY DIV WRIGHT-PATTERSON AFB OH A I BETTINOV ET AL. 08 MAR 84 FTD-ID(RS)T-1205-83 2/6

UNCLASSIFIED F/G 9/3 NL

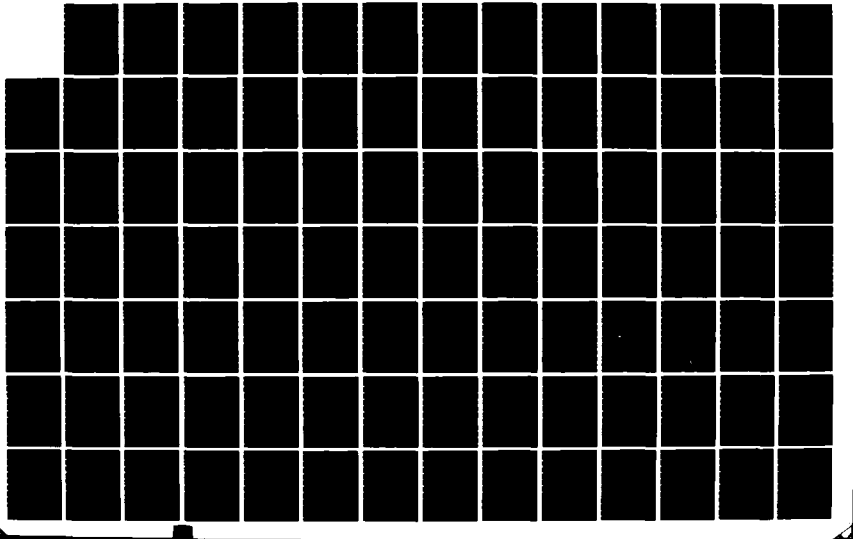

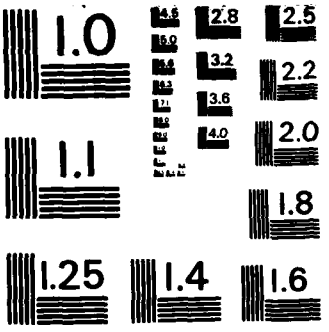

MICROCOPY RESOLUTION TEST CHART
NATIONAL BUREAU OF STANDARDS - 1963 - A

passes perpendicularly to the rotational axis of machine. Theoretical (taking into account the distribution of the n. s.) conductivity Λ_1, conductivity Λ_2 and series-connected in pairs conductivities Λ_3 and Λ_4 (Fig. 3-2a and b) are carried out to the clamps of source n. s. Allowed in this case errors, caused by a drop in the magnetic potential in steel (taking into account saturation by armature field of rotor F_p and stator F_c can be taken into account by the coefficients

$$k_1 = \frac{F_\delta - F_c}{F_\delta} = 1 - \frac{F_c}{F_\delta};$$

$$k_2 = \frac{F_\delta - F_c - F_p}{F_\delta} = \frac{k_\delta F_\delta}{F_\delta},$$

where F_δ - drop in the magnetic potential in the working gaps;

$k_\delta > 1$ - coefficient, which considers a drop in the magnetic potential in the structural/design gaps of machine.

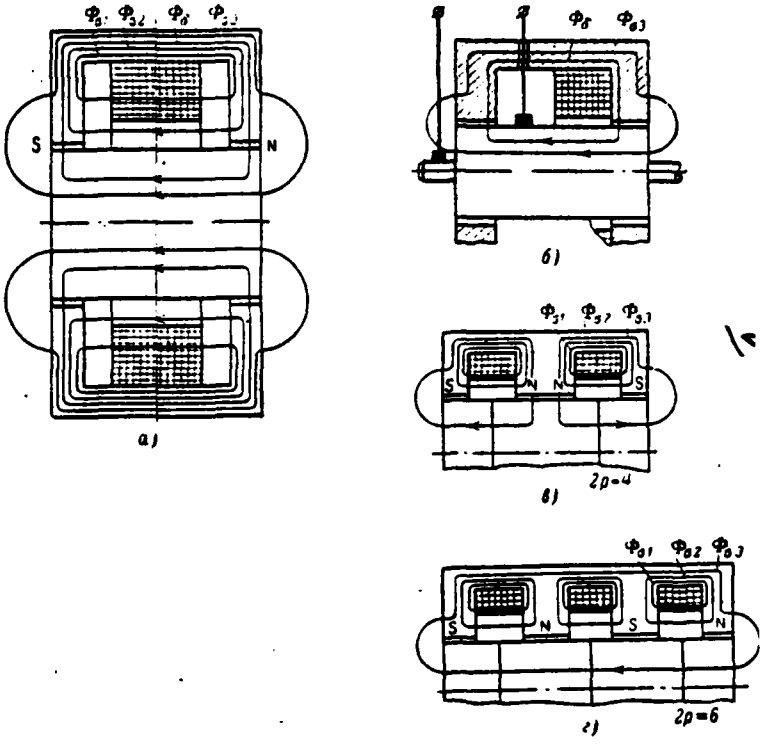

Fig. 3-1. Location of magnetic fluxes of UM with the massive cylindrical rotor. a, b) for the bipolar machine; c) for the multipole with even number of pole pairs; d) for the multipole with the odd number of pole pairs.

Page 55.

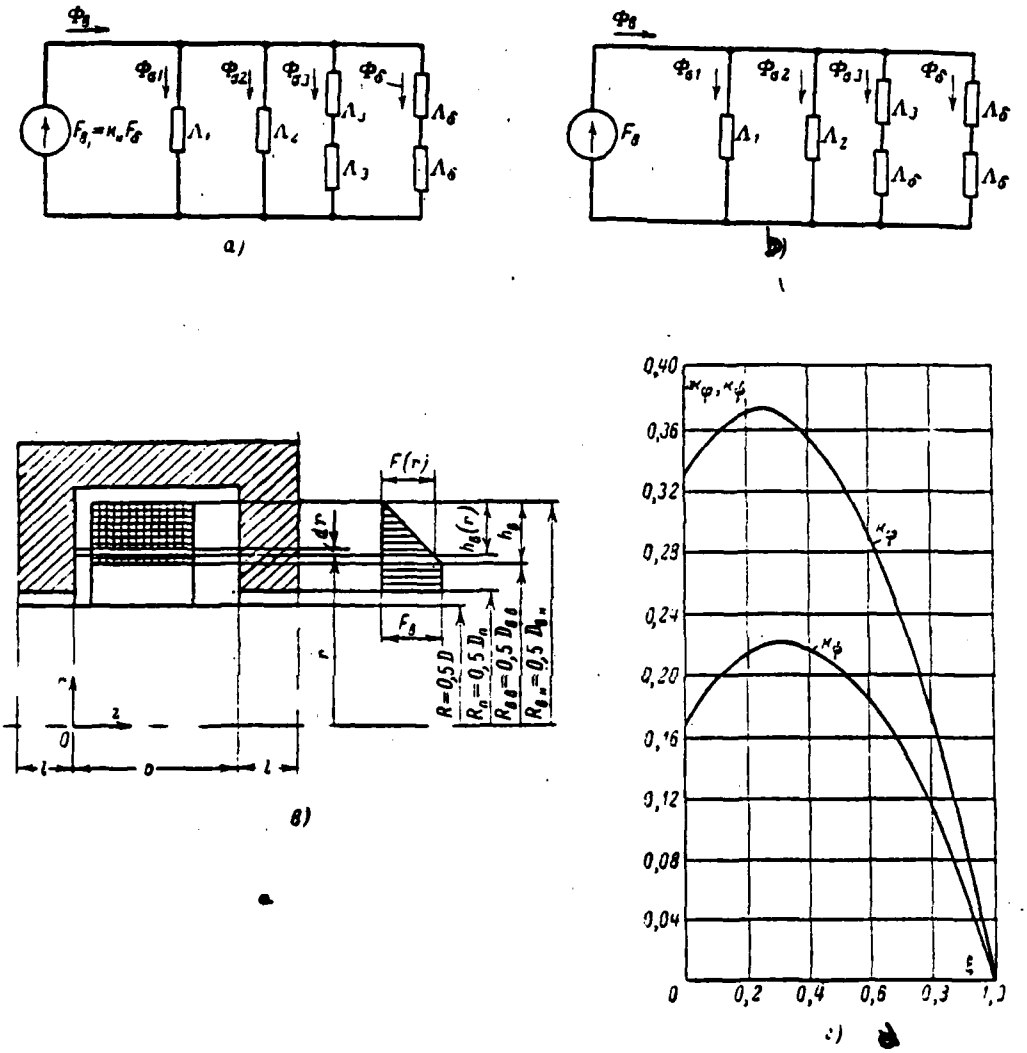

Fig. 3-2. Illustration to the calculation of magnetic circuit of UM with the massive cylindrical rotor. a) the equivalent diagram of the magnetic circuit of two-pole UM (or the circuits of the extreme poles of multipole of UM with the odd number of pole pairs); b) the equivalent diagram of the magnetic circuit of multipole UM with even

number of pole pairs; c) illustration to the calculation of permeance and flows of scattering rectangular circular field coil; d) plotted functions $\lambda_\delta = f(\delta)$ and $\lambda_\varphi = f(\delta)$.

Page 56.

3.2. Calculation of permeance and leakage fluxes the excitation windings of cylindrical ones mind with the solid rotor.

For simplification in the calculation let us take the following assumptions.

1. Flux lines $\Phi_{\sigma 1}$ and $\Phi_{\sigma 2}$ are directed in parallel to the rotational axis of machine and are normal toward the end-type walls of the turning of stator.

2. The material of the conductors of winding is nonmagnetic.

3. Magnetizing force of excitation $F_в$ evenly distributed over the cross section of coil.

Let us consider the general case of the location of rectangular coil (Fig. 3-2c). Should be distinguished the values of permeance of scattering excitation winding in the steady-state and transient

conditions. During the calculation of magnetic circuit it is necessary to consider the true flow value $\Phi_\sigma = \Phi_{\sigma 1} + \Phi_{\sigma 2}$ of scattering winding. In this case theoretical conductivity Λ_1 must be calculated from flow $\Phi_{\sigma 1}$. In transient conditions the inducing action of leakage flux has a value; therefore $\Lambda_{1\Phi}$ it is necessary to calculate from the average/mean flux linkage of the turn of winding. Conductivity determined thus is used during the calculation of inductance and time constant excitation winding. Since flow $\Phi_{\sigma 2}$ is engaged with all turns of winding, the value of conductivity Λ_2 will be identical both for that being steady and the transient conditions of work of the UM.

Conductivity $\Lambda_{0\Phi} = \Lambda_{1\Phi} + \Lambda_2$ on the flux linkage can be determined, using expression for the magnetic energy H in cylindrical coordinates r, φ, z.

Magnetic energy in volume element dV

$$dW = \frac{B(r)H(r)}{2}dV = \mu_0 \frac{H^2(r)}{2}dV,$$

where volume element in cylindrical coordinates

$$dV = r\,dr\,d\varphi\,dz; \quad B(r) = \mu_0 H(r)$$

and

$$\mu_0 = 0{,}4\pi \cdot 10^{-6}, \ \text{H/m}.$$

Magnetic field energy in the space in question will be represented by the expression

$$W=\frac{\mu_0}{2}\iiint_V H^2(r)\,dV=\frac{\mu_0}{2}\int_{r_1}^{r_2}\int_0^{2\pi}\int_0^{b} H^2(r)\,r\,dr\,d\varphi\,dz, \qquad (3\text{-}1)$$

moreover in accordance with the adopted designations of geometric dimensions (Fig. 3-2c)

$r_1=R_{в.в}$ (1) и $r_2=R_{в.н}$ (2) при расчете $\Lambda_{1\phi}$;
$r_1=R_н$ и $r_2=R_{в.в}$ при расчете Λ_2.

Key: (1). and. (2). with calculation.

According to the adopted assumptions for n. s. F(r) on the circle/circumference of the arbitrary radius r is correct

$$\oint_l \mathbf{H}(r)\,d\mathbf{l}\approx\int_0^b H(r)\,dz=H(r)\,b\approx F(r). \qquad (3\text{-}2)$$

In accordance with (3-2), after taking into account diagram n. s. (Fig. 3-2c), let us determine the strength of field on the circle/circumference of radius r:

$$H(r)=\frac{F(r)}{b}=\frac{F_в}{b}\,\frac{R_{в.в}-r}{R_{в.в}-R_{в.в}}=\frac{F_в}{b}\,\frac{\overline{h_в(r)}}{h_в}, \qquad (3\text{-}3)$$

which we use during calculation $\Lambda_{1\phi}$.

During the determination of Λ_2 the intensity/strength of the field

$$H(r)=\frac{F_в}{b}=\text{const}.$$

Let us note that with the nonrectangular form of the section of coil $F(r) = (\alpha + \beta r^{\gamma}) F_{\text{п}}$, where α, β and γ - constants, which depend on location and layout of coil.

Producing the integration of expression (3-1) taking into account (3-3) and relationships/ratios $W = \frac{1}{2} F_{\text{п}}^2 \Lambda_{\phi}$, we find:

$$\left.\begin{aligned} \Lambda_{1\phi} &\approx \frac{D_{\text{в.н}}^2}{b} k_{\phi}(\xi)\, 10^{-6},\ \overset{(1)}{\text{ом·сек}}; \\ \Lambda_{2\phi} &\approx \frac{D_{\text{в.н}}^2}{b} (\xi^2 - \varkappa^2)\, 10^{-6},\ \overset{(1)}{\text{ом·сек}}, \end{aligned}\right\} \qquad (3\text{-}4)$$

Key: (1). Ω·s.

where

$$D_{\text{в.н}} = 2R_{\text{в.н}};\quad \xi = \frac{D_{\text{в.в}}}{D_{\text{в.н}}};\quad D_{\text{в.в}} = 2R_{\text{в.в}};$$

$$\pi^2 \approx 10;\quad \varkappa = \frac{D_{\text{п}}}{D_{\text{в.н}}};\quad k_{\phi}(\xi) = \frac{1}{0}(1 + 2\xi - 3\xi^2).$$

Page 58.

As can be seen from (3-4), $\Lambda_{2\phi}$ coincides with real permeance:

$$\Lambda_{\text{п}} = \frac{\mu_0}{b} \int_{R_{\text{п}}}^{R_{\text{в.в}}} 2\pi r\, dr = \frac{\pi\mu_0}{4b}(D_{\text{в.в}}^2 - D_{\text{п}}^2) \approx \frac{D_{\text{в.н}}^2 10^{-6}}{b}(\xi^2 - \varkappa^2),\ \overset{(1)}{\text{ом·сек}}. \qquad (3\text{-}5)$$

Key: (1). Ω·s.

The admittance of scattering on the flux linkage and the inductance of excitation winding

$$\Lambda_{0\phi} = \frac{D_{в.н}^2}{6b}(1 + 2\xi + 3\xi^2 - 6\varkappa^2)\cdot 10^{-6},\ {}^{(1)}_{ом\cdot сек}; \qquad (3\text{-}6)$$

$$L_в = w_в^2 \Lambda_{0\phi},\ {}^{(2)}_{гн},$$

Key: (1). Ω·s. (2). H.

where $w_в$ - number of turns in the coil.

Conductivity $\Lambda_{1\phi}$ can be determined also, integrating the value of the flux linkage of stray field in the limits of the coil

$$\Psi_1 = \int_{R_{в.в}}^{R_{в.н}} d\Psi_1(r) = \frac{I_в w_в^2 D_{в.н}^2 \cdot 10^{-6}}{b} \frac{1 + 2\xi - 3\xi^2}{6};$$

$$\Psi_1 / I_в = L_1 = w_в^2 \Lambda_{1\phi},$$

where $I_в$ — field current, a; L_1 - inductance, H.

Let us calculate permeance $\Lambda_в = \Lambda_1 + \Lambda_2$ from the leakage flux $\Phi_{в0}$. Magnetic conductivity and the flow of elementary field tube

$$d\Lambda_1 = \frac{2\pi\mu_0 r\, dr}{b};\quad d\Phi_{в1} = F(r)\, d\Lambda_1 = \frac{2\pi\mu_0 F_в (D_{в.н} - 2r)}{b(D_{в.н} - D_{в.в})} r\, dr. \qquad (3\text{-}7)$$

Integrating (3-7) in the limits of coil, we find:

$$\Phi_{в1} = \frac{2\pi\mu_0 F_в}{b(D_{в.н} - D_{в.в})} \int_{R_{в.в}}^{R_{в.н}} (D_{в.н} - 2r) r\, dr = \frac{F_в D_{в.н}^2 10^{-6}}{3b}(1 - \xi - 2\xi^2),\ {}^{(1)}_{вб}, \qquad (3\text{-}8)$$

Key: (1). Wb.

moreover it is accepted that $\pi^2 \approx 10$. Since $\Phi_{в1} = F_в \Lambda_1$, the calculated according to the flow value conductivity

$$\Lambda_1 = \frac{D_{в.н}^2}{b} k_\phi(\xi)\cdot 10^{-6};\quad k_\phi(\xi) = \frac{1 + \xi - 2\xi^2}{3}. \qquad (3\text{-}9)$$

Magnetic flux $\Phi_{\sigma 2} = F_\delta \Lambda_2$; Λ_2 is determined from (3-5). Complete permeance and the total leakage flux of excitation winding

$$\Lambda_\sigma = \frac{D^2_{\text{в.н}}}{b}(k_\varphi + \xi^2 - \varkappa^2)\cdot 10^{-6};$$

$$\Phi_{\sigma 0} = \frac{F_\delta D^2_{\text{в.н}}\cdot 10^{-6}}{3b}(1 + \xi - \xi^2 - \varkappa^2).$$

Taking into account coefficient k_1: $\Lambda'_\sigma = k_1\Lambda_\sigma$; $\Phi'_{\sigma 0} = k_1\Phi_{\sigma 0}$.

On the basis (3-4) and (3-9) we obtain the equality

$$\frac{\Lambda_1}{\Lambda_{1\phi}} = \frac{k_\varphi(\xi)}{k_\phi(\xi)},$$

which characterizes the relationship/ratio of the values of real leakage flux and equivalent on its inducing action magnetic flux within limits of doughnut coil with evenly distributed over its cross section n. s. Research of functions $k_\varphi = f(\xi)$ and $k_\phi = f(\xi)$ shows that $k_\varphi = k_{\varphi\,\text{макс}} = \frac{3}{8}$ when $\xi = \frac{1}{4}$; $k_\phi = k_{\phi\,\text{макс}} = \frac{1}{6}$ with $\xi = 1/3$. True leakage flux is more than equivalent on the inducing action, which is caused by a difference in the flux linkages of the separate turns of distributed winding. For convenience in the calculations graphs/curves $k_\varphi(\xi)$ and $k_\phi(\xi)$ are represented in Fig. 3-2d.

3.3. Calculation of conductivity and leakage flux between the surfaces of the magnetic circuit.

The calculation of conductivity Λ_δ between faces of stator-rotor

unit is carried out by the method of the possible (expected) paths of magnetic flux [83].

In the general case face of stator can be implemented by conical for facilitating the weight of inductor (Fig. 3-3).

Page 60.

As a result of calculation in accordance with the designations of geometric dimensions, given in Fig. 3-3, it is obtained:

a) with $\frac{D_a - D_a}{2\cos\theta} < \frac{D}{2}$

$$\Lambda_\delta \approx (D+\delta)\left[10^{-6} + \frac{\pi\mu_0}{\pi+\theta}\ln\left(1+\frac{2}{\cos\theta}+\frac{D_a-D}{\delta\cos\theta}\right)\right]; \quad (3\text{-}10)$$

b) with $\frac{D_a - D_a}{2\cos\theta} \geqslant \frac{D}{2}$

$$\Lambda_\delta \approx (D+\delta)\left[10^{-6} + \frac{\pi\mu_0}{\pi+\theta}\ln\left(1+\frac{D}{\delta}\right)\right]. \quad (3\text{-}11)$$

In the case of flat/plane faces of inductor in (3-10) and (3-11) one should take $\theta=0$. Knowing values of Λ_δ in the replacement schemes, depicted in Fig. 3-2a, b, we find flow value $\Phi_{\sigma\delta}$.

For the machines with odd p

$$\overline{\Phi_{\sigma\delta}} = \frac{1}{2} F_\delta \Lambda_\delta;$$

for the machines with even p

$$\Phi_{\sigma\delta} = F_\delta \frac{\Lambda_\delta \cdot \Lambda_\delta}{\Lambda_\delta + \Lambda_\delta},$$

where permeance of gap under the pole

$$\Lambda_\delta = \frac{2\pi\mu_0 l}{\int_{D/2}^{D/2+\delta} \frac{dr}{r}} \approx \frac{8\cdot 10^{-9} l}{\ln\left(1+\frac{2\delta}{D}\right)}, \text{ (1) } \text{ом}\cdot\text{сек};$$

Key: (1). Ω·s.

l - axial length of pole, m.

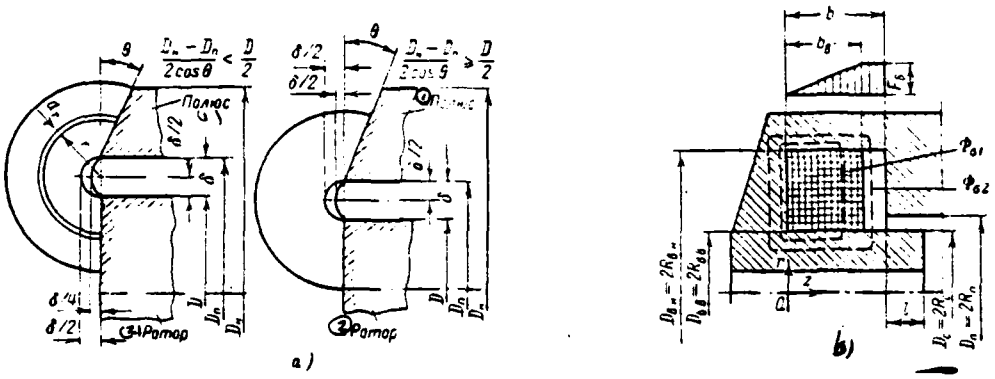

Fig. 3-3. Illustration to the calculation of conductivity Λ_δ and coefficient of scattering k_δ. a) to the calculation of conductivity between faces of UM; b) to the calculation of coefficient of scattering of UM with the hollow rotor.

Key: (1). Pole. (2). Rotor.

Page 61.

Usually $\delta << D$; therefore Λ_δ it is possible to compute according to the simpler formula

$$\Lambda_\delta \cong \frac{4 \cdot 10^{-9} Dl}{\delta}, \text{ ом·сек.} \quad (1)$$

Key: (1). Ω·s.

Taking into account a potential drop in steel

$$\Lambda'_\delta = k_2 \Lambda_\delta; \quad \Lambda'_\delta = k_2 \Lambda_\delta.$$

Computing Λ_δ for multipolar machines with odd p, coefficient k_2

should be determined according to the expression

$$k'_2 \cong \frac{F_\delta - p(F_c + F_p)}{F_\delta},$$

moreover F_δ — isthe n. s. of one coil, since n. s. of the remaining (p-1) coils, included by the duct/contour of flux line $\Phi_{\sigma 3}$, average out. Let us note that if the extreme poles of multipole UM with even p are not used on the voltage/stress, then $\Phi_{\sigma 3}$ is not the leakage flux for it.

3.4. Coefficient of scattering mind with the massive cylindrical rotor.

Magnetic flux in "neutral" (taken plane of the location of source n. s.) of the inductor

$$\Phi_\delta = \Phi_\delta + \Phi_\sigma,$$

where $\Phi_\sigma = \Phi_{\sigma 0} + \Phi_{\sigma 3}$ - leakage flux. Coefficient of scattering for the inductor (stator)

$$k_{\sigma c} = \frac{\Phi_\delta}{\Phi_\delta} = 1 + \sigma_0,$$

moreover $\sigma_0 = \frac{\Phi_\sigma}{\Phi_\delta}$ it is possible to express through permeance.

Page 62.

In accordance with the replacement scheme, represented in Fig. 3-2a,

$$\Phi_\delta = \frac{1}{2} F_\delta \Lambda_\delta;$$

for the machines with odd p

$$\Phi_\sigma = F_\delta (\Lambda_1 + \Lambda_2 + 0{,}5\Lambda_3);$$

for the machines with even p

$$\Phi_\sigma = F_3(\Lambda_1 + \Lambda_2 + \Lambda_3);\ \Lambda_3 = \frac{\Lambda_4\Lambda_5}{\Lambda_4+\Lambda_5}.$$

In this case, after introducing the relative values of the conductivities

$$\overset{*}{\Lambda}_5 = 1;\ \overset{*}{\Lambda}_i = \frac{\Lambda_i}{\Lambda_5},\ (i = 1, 2, 3);\ \overset{*}{\Lambda}_3 = \frac{\Lambda_3}{\Lambda_5},$$

we will obtain:

$$\sigma_c\big|_{p=1,3,5\ldots} = 2(\overset{*}{\Lambda}_1 + \overset{*}{\Lambda}_2) + \overset{*}{\Lambda}_3;\ \sigma_c\big|_{p=2,4,6\ldots} = 2(\overset{*}{\Lambda}_1 + \overset{*}{\Lambda}_2 + \overset{*}{\Lambda}_3).$$

Thus,

$$k_{\sigma c} = 1 + \overset{*}{\Lambda}_\sigma, \qquad (3\text{-}12)$$

where $\overset{*}{\Lambda}_\sigma = \sigma_\sigma$ - relative conductivity of scattering.

Magnetic flux in rotor $\Phi_p = \Phi_\delta + \Phi_{\sigma 3}$. It is similar to previous, coefficient of scattering for the rotor

$$k_{\sigma p} = 1 + \overset{*}{\Lambda}_3 \ (\overset{(1)}{\text{при}}\ \text{нечетном}\ p);$$
$$k_{\sigma p} = 1 + \overset{*}{\Lambda}_3 \ (\overset{(2)}{\text{при}}\ \text{четном}\ p).$$

Key: (1). with odd p. (2). with even p.

3.5. Magnetic flux, conductivities and coefficient of scattering mind with the hollow cylindrical rotor.

During the calculation of UM with the hollow rotor let us take into account the leakage flux of excitation winding $\Phi_\sigma = \Phi_{\sigma 1} + \Phi_{\sigma 2}$, which

corresponds to one pole pair.

Page 63.

After taking in accordance with the special features/peculiarities of the magnetic system of machine the radial direction of flux line (Fig. 3-3b), we will obtain:

$$\Phi_{\sigma 1}=\int_0^{b_в}\frac{F_в z\,dz}{\int_{\frac{D_{в.н}}{2}}^{b_в}\frac{dr}{2\pi\mu_0 r}}=\frac{\pi\mu_0 b_в F_в}{\ln\frac{D_{в.н}}{D_{в.в}}}, \qquad (3\text{-}13)$$

$$\Phi_{\sigma 2}=\int_{\frac{D_{в.в}}{2}}^{\frac{D_{в.н}}{2}}F_в\,d\Lambda_z=\frac{F_в}{\int_{\frac{D_{в.в}}{2}}^{\frac{D_{в.н}}{2}}\frac{dr}{2\pi\mu_0(b-b_в)r}}=\frac{2\pi\mu_0(b-b_в)F_в}{\ln\frac{D_{в.н}}{D_{в.в}}}, \qquad (3\text{-}14)$$

$$\Phi_\sigma=\frac{2\pi\mu_0 b_в F_в}{\ln\frac{D_{в.н}}{D_{в.в}}}(1-0{,}5\beta)\approx\frac{b_в F_в\cdot 10^{-6}}{\ln\frac{D_{в.н}}{D_{в.в}}}(8-4\beta),\ (1)\ вб, \qquad (3\text{-}15)$$

Key: (1). Wb.

where b, $b_в$, $D_{в.н}$, $D_{в.в}$ - geometric dimensions in accordance with Fig. 3-3b, m;

$\beta=b/b_в$;

$F_в$ - n. s. of the field coil.

Since $\Phi_{el} = F_{в}\Lambda_{1}$, the theoretical conductivity, designed along this flow, on the basis (3-13) for UM with the hollow rotor

$$\Lambda_1 = \frac{\pi\mu_0 b_{в}}{\ln\frac{1}{\xi}},$$

where

$$\xi = \frac{D_{в.в}}{D_{в.н}} < 1.$$

Conductivity $\Lambda_{1\psi}$ on the flux linkage is determined with the help of the magnetic energy

$$W = \frac{1}{2\mu_0}\int\limits_{R_{в.в}}^{R_{в.н}}\int\limits_{0}^{2\pi}\int\limits_{0}^{b_{в}} B^2(r, z)\, r\, dr\, d\varphi\, dz =$$

$$= \frac{\pi}{\mu_0}\int\limits_{R_{в.в}}^{R_{в.н}}\int\limits_{0}^{b_{в}} B^2(r, z)\, r\, dr\, dz.$$

Page 64.

Magnetic flux of elementary field tube

$$d\Phi = B\, dS = 2\pi B r\, dz,$$

whence

$$B = \frac{d\Phi}{2\pi r\, dz}.$$

On the other hand,

$$d\Phi = F(z)\, d\Lambda = \frac{F_{в} z}{b_{в}\frac{dr}{2\pi\mu_0 r\, dz}},$$

consequently,

$$B(r, z) = \frac{F_{в} z}{2\pi b_{в} r\, dz\frac{dr}{2\pi\mu_0 r\, dz}}$$

and

$$B^2(r, z) = \frac{\mu_0^2 F_{в}^2 z^2}{b_{в}^2 (dr)^2}.$$

Thus,

$$W=\frac{\pi}{\mu_0}\int_0^{b_\delta}\frac{\mu_0^2F_\delta^2z^2dz}{b_\delta^2\int_{R_{\delta.\delta}}^{R_{\delta.\delta}}\frac{dr}{r}}=\frac{\pi\mu_0F_\delta^2b_\delta}{3\ln\frac{R_{\delta.\delta}}{R_{\delta.\delta}}}.$$

Taking into account expression $W=\frac{1}{2}F_\delta^2\Lambda_{1\phi}$, let us find the conductivity

$$\Lambda_{1\phi}=\frac{2\pi\mu_0b_\delta}{3\ln\frac{1}{\xi}},$$

where

$$\xi=\frac{D_{\delta.\delta}}{D_{\delta.\delta}}<1;\ D_{\delta.\delta}=2R_{\delta.\delta};\ D_{\delta.\delta}=2R_{\delta.\delta}.$$

Page 65.

Conductivity $\Lambda_{1\phi}$ can be, as this was done above for the cylindrical machine with the solid rotor, determined by the integration of the elements/cells of the flux linkage of stray field in the limits of field coil:

$$d\Psi_1=w_\delta(z)\,d\Phi=\frac{w_\delta z}{b_\delta}\frac{F_\delta z}{b_\delta\frac{dr}{2\pi\mu_0r\,dz}},$$

where $F_\delta=I_\delta w_\delta$ - n. s. of excitation UM with the hollow rotor.

Since

$$\Psi_1=\int_0^{b_\delta}\frac{I_\delta w_\delta^2z^2dz}{b_\delta^2\int_{R_{\delta.\delta}}^{R_{\delta.\delta}}\frac{dr}{2\pi\mu_0r}}=\frac{I_\delta w_\delta^2b_\delta}{\frac{3}{2\pi\mu_0}\ln\frac{R_{\delta.\delta}}{R_{\delta.\delta}}}$$

and

$$\Psi_1/I_\delta=L_1=w_\delta^2\Lambda_{1\phi},$$

that as a result we obtain:

$$\Lambda_{1\phi}=\frac{2\pi\mu_0 b_\delta}{3\ln\frac{1}{\zeta}},$$

which coincides with the expression, caused by energy of stray field.

From that presented it is evident that for the UM with the hollow cylindrical rotor is correct the relationship/ratio:

$$\frac{\Lambda_1}{\Lambda_{1\phi}}=1{,}5.$$

Permeance for flow $\Phi_{\sigma 2}$ comprises

$$\Lambda_2=\frac{1}{\int\limits_{R_{2.1}}^{R_{2.2}}\frac{dr}{2\pi\mu_0(b-b_\delta)r}}=\frac{2\pi\mu_0(b-b_\delta)}{\ln\frac{1}{\xi}}.$$

Page 66.

Coefficient of scattering field coil

$$k_\sigma=1+\frac{\Phi_\sigma}{\Phi_\delta}=1+\frac{\Lambda_1+\Lambda_2}{\Lambda_\delta},$$

where $\Phi_\delta=F_\delta\Lambda_\delta$ and Λ_δ - magnetic flux in the working gap and permeance of the nonmagnetic gap/interval between the pole and the internal magnetic circuit of stator of UM.

Assuming hollow rotor nonmagnetic, it is possible in accordance with the designations of sizes/dimensions, given in Fig. 3-3b, to obtain:

$$\Lambda_\delta\approx\frac{2\pi\mu_0 l}{\int\limits_{R_c}^{R_a}\frac{dr}{r}}=\frac{2\pi\mu_0 l}{\ln\frac{R_a}{R_c}}.$$

With the hollow magnetic rotor

$$\Lambda_\delta = \frac{2\pi\mu_0 l}{\ln\left(1+\frac{\delta+\delta_1}{R_c}\right)},$$

where δ and δ_1 are the working and additional gaps.

After introducing relative units, let us find:

$$k_c = 1 + \mathring{\Lambda}_1 + \mathring{\Lambda}_2, \quad \mathring{\Lambda}_i = \frac{\Lambda_i}{\Lambda_\delta}, \quad i = 1, 2.$$

3.6. Permeance and the leakage fluxes of disk machines.

Magnetic flux distribution and designation of the sizes/dimensions of two-pole UM with the conical nonmagnetic rotor are shown in Fig. 3-4a. The direction of leakage fluxes $\Phi_{\sigma 1}$ and $\Phi_{\sigma 2}$ is accepted by the parallel to the direction of working flow Φ_δ.

Leakage flux $\Phi_{\sigma 2}$ should be considered only for the machines with the ferromagnetic shafts; for the simplification into the calculation we will accept only its part in the limits of length l_1 out of the zone between the current pickups. Within this zone in the shaft of machine from flow $\Phi_{\sigma 2}$ emf, which coincides in the direction with emf of the disk of the armature, is induced.

Page 67.

Each pole pair of multipolar machine has the similar pattern of

scattering. The structure of the replacement scheme of magnetic circuit disk type of UM is similar to the structure of the diagram, given in Fig. 3-2a. In the UM with the nonmagnetic disk coefficients k_1 and k_2 are close to one

$$k_1 = k_2 = \frac{F_\delta - F_c}{F_\delta} = \frac{k_\sigma F_\delta}{F_\delta} \cong 1{,}1 \div 1{,}15,$$

since nonmagnetic space between the poles is relatively great and $F_\delta \gg F_c$.

Conductivities $\Lambda_{1\phi}$ and Λ_1, taking into account the designations of the sizes/dimensions of Fig. 3-4a are expressed by the formulas analogous (3-4) and (3-9).

The conductivity $$\Lambda_2 = \frac{D_{\text{в.н}}^2 \cdot 10^{-8}}{c} (\xi^2 - \varkappa^2);$$

$$\xi = \frac{D_{\text{в.в}}}{D_{\text{в.н}}};\ \varkappa = \frac{D}{D_{\text{в.н}}},$$

moreover in the particular case when $D_{\text{в.в}} = D$ it will be $\varkappa = \xi$ and $\Lambda_2 = 0$.

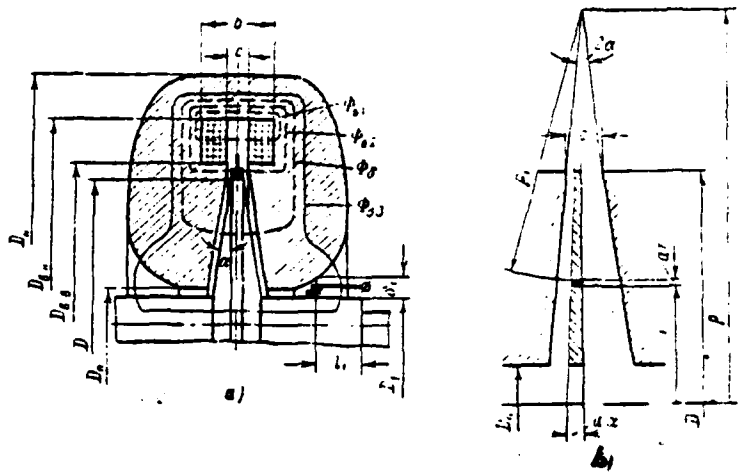

Fig. 3-4. Illustrations to the calculation of the magnetic circuit of disk of UM. a) the magnetic fluxes of disk of UM with conical nonmagnetic rotor; b) to the calculation of permeance of the interpolar space of disk of the UM.

Page 68.

Admittance and the leakage flux of excitation winding

$$\left.\begin{aligned} \Lambda_0 = \Lambda_1 + \Lambda_2 = \frac{D_{a.H}^2}{b}\left[k_\varphi(\xi) + \beta(\xi^3 - x^3)\right] 10^{-6}; \\ \beta = \frac{b}{c}; \\ \Phi_{\sigma 0} = F_2 \Lambda_0. \end{aligned}\right\} \qquad (3\text{-}16)$$

The conductivity Λ_1, which corresponds to one pole, is determined according to the method of the expected magnetic paths in accordance with Fig. 3-4a.

$$\Lambda_3 \approx 2D_1\left(1+\frac{2}{\theta_1}\ln\frac{1+\frac{l_1}{\delta_1}\operatorname{tg}\theta_1}{1+\operatorname{tg}\theta_1}\right)10^{-6},\ \text{ом}\cdot\text{сек}. \quad (3\text{-}17)$$

(1)

Key: (1). Ω·s.

During conclusion/output (3-17) it is accepted that the surface of the pole of magnetic circuit, converted to the shaft, in the limits of length l_1 is conical. Leakage flux $\Phi_{a3}=0{,}5F_\delta\Lambda_3$.

The permeance of interpolar space mind with the nonmagnetic disk of the equal thickness

$$\Lambda_\delta=\int_{0.5D_\text{п}}^{0.5D}\frac{2\pi\mu_0 r\,dr}{c}=\frac{\pi\mu_0(D^2-D_\text{п}^2)}{4c}\cong\frac{D^2-D_\text{п}^2}{c}10^{-6},\ \text{ом}\cdot\text{сек}, \quad (3\text{-}18)$$

(1)

Key: (1). Ω·s.

where D, $D_\text{п}$ - diameters of pole;

$c=2\delta+b_\text{п}$ - distance between the poles;

δ and $b_\text{п}$ - one-sided gap and the thickness of disk;

$\mu_0=0{,}4\pi\cdot10^{-6}$ (1) гн/м; $\pi^2\approx10$.

Key: (1). H/m.

In accordance with the designations of sizes/dimensions, given in Fig. 3-4b, the reluctance of interpolar space of the UM with the

conical nonmagnetic disk

$$R_\delta = \int_0^{2\alpha} \frac{d\alpha}{\dfrac{0{,}5D}{2\pi\mu_0 \int_{0{,}5D_\text{ш}} \frac{r\,dr}{\rho - r}}} = \frac{\alpha}{\dfrac{0{,}5D}{\pi\mu_0 \int_{0{,}5D_\text{ш}} \frac{r\,dr}{\rho - r}}},$$

where

$$\rho = 0{,}5\left(D + \frac{c}{\operatorname{tg}\alpha}\right);\quad \rho - r = \rho_1.$$

Page 69.

Permeance of space between the poles

$$\Lambda_\delta = \frac{1}{R_\delta} = \frac{\pi\mu_0}{\alpha}\left(\rho \ln \frac{2\rho - D_\text{ш}}{2\rho - D} - \frac{D - D_\text{ш}}{2}\right). \qquad (3\text{-}19)$$

Conductivity $\bar{\Lambda}_\delta$ can be calculated also from the simplified approximation formula. If we take the average distance between conical poles $l_{\text{ср}} = 2a\rho_{1\text{ср}} = a\left(\frac{D - D_\text{ш}}{2} - \frac{c}{\operatorname{tg}\alpha}\right)$ and assume in view of the small value of angle tg $\alpha = \alpha$, then

$$\Lambda_\delta \approx \frac{D^2 - D_\text{ш}^2}{a\left(D - D_\text{ш} - 2\frac{c}{\alpha}\right)} 10^{-6};\quad a = \frac{\alpha\cos\alpha}{2} \approx \frac{\alpha\sqrt{1 - \alpha^2}}{2}.$$

The scattering factor of UM with the nonmagnetic disk (similar to that presented in S 3-4)

$$k_\sigma = \frac{\Phi_\delta + \Phi_\sigma}{\Phi_\delta} = 1 + \mathring{\Lambda}_\sigma; \qquad (3\text{-}20)$$

where $\mathring{\Lambda}_\sigma = \mathring{\Lambda}_1 + \mathring{\Lambda}_2 + 0{,}5\mathring{\Lambda}_3$. $\qquad \mathring{\Lambda}_\sigma = \frac{\Lambda_\sigma}{\Lambda_\delta}$,

For the disks of UM with the shaft from the nonmagnetic material is taken $\Lambda_3 = 0$; $\Phi_{\sigma 3} = 0$.

Coefficient of scattering of UM with the magnetic disk in the first approximation, can be computed according to the expression, similar (3-20). In actuality flow distribution of scattering in them is more complicated due to the presence of the flows, which close through the periphery of disk. With the asymmetry of these flows is connected the one-sided attraction of rotor of UM to the pole of stator. The calculation of the flows indicated presents considerable difficulties.

Page 70.

3.7. Calculation of magnetic circuit. Drop in the magnetic potential in the ferromagnetic cylindrical armature.

Magnetic circuit of UM for convenience in the analysis and calculation in the general case sectionalize, through which is passed the flow of mutual induction: the back of stator, pole cores, working gaps, armature core, and design gaps. Through the back of stator, pole cores and structural/design gaps, besides the flow of mutual induction Φ_{δ}, the appropriate leakage fluxes Φ_{σ} are passed. The magnetic flux of mutual induction Φ_{δ} causes the induction of emf in the armature of machine, and flows Φ_{σ} determine scattering the

primary circuit.

Magnetizing force of excitation winding of UM with the idling compensates a drop in the magnetic potential in the sections of magnetic circuit with the passage of the magnetic flux of the idling

$$F_в = \oint_l \mathrm{H}(l)\,dl = \sum_{i=1}^{m} \int_{a_i}^{b_i} H(l)\,dl = \sum_{i=1}^{m} F_i = F_р + 2F_м + F_{с.с} + F_б + F'_б;$$

$$F_б + F'_б = k_в F_б;\quad k_в = 1 + F'_б/F_б;\quad F_с = 2F_м + F_{с.с},$$

where $F_i = H_i l_i$ - drop in the magnetic potential in the i section of the magnetic circuit:

$F_р$ - in the rotor;

$F_м, F_{с.с}$ in pole and core of stator;

$F_б, F'_б$ - in the working and structural/design gaps.

The special features/peculiarities of the calculation of a drop in the magnetic potential escape/ensue from the three-dimensional/space, but not plane-parallel character of the distribution of magnetic field in the magnetic circuit of the UM.

Is presented below the calculation of a drop in the magnetic potential in different sections of magnetic circuit of UM of different construction/design.

Let us determine the drop in the magnetic potential in the rotor with the idling, taking into account the nonuniformity of magnetic field, using expressions (2-7) and (2-8).

With the idling the component of induction $B_\varphi(r, z)=0$ and the resulting induction at any point of rotor will be determined by two components

$$B(r, z)=\sqrt{B_r^2(r, z)+B_z^2(r, z)}.$$

Page 71.

Taking into account that presented and using the adopted assumption on the constancy of the magnetic permeability, let us register the equation of Maxwell for the magnetic energy in the space of the rotor

$$W=\frac{1}{2\mu_a}\iiint_V B^2(r, z)\,dV$$

or

$$W=\frac{1}{2\mu_a}\int_0^R\int_0^{2\pi}\int_0^{L_a}\left[B_r^2(r, z)+B_z^2(r, z)\right]r\,dr\,d\varphi\,dz. \qquad (3\text{-}21)$$

Substituting in (3-21) values $B_r(r, z)$ and $B_z(r, z)$ from (2-7) and (2-8) and taking into account the orthogonality of functions $\sin[\varphi_m(z+0{,}5L_a)]$ and $\cos[\varphi_m(z+0{,}5L_a)]$ on segment $[0;\ 0{,}5L_a]$ after integration (3-21) and series/row of conversions we find:

$$W=\frac{32}{\pi^3}\frac{B_\delta^2}{\mu_a}RL_u^2\sum_{m=0}^{\infty}Q_m\frac{I_0(\varphi_m R)}{I_1(\varphi_m R)}, \qquad (3\text{-}22)$$

where

$$Q_m=\left(\frac{\pi}{\varphi_m L_u}\right)^3\sin^2(0{,}5\varphi_m l)\cos^2[0{,}5\varphi_m(2L_u-l)];$$

$$\varphi_m=\frac{2m+1}{L_u}\pi;\quad R=0{,}5D.$$

On the other hand, magnetic field energy of the armature

$$W=\frac{1}{2}F_p\Phi_p=\pi RlB_\delta F_p, \qquad (3\text{-}23)$$

where $\Phi_p=k_{ep}\Phi_\delta\approx\Phi_\delta=2\pi RlB_\delta$ - magnetic flux in the rotor.

Using expressions (3-22) and (3-23), we determine the refined expression of a drop in the magnetic potential in rotor F_p for the general case:

$$F_p=\frac{32}{\pi^3}\frac{B_\delta L_u^2}{\mu_a l}\sum_{m=0}^{\infty}Q_m\frac{I_0(\varphi_m R)}{I_1(\varphi_m R)}. \qquad (3\text{-}24)$$

Page 72.

Magnetic permeability μ_a in the weak magnetic fields is determined by the straight portion of curve of magnetization B=f(H) the material of rotor.

In the strong fields it is possible approximately to determine μ_a with induction $B=f(H)$ in accordance with the engineering calculation procedure.

In the approximate computations of magnetic circuit without

taking into account the nonuniform distribution of magnetic field a drop in the magnetic potential in the rotor is determined by the expression

$$F'_p \cong H_p l_p = H_p (L_u - l + R);\ H_p = \frac{B_p}{\mu_a}. \qquad (3\text{-}25)$$

Using (3-24) and (3-25), we will obtain the expression of the coefficient, which considers the nonuniformity of the distribution of induction in the rotor:

$$\zeta_p = \frac{F_p}{F'_p} = \frac{32}{\pi^2} \frac{L_u^2 B_\delta}{B_p l (L_u - l + R)} \sum_{m=0}^{\infty} Q_m \frac{I_0(\gamma_m R)}{I_1(\gamma_m R)}. \qquad (3\text{-}26)$$

Taking into account scattering rotor (S 3-4)

$$F_p = \zeta_p F'_p = \zeta_p \frac{k_{sp} B_p}{\mu_a} (L_u - l + R). \qquad (3\text{-}27)$$

For the special case, when the geometric dimensions of cylindrical UM have relationships/ratios $l \approx 0{,}25 L_u$ and $R \approx 0{,}5 L_u$, from (3-24) follows that

$$F_p = 4{,}13 \frac{B_\delta L_u}{\mu_a} \sum_{m=0}^{\infty} Q_m \frac{I_0\left(\frac{2m+1}{2}\pi\right)}{I_1\left(\frac{2m+1}{2}\pi\right)}, \qquad (3\text{-}28)$$

moreover

$$Q_m = \frac{1}{(2m+1)^2} \sin^2\left(\frac{2m+1}{8}\pi\right) \cos^2\left[\frac{7(2m+1)}{8}\pi\right].$$

Approximate value F'_p from (3-25) it comprises:

$$F'_p \approx 1{,}25 \frac{B_\delta}{\mu_a} L_u.$$

On the basis of latter/last expression and (3-28) we will obtain the value of coefficient ζ'_p for the special case, most widely used in practice:

$$\zeta'_p \approx 3{,}3 \sum_{m=0}^{\infty} Q_m \frac{I_0\left(\frac{2m+1}{2}\pi\right)}{I_1\left(\frac{2m+1}{2}\pi\right)},$$

moreover $B_p \approx B_\delta$ with the geometric relationships/ratios in question.

Page 73.

The value of coefficient ζ'_p with the limited number of terms of series/row comprises $\zeta'_p \approx 0{,}7$. Thus, with the frequently encountered geometric relationships/ratios of the sizes/dimensions of cylindrical UM is the refined value of a drop in the magnetic potential in the armature

$$F_p \cong 1{,}25\zeta'_p \frac{k_{\sigma p} B_\delta}{\mu_a} L_a \cong 0{,}875 \frac{k_{\sigma p} B_\delta}{\mu_a} L_a.$$

3.8. Drop in the magnetic potential in the magnetic circuit of the stator of cylindrical machine.

The magnetic circuit of stator (Fig. 3-5a) let us divide into two parts: poles (аб, вг) and the core of stator (бв).

If poles are carried out so that the magnetic induction on their height/altitude is constant/invariable, then a drop in the magnetic potential in the poles is found in the usual way, using the curve of magnetization B=f(H), from which they determine H_a by B_a and then value

$$F_a = H_a l_a.$$

where $l_п$ — length of flux line in the pole.

Induction on the height/altitude of pole $B_п$ is constant/invariable, if the width of the pole, shaped along a radius, is changed according to the law

$$b_п(r) = \frac{\Phi_п(r)}{2\pi r B_п} \approx \frac{\Phi_б + \Phi_с(r)}{2\pi r B_п} \approx \frac{\Phi_б + \Phi_{оп}}{2\pi r B_п},$$

where $b_п(r)$ and $\Phi_п(r)$ — width and the flow of pole on the circle/circumference of radius r.

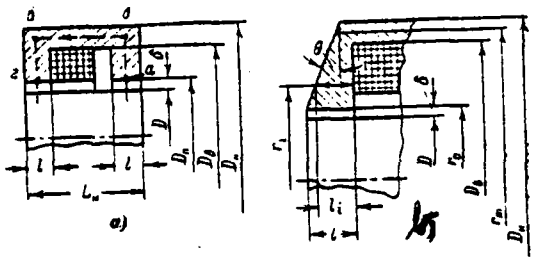

Fig. 3-5. On the calculation of the magnetic circuit of cylindrical UM. Poles: a) with flat/plane face; b) from that chamfered (by conical face).

Page 74.

Flow $\Phi_n(r)$ is changed on the height/altitude of pole as a result of a change in the leakage flux. They usually conduct calculation on the average/mean value of the flow of scattering Φ_{on} according to the height/altitude of pole.

Analogously is determined a drop in the magnetic potential in the core of the stator, in which the induction is usually constant. Thus, a drop in the magnetic potential in the magnetic circuit of the stator

$$F_c = 2H_n l_n + H_c l_c.$$

In the general case the induction with respect to the height/altitude of pole is not identical, and a drop in the magnetic

potential in it can be determined by the different methods, of which are examined below the approximation methods of the curve B=f(H) and the approximative integration.

The first method (approximations) is suitable for the simple forms of magnetic circuit. Curve of magnetization B=f(H) is approximated by one of known expressions [84], for example,

$$H=\alpha \operatorname{sh}\beta$$

or

$$H=\sum_{k=0}^{n}\alpha_{2k+1}B^{2k+1}. \qquad (3\text{-}29)$$

After determining then in the section of magnetic circuit sectional area $S_i(l_i)$, normal to the flow, we will obtain $H_i=f\left[\frac{\Phi_i}{S_i(l_i)}\right]$. In particular, for (3-29) with n=1 we have:

$$H_i(l_i)=\alpha_1\frac{\Phi_i}{S_i(l_i)}+\alpha_3\frac{\Phi_i^3}{S_i^3(l_i)}.$$

Coefficients α_1 and α_3 are determined on Metol of selected points [84].

Let us find a drop in the magnetic potential in the pole with flat/plane faces, assuming/setting direction of flow Φ_π by radial and distribution of induction by uniform. In accordance with the designations of sizes/dimensions, given in Fig. 3-5a.

$$F_{\text{п}} = F_{\text{аб}} = F_{\text{вг}} = \int_{r_a}^{r_б} \left[\alpha_1 \frac{\Phi_{\text{п}}}{2\pi r l} + \alpha_3 \frac{\Phi_{\text{п}}^3}{(2\pi r l)^3} \right] dr =$$

$$= \frac{\alpha_1 \Phi_{\text{п}}}{2\pi l} \ln \frac{r_б}{r_a} + \frac{\alpha_3 \Phi_{\text{п}}^3}{16\pi l^3} \left(\frac{1}{r_a^2} - \frac{1}{r_б^2} \right).$$

Page 75.

The use/application of this method to the determination of a potential drop in the framework of stator with the constant cross section and the constant/invariable induction is irrational, since it leads to the expression $F_{\text{с.с}} = F_{\text{бв}} = \int_{z_б}^{z_в} M dz = M (L_{\text{н}} - l);$

$$M = \frac{4\alpha_1}{\pi} \frac{\Phi_{\text{с}}}{D_{\text{н}}^2 - D_{\text{в}}^2} + \frac{64\alpha_3}{\pi^3} \frac{\Phi_{\text{с}}^3}{(D_{\text{н}}^2 - D_{\text{в}}^2)^3}.$$

Here the use of an approximation is not justified, and $F_{\text{бв}}$ it is necessary to find by usual method with the help of the curve B=f(H). Thus,

$$F_{\text{с}} = 2F_{\text{п}} + F_{\text{с.с}} = F_{\text{аб}} + F_{\text{бв}} + F_{\text{вг}}.$$

With the complicated configurations of magnetic circuit sometimes the integration does not succeed in fulfilling in the quadratures, then should be expanded integral in series/row.

The second method - the approximative integration - with some forms of magnetic circuits is more convenient than the method of approximation. Let us consider its use/application based on the

example of the calculation of a potential drop in the pole with conical face. In accordance with the designations of geometric dimensions (Fig. 3-5b)

$$r_0=\frac{D_в}{2};\quad l_0=l;\quad r_m=\frac{D_в+D_н}{4};\quad H_i=f(B_i);\quad B_i=\frac{\Phi_в}{S_i};$$

$$S_i=2\pi r_i l_i;\quad l_i=l-\left(r_i-\frac{D_в}{2}\right)\operatorname{tg}\theta;\quad r_i=r_0+i\frac{r_m-r_0}{m}.$$

Section AB along a radius from r=r$_0$ to $r=r_m$ conditionally is divided into m of equal parts. Then some formulas of approximative integration [85] are applicable.

Page 76.

a) The formula of the rectangles

$$F_{аб}=\int_{r_0}^{r_m}H(r)\,dr=\frac{r_m-r_0}{m}\sum_{i=0}^{m-1}H_i(r_i)\ =\frac{r_m-r_0}{m}[H_0(r_0)+H_1(r_1)+\ldots+H_{m-1}(r_{m-1})].$$

b) The trapezoid rule

$$F_{аб}=\int_{r_0}^{r_m}H(r)\,dr=\frac{r_m-r_0}{2m}\left[H_0(r_0)+2\sum_{i=1}^{m-1}H_i(r_i)+H_m(r_m)\right]=\frac{r_m-r_0}{2m}[H_0(r_0)+2H_1(r_1)+2H_2(r_2)+$$
$$+\ldots+H_m(r_m)].$$

c) The formula of parabolas (Simpson) with even m

$$F_{аб}=\int_{r_0}^{r_m}H(r)\,dr=\frac{r_m-r_0}{3}\left[H_0(r_0)+4\sum_{k=0}^{0.5m-1}H_{2k+1}(r_{2k+1})+\right.$$
$$\left.+2\sum_{k=1}^{0.5m-1}H_{2k}(r_{2k})+H_m(r_m)\right]=\frac{r_m-r_0}{3m}[H_0(r_0)+4H_1(r_1)+2H_2(r_2)+$$
$$+4H_3(r_3)+2H_4(r_4)+\ldots+2H_{m-2}(r_{m-2})+4H_{m-1}(r_{m-1})+H_m(r_m)].$$

Let us note that the formula of parabolas (with m=2) is used for

calculating the drop in the magnetic potential in the teeth with the not in parallel walls during the design of electrical machines. All given formulas are more precise, the greater m number of the parts of the separation of the section of magnetic circuit. With identical m the formula of parabolas is more precise than the trapezoid rule, and the latter is more precise than the formula of rectangles. With respect to complexity they are approximately/exemplarily identical; therefore the formula of parabolas is more preferable. For achievement of the in practice sufficient authenticity of calculation it is possible to recommend its use with m=4 or by 6. In these cases

$$F_{a6}=H_{расч}l_{ср};\ l_{ср}=r_m-r_0,$$

where for m=4

$$H_{расч}=\frac{1}{12}(H_0+4H_1+2H_2+4H_3+H_4);$$

for m=6

$$H_{расч}=\frac{1}{18}(H_0+4H_1+2H_2+4H_3+2H_4+4H_5+H_6).$$

For the refined calculations with the increased authenticity of calculations it is possible to use Newton-Cotes formulas [86]. For Newton-Cotes formula with m=6 ($l_{ср}=r_6-r_0$)

$$H_{расч}=\frac{1}{840}(41H_0+216H_1+27H_2+272H_3+27H_4+216H_5+41H_6).$$

Page 77.

During calculations of a potential drop is possible the use/application of formulas, similar to those indicated, but based on the use of values H_i, which relate to the middle of the i part of the

section of circuit, and also the methods of the approximative integration of Chebyshev, Gauss, etc. [85, 86].

During the calculation of a drop in the magnetic potential of disk UM the distribution of magnetic circuit in the sections, which have the shape of simple geometric solids, is difficult. Taking into account that the magnetic circuits are projected/designed with the greatest quality (S2-3) and identical B and H in the separate elements/cells of stator, it is possible to reduce calculation to the calculation of line integrals. However, in view of the complexity of integrands to more conveniently find the length of center line from the outline of magnetic circuit (for example, with the help of the curvimeter) and to determine $F_{a6}=Hl_{cp}$ (with H=const).

3.9. Drop in the magnetic potential in the working gap of cylindrical and the nonmagnetic space of disk mind.

a) A drop in the magnetic potential in the working gaps of cylindrical UM (Fig. 3-5) on the pole pair will be determined by the expression

$$F_\delta=2\Phi_\delta R_\delta=\frac{B_\delta D}{\mu_0}\ln\left(1+2\frac{\delta}{D}\right),$$

where

$R_\delta=\int_R^{R_a}\frac{dr}{\mu_0 2\pi r l}=\frac{1}{2\pi l\mu_0}\ln\frac{R_a}{R}$ — the reluctance of working gap;

$$R=0{,}5D;\quad R_п=0{,}5D_п;$$

$\Phi_б=2\pi RlB_б$ — flow in the working gap.

Since $2\delta<<D$ and $\ln\left(1+2\frac{\delta}{D}\right)\approx 2\frac{\delta}{D}$, it is possible to use the approximation

$$F_б\approx\frac{2\delta B_б}{\mu_0}\approx 1{,}6\delta B_б\cdot 10^6, А.$$

Page 78.

b) А drop in the magnetic potential in the interpolar space of UM with the nonmagnetic disk of equal thickness we obtain, using (3-18):

$$F_б=\Phi_б R_б=\frac{2\delta+b_п}{\mu_0}B_б,$$

where

$$R_б=\frac{4}{\pi\mu_0}\frac{2\delta+b_п}{D^2-D_п^2}\text{ and }\Phi_б=\frac{\pi}{4}(D^2-D_п^2)B_б$$

- the reluctance of interpolar space of UM with the nonmagnetic disk of equal thickness and flow in the working gap.

c) А drop in the magnetic potential in the interpolar space of UM with the conical nonmagnetic disk let us register, using (3-19):

$$F_б=\Phi_б R_б=\frac{\alpha\Phi_б}{\pi\mu_0\left(\rho\ln\frac{2\rho-D_п}{2\rho-D}-\frac{D-D_п}{2}\right)},$$

where

$$R_б=\frac{\alpha}{\pi\mu_0}\left(\rho\ln\frac{2\rho-D_п}{2\rho-D}-\frac{D-D_п}{2}\right)^{-1}=\frac{1}{\Lambda_б}$$

- reluctance of interpolar space of UM with the nonmagnetic conical disk;

$$\Phi_\delta = 0{,}25\pi \frac{B_\delta}{\cos\alpha}(D^2 - D_a^2)$$

- magnetic flux in the working gap.

Presented in this chapter results can be used also during calculations of electrical machines with another construction/design of magnetic system and unipolar magnetization.

Chapter Four.

ARMATURE REACTION IN ACYCLIC MACHINES WITH LIQUID-METAL CURRENT PICKUP.

4.1. Special features of armature reaction in acyclic machines.

By phenomenon of armature reaction the effect of mag. force of armature (secondary duct/contour) on mag. force of excitation (core circuit) is understood.

Armature reaction in acyclic machines is one of the fundamental questions of theory and calculation of these machines, since the high values of armature current and its field substantially affect work of UM. Relative value of mag. force of armature $F_я$ in UM is considerably higher than in the bipolar machines of direct current, i.e.

$$\left(\frac{F_я}{F_в}\right)_{ум} \gg \left(\frac{F_я}{F_в}\right)_{биполя}. \qquad (4\text{-}1)$$

In the general case axes of magnetic force of excitation and magnetic force of the armature of electrical machine are displaced between themselves to certain angle and, therefore, magnetic force of armature has longitudinal and transverse components according to the

relation of magnetic force of excitation, which is accepted as longitudinal.

In the synchronous machines the character of armature reaction is determined by type of load, in collector direct-current machines - by brush shift from normal neutral plane, while in acyclic machines of direct current - by construction/design of current pickup.

The latter is not obvious without the explanation. As it was shown above, there are two varieties of current pickups of UM: circular and zonal.

In the first case UM can have only transverse component of armature reaction, and the second - transverse and longitudinal components.

Page 80.

Thus, during the circular liquid-metal current pickup, just as with the brush with the symmetrical location of brushes in the circle/circumference of rotor, magnetic force of longitudinal armature reaction in UM is absent. The concept of normal neutral plane for UM becomes meaningless, but longitudinal magnetic force does not appear also with any simultaneous shift/shear of all

brushes. It appears only in UM with the asymmetric magnetic system or during the nonuniform distribution of brushes according to the circle/circumference of armature and is caused by the eddy currents in the rotor, whose magnetic force demagnetizes machine in the generator mode and magnetizes - in the engine. In the rotor UM with the brush current pickup (or with the zonal liquid-metal) appear the cross currents, which create also longitudinal magnetic force of peculiar commutation armature reaction. The latter in the generator mode functions by the demagnetizing form, in the engine - magnetizing. Transverse armature reaction in UM with the brush current pickup distorts field and leads to current displacement to brush toe, which can entail sparking under it as a result of the excessive current density.

As has already been indicated, in UM with the circular liquid-metal current pickup similar phenomena are absent and there is only a transverse armature reaction.

If the operating point of machine lies/rests in the straight portions of magnetization curve, i.e. when the magnetic circuit of machine is not saturated by the resulting magnetic field or is strongly saturated, then the distortion of ground field in steel does not lead to a decrease in induced emf. However, since usually the operating point of machine lies/rests on the nonlinear the sections

of curve of magnetization (on the "elbow"), i.e. magnetic circuit has "average/mean" saturation, then a decrease in the total flux and the corresponding decrease of emf occurs. For retaining/preserving/maintaining the value of emf they increase field current (magnetic force). Thus, further field current compensates the demagnetizing effect of transverse armature reaction F_{qd}.

Here F_{qd} — "longitudinal" component of transverse reaction F_q. Back induction magnetic force of transverse armature reaction in UM is exhibited considerably stronger than in the DC commutating machines. This is caused by relationship/ratio (4-1), and also fact that relative value of the reluctance of quadrature circuit R_{Mq} (in comparison with the resistor/resistance to longitudinal circuit R_{Md}) for UM considerably less than the bipolar ones, i.e., has.

$$\left(\frac{R_{Mq}}{R_{Md}}\right)_{УМ} \ll \left(\frac{R_{Mq}}{R_{Md}}\right)_{биполя}, \qquad (4\text{-}2)$$

moreover $(R_{Mq}/R_{Md})_{биполя} \approx 1$, since longitudinal $\Phi_в$ and transverse $\Phi_я$ magnetic fluxes meet on their path in the magnetic circuit of the bipolar machines of the resistor/resistance of air gaps.

Page 81.

In UM $R_{Mq} \ll R_{Md}$, since the cross flow of armature field is closed in the continuous massive magnetic circuits, and main longitudinal flow must twice pass through the working gap. On the basis (4-1) and (4-2) it

is possible to conclude that the saturation of magnetic circuit the resulting field in UM and, consequently, also value of magnetic force F_{qd} of the longitudinal effect of transverse armature reaction will be more than in the bipolar ones. From the point of view of the decrease of the relative back induction magnetic force F_{qd} it is expedient so that the magnetic circuit of UM would be saturated by main field of excitation. In this case the reluctance of circuit during all operating modes to idling from considerable overloadings varies lower.

The saturation of magnetic circuit decreases the possibilities of regulating the voltage/stress of UM. If necessary for wide regulating should be compensated the armature reaction with the help of the special "windings". In those compensated UM descends the necessary power of excitation winding and its sizes/dimensions. Questions of compensation and decrease of the armature field demagnetizing effects in UM have important value.

As a result of the absence of magnetic reversal and hysteresis losses an increase in the resulting induction with the load does not produce an increase in the "losses in steel", but equalizing (eddy currents in the armature of UM with the zonal current pickup cause incremental losses in it and supplemental heat of machine. Procedure of calculation of magnetic force of the commutation armature reaction

and incremental losses in UM is worked out insufficiently. Special feature/peculiarity of UM with the solid rotor and circular liquid-metal current pickup is the impossibility of the "tilting/reversal of field" in the working gap, since in contrast to the DC commutating machines UM have single-pole

magnetic system. In UM with bar winding "tilting/reversal" can occur under the insignificant part of the pole. There is theoretical interest in research of the completely unstudied question about the armature reaction in the magnetoelectric UM; however, such machines yet did not win acceptance.

Up to the present time there are no approved engineering methods of quantitative account of magnetic force F_{qd} in UM. For a special case of cylindrical UM with the rotor expansion this problem is solved by the graph-analytic method of successive approximations [58]. This method, which requires however, the large space of graphic constructions, can be used also for other UM (disk; for the solid rotor of cylindrical ones).

Page 82.

Below are stated principles of theory, engineering methods of account and ways of the compensation for transverse armature reaction

in the cylindrical and the disk UM with the circular current pickup and the symmetrical magnetic system, in essence in connection with the generator mode of their work. Experimental research is given in Chapter 10.

4.2 Theory of armature reaction in UG with the circular liquid-metal current pickup.

Let us consider cylindrical UG with the flat massive ferromagnetic rotor, with the hollow rotor and disk UG. During the circular current pickup in all these UM the armature reaction is purely transverse. The directions of the magnetic fluxes of the fields of exictation $\Phi_в$ and armature $\Phi_я$ with the load UG are shown in Fig. 4-1.

For any duct/contour of circuit/bypass magnetic force of excitation winding according to the laws of full current it is valid the relationship/ratio

$$F_в = \oint_{l_{di}} \mathbf{H}_{вi} d\mathbf{l} = I_в w_в,$$

where $F_в$, $I_в$, $w_в$ — magnetic force, current and a number of turns of excitation winding; $H_{вi}$ — intensity/strength of the field of exictation, accepted by longitudinal, on the i duct/contour of integration.

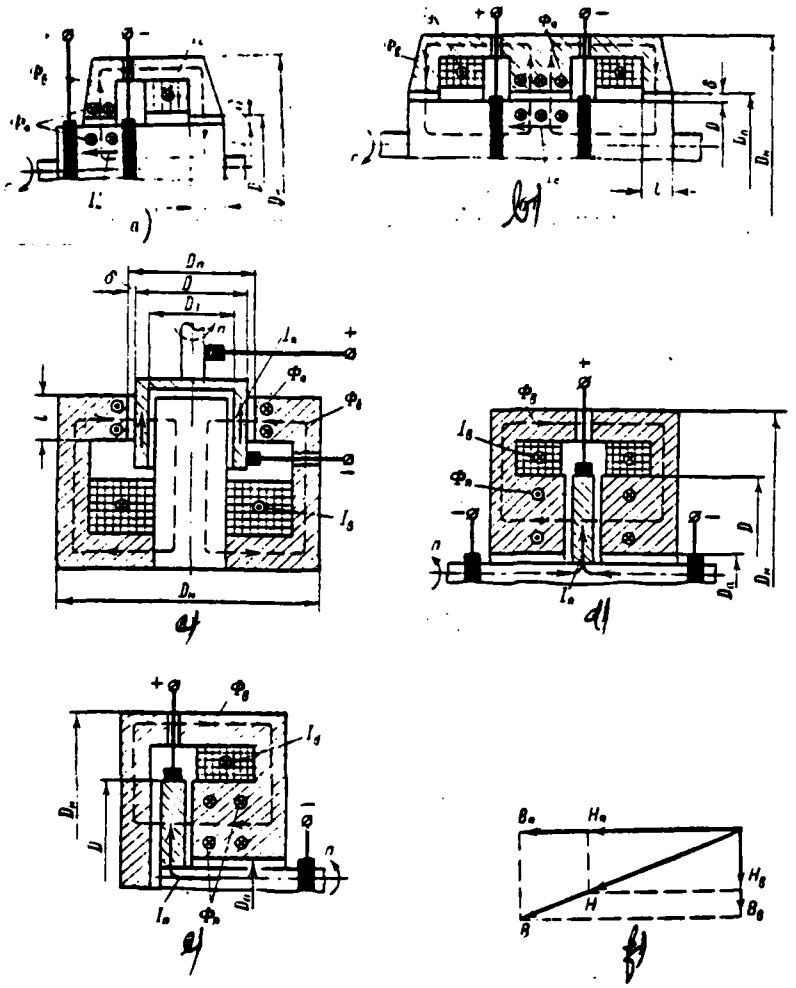

Fig. 4-1. Magnetic fluxes with the load of UG. a, b) cylindrical with the solid rotor with 2p=2 and 2p=4; c) cylindrical with the hollow rotor; d, e) disk with the bilateral and one-sided current pickup on the shaft; f) vector diagram of magnetic fields.

In the case of axial symmetry it is analogous for any i duct/contour of circuit/bypass, pierced by armature current, is correct

$$F_{ai}=\oint_{l_{qi}} H_{ai}dl=\int_0^{2\pi}\frac{H_{ai}d_i}{2}d\varphi=I_{ai}, \qquad (4\text{-}3)$$

where I_{ai}, F_{ai} — the full current, included by the duct/contour of integration, and corresponding magnetic force (number of the "turns" of armature $w_a=1$);

H_{ai} — strength of transverse (tangential) field.

As the ducts/contours of circuit/bypass l_{qi} are selected the concentric circles/circumferences with diameters of d_i with the centers on the rotational axes of UM. In the form of an example let us consider cylindrical UM. For the arbitrary section at the active length l of machine (Fig. 4-1a) let us determine the resulting intensity/strength and the induction of magnetic field on the arbitrary circle/circumference with a diameter of d_i.

Let us recall that arbitrary diameter d_i in the armature varies within the limits $d_a<d_i<D$ in the presence of the isolated/insulated shaft with a diameter of d_a and $0<d_i<D$, if there is no opening/aperture and to current carriers it is all the section of armature ($d_a=0$).

In stator d_i it varies within the limits $(D+2\delta)<d_i<D_н$, while in the working gap in limits $D<d_i<(D+2\delta)$; $D+2\delta=D_н$.

Armature current, included by unit magnetic flux, which passes at a distance $d_i<D$ from the rotational axis of armature,

$$I_{яi}=I_я\frac{\overset{*}{d}_i^2-\overset{*}{d}_в^2}{1-\overset{*}{d}_в^2}=j_я S_{яi}=j_я\frac{\pi D^2}{4}(\overset{*}{d}_i^2-\overset{*}{d}_в^2),$$

where

$j_я=\frac{I_я}{S_я}=\frac{4}{\pi D^2}\frac{I_я}{1-\overset{*}{d}_в^2}=$ const — the current density of armature;

$$\overset{*}{d}_i=\frac{d_i}{D};\quad \overset{*}{d}_в=\frac{d_в}{D}.$$

Page 84.

It is obvious that when $d_i\geqslant D$ current $I_{яi}=I_я=$const. Taking into account that presented, let us determine the magnetic intensity of armature in the rotor on the circle/circumference with a diameter of $d_i<D$:

$$H_{яi}=\frac{I_{яi}}{\pi d_i}=\frac{I_я}{\pi d_i}\cdot\frac{\overset{*}{d}_i^2-\overset{*}{d}_в^2}{1-\overset{*}{d}_в^2}=0{,}25 j_я D\frac{\overset{*}{d}_i^2-\overset{*}{d}_в^2}{\overset{*}{d}_i}.$$

It is analogous for the stator $(d_i\geqslant D+2\delta=D_н)$:

$$H_{яi}=\frac{I_я}{\pi d_i}=0{,}25 j_я D\frac{1-\overset{*}{d}_в^2}{\overset{*}{d}_i}.$$

The magnetic inductions, which correspond to these values $H_{яi}$, are equal to:

$$B_{яi}=\mu_{яi}H_{яi},$$

moreover $\mu_{яi}$ — magnetic permeability in the i section of rotor or

stator, caused by the resulting field.

For the clarity Table 4-1 gives values H_{ni} and are given the limits of change d_i in the rotor, the stator and the working gap for the different constructions/designs of UM.

Table 4-1. Values $H_{\pi i}$ and the ranges of change d_i in the rotor, the stator and the working gap of different types of UM.

(1) Конструкция генератора	(2) Участок магнитной цепи		
	(3) Ротор	Статор (4)	(5) Зазор
(6) Цилиндрический с массивным ротором	$H_{\pi i} = \frac{I_\pi d_i}{\pi D^2}$ $0 < d_i \leqslant D$	$H_{\pi i} = \frac{I_\pi}{\pi d_i}$ $D_a \leqslant d_i \leqslant D_a$	$H_{\pi\delta} = \frac{I_\pi}{\pi (D+\delta)}$ $d_i = D + \delta$
(7) Цилиндрический с полым ротором	$H_{\pi i} = \frac{I_\pi}{\pi d_i} \frac{d_i^{*2} - D_1^{*2}}{1 - D_1^{*2}}$ $D_1 \leqslant d_i \leqslant D$	$H_{\pi i} = \frac{I_\pi}{\pi d_i}$ $D_a \leqslant d_i \leqslant D_a$	$H_{\pi\delta} = \frac{I_\pi}{\pi (D+\delta)}$ $d_i = D + \delta$
(8) Дисковый		$H_{\pi i} = \frac{kI_\pi}{\pi d_i}$ $D_a \leqslant d_i \leqslant D_a$	$H_{\pi\delta i} = \frac{kI_\pi}{\pi d_i}$ $D_a \leqslant d_i \leqslant D_a$

Key: (1). Construction/design of generator. (2). Section of magnetic circuit. (3). Rotor. (4). Stator. (5). Gap. (6). Cylindrical with the solid rotor. (7). Cylindrical with the hollow rotor. (8). Disk.

Page 85.

In this case the following positions were considered:

a) in the internal core of stator UG with the hollow rotor and in the rotor disk UG there is no imposition of the longitudinal and cross fields (disk it is accepted sufficiently to thin ones);

b) in accordance with §2-4 is accepted axially-uniform current distribution in the rotors of cylindrical UM and the current carrying shaft of disk UM.

Coefficient k=1 for disk UG with the one-sided current pickup on the shaft and k=0.5 with the bilateral ($I_я$ — full current of generator armature). Values $H_{яi}$ in the gaps are given for the mean diameter in the gap, since $\delta<<D$.

For the more demonstrative understanding of the essence of the physical phenomena, which occur with the load UG, let us connect of the replacement of their magnetic circuit.

In this case the magnetic circuit of machine is conditionally divided into two zones: active and inactive.

By active region/core the sections of magnetic circuit, magnetized simultaneously by longitudinal and cross fields, are implied. In the axial direction it is limited to the planes, in which the current pickups are arranged/located.

The remaining part of the magnetic circuit is magnetized only by longitudinal field. Let us divide stator, and also solid rotor, cylindrical UM and the stator of disk UM into m sections, in the

limits of each of which magnetic permeability of material μ_{ai} can be considered constant/invariable. Special feature/peculiarity relative to thin hollow cylindrical (ferromagnetic) rotor will be m=1. In the active region/core value μ_{ai} is determined by the effect of resulting magnetic field $H_i=H_{bi}+H_{ri}$, in the inactive - only longitudinal fields H_{bi}, since here $H_{ri}=0$. During the calculation of the reluctances of the i sections of magnetic circuits virtually it suffices to consider the cases of continuous and it is gentle cylinders in different directions of the passage of magnetic flux in UG, to them it is possible to reduce the sections, in which the magnetic circuits (Table 4-2) are decomposed. Furthermore, Table 4-2 gives the calculation formulas of resistors/resistances for some typical sections of magnetic circuit of UM.

The reluctances of sections R_{mdi} for the longitudinal flow compute during the determination of magnetic force F_{qd} from the method, presented in §4-3. It is useful to know the reluctances of sections for the cross flow, for example, during the estimation of the efficiency of nonmagnetic radial separators in the magnetic circuit for decreasing the flow of armature field (§4-5).

Pages 86-87.

Table 4-2. Calculation formulas for the reluctances.

Название (1)	(2) Формула	
(3) Сопротивление сплошного цилиндра для $\Phi_в$ в осевом направлении	$R_{\mu di} = \frac{4l_i}{\pi\mu_{ai}D_i^2}$	(1)
(4) Сопротивление полого цилиндра для $\Phi_в$ в осевом направлении	$R_{\mu di} = \frac{4l_i}{\pi\mu_{ai}(D_{ni}^2 - D_{ai}^2)}$	(2)
(5) Сопротивление полого цилиндра для $\Phi_в$ в радиальном направлении	$R_{\mu di} = \frac{1}{2\pi\mu_{ai}l_i}\ln\frac{D_{ni}}{D_{ai}}$	(3)
(6) Сопротивление полого цилиндра для $\Phi_в$ в тангенциальном направлении	$R_{\mu qi} = \frac{\pi(D_{ni} + D_{ai})}{\mu_{ai}l_i(D_{ni} - D_{ai})}$	(4)
(7) Сопротивление воздушных зазоров для $\Phi_в$ цилиндрической машины	$R_{\delta d} = \frac{1}{\pi\mu_0 l}\ln\left(1 + 2\frac{\delta}{D}\right)$	(5)
(8) Сопротивление полого ротора для $\Phi_в$ цилиндрической машины	$R_{\mu dп} = \frac{1}{\pi\mu_{cp}l}\ln\frac{D}{D_1}$	(6)
(9) Сопротивление межполюсного пространства для $\Phi_в$ дисковой машины с плоским немагнитным ротором	$R_{\delta d} = \frac{4c}{\pi\mu_0(D^2 - D_п^2)}$	(7)
(10) То же, что (7), для машины с коническим немагнитным ротором	$R_{\delta d} = \frac{\alpha}{\pi\mu_0\left(\rho\ln\frac{2\rho - D_п}{2\rho - D} - \frac{D - D_п}{2}\right)}$, $\rho = 0{,}5(D + c\operatorname{ctg}\alpha)$	(8)

(11) Эквивалентное сопротивление для $\Phi_в$ цилиндрической машины на пару полюсов	$R_{вd} = \left[\left(\sum_{i=1}^{m} R_{вdi}\right)_а + \left(\sum_{i=1}^{m} R_{вdi}\right)_{н.а}\right]_р + k_в R_{бd} + \left[\left(\sum_{i=1}^{m} R_{вdi}\right)_а + \left(\sum_{i=1}^{m} R_{вdi}\right)_{н.а}\right]_с$ (9)
(12) Эквивалентное сопротивление для $\Phi_в$ дисковой машины на пару полюсов	$R_{вd} = \left[\left(\sum_{i=1}^{m} R_{вdi}\right)_а + \left(\sum_{i=1}^{m} R_{вdi}\right)_{н.а}\right]_с + k_в R_{бd}$ (10)
(13) Эквивалентное сопротивление для $\Phi_в$ в статоре и воздушном зазоре цилиндрической машины	$R_{вq} = \frac{1}{\left(\sum_{i=1}^{m} \frac{1}{R_{вqi}}\right)_а + \frac{1}{R_{бq}}}$ (11)
(14) То же, что (11), для дисковой машины	$R_{вq} = \frac{1}{\left(\sum_{i=1}^{m} \frac{1}{R_{вqi}}\right)_а + \sum_{i=1}^{m} \frac{1}{R_{бqi}}}$ (12)

Note. The interpretation of indices in (9)-(12): a - active region/core; н.а - inactive zone; р - rotor; с - stator.

Key: (1). Name. (2). Formula. (3). Resistor/resistance of continuous cylinder for in the axial direction. (4). Resistor/resistance of hollow cylinder for in the axial direction. (5). Resistor/resistance of hollow cylinder for in the radial direction. (6). Resistor/resistance of hollow cylinder for in the tangential direction. (7). Resistor/resistance of air gaps for the cylindrical machine. (8). Resistor/resistance of hollow rotor for the

cylindrical machine. (9). Resistor/resistance of interpolar space for the disk machine with the flat/plane nonmagnetic rotor. (10). The same as (7), for the machine with the conical nonmagnetic rotor. (11). Equivalent resistance for the cylindrical machine to the pole pair. (12). Equivalent resistance for the disk machine to the pole pair. (13). Equivalent resistance for in stator and air gap of cylindrical machine. (14). The same as (11), for the disk machine.

The formulas, indicated in Table 4-2, are used during the calculation of the resistors/resistances: the internal core of stator in UG with hollow rotor (1); the framework of stator UM of any construction/design (2); the i layer in the pole of the stator of cylindrical machine (3); the i layer of magnetic circuit for the cross flow of UM of any construction/design (4). In the formulas l_i, D_{ai}, D_{bi} indicated - axial length, external and cylinder bores; μ_{ai} it is determined for the mean diameter of layer $D_i=0,5\ (D_{ai}+D_{bi})$. Formula (5) is derived on the basis (3) for two gaps of UM (to the pole pair). Formula (6) is also designed for the pole pair, moreover μ_{cp} is determined for the diameter, equal to 0.5 $(D+D_1)$, and with nonmagnetic rotor $\mu_{cp}=\mu_0$.

Page 88-89.

In formulas (7) and (8) c - distance between the poles [in the expression (8) - at diameter D]. With the magnetic disk the formula of the resistor/resistance of two gaps takes the form

$$R_{\delta\delta} = \frac{8\delta\cos\alpha}{\pi\mu_0(D^2 - D_{\text{п}}^2)},$$

where δ - one-sided gap, α - angle of taper (for the flat/plane disk cos α=1).

Coefficient $\mu_{\text{в}} > 1$, entering formulas (9) and (10), considers the resistor/resistance of structural/design gaps. For UM with the hollow rotor instead of the expression in the first brackets into formula (9) must be substituted $R_{\text{маг}}$ from expression (6). For the machine with the magnetic rotor in formula (10) it is necessary to supplement component/term/addend $R_{\text{маг}}$ from expression (2). Resistance $R_{\text{эф}}$ in formula (11) is calculated from formula (4) when $D_{\text{вн}} = D_{\text{в}} = D + 2\delta$; $D_{\text{нн}} = D$; $l_1 = l$; $\mu_{\text{эф}} = \mu_0$. In formula (12) resistor/resistance $R_{\text{эф}}$ is calculated from (4) when $l_1 \cong \delta$; $\mu_{\text{эф}} = \mu_0$.

In accordance with formulas (9) and (10) table 4-2 are constructed the replacement schemes for "the longitudinal axis "the

magnetic circuit of cylindrical and disk UM; in accordance with (4) (11) and (12) - replacement schemes for the quadrature circuit in the active region/core of the solid rotor of cylindrical UM, and also stator and air gap of disk or cylindrical UM (Fig. 4-2).

The analysis of the replacement schemes of magnetic circuit of UM makes it possible to make the following conclusions:

1) $R_{\text{мd}} > R_{\text{мq}}$, since the cross flow does not meet with resistance air gaps;

2) into UM with the nonmagnetic disk for creation $\Phi_{\text{в}}$, identical to the flow in cylindrical UM with the ferromagnetic rotor, is required large magnetic force $F_{\text{в}}$, since in this case $(R_{\text{bd}})_{\text{диск}} > (R_{\text{bd}})_{\text{цил}}$;

3) the relative value of magnetic force of armature in UM with the nonmagnetic disk is less than in UM with the ferromagnetic cylindrical rotor

$$\left(\frac{F_{\text{я}}}{F_{\text{в}}}\right)_{\text{диск}} < \left(\frac{F_{\text{я}}}{F_{\text{в}}}\right)_{\text{цил}}.$$

4) $R_{\text{bq}} \gg R_{\text{мqi}}$ both in the disk and the cylindrical UM; therefore the branching of the parallel parts of flow $\Phi_{\text{я}}$ into the gap is insignificant; basic part of flow $\Phi_{\text{я}}$ is closed on the massive ferromagnetic parts of the circuit in the active region/core of UM.

Cross field $H_{пi}$ produces the increase of strength H_i of the resulting field with the load in each i section in the active region/core of UM. Since the longitudinal and cross fields are orthogonal, resulting field $H=H_{вi}+H_{пi}$ in the value it will comprise:

$$H_i=\sqrt{H_{вi}^2+H_{пi}^2}. \qquad (4\text{-}4)$$

Consequently, $H_i>H_{вi}$, which involves the decrease of permeability $\mu_{вi}$ (Fig. 4-3a) and the increase of magnetic equivalent resistance $R_{вi}$ for flow $\Phi_в$, which when $F_в=\text{const}$ is reduced in comparison with its value with the idling. As corollary is reduced emf of the machine

$$e=\Phi_в n,$$

where n=const - speed of rotation of rotor. To avoid this it is necessary to create supplementary magnetic force of excitation winding $\Delta F_в$, which is necessary for maintenance $\Phi_в=\text{const}$ during increased resistor/resistance $R_{вд}$.

We assume/set the materials of magnetic circuits by isotropic ones, in this case in each section

$$\frac{B_в}{H_в}=\frac{B_п}{H_п}=\frac{B}{H}=\mu_а. \qquad (4\text{-}5)$$

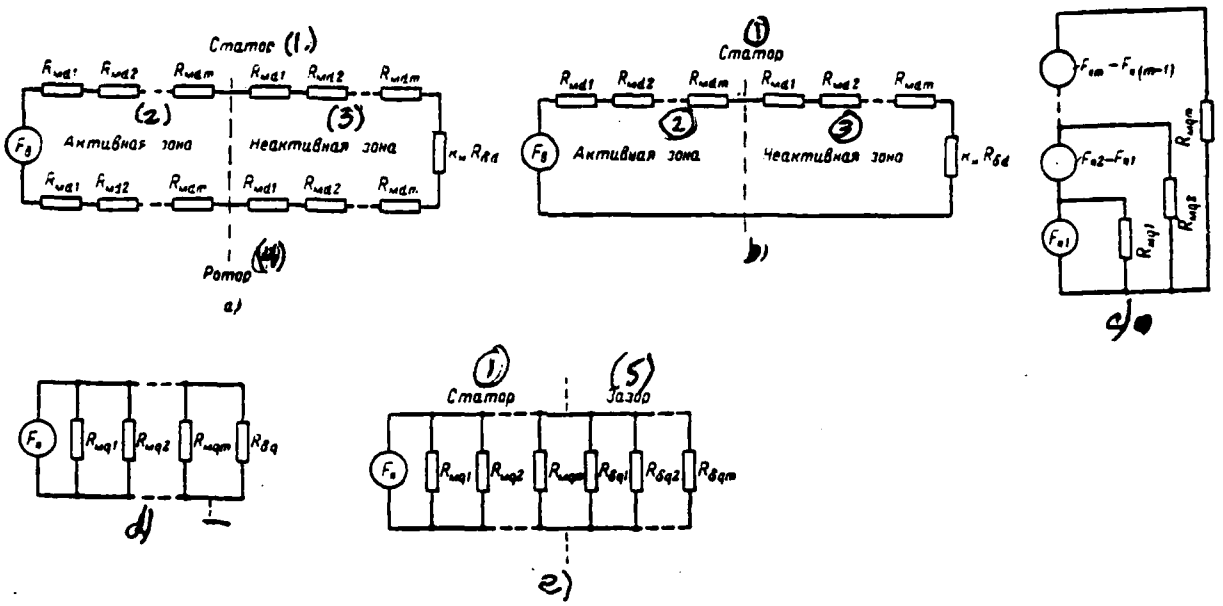

Fig. 4-2. Replacement schemes, which correspond to pole pair of UM. a) for the longitudinal circuit of cylindrical machine; b) the same of disk machine; c) for the quadrature circuit of the active region/core of massive cylindrical rotor; d) the same of stator and gap of cylindrical machine; e) the same of stator and gap of disk machine.

Key: (1). Stator. (2). Active region/core. (3). Inactive zone. (4). Rotor. (5). Gap.

Page 90.

The intensity/strength of field $\overline{H_{\delta 1}}$ is determined on the curve of magnetization B=f(H) material for the given ones of flow Φ_δ in

induction $B_{\text{вi}x.x}$ with the idling. The values of field H_{ni} with the assigned armature current for the different constructions/designs of UM are given in Table 4-1. The intensity/strength of resulting field H_i with known ones $H_{\text{вi}}$ and H_{ni} is determined by relationship/ratio (4-4). The density of field of excitation with the load on the basis (4-5)

$$B_{\text{вi}} = B_i \frac{H_{\text{вi}}}{H_i},$$

where B_i is determined on the curve of magnetization B=f(H) for $H=H_i$. The induction of armature field in this case comprises:

$$B_{\text{ni}} = \sqrt{B_i^2 - B_{\text{вi}}^2} \text{ or } B_{\text{ni}} = B_i \frac{H_{\text{ni}}}{H_i}.$$

Thus, are described longitudinal, transverse and resulting magnetic fields in UM Fig. 4-3b gives the curves of the field distribution of armature along a radius for the cylindrical UM. With the help of (5-5) analogous curves it is possible to find for intensity/strength and inducting all fields of UM.

From the point of view of the induction of assigned emf it is important so that normal component of induction in gap $B_{\text{вi}}$ would not be reduced with the load. Therefore the determination of the value of the current of armature with intended sizes of machine, for which the armature field does not cause the decrease of emf, is of interest.

As an example let us consider cylindrical UG with the solid rotor. As can be seen from Fig. 4-3, the greatest value intensity/strength H_{ai} reaches on the nearest to the gap $i-x$ layers of rotor (i=m) and stator (i=1).

Let us take for simplicity of the calculation

$$(B_{\delta m})_p \simeq (B_{\delta 1})_c \approx B_{\delta\delta}; \quad (\mu_{\delta m})_p \approx (\mu_{\delta_1})_c;$$

then

$$(H_{\delta m})_p \approx (H_{\delta 1})_c \approx H_{\delta\cdot}$$

Furthermore, let us assume $(H_{\delta m})_p \approx (H_{\delta 1})_c \approx H_{\delta\delta} = H_{\delta\cdot}$ Taking into account that $D \gg \delta$, it is possible to count $H_\delta \approx I_\delta/\pi D$. For the most widely used magnetic materials of overall use/application the linear section of curve of magnetization B=f(H) lies/rests within the limits of fields with the intensity/strength to 1000-1500 a/m. Not to consider the back induction of armature field in UG is possible with the intensities/strength of the resulting field

$$H = \sqrt{H_\cdot^2 + H_\delta^2} < 1\,000 \div 1\,500\ a/\text{м}, \qquad (4\text{-}6)$$

not causing the saturation of machine. Inequality (4-6) is satisfied with

$$I_\delta < \pi D \sqrt{(10^6 \div 2\cdot 10^6) - H_\cdot^2},\ a.$$

Page 91.

Latter/last expression makes sense for unsaturated UG, the strength

of field of which

$$H_в < 1\,000 \div 1\,500 \ a/м.$$

In order to determine the greatest possible decrease in emf under the action of armature field, let us consider the limiting case: magnetic circuit is not saturated by main field (i.e. $H_в < 1\,000 \div 1\,500$ a.m. $B_{в.х.х} \approx 1.3$ T), but armature field strongly saturates it ($H_я \geqslant 15\,000$ a/м, $B_я \approx 1{,}95$ T).

With this

$$H = \sqrt{1\,000^2 + 15\,000^2} \approx H_я; \quad B \approx 1{,}95 \ \text{T}.$$

$$B_в = B\frac{H_в}{H} = 1{,}95\frac{1\,000}{15\,000} = 0{,}13 \ \text{T}; \quad \frac{B_{в.х.х}}{B_в} = \frac{1.3}{0{,}13} = 10.$$

Thus, in the extreme case is possible weakening induction and decrease of emf approximately/exemplarily 10 times. For the machines, whose magnetic circuit is saturated by field $H_в$, a decrease in emf will be less.

The armature reaction in UM, which functions by means of the saturation of magnetic circuit, is the phenomenon, substantially nonlinear. Its effect can be taken into consideration by approximation methods.

4.3. Quantitative account of the demagnetizing effect of transverse armature field.

a). Method, based on the calculation of the resistors/resistances of the replacement schemes of magnetic circuit. The task of method is the determination of value of magnetic force $\Delta F_{\text{в}}$, numerically equal to $F_{\text{ад}}$, by which it is necessary to increase of magnetic force of excitation winding with the load so that emf UG would remain constant in comparison with emf of idling.

With this magnetic force of excitation winding $F_{\text{в.в}}=F_{\text{в}}+\Delta F_{\text{в}}$

$$\Phi_{\text{в}}=\frac{F_{\text{в}}}{R_{\text{мдх.х}}},$$

Pages 92-93.

Magnetic flux with the idling

where $F_{\text{в}}=k_{\text{в}}F_{\text{з}}+F_{\text{р}}+F_{\text{с}}$ is calculated for the appropriate construction/design of UG according to the formulas, led in chapter 3.

So that the value $\Phi_{\text{в}}$ would not be changed, it is necessary to have:

$$\frac{F_{\text{в}}}{R_{\text{мдх.х}}}=\frac{F_{\text{в}}+\Delta F_{\text{в}}}{R_{\text{мдн}}},$$

whence

$$\Delta F_{\text{в}}=F_{\text{в}}\left(\frac{R_{\text{мдн}}}{R_{\text{мдх.х}}}-1\right);\quad R_{\text{мдн}}>R_{\text{мдх.х}}.$$

Equivalent resistance $R_{нд}$ is computed from the appropriate formulas, given in Table 4-2. With the idling permeability $\mu_{ад}$ is determined only by field $H_{вд}$, while with the load of machine $\mu_{ад}$ for the sections of active region/core it is determined by resulting field H_f (in the inactive zone when $\Phi_в = const$ permeability is not changed). Value $\mu_{ад}$ is found with the help of curves $\mu_а = f(H)$ when $H = H_f$ (Fig. 4-3a), which can be constructed on the curves of magnetization of material. The intensity/strength of field H_f is computed from (4-4). For UG with the hollow magnetic rotor, taking into account the relatively small wall thickness of cylinder, the intensity/strength of armature field in the rotor it is possible to take for its mean diameter

$$H_{я.ср} = \frac{I_я}{\pi D} \cdot \frac{0{,}5 + \zeta - 1{,}5\zeta^2}{1 + \zeta - \zeta^2 - \zeta^3}; \quad \zeta = \frac{D_1}{D} < 1.$$

By knowing $\Phi_в$ and after calculating $R_{нд.х.}$ it is possible to find $F_в$ by this to check the calculation of magnetic circuit with the idling.

b). Method, based on the use of curves of simultaneous magnetization. According to this method it is determined directly by magnetic force $F_{в.н}$ taking into account the demagnetizing effect of reaction $F_{ид}$. During the calculation are used the curves of the simultaneous magnetization of materials by two orthogonal fields

H_d, B_d and H_q, B_q. Fig. 4-4a depicts the family of such curved in the form graphs $B_d=f(H)_d$ on H_q for magnetically soft steel. Three-dimensional/space dependence $B_d=f(H_d, H_q)$ corresponds to this family of curves.

The curves of simultaneous magnetization for the isotropic material can be obtained experimentally in the special toroidal samples/specimens with the orthogonal magnetizing coils or constructed according to the data of calculation with the use by usual curve of uniaxial magnetization, being based on the property of isotropy (4-5). For the construction they assign H_d and H_q, are found $H=\sqrt{H_d^2+H_q^2}$ and B for this value of H through the magnetization curve. Then $B_d=$ [redacted] compute

The calculation of value $F_{s.n}$ is produced in the following sequence:

1. Magnetic circuit with the idling on the sections is calculated, and induction B_{mxx} in each section is determined.

2. The intensity/strength of armature field H_{ni} in each section with assigned current I_n. is calculated

3. For retaining/preserving/maintaining the values of emf and

flow Φ_δ constant/invariable with the load must be correctly the equality $B_{\delta ix} = B_{\delta ix.x}$.

Knowing $B_{\delta ix.x}$ and H_{si} in the section, on the curve of simultaneous magnetization (Fig. 4-4), for which $H_{ci} = H_{si}$, they find $H_{si} = H_{di}$ for given value

4. Value of magnetic force $F_\delta + \Delta F_\delta$, which corresponds to one pole pair

$$F_{\delta.\delta} = \sum_{i=1}^{m} H_{si}\Delta l_i + k_\delta F_\delta,$$

is determined, where $k_\delta F_\delta$ - drop in the magnetic potential in the gaps;

Δl_i - length of the line of longitudinal flow in the i section.

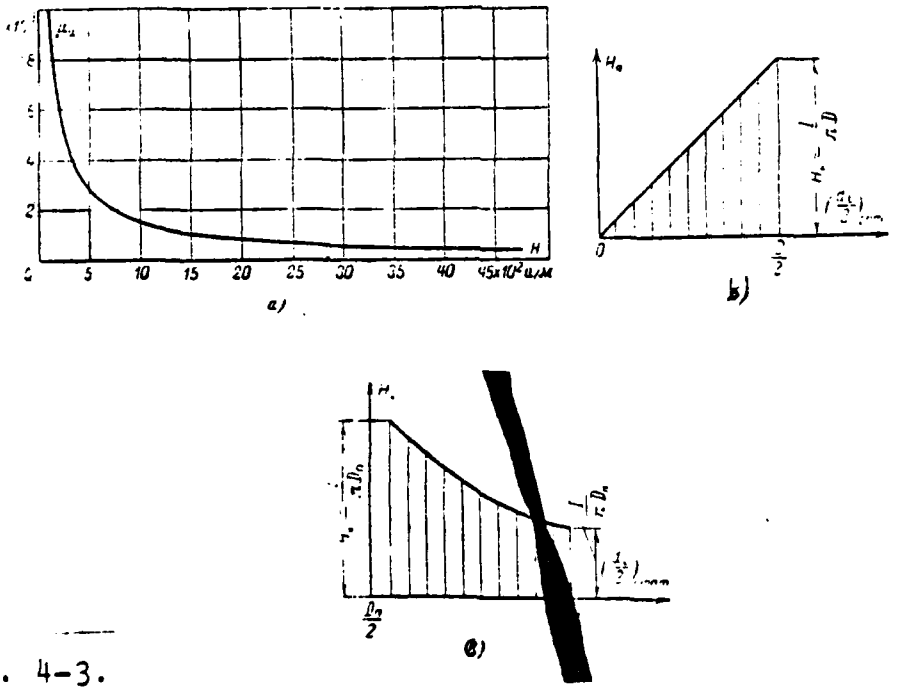

Fig. 4-3.

Fig. 4-3. Curves of a change in magnetic permeability and strength of field of UM. a) the dependence of magnetic permeability on the intensity/strength of field [illegible] for the magnetically soft material (of type of Armco); b) the field distribution of the armature of cylindrical UM in the rotor; c) the same in the stator.

Page 94.

In the absence among curves (Fig. 4-4) of dependence $B_d=f(H_d)$ on that obtained H_{qi} use interpolation.

The most analytical possible development of the set-forth method. The curves of simultaneous magnetization are approximated sufficiently well by the function of the form

$$H_d=\alpha_i \operatorname{sh} \beta_i B_d. \qquad (4\text{-}7)$$

Coefficients α_i and β_i with appropriate H_{qi} are determined according to the method of two selected points [84] on the basis of the relationships/ratios:

$$H_{d_1}=\alpha_i \operatorname{sh} \beta_i B_{d_1};\quad H_{d_2}=\alpha_i \operatorname{sh} \beta_i B_{d_2};$$

$$(H_{d_2}>H_{d_1}),$$

$$\frac{H_{d2}}{H_{d1}}=\frac{\operatorname{sh}(\beta_i B_{d2})}{\operatorname{sh}(\beta_i B_{d1})}=\frac{\exp(\beta_i B_{d2})-\exp(-\beta_i B_{d2})}{\exp(\beta_i B_{d1})-\exp(-\beta_i B_{d1})},$$

where $\exp(\beta_i B_{d_1})=e^{\beta_i B_{d_1}}$ and so forth.

Choosing point (H_{d_1}, B_{d_1}) so, in order to $\exp(-\beta_i B_{d_1}) \ll \exp(\beta_i B_{d_1})$ in this

case of peak (H_{d2}, B_{d2}) a similar inequality knowingly it is satisfied], we obtain:

$$\frac{H_{d2}}{H_{d1}} = \exp[\beta_i (B_{d2} - B_{d1})]; \quad \beta_i = \frac{\ln \frac{H_{d2}}{H_{d1}}}{B_{d2} - B_{d1}};$$

$$\alpha_i = \frac{H_{d2}}{\operatorname{sh}(\beta_i B_{d2})} \approx \frac{H_{d1}}{\operatorname{sh}(\beta_i B_{d1})}.$$

At the high values of argument $\beta_i B_{d2} > 6$ is correct $\alpha_i \cong 2H_{d2}\exp(-\beta_i B_{d2})$.

The values of coefficients α_i and β_i obtained for the plotted curves, given Fig. 4-4a, gives in the form of graphs in Fig. 4-4b as function of H_q.

With the analytical expression of the curves of magnetization of value H_{Bi} and $F_{B.H}$. (in sequence 3 and 4 presented above sequence of calculation) they find through the expressions:

$$H_{Bi} = \alpha_i \operatorname{sh}(\beta_i B_{Bi}); \quad F_{B.H} = \sum_{i=1}^{m} \alpha_i \operatorname{sh}(\beta_i B_{Bi}) + k_H F_b,$$

where α_i and β_i are determined from the curves, represented in Fig. 4-4b, for $H_q = H_{Bi}$.

Page 95.

In Fig. 4-4a as an example are compared experimental-design and analytical dependences $B_d = f(H_d)$ when $H_q = 70$ *a/cm*. Analytical curve (dotted line) is designed on (4-7).

c). Method is graph-analytic, successive approximations (B. S.

Khlusevich's method). Let us consider the methodology of account of magnetic force F_{qd}. briefly which is presented in [58] in connection with cylindrical generators with the expanded rotor. Methodology in the principle can be used also for acyclic machines of another construction/design.

For retaining/preserving/maintaining the value of emf is necessary the constancy of longitudinal flow Φ_δ, the invariability of induction $\overline{B_{\delta i}}$ in each section with a change in the load of armature from the idling to the nominal. It is possible to achieve the constancy of induction $\overline{B_{\delta i}}$ if increase magnetic force of excitation winding on

$$\Delta F_\delta = \sum_{i=1}^{m} \Delta F_{\delta i}, \qquad (4\text{-}8)$$

where $\Delta F_{\delta i}$ - necessary increment of magnetic force of excitation for the i section.

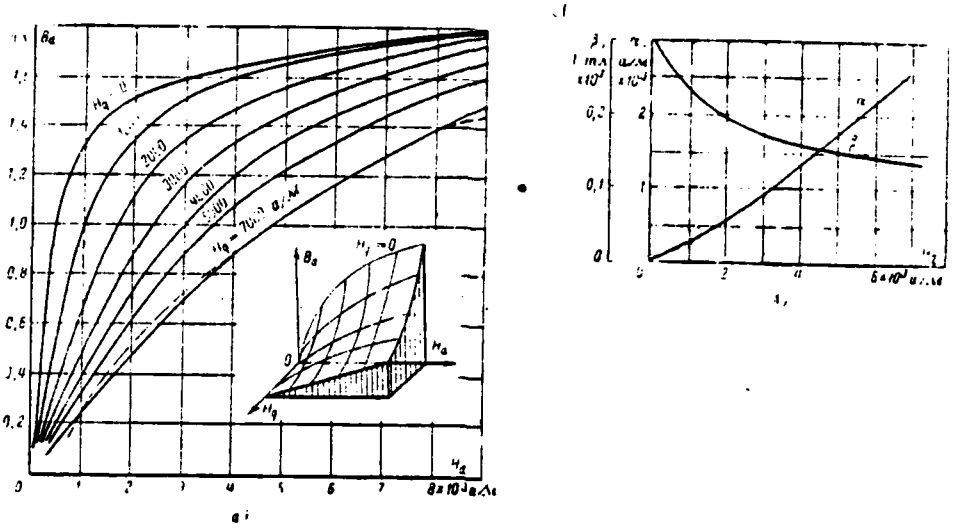

Fig. 4-4. On the calculation of magnetic circuit taking into account the demagnetizing effect of transverse armature field. a) the curves of simultaneous magnetization and three-dimensional/space dependence $B_d=f(H_d, H_q)$; b) the dependence of coefficients α_i and β_i on H_q (magnetically soft steel of the type of Armco).

Page 96.

According to [58] this increment can be determined in a following manner (let us consider method based on the example of cylindrical generator with the hollow rotor). Let us divide stator in the active region/core into m layers with thickness

$$\Delta l_i = \frac{D_a - D_a}{2m}.$$

We assume/set flow Φ_δ passing in the radial direction. For each

layer a drop in the magnetic potential with the idling along the longitudinal axis (partial magnetic force of excitation) comprises:

$$F_{ai} = H_{ai}\Delta l_i = \frac{H_{ai}(D_a - D_a)}{2m}.$$

Resulting magnetic force in the i section with the load

$$\mathbf{F}_i = \mathbf{F}_{ai} + \mathbf{F}_{ri}; \quad F_i = (F_{ai}^2 + F_{ri}^2)^{1/2},$$

where $F_{ri} = I_r$-magnetic force of armature, which functions along the transverse axis.

We construct diagram (Fig. 4-5), assuming material by isotropic, and also considering that hysteresis effects are absent and the corresponding vectors B and H coincide in the direction.

Resulting magnetic force $\overline{F_i}$ creates induction $\overline{B_i}$ of the resulting field, according to assumption vectors F and B coincide in the direction. After plotting along the axis of ordinates vector and along the axis of abscissas vector $\overline{F_{ai}}$ we find vector $\overline{F_r}$ by addition $\overline{F_{ai}}$ and $\overline{F_r}$ through the rule of parallelogram. After continuing $\overline{F_i}$ we will obtain direction of beam 01, on which vector $\overline{B_i}$ of the induction of the resulting field lies/rests. Value $\overline{B_i}$ thus far is not known, since permeability μ_{ai} is not known.

Let us decompose predicted vector $\overline{B_i}$ into two components: in the direction of longitudinal field $B_{ai(r)}$ (axis of ordinates) and in the direction of cross field $\overline{B_{ri}}$ (axis of abscissas), i.e., to the

orthogonal vectors of the induction of field of exictation with the load and the armature fields: $B_{в(н)} \perp B_{яf}$. Vectors $\bar{B}_f$, $B_{в(н)}$ and $B_{яf}$ are obtained tentatively taking into account the saturation of the active region/core of magnetic circuit with the load of machine, therefore, $B_{в(н)} < B_{в(х.х)}$. For satisfaction of condition $B_{в(н)} = B_{в(х.х)}$ it is necessary that by the hodograph of vectors B_f there would be straight line 2-2 (Fig. 4-5), which passes at height/altitude $B_{в(х.х)}$ from the origin of coordinates, value $B_{в(х.х)}$ was known from the calculation of the magnetic circuit of machine with the idling. On the other hand, with the fixed/recorded load of machine $I_н = \text{const}$ there will be $F_{яf} = \text{const}$ and $H_{яf} = \text{const}$ for each layer of the magnetic circuit of stator. Consequently, the hodograph of vectors F_f is straight line 3-3.

Page 97.

The determination of supplementary magnetic force for the i section

$$\Delta F_i = F_{вδi} - F_{яi}$$

in accordance with that presented is produced while the conducting on vector diagram of ray/beam 04 on the following diagram (by successive approximations):

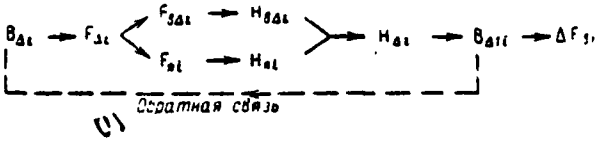

Key: (1). Feedback.

Feedback serves for comparison $B_{\Delta i}$ and $B_{\Delta ii}$: if the obtained value of the induction of resulting field $B_{\Delta ii}$ differs little from selected value $B_{\Delta i}$, then supplementary magnetic force $\Delta F_{\Delta i}$ is found correctly.

Otherwise is conducted another ray/beam, for example 05, and entire process of calculations is repeated before reaching/achievement of the equality

$$B_{\Delta ii} \approx B_{\Delta i}.$$

The checking indicated can be led, also, on the basis of the proportion

$$\frac{B_{\Delta i}}{H_{\Delta i}} = \frac{B_{\text{в}\Delta i}}{H_{\text{в}\Delta i}} = \mu_{\text{в}i},$$

with the help of the magnetization curve.

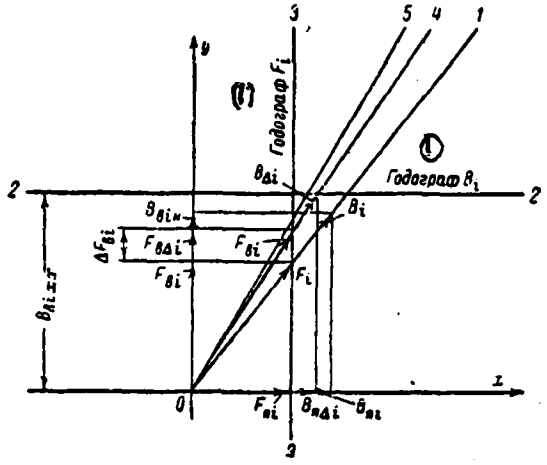

Fig. 4-5. Vector diagram for determining supplementary magnetic force in the i section of magnetic circuit.

Key: (1). Hodograph.

Page 98.

After making the similar actions m of times (with respect to a number of sections of separation) it summed up $\Delta F_{\delta i}$ according to formula (4-8), we will obtain the unknown increment of magnetic force of excitation winding, equal numerically to value of magnetic force $F_{\delta i}$.

The methods presented are suitable for all constructions/designs of UG of direct current with the electromagnetic excitation during

the circular current pickup. It is possible to spread them to engine operating mode of UM. The accuracy of methods is higher, the greater the number of sections m, but the labor expense for calculation simultaneously with increase of m increases. As showed the series/row of the calculations conducted for UG of different construction/design usually sufficient to take m=4-6. With increase in m doubly the accuracy is raised insignificantly.

Two first methods ensure the virtually identical accuracy of calculations.

From the work experience it came to light, that the method, based on the use of curves of simultaneous magnetization, is more convenient.

4.4. On performance calculation of UG with the help of the reactive/jet triangle.

After determining $\Delta F_0 - F_{ad}$ for different currents I_a and also a voltage drop in internal circuit of armature, from these parameters it is possible to construct for each value of armature current reactive/jet (characteristic) triangle UG. Its difference from the same for the DC commutating machines consists of a change in horizontal leg F_{ad} also in the straight portion of no-load

characteristic (with the low currents of excitation). In the machines of direct current this leg is received in the linear section of this characteristic as constant/invariable, since it is determined in essence by longitudinal armature reaction. In UG it is caused only by the longitudinal effect of transverse reaction. With the help of the reactive/jet triangles and no-load characteristic of UG, calculated by usual methods, it is possible to construct when $I_{в.-var}$ all other characteristics of UG (load, external, regulating, short-circuiting). The methods of construction are similar used in the DC commutating machines [7]. Calculated and experimental characteristics of experimental model of UG are compared in Chapter 10.

Page 99.

4.5. Devices/equipment for compensation and decreasing the back induction of armature field.

a). Subdivision of devices/equipment.

Longitudinal-demagnetizing magnetic force of transverse armature reaction in UG according to the data of the calculations conducted and experiments can comprise to 80-90% of magnetic force of excitation with the idling. This increase in magnetic force for the maintenance by constant/invariable emf UG causes a considerable

increase in the space of the excitation winding and sizes/dimensions of machine. Furthermore, the saturation of magnetic circuit by armature field decreases ranges of adjustment of voltage/stress UG with the load. For the purpose of the elimination of these deficiencies/lacks different devices/equipment for compensation and decreasing the back induction of armature field are applied. Let us note that in the DC commutating machines pole face winding serves as means for the distortion elimination of main field and decrease in the maximum voltage/stress between the adjacent plates of collector/receptacle [7].

The devices/equipment indicated according to the operating principle are identical for all UM and can be divided into two groups.

First group - compensative "windings", included consecutively/serially in the circuit of armature of UM, but having direction of flow, opposite to its direction in the armature.

The second group - devices/equipment, which increase reluctance for the cross flow how is achieved a decrease in the demagnetizing effect of magnetic force of armature.

In the UM different combinations from these devices/equipment,

which relate to the different groups, are possible. Overall deficiency/lack in the given devices/equipment - complication of construction/design of UM, and also in the majority of the cases the undercompensation for armature reaction. To completely compensate armature field of UM is possible only in the case, when the spatial distributions of currents in pole face winding and armature will be the mirror images. The classification of devices/equipment conducted of the groups made it possible to propose some of their new varieties for separate acyclic machines. Let us consider construction/design, elements of calculation and characteristic of devices/equipment of both groups based on the examples of different UM.

Pages 100-101.

B). Compensative "windings" in the circuit of armature.

Pole face winding in the form of the hollow cylinder, arranged/located coaxially with the massive or hollow rotor of cylindrical UM, it is shown in Fig. 4-6a, b. Winding can be implemented from the ferromagnetic or nonmagnetic (copper) material. Is compensated armature field only in the stator, its demagnetizing effect in the ferromagnetic cylinder is not prevented. Magnetic field in the limits of cylinder from passing on it current I_a

$$H_{\text{вн}} = \frac{I_a}{\pi d_i} \frac{x^2 - \zeta^2}{1 - \zeta^2}; \quad x = \frac{d_i}{D_{\text{в.н}}};$$

$$\zeta = \frac{D_{\text{в.в}}}{D_{\text{в.н}}}; \quad D_{\text{в.в}} \leqslant d_i \leqslant D_{\text{в.н}}.$$

The diagrams/curves of the magnetic fields of armature, pole face winding and resulting field (it is shaded) are represented in Fig. 4-6. An increase in the nonferromagnetic gap/interval for flow Φ_δ in the machine is a deficiency/lack in copper pole face winding. As a result of the smaller electrical conductivity of magnetic material the thickness of pole face winding prepared from it proves to be considerable. In this case the part of the magnetic circuit of stator in the limits of winding is compensated not completely. In UM with the hollow nonmagnetic rotor and by nonmagnetic pole face winding is achieved complete (100%-) compensation. It occurs also in UM with two hollow nonmagnetic rotors, which revolve in opposite sides [87]. Similar UM can be named autocompensated (self-compensated). Complete compensation can be reached in UM with rod armature and pole face windings. Deficiency/lack in bar windings - presence in working gap of UM radial component fields separate rods, distorting main field, and also appearance of pulsating losses.

Internal and outside diameters of cylindrical pole face winding:

$$D_{\text{в.к}} = D + 2\delta; \quad D_{\text{н.к}} = \sqrt{D^2_{\text{в.к}} + \frac{4I_\text{п}}{\pi j_{\text{к.о}}}}. \qquad (4\text{-}9)$$

For the steel windings one should tentatively accept:

$$j_{\text{к.о}} \approx j_\text{м} \sqrt{\frac{\rho_\text{м}}{\rho_\text{с}}},$$

where $j_{\text{к.о}}$ - current density in the winding;

$j_м$ - permissible for reasons of heating current density in copper;

$\rho_м, \rho_с$ - the specific resistances of copper and steel.

The removal/diversion of current is the limiting case of compensation with the help of the magnetic winding directly through the body of the magnetic circuit of stator (Fig. 4-6c). The parts of the magnetic circuits, which have the electric potentials of different signs, must be isolated of each other.

The compensators of disk UM (Fig. 4-6e, f) should be implemented in the form of the system of the discharge ring busbars and cylindrical plugs, coaxial with the current carrying shaft of machine. The sizes/dimensions of plug are determined by the relationships/ratios, similar (4-9). Thickness of disk busbar at the appropriate diameter

$$b_i = \frac{kI_н}{\pi j_i d_i},$$

where k=1 during the one-sided current pickup on the shaft and k=0.5 with the bilateral; j_i - current density in the busbar at diameter d_i.

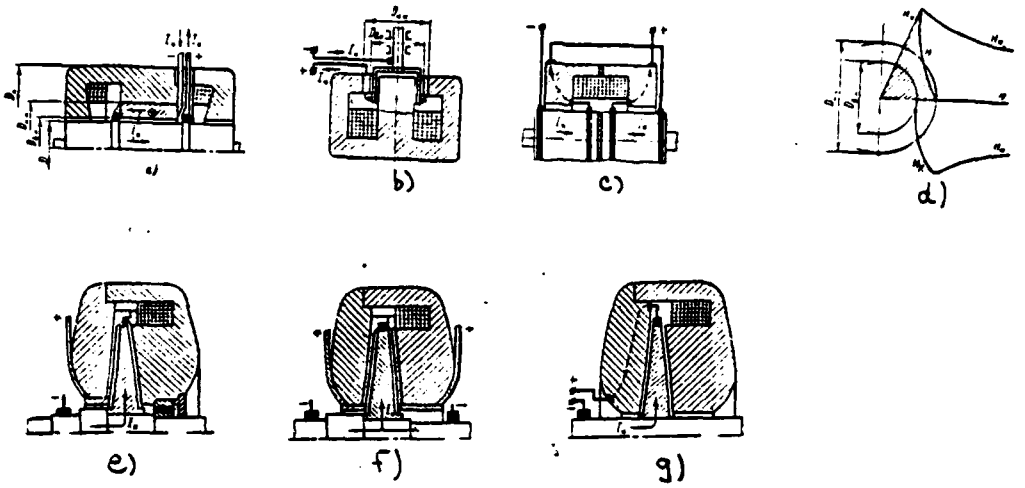

Fig. 4-6. Unipolar electrical machines with the compensators. a, b) cylindrical UM with the massive and hollow rotors and compensative "windings" (cylindrical "bifilar"); c, g) cylindrical and disk UM with the removal/diversion of current on the stator; e, f) the compensated disk UM with one- and bilateral current pickup on the shaft; d) the diagram/curve of the resulting magnetic field of armature current in the cylindrical UM with the compensative "winding".

Pages 102-103.

The electrical resistance of the busbar of conical profile/airfoil is computed from the formula, analogous (2-22). Deficiencies/lacks in the nonmagnetic discharge busbars and discharge rods are similar indicated above for the cylindrical machines. In the disk UM is also possible the use of a magnetic circuit of stator for

the current tap (the limiting case of compensation, Fig. 4-6g).

C) devices/equipment for an increase in the reluctance to the cross flow of machine.

An increase of the reluctance in the quadrature circuit is achieved by introduction on the magnetic path Φ_a of the nonmagnetic separators, arranged/located radially in the planes, passing through UM the rotational axis. As experiments showed, the demagnetizing effect of armature field with the help of such separators is weakened/attenuated to a considerable degree. The device/equipment of the stator of cylindrical machine with three separators is shown in Fig. 4-7a. Magnetic circuit it is possible and not to cut completely on a radius (Fig. 4-7b). Construction/design with the internal slots/grooves is correct, since armature field near the external surface of stator is weaker than about the internal. The thickness of nonmagnetic separator can be approximately determined according to the expression

$$\delta_{\text{м}} \approx \frac{I_a - 0{,}5H_{a.cp}(D + D_a + 2\delta)}{m_{\text{м}}\left(\frac{1}{\mu_0} B_{a.cp} - H_{a.cp}\right)}, \qquad (4\text{-}10)$$

where $m_{\text{м}}$ - number of separators; $H_{a.cp}$, $B_{a.cp}$ - permissible for reasons saturations the parameters of armature field at the mean diameter of the magnetic circuit of stator. The equivalent reluctance of linings for the cross flow must comprise

$$R_{\text{м.в}} = \frac{2m_{\text{м}}\delta_{\text{м}}}{\mu_0 l_{\text{в}}(D_{\text{в}} - D)} \gg R_{\text{м}q},$$

where $l_{\text{н}}$ - axial length of nonmagnetic separator in the active region/core.

Estimate of the magnitude $H_{\text{н.ср}}, B_{\text{н.ср}}, R_{\text{нн}}$ is given in §4-2. The number of linings $m_{\text{н}}$ must be chosen so that the inequality $\delta_{\text{н}}<2\delta$ would be correct. In this case the branching of the parts of flow $\Phi_{\text{н}}$ around the separator through the working gap of UM is insignificant. Radial separators it is possible to weld, also, into the magnetic cylinder of pole face winding (Fig. 4-7c) for decreasing the consequences of undercompensation in this section of magnetic circuit. Size/dimension $\delta_{\text{н}}$ is determined similarly (to 4-10). Analogous devices/equipment it is possible to use in the active region/cores of cylindrical UM with the hollow rotor and disk UM.

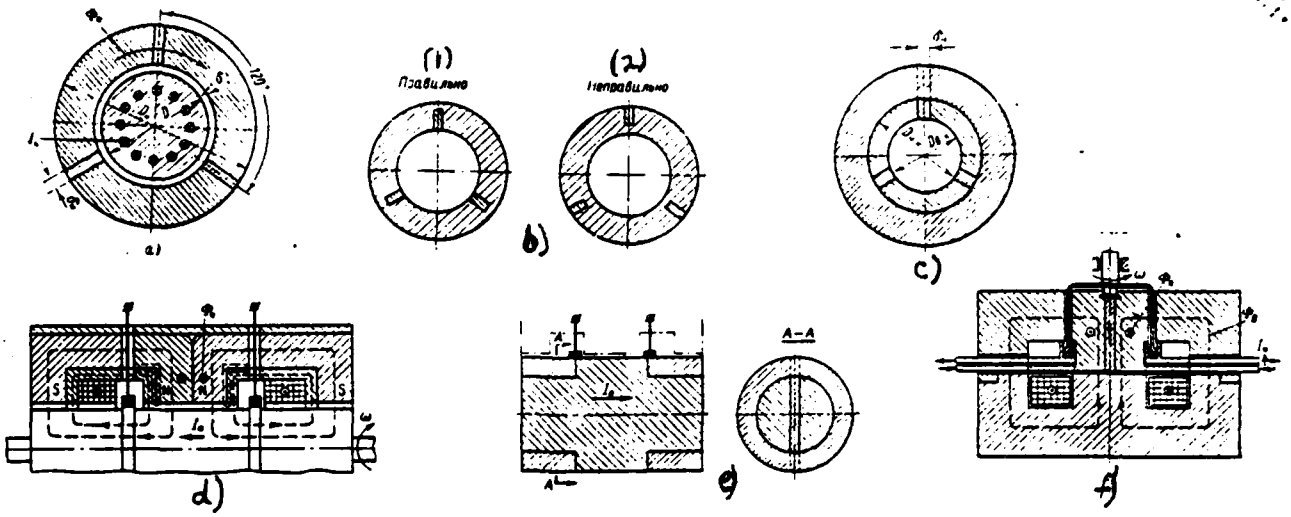

Fig. 4-7. Devices/equipment for decreasing the demagnetizing effects armature of UM. a) nonmagnetic separators in the stator; b) the same with the incomplete radial section of stator; c) nonmagnetic separators in the ferromagnetic compensative cylinder; d) inductor from the permanent magnets; e) nonmagnetic insert in the rotor; f) the compensated machine with the hollow rotor and the nonmagnetic separator in the internal magnetic circuit of stator.

Key: (1). It is correct. (2). It is incorrect.

Page 104.

The limiting case of these devices/equipment is excitation of UM from the permanent magnets. The reluctance of the inductor of these UM is great. In those proposed [76] UM with the combined excitation

the magnetic shunts, utilized with regulating of voltage/stress, have the radial gashes, which prevent their saturation by armature field (Fig. 4-7d).

As an example of the use/application of nonmagnetic separators in the massive rotor of UM, where a drop in the magnetic potential with the load is especially considerable, serves proposition [88]. Rotor has the special construction/design, which ensures its mechanical strength (Fig. 4-7e). During the circular current pickup the lateral surface of rotor is equipotential, and nonmagnetic separator will not cause the pulsations of current. Structural/design advantages possesses [89] compensated proposed UM with the hollow rotor. Its difference is in the passage of the current of the circuit of armature on the internal core of stator in the direction, opposite to direction of flow in the rotor. In this case the compensation for field in the external magnetic circuit of stator (Fig. 4-7d) is achieved. For preventing the saturation by the field of the current, occurring in terms of the internal core, the latter is divided by nonmagnetic radial separator. Thus, given UM represents an example of the use/application of devices/equipment of both groups.

Compensated UM (or with the nonmagnetic separators) can have higher ampere-conductors per inch, better use of active materials, smaller over-all payload ratio, and with the identical

electromagnetic loads with those not compensated UM and larger efficiency. A question about the advisability of applying one or the other device/equipment must be solved by the appropriate calculation during the design of concrete/specific/actual machine. Let us note that in contrast to the bipolar machines an increase of the working gap in UM leads only to to the relative (in comparison with F_δ) decrease of magnetic force F_{ma}. In the progressive/forward UM (electromagnetic pumps, MHD generators) the back induction of magnetic force of armature is relatively small, since flow Φ_δ passes through nonmagnetic gaps. In them has a value the distortion of field by transverse armature reaction, adversely affecting the working process. For eliminating this effect the shaping of channels in the active region/core of machines and different compensators are used.

Page 105.

Chapter Five.

LIQUID-METAL SLIDE CONTACT OF HOMODYNAMO.

5.1. Problem of slide contact for acyclic machines.

The movable electrical contact of current-tap apparatus - most complicated part is the UM of direct current. In the UM there is no collector/receptacle, which consists of the separate isolated/insulated plates, and there is no clearly expressed commutation with a change of direction of flow in the conductors of armature. With the realization of current pickup into the UM the process of the concealed/latent commutation, during which external circuit is closed all by new elementary conductors, occurs. Armature of UM of any type is as if commutator, which has an infinite number of elements/cells. The process of commutation of UM during the brush and circular liquid-metal current pickup is clarified with the help of Fig. 5-1. Circular liquid-metal current-tap apparatus is accepted

by conditionally consisting of the infinite series of parts. The fundamental need for commutation into the UM of direct current escape/ensues from the following relationships/ratios for the emf and the magnetic flux:

$$e = -w_a \frac{d\Phi_s}{dt} = \text{const};$$

$$\int e\,dt = -\int w_a d\Phi_s;$$

$$\Phi_s = -\frac{e}{w_a} t + \frac{C}{w_a},$$

where C - arbitrary integration constant.

Page 106.

With $e \neq 0$ flow Φ_s in the unchanging duct/contour of the circuit of armature must continuously grow in the absolute value with an increase in time t, which is impossible.

There is also a proof of the need for slide contact into the UM based on the geometric theory of electrical circuits [90].

As a result of the special features/peculiarities of magnetic system of the UM is series connection of the conductors of armature winding for the purpose of an increase in the voltage/stress due to an increase in the number of "turns" w_a possibly only by means of the slide contacts. Separate rods or groups of the rods of winding are derived/concluded to the independent pair of slip rings. Each

current-tap apparatus must rely on complete operating current. Therefore during the brush current pickup due to the large losses in the contact of UM they did not have advantages in comparison with the appropriate commutator machines, and attempts at the use UG to the voltages/stresses 200-500 V were not justified. With the low voltages of UM with massive armature ($w_a = 1$) and brush current pickup they can possess some advantages over commutator machines. However, with the high currents, characteristic of the UM, a number of brushes in the slide contact it is great, and it is difficult to ensure uniform current distribution between them due to the special features/peculiarities of the conductivity of sliding contact. This fact leads to the overloading of separate brushes and their output from the system; therefore the reliability of the operation of the large groups of brushes is low. For an improvement in the work of brush apparatus the blowout and water cooling [9, 57, 91] are applied, but these measures do not give the radical resolution of the problem of brush current pickup.

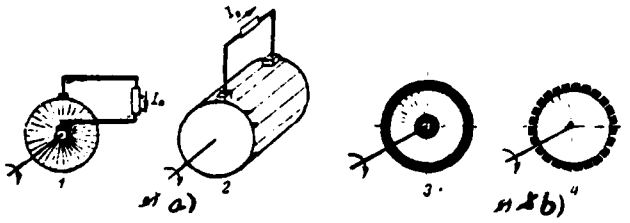

Fig. 5-1. Explanation of the process of commutation into the UM. a) for the disk (1) and cylindrical (2) of machines with the brush current pickup; b) for machines with the circular liquid-metal current pickup; 3 - real picture; 4 - conditional.

Page 107.

Different brands of brushes for the electrical machines allow/assume the relative speed in slide contact $v_к$=10—45 m/s and current density $j_к$=(6-20)10⁴ A/m² (on special TU for the brushes МГС-7 $v_к$=55 m/s and $j_к$=27·10⁴ A/m²) on the collector/receptacle. On the slip rings it is possible to allow a somewhat larger value $v_к$. At the increased speeds the stability of the work of contact due to the vibrations is broken and sharply grow losses to friction, especially with the high currents and in the considerable surface areas of friction, caused by low value $j_к$.

With the contact of the metal electrodes of contact the so-called contact resistance is formed. It is caused by the cover

"films of fogging" (or by admixed films), that consist of oxides, sulfides of metal, water compounds, adsorbed gases, etc. These films appear with surface contact of electrode with the surrounding atmosphere. By their physical nature they are dielectrics or semiconductors and cause a voltage drop, as a rule, which exceeds in the value a voltage drop on entire electrode. Furthermore, the surfaces of solid electrodes even during the careful working/treatment are not ideally flat, on them there are flanges, protuberances/prominences of roughness. Because of this the contact of two solid electrodes it occurs not by the entire apparent geometric surface area, but only in the series/row of isolated points, on which is passed the electric current through the contact.

The value of contact resistance depends on specific pressure on the electrodes, since with an increase in the pressure the cover films are destroyed in the separate places, a quantity of points of contact of electrodes grows. The decomposition of films leads to the appearance of a local metallic contact between the electrodes. But even in the absence of this contact of film they allow/assume the passage of electric current due to the intrinsic conduction, which depends on physical nature of films.

Contemporary theory [92, 93] gives qualitative and partially quantitative prerequisites/premises for determining the contact

resistance in essence. experimental data play sizable role in this question. This is explained by the complexity of physical processes in the electrical contact and by their dependence on a large number of environmental factors.

The basic condition/positions of the theory of motionless electrical contact can be spread to the case of relative electrode travel.

Thus, the contact of solid electrodes occurs not over the entire apparent contact surface, but on the small regions, called a-spots, where the material of electrodes at the contact pressure reaches the boundary of yield.

Page 108.

With the connection to the electrodes of voltage/stress the effect of the contraction of current to a-spots [92] is created, and current is distributed unevenly in the plane of contact transition/junction. In the absence of metallic contact in the fields of contraction the conductivity is created by contact effects. They distinguish the following three effects.

Tunnel effect, or the passage of microparticle (electron)

through the potential threshold, i.e., through the region of space on the boundary of electrodes, in which potential energy of the particle of more than its total energy. Tunnel effect appears at the contact pressure, sufficient for decreasing the thickness of cover films to the monomolecular. The conductivity of contact transition/junction has electronic character. The voltage/stress applied to the electrodes creates the electric field, which reduces the potential threshold for the electrons on the surface of metal, ensuring the conductivity of contact.

The effect of warping (quetsch-effect), i.e., formation/education at the relatively larger contact pressures of cracks and slots in the films, when between the electrodes metallic bridges appear.

The fritting-effect, i.e., the formation/education of metallic bridges under the action of high electric intensities in the films (on the order of 10^{8} V/m), which cause the electrical breakdown of films, then by thermal test/sample and the fusing of electrodes in the contact regions of contraction.

The electrodes of brush contact are covered relative to with thick film, and conductivity is determined by the fritting-effect. For achievement of breakdown electric intensity they are necessary

depending on the material of electrodes contact voltages/stresses $\Delta U_к \approx 0{,}3 \div 0{,}7$ V. This causes considerable electrical losses. For example, with current $I_к = 10^4$ a and $\vartheta_к = 60$ m/s total (mechanical and electrical) losses in the brush current pickup can reach 70 kW, that the UM decreases efficiency and it complicates the construction/design of catalytic gas recombiner (Fig. 1-2).

Overcoming deficiencies/lacks in the brush contact is possible with the help of the current pickup on the base of liquid metal. In the bipolar machines of direct current its use/application in principle is excluded, since liquid metal would close shortly the plates of collector/receptacle. In acyclic machine the contact surface of armature is equipotential.

During the liquid current pickup the space between the solid electrodes is filled with molten metal, which covers entire apparent contact surface. Because of a good wetting metallic or quasi-metallic contact is created over the entire surface.

Page 109.

Considerable current is passed already with small contact voltages/stresses due to the large area and the small thickness of cover film, in spite of its high specific resistor/resistance.

Fritting effect (and partially tunnel effect in the liquid-metal contact occurs more intensely than in the brush; even at a small hydrostatic pressure in this case is formed more than the a-spots. For the onset of fritting-effect and reaching/achievement of the intensities/strength of field $\approx 10^8$ V/m the voltage/stress in the contact only of order 0.01 V is required. A good thermal conductivity of contact liquid contributes to the best cooling of current pickup, which makes it possible to allow current densities in contact on the order of 10^7 A/m^2 (highest $j_к$ they are attained in the contacts with the circulation of the liquid metal, cooled in the special devices/equipment).

In this case the necessary surface area of current pickup will be small, which makes it possible to allow speeds $v_к \approx 100$ m/s and it is above. Both electrical and mechanical losses in the liquid contact it is less than in the brush.

The liquid metal (mercury) they began to apply for the electrical contact (disruptive and sliding) already long ago: M, Faraday in 1822, P. Barlow in 1824, G. Ampere in 1828-1833 and so forth [1-3]. N. Tesla later proposed several slide contacts, in which mercury was placed in the revolving jacket/case/housing, and disk was stationary electrode. However, these contacts were unsuitable for the high currents and the speeds. The knife zonal contact worked out by

B. I. Ugrimov [6] was the first attempt at the use/application of a liquid-metal contact in large/coarse UG. It made it possible to remove/take current to 400 A at the relative speed of mercury in the revolving rim of disc armature UG $v_к \approx 300$ m/s (Fig. 5-3). For the cooling from above mercury the water filled. During the calculation of the depth of the furrow of rim and insertion/immersion of knife into the liquid its motion was considered as the motion of vessel in the channel of insignificant depth. Problem was solved on the basis of the corresponding equation of N. Ye. Zhukovskiy, the action of gravitational force on the liquid was substituted by the action of centrifugal force, the curvature of channel was not considered. Experiments came to light/detected/exposed the greater consumption of mercury as a result of the evaporation on the knife and to a lesser degree due to the sputtering (about 14 g/h), which made a contact virtually unsuitable. Subsequently it was substituted brush. Let us note that such high speeds ($v_к$) in the liquid-metal contact are not achieved/reached, until now. In the contemporary stage use as the working fluids of contacts mercury, its alloys, and also light alkali metals. The alloy of sodium and potassium with eutectic composition of 22% Na, 78% K has a melting point $t_{пл} \approx -11°C$, thanks to which it are conveniently used in the current-tap apparatus.

AD-A139 778 UNIPOLAR ELECTRIC MACHINES WITH LIQUID-METAL CURRENT PICKUP(U) FOREIGN TECHNOLOGY DIV WRIGHT-PATTERSON AFB OH A I BETTINOV ET AL. 08 MAR 84 FTD-ID(RS)T-1205-83 3/6

UNCLASSIFIED F/G 9/3 NL

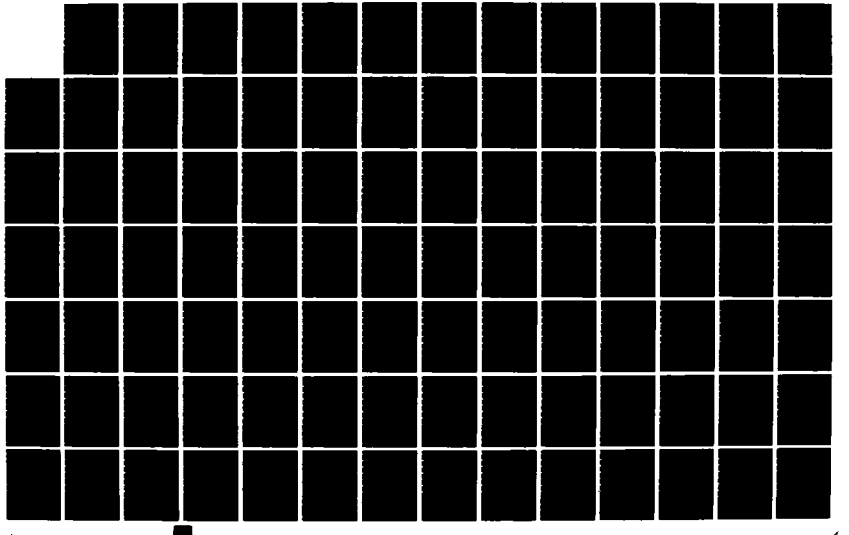

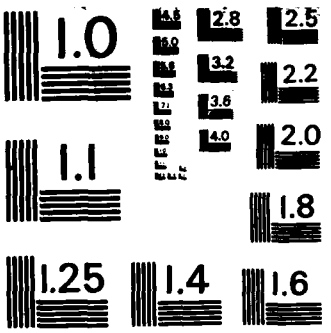

MICROCOPY RESOLUTION TEST CHART
NATIONAL BUREAU OF STANDARDS-1963-A

In recent years for the electrical machines gas contact [94] is proposed also. Contact can be unguided or can have control electrode, similar to the grid of tube. Is of interest research of the possibilities of applying such contacts in the current pickup of the UM.

The exemplary/approximate classification of movable electrical contacts of UM is represented in Fig. 5-2. Liquid-metal current pickup is feasible two forms: continuous circular and zonal - jet-edge or knife. On the technological reasons (thermal expansion, bearing clearances, decomposition from the corrosion) the submersion depth of electrode into the metal and its width must be not less than 0.5-0.8 mm. With the large diameters of rotors this gives the considerable area of the moistened surface in the slit ring terminal. Therefore at speeds $v_к$=120 m/s mercury current pickup (to avoid excessive losses to friction due to the large specific specific gravity/weight of mercury) is made only by the jet-edge [95, 96]. Some types of liquid contacts are shown in Fig. 5-3. The complete insertion/immersion of rotor of UM into liquid metal [46] is the limiting case of continuous circular current pickup. By the example to constructions/designs of UM, by the differing hermetic sealing/pressurization of liquid-metal contact and as its automatic filling under the action of the helical spindles, serves the proposed in the MAI converter of an alternate-constant current with disk of UG and shielded induction motor (Fig. 5-4).

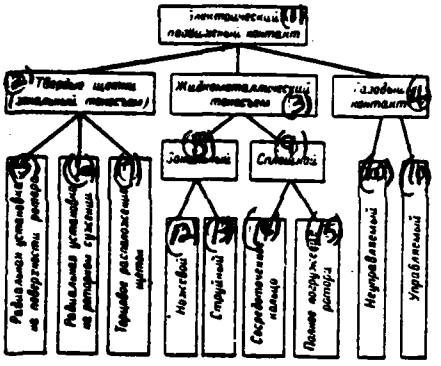

Fig. 5.2. Diagram of the classification of slide contacts for the unipolar electrical machines.

Key: (1). Electrical movable contact. (2). Solid brushes (zonal current pickup). (3). Liquid-metal current pickup. (4). Gas contact. (5). Radial surface mounting of rotor. (6). Radial installation during the rotor contraction. (7). End-type arrangement of brushes. (8). Zonal. (9). Continuous. (10). Uncontrollable. (11). Controlled. (12). Knife. (13). Jet-edge. (14). Concentrated ring. (15). Complete insertion/immersion of rotor.

Page 111.

Contact with the automatic filling with liquid metal, but based on other principle (pumping action of the eccentrically arranged/located electrodes), is described in [97].

In works [14, 47, 48, 87] slow ($v_к$ <20 m/s) slit ring terminals UG with the hollow rotor are investigated. It is indicated that for the more stable work of contact the rotating electrode (Fig. 5-3b) must be external with respect to the motionless. In the stable position of the liquid metal, which has in similar contacts the form of gently one-and-a-half, is necessary the equilibrium of four forces, which function on the metal: gravitational, centrifugal, electromagnetic (caused by interaction of electric current in the contact with the stray field of UG and by proper field of current) and frictional force.

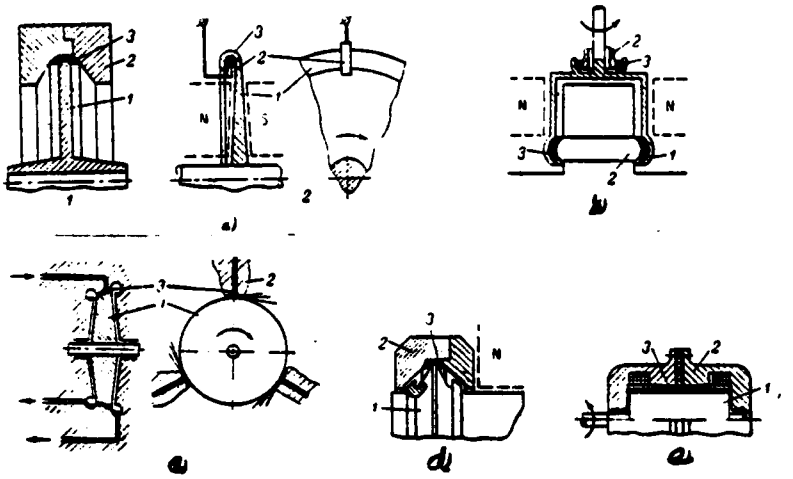

Fig. 5-3. Varieties of liquid-metal contacts. a) B. I. Ugrimov's contacts - initial circular (1) and knife zonal (2); b) the slit ring terminals of the semitoroidal type of D. A. Watt; c) the jet-edge shaped contact of P. Klaudi with the channels for the collection of mercury; d) the circular "floating" contact of Yu. Yu. Kaunas (development of the initial ideas of B. I. Ugrimov); e) the complete insertion/immersion of rotor into the liquid metal; 1 - rotating electrode; 2 - stationary electrode; 3 - liquid metal.

Page 112.

Mercury contacts of such type are more stable with the current overloadings, than contacts on the base of light metals, since the latter the action of electromagnetic forces relatively more strongly affects. In the high-speed slit ring terminals the effect of centrifugal force prevails and they are more stable.

The development of different liquid contact systems made it possible in essence to solve the problem of current pickup for UG over a wide range of power. In contemporary UG of large power is applied the sodium-potassium contact both jet-edge with $v_ж \approx 165$ m/s [20] and circular with $v_ж \approx 150$ m/s [13, 16-18].

In the machines of a small and average/mean power they are used both mercury (or mercury-indium) and sodium-potassium current pickups of both forms [12, 15, 46, 48, 96]. Further progress is feasible during the improvement of protective coatings for guaranteeing the prolonged service life of electrodes during the flow of liquid metal and the creation of the reliably hermetically sealed constructions/designs of UM, not allowing/assuming the leak/leakage of inert gas and vapors of metal.

Circular current pickup on the base of light metals is most promising, since the UM does not require special circulation loops with the auxiliary liquid-metal pumps and does not break electromagnetic symmetry. During the correct design in it it is possible to ensure low losses to friction at the high linear velocities.

Let us note that in the unipolar electric motors (UD) in contrast to UG the use/application of those systems of the liquid-metal contacts, which allow/assume the supply of metal into the current pickup only during the rotation of rotor, is undesirable. The use/application of such contacts would complicate launching/starting engine due to a break in the circuit of armature.

Liquid-metal contacts of UD are examined in Chapter 8.

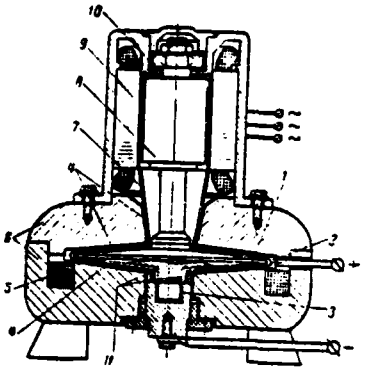

Fig. 5-4. Construction/design of the converter of an alternate-constant current with the shielded engine and non-polar dynamo, which has the airtight liquid-metal contact (MAI). 1 - rotor UG; 2 - peripheral contact; 3 - axial liquid-metal contact and journal bearing; 4 - electrical insulation; 5 - excitation winding; 6 - magnetic circuit of stator of UG; 7 - metal shield; 8 - rotor of induction motor; 9 - stator of engine with the three-phase winding; 10 - insulating plug; 11 - screw thread.

Page 113.

5.2. Hydrodynamic, magnetohydrodynamic, electromagnetic and surface phenomena in the contact.

The simplest model of slide contact of UG is schematically shown in Fig. 5.5a. During the analysis of hydrodynamic processes [1] with the help of the boundary-layer theory [98] they usually disregard the

axial displacements of liquid in the end-type gap s between the jacket/case/housing and the disk, and phenomena in the radial clearance lead to the same in the end-type gap by the corresponding increase of the diameters of jacket/case/housing $D_{2к}$ and disk $D_к$.

FOOTNOTE [1]. In more detail questions of hydrodynamics of contact are examined in Chapter 8 in connection with work of UD. ENDFOOTNOTE.

The design of collector shoe gear is produced, on the basis of the conditions:

a) the normal position of liquid-metal layer in the circular device/equipment;

b) the minimum losses of friction, which is determined by the layout of electrodes and by air-gap clearance;

c) minimum electrical losses in the zone of current pickup.

The solution of the first two problems is most complicated.

In the correctly planned liquid-metal collector shoe gear liquid layer must occupy normal position of equilibrium in the annular channel, without escape/ensuing from it during all possible operating

modes of the UM.

In the general case to the liquid layer in the annular channel there acts the forces: centrifugal, appearing as a result of rotating the rotor, electromagnetic, being corollary interactions of the current of load, passing through the contact liquid, and magnetic field in the contact zone, gravitational and frictional force.

Page 114.

The complexity of problem is determined by the fact that the value and the direction of these forces complicatedly and differently depend on the physical properties of liquid and magnetic intensity in the zone of contact, geometry and quality of working/treatment of channel, strength of current of load and speed of rotation of rotor.

The problem of calculating the contact consists in during all operating modes cumulative effect of all forces in the contact liquid not breaking its position of equilibrium and, therefore, would be ensured reliable efficiency of UM.

With the work of UM the position of liquid in the annular channel is determined by interaction of centrifugal and electromagnetic forces, gravitational forces are usually small and

have a value only at small linear velocities in the contact, when centrifugal forces are insignificant.

The frictional forces, directed tangentially, on the position of contact liquid in the cross section of circular current pickup virtually an effect do not have.

The calculation of the position of liquid metal in the slit ring terminal of UG with the horizontal rotational axis upon consideration of electromagnetic forces is carried out in work [128]. Contact with the rounded electrodes [128, Fig. 66] is analyzed by the authors, in which liquid metal has a form of gently one-and-a-half. Internal electrode is revolving.

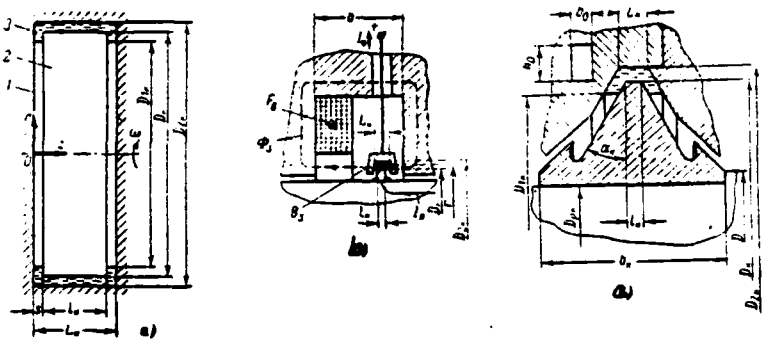

Fig. 5.5. Liquid-metal contact devices. a) the designation of the sizes/dimensions of the simplest model of slit ring terminal; b) to the calculation of the longitudinal (tangential) electromagnetic force, which functions on the liquid metal of contact; c) the designation of the calculated sizes/dimensions of slit ring terminal.

Page 115.

Calculations showed that the determining influence on the position of liquid metal exert the centrifugal forces. One should, however, note that the experimental functional check of the in question in [128] type of slit ring terminal is necessary.

Mechanical losses in contact $P_{к.т}$ are proportional to the product of the angular velocity ω to the moment of friction $M_т$, i.e. $P_{к.т}=\omega M_т$.

For determining the moment of friction of the moistened surface of rotary disk it is necessary to find specific tangential frictional force $\tau_н$, shearing stresses of frictional forces.

In accordance with Fig. 5.5a it is possible to examine shearing stresses and friction moment in two zones of friction:

a) faces of two sides of disk (M');

b) the surface between two concentric cylinders in the radial clearance (M").

Each force component of friction forms the appropriate friction moment.

The friction moment, which is determining mechanical losses in the contact, is equal to the sum of the friction moments, which function in the contact, i.e., $M_r = M' + M''$.

The physical picture of the processes, which occur in the gap between the rotary disk, submerged in the liquid, and the motionless jacket/case/housing, they depend on a number of Reynolds Re, sizes/dimensions of the end-type gap s and the properties of liquid.

Are distinguished two fundamental types of the motion of the liquid: viscous motion and turbulent. In the first case the layers of liquid are moved relative to each other, without being agitated, the secondly - the particle of liquid they move disorderly, in the fluid

flow they appear turbulence. As the criterion, by which they judge the character of the motion of liquid, serves the Reynolds number, directly proportional to the linear velocity of the particle motion of the liquid and the characteristic geometric dimension of hydraulic channel and the inversely proportional to the kinematic viscosity of liquid. The critical Reynolds numbers $Re_{кр}$, which are determining the boundary of the transition/junction of laminar flow into the turbulent, depend on the form of hydraulic channel and properties of liquid. In the general case during the motion of liquid it is possible to conditionally isolate two regions: the thin layer of liquid near the boundaries of the channels, where occurs a fundamental change in the particle speed of the liquid, called boundary layer, and the remaining mass of liquid, called flow core or external flow. For the proximate analysis of processes in the slit ring terminal it is possible to use basic condition/positions of boundary-layer theory.

Let us enumerate some cases of the work of the model of contact.

Page 116.

1. When $s<\delta_п$, when the end-type gap s is less than the boundary layer thickness $\delta_п$, separate boundary layers about faces of disk and jacket/case/housing vanish, in the gap has the place the so-called

"flow of Couette" [98, 99].

With laminar flow Reynolds number

$$\mathrm{Re}=\frac{\omega D_к^2}{4\nu}=\frac{v_к D_к}{2\nu}<10^5,$$

where

$$v_к=\pi D_к n \text{ and } \omega=2\pi n;$$

boundary layer thickness $\delta_п<10(\nu/\omega)^{0.5}$ and does not depend on a radius.

During the turbulent flow of the liquid metal, when $\mathrm{Re}>3\cdot10^5$, boundary layer thickness $\delta_п<10\,r^{0.8}(\nu/\omega)^{0.2}$ depends on a radius. In both cases ν - the kinematic viscosity of liquid.

2. When $s>2\delta_п$ about the surfaces of disk and jacket/case/housing appear the separate boundary layers, between which revolves the "flow core" of liquid with an angular velocity of $\beta\approx0.5\omega$. Each of the boundary layers has a distribution of velocities, characteristic for flow of Couette. In the latter case the friction moment is reduced approximately/exemplarily doubly in comparison with case $s<\delta_п$.

Moment/torque $M_т$ does not depend on air-gap clearance s between the jacket/case/housing and the disk. However, with the ample clearances the component of the velocity gradient in axial direction

$\frac{\partial v_z}{\partial z}$ increases and increases braking effect of the lateral surface of jacket/case/housing; therefore to provide for wide gaps is undesirable.

3. The smallest losses to friction in the contact are obtained when $s \approx 2\delta_п$, since in this case the velocity gradient in the axial direction is smallest. This case is investigated [100] taking into account the effect of radial clearance between the electrodes in the current pickup.

Page 117.

Total moment of friction

$$M_т = c\rho_ж l_п D_п^4 \omega^2, \qquad (5\text{-}1)$$

where $\rho_ж$ - density of liquid;

$$c = \mathrm{Re}^{-0,188}\left(\frac{D_п - D_{1п}}{l_п} + 0,8\right)\varphi_п(\lambda) \qquad (5\text{-}2)$$

- moment coefficient of resistor/resistance (coefficient of friction);

$$\varphi_п(\lambda) = 5,8 \cdot 10^{-3}\frac{1,8\lambda^2 - 0,4\lambda - 1}{\lambda^2 + 1,5\lambda - 2};$$

$$\lambda = \frac{D_{2п} - D_{1п} + 0,84L_п}{D_п - D_{1п} + 0,8l_п} \qquad (5\text{-}3)$$

- coefficient of hydrodynamic drag;

$L_к$ - width of jacket/case/housing.

In expression (5-2) Reynolds number

$$\mathrm{Re}=\frac{\omega D_к^2}{\nu}=4\,\mathrm{Re}.$$

On the basis of experimental research Yu. Yu. Kaunas established that a change in the velocity in the boundary layer of liquid occurs according to the law

$$v_\varphi=r(\omega-\beta)\left[1-\left(\frac{z}{\delta}\right)^{1/8}\right]+r\beta, \qquad (5\text{-}4)$$

which better will be coordinated with experiment than with the exponent of ratio (z/δ), T. Karman [99] equal to 1/7 in a similar to expression (5-4) formula. Expressions (5-1)-(5-4) are valid for the turbulent flows with $\mathrm{Re}\geqslant 10^4$, which usually occurs in the contacts of UG of this type.

4. Let us consider the effect of the roughness of the surface of electrodes. At the height/altitude of the protuberances/prominences of roughness $h_ш$, considerably less than the thickness of laminar sublayer $\delta_{л.т}$ of the turbulent flow, they do not affect the hydraulic resistor/resistance and losses in the contact. In the first approximation, not to consider roughness is possible when $h_ш\approx\delta_{л.т}$. In the mode/conditions of "developed roughness" $h_ш>\delta_{л.т}$ occurs detached flow of protuberances/prominences. Flow pattern in this case becomes the independent variable from the Reynolds number and hydraulic resistor/resistance can substantially increase. The approximate

estimate of the magnitude $\delta_{\text{п.л}}$ conducted showed that for the contacts of UM to avoid flows with the developed roughness must occur inequality $h_{\text{ш.ср}} < 0.01$ mm. The class of the cleanliness of working/treatment ∇6 according to GOST 2789-51 corresponds to this.

Magnetohydrodynamic phenomena in the slit ring terminal are caused by the presence of the transverse to the direction motion of the liquid metal of the magnetic field of scattering and longitudinal (tangential) field from the current, which passes in the contact.

Page 118.

1. According to the representations of applied magnetohydrodynamics under the action of transverse velocity distribution pattern of liquid during the laminar flow is equalized, and the velocity gradient about the wall increases and, therefore, increase losses to friction. For the exemplary/approximate evaluation/estimate of the increase of hydraulic resistor/resistance it is possible to use an expression of efficient viscosity [101] of fluid flow in the rectilinear channel, disregarding in the first approximation, the curvature of slit ring terminal.

During the evaluation/estimate should be accepted the series/row of the different values of the ratio of Reynolds number Re to a

number of Hartman

$$M_m = sB_0\sqrt{\frac{\gamma}{\rho\nu}}.$$

where s, B_0, γ - the width of channel, the induction of stray field and electrical conductivity of liquid metal.

Longitudinal magnetic field, evidently, does not have an effect on laminar flow of liquid. Thus, magnetohydrodynamic effect widens the regions of laminar flow in the direction of greater velocities than in the absence of cross field.

2. In the turbulent flow the stray field will lead to the equalization of the velocities in the middle part of the flow and damping of the turbulent pulsations of velocity. The velocity gradient in the middle part of the flow decreases, and in walls it will increase. As experimental research [102] showed, the hydraulic resistor/resistance of annular channel over a wide range of variation $\frac{M_m}{Re}$ varies insignificantly. The coefficient of hydrodynamic drag to flow of different bodies in this channel can increase several times with an increase in ratio M_m/Re [121].

Longitudinal field damps turbulent pulsations and somewhat decreases resistor/resistance.

Since for the contacts of UG the turbulent flows with the large

Re numbers are characteristic, and the induction of stray field and number M_m are small, in the first approximation, these magnetohydrodynamic phenomena can be not considered.

Interaction of current in the contact with the proper magnetic field causes the electromagnetic forces, directed inside the space of liquid metal. They attempt to press metal, to decrease the area of the section (pinch effect) pierced by current. Under the effect of these forces a change in the form of the floating surface of metal and its expulsion from the slow contacts of some constructions/designs with the current overloadings is possible. In the high-speed/high-velocity contacts pinch effect it is possible not to consider.

Page 119.

The electromagnetic force, caused by interaction of current with the stray field, in accordance with the designations Fig. 5-5b will comprise in the first approximation,

$$T_э \approx \int_{D_н/2}^{D_{эк}/2} \int_{0}^{2\pi} \int_{0}^{0.5(L_н+l_н)} \mu_0 \frac{I_н F_э \, dr \, d\varphi \, dz}{3\pi (l_н+L_н) b} = \mu_0 I_н F_э \frac{D_{эк} - D_н}{6b}.$$

In the homopolar dynamo force $T_э$ attempts to move liquid metal against the direction of rotation of rotor, producing certain increase of losses to friction in the current pickup.

During the design of slit ring terminals it is necessary to consider electromagnetic force $T'_э$, transverse to the direction of the flow of liquid metal caused by interaction of current in the contact with the magnetic field of armature. This force (in contrast to longitudinal, force of periphery $T_э$) has an effect on the position of liquid metal relative to rotating electrode in the cross section of channel (Fig. 5-5). Let us consider the equilibrium (symmetrical) position of liquid in the transverse direction under the action of the force of gravity (gravitational), centrifugal force and electromagnetic, that fall per unit volume of liquid metal. We will assume that the rotational axis of contact is horizontal; centrifugal force is directed radially from the rotational axis; in the upper position of the particle of liquid metal gravitational force is directed radially toward the rotational axis; we also consider electromagnetic force in the worst case directed radially toward the rotational axis. In this case the equation of equilibrium takes the form:

$$\frac{2}{3}\beta^2 r\rho_t - g\rho_t = jB_R \sin\alpha,$$

where $\beta=0.5\omega$ - angular velocity of liquid metal in the "kernel" of flow;

r - distance from the rotational axis to the liquid metal;

g=9.81 m/s² - free-fall acceleration;

ρ_t - density of liquid metal;

j - current density in the liquid metal of contact;

$B_я$ - the density of field of armature;

α - angle between directions $B_я$ and j.

Let us take for upper limit: current density in the contact to equal maximum value $j=j_к$, current density on the surface of internal (revolving) electrode; magnetic induction - equal to

$$B_я=\mu_0 H_я=\frac{\mu_0 I_я}{\pi D_{1к}},$$

in this case $r=0{,}5D_{1к}$.

Page 120.

The crossed electrical and magnetic fields we consider perpendicular to each other, i.e., sin α=1.

In view of the relative smallness of value $g\rho_t$ in comparison with

others components/terms/addends it is disregarded by the effect of the force of gravitation. In this case for the normal equilibrium operation of contact it is necessary to have:

$$\frac{\mu_0 j_\kappa I_\kappa}{\pi D_{1\kappa}} < \frac{\beta^2 D_{1\kappa} \rho_t}{2}$$

or

$$\frac{\mu_0 j_\kappa I_\kappa}{\pi} < \frac{\omega^2 D_{1\kappa}^2 \rho_t}{8} \approx \frac{1}{2} v_\kappa^2 \rho_t,$$

where $v_\kappa \approx 0{,}5\omega D_{1\kappa}$. If j_κ, I_κ will achieve such value, that this inequality will be broken, will be begun, the displacement of liquid in the transverse direction.

Surface tension and wettability, and also density and kinematic viscosity of liquid sodium and alloy NaK is very close to the corresponding parameters of water. This makes it possible to simulate hydrodynamic processes in the contacts on base of Na, NaK with the help of the water. A similar reception/procedure is used by the authors with the experimental investigation of the model of slit ring terminal. In the slide contacts with relatively greater v_κ of the force of surface tension it is possible not to consider.

With the wetting with the liquid metal of the cleaned surfaces of electrodes the contact resistance virtually is absent [103]. The resistor/resistance of the layer of liquid metal in the interelectrode space is very small. According to data of the measurements of different authors (for example, [46], etc.), the

transient contact voltage drop, caused by the presence of surface film on the electrodes, for different pairs of solid and liquid metals comprises

$$\Delta U_к \approx 0{,}01 \text{ V}.$$

Wettability increases with an increase in the temperature, which is explained by the dissolution of the pollution/contamination of electrodes in the liquid metal. For guaranteeing the wetting the washing of contact surfaces with special compositions [15] is recommended.

The protective coatings of electrodes and the atmosphere of inert gas prevent increase in the film of oxides and admixtures/impurities, pollution/contamination of liquid metal. The static and dynamic corrosive effect of different liquid metals on the solid ones and the solubility of the latter they are characterized in [104]. The given in this work recommendations must be considered during the design of coatings of contact surfaces.

5.3.

Calculation of Liquid-metal Contact.

The common procedure of calculation of different contacts there does not exist. Some authors use empirical formulas.

In the work of P. Klaudi [96] for calculating the losses to friction in the contact, depicted in Fig. 5.5a, the dependence

$$P_{\text{м.т}} = \varkappa S_{\text{к}} v_{\text{к}}^3,$$

is experimentally obtained where $\varkappa$ - coefficient, proportional to the ratio of the viscosity of liquid to the value of radial clearance between the electrodes, $s_{\text{к}}$ - area of the moistened surface. In work [47] D. Vatt determines experimentally the sizes/dimensions of contact (Fig. 5-3b), which correspond to the smallest losses to friction for various forms of electrodes. Friction moment in the contacts in this case is expressed by the empirical dependence

$$M_{\text{т}} = \left(\frac{D_{\text{к}}}{D_{\text{э}}}\right)^3 y v_{\text{к}}^x,$$

where $D_{\text{к}}$, $D_{\text{э}}$ - diameters of the projected/designed and standard contact;

x, y - experimental values for the assigned form of standard contact.

Separate theoretical dependences for calculating the losses to friction give considerable divergence from the experimental indices.

Hydrodynamic processes are determining with the work of high-speed/high-velocity liquid-metal contact. Most important problems of calculating the contact - determination of the optimum geometric dimensions, which cause the smallest losses to friction, and the determination of magnitude of losses. In connection with slit ring terminal good agreement of designing-theoretical and experimental data gives research [100]. In work [22] Yu. Kaunasom is proposed the floating contact, which is the development of the initial ideas B. I. Ugrimov (Fig. 5-3d).

Below is stated the worked out on the basis [22, 100] procedure for of calculation of the slit ring terminal, the designation of sizes/dimensions of which is given in Fig. 5-5c.

Page 122.

1. Velocity of the surface of the armature

$$v=\pi Dn, \quad \text{m/s},$$

where n, r/s, and D, m - rotational speed and the active diameter of rotor.

2. The outside diameter of the flange of the rotating electrode

$$D_к = \frac{v_к}{\pi n}, \text{ м},$$

where $v_к = \dot{D}_к v$ - linear relative velocity in contact, m/s;

$$\dot{D}_к = \frac{D_к}{D} > 1.$$

3. The width of rotating electrode on the surface of the rotor

$$b_к = \frac{I_д}{\pi D_{р.к} j_{р.к}}, \text{ м},$$

where $D_{р.к} = \dot{D}_{р.к} D$ - diameter of rotor in the zone of the pressing of electrode;

$$\dot{D}_{р.к} = \frac{D_{р.к}}{D} < 1.$$

During the use for the electrical contact with the rotor of face of electrode $D_{р.к} = k_{р.к} D$, moreover

$$k_{р.к} = \sqrt{1 - \frac{4I_д}{\pi D^2 j'_{р.к}}},$$

where $j'_{р.к} = j_{р.к} \approx (50\text{-}100)10^4$ - current density in make-before-break contact between the rotor and rotating electrode, A/m².

In this case $b_к$ - structural/design size/dimension.

4. Width of the sharpening of rotating electrode.

If it is accepted that $S_{кl} = \pi D_к l_к$ composes one third of surface of rotating electrode moistened by liquid metal, then

$$l_к \approx \frac{I_д}{3\pi D_к j_д}, \text{ м},$$

where $j_к$ - current density in the liquid contact on the end-type and lateral surfaces of flange; it is assumed that the current density is distributed evenly. For the construction-engineering reasons $l_к \geqslant 0.001$ m.

5. Diameter of the insertion/immersion of the contact

$$D_{1к} = D_к - 2l_к \cos \alpha_к, \text{ м}.$$

Page 123.

According to the construction-engineering reasons, the angle of throat of contact $\alpha_к \approx 35°$ ($\cos \alpha_к = 0.819$), therefore,

$$D_{1к} \approx D_к - 1{,}64 l_к; \frac{D_{1к}}{D_к} = 1 - 1{,}64 \frac{l_к}{D_к};$$

$$0{,}5(D_к - D_{1к}) = l_к \cos \alpha_к \approx 0{,}819\, l_к.$$

6. Optimum sizes/dimensions (lengths and diameter) of the turning of stationary electrode, which correspond to the minimum of losses to friction [100],

$$L_к = l_к + 0{,}3 D_к \, \mathrm{Re}^{-0{,}182};$$

the gap

$$s \approx 0{,}5(L_к - l_к) = 0{,}15 D_к \mathrm{Re}^{-0{,}182}$$

and

$$D_{2к} = D_к (1 + 0{,}32 \, \mathrm{Re}^{-0{,}182}), \text{ м}.$$

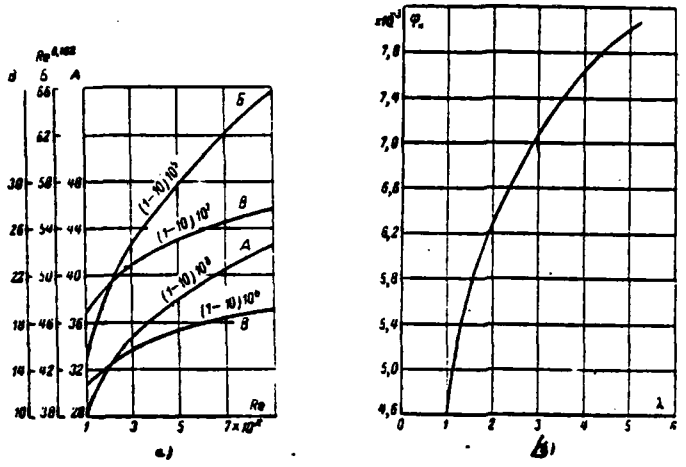

Fig. 5-6. On the calculation of slit ring terminal. a) dependence $Re^{0,182}=f(Re)$; b) dependence $\varphi_к=f(\lambda)$.

Page 124.

Optimum thickness of the layer of the contact liquid

$$s_{max}=0,5(D_{2к}-D_к)=0,16D_к\,Re^{-0,182},$$

where

$$Re=\frac{2D_к v_к}{\nu_t}=4Re;$$

ν_t, m^2/s - kinematic viscosity of liquid metal at expected operating temperature of contact.

Values $Re^{0,182}=f(Re)$ are represented in Fig. 5-6a.

7. Losses of friction in the contact.

Hydraulic losses taking into account (5-1) comprise:

$$P_{\text{к.т}} = 8c\rho_t l_{\text{к}} D_{\text{ж}} v_{\text{к}}^3, \ \text{W}, \qquad (5\text{-}5)$$

where ρ_t - density of liquid metal at a temperature t°C (or with respect to °K), kg/m³.

The coefficient of friction, using (5-2), let us register in the form

$$c = \frac{D_{\text{к}} - D_{1\text{к}} + 0{,}8l_{\text{к}}}{l_{\text{ж}}\,\text{Re}^{0{,}182}}\,\varphi_{\text{к}}(\lambda).$$

The values of function $\varphi_{\text{к}}(\lambda)$ for

$$\lambda = \frac{D_{2\text{к}} - D_{1\text{к}} + 0{,}84L_{\text{к}}}{D_{\text{к}} - D_{1\text{к}} + 0{,}8l_{\text{к}}} < 6$$

are given in the form of curve in Fig. 5-6b.

8. Electrical losses in the contact

$$P_{\text{к.э}} = I_{\text{к}}\Delta U_{\text{к}} + I_{\text{к}}^2 R_{\text{ж}}, \ \text{W}, \qquad (5\text{-}6)$$

where $\Delta U_{\text{к}}$ - voltage drop in contact resistance of contact.

Approximate value of the electrical resistance of the layer of the liquid metal of the slit ring terminal

$$R_{\text{ж}} \approx \frac{1}{3\pi\gamma_t (L_{\text{к}} + l_{\text{к}})} \ln\frac{D_{2\text{к}}}{D_{1\text{к}}},$$

where γ_t - the specific conductivity of metal at operating temperature of contact, $1/\Omega \cdot m$.

Page 125.

For the removal/outlet of losses in contact $P_{к.т}+P_{к.э}$ gas, liquid or evaporative cooling can be used. The cooling agent - the heat-transfer agent, which takes place along the special channels (Fig. 5-5c), is isolated/insulated from the internal cavity of slit ring terminal.

As the heat-transfer agent they can be used: water, combustible (kerosene), oil, organic liquids and liquid metal. The necessary coolant flow rate is approximately determined by the expression

$$Q \approx \frac{P_{к.т}+P_{к.э}}{\rho_{ж} C_{ж} (T_1 - T)}, \text{ м}^3/\text{с},$$

where $\rho_{ж}$, кг/м^3; $C_{ж}$, J/kg·°K - density and the specific heat of heat-transfer agent at a temperature of contact;

T_1, °K - permissible temperature of heat-transfer agent and the temperature of contact;

T_1-T, °K - temperature excess of heat-transfer agent.

The sectional area of the window of the channel

$$S_0 = b_0 h_0 = \frac{Q}{v_m}, \ м^2,$$

where v_m - average/mean rate of flow of the cooling fluid in channel, m/s.

Experimental research of slit ring terminal is stated in Chapter 10.

In conclusion let us present some recommendations by choice of the type of liquid for the current pickup of the UM.

The liquid, used for the current pickup, must satisfy the following requirements:

a) to be found in the liquid state at operating temperature of contact, i.e., the melting point of this liquid must be below, and boiling point - is higher than operating temperature of contact;

b) to produce smallest possible losses to friction, i.e., to possess by low ones specific density and viscosity, and it is good to wet contact surface;

c) to cause smallest possible electrical losses, i.e., to possess high specific conductivity and low contact resistance between the contact liquid and the surface of electrodes;

d) to provide a good cooling of contact, i.e., to possess high thermal conductivity and specific heat;

e) to satisfy the requirements safety engineering with respect to the toxicity of vapors of liquid and their nonflammability at operating temperatures in the conditions of the ambient contact medium;

f) to have stable physicochemical properties for guaranteeing the operational stability of contact.

Page 127.

Table 5-1 gives the properties of low-melting metal ($t_{пл}$ <200°C) and their alloys, some of them can be considered as possible contact liquids.

A selection of the type of contact liquid depends on operating temperature of contact, relative velocity of the movable electrode of contact and construction/design of UM.

Table 5-1. Parameters of some low-melting metal and alloys (T, °K=t, °C+273.15°).

(1) Металл или сплав	(2) Химическое обозначение	(3) Точка, °С: (4) плавления	(3) Точка, °С: (5) кипения	(6) Плотность $\rho_t \cdot 10^{-3}$, кг/м³, при t, °С		(7) Удельное электрическое сопротивление, мком·м, при t, °С		(8) Кинематическая вязкость $\nu \cdot 10^6$, м²/сек, при t, °С		(9) Примечание
(10) Ртуть	Hg	−39	357	13,6	20°	0,958	20°	11,4	20°	Пары токсичны (11)
(12) Цезий	Cs	28,5	705	1,8	100°	0,37	30°	47,0	100°	Самовоспламеняется на воздухе (13)
(14) Галлий	Ga	30	1 983	6,0	50°	0,29	50°	32,0	50°	—
(15) Рубидий	Rb	39	688	1,44	100°	0,245	100°	48,0	100°	Самовоспламеняется на воздухе (16)
(17) Калий	K	63,7	760	0,82	100°	0,155	100°	56,0	100°	—
(18) Натрий	Na	97,8	883	0,93	100°	0,97	100°	77,0	100°	—
(19) Индий	In	159	2 087	7,0	200°	0,31	200°	—	—	—
(20) Литий	Li	179	1 317	0,51	200°	0,45	200°	111,0	200°	—
(21) Сплав	50% Hg 50% In	—	—	9,5	20°	—	—	—	—	Мало исследован. (21)
(22) Сплав	22% Na 78% K	−11	784	0,85	100°	0,42	100°	60,0	100°	Эвтектика (22)
(23) Сплав	Bi, Pb, In, Sn, Cd	47	—	10	50°	—	—	—	—	Состав эвтектический (23)
(24) Сплав	Bi, Pb, Sn, Cd	68	—	10	50°	0,52	0°	—	—	Сплав Вуда (24)
(25) Сплав	44,5% Pb 55,5% Bi	125	1 670	10,5	200°	1,13	200°	24,3	200°	—

Key: (1). Metal or alloy. (2). Chemical designation. (3). Point. (4). melting. (5). boiling. (6). Density ·10³, kg/m³, with. (7). Resistivity, μΩ·m, at. (8). Kinematic viscosity $\nu \cdot 10^6$, m²/s, with. (9). Note. (10). Mercury. (11). Pairs are toxic. (12). Cesium. (13). It self-ignites in air. (14). Gallium. (15). Rubidium. (16). Potassium. (17). Sodium. (18). Indium. (19). Lithium. (20). Alloy. (21). Little it is investigated. (22). Eutectic. (23). Composition is eutectic. (24). Wood's alloy.

Page 127.

Operating temperature of contact - the temperature of contact liquid in the general case can be changed over wide limits; at low temperatures to 200°C, average/mean to 500°C and it is high more than 500°C.

The linear velocity on the periphery of the movable electrode of liquid-metal contact in the general case also can be changed over wide limits: at the low speeds to 50, average/mean - to 150 and high - it is more than 150 m/s. Current density in the contact can reach value from 400 to 4000-6000 A/cm^2.

For the contacts of average/mean and high velocities the relative value of the losses of friction of which is great, should be chosen contact liquids with the low values of the density of mass (sodium, potassium, lithium, sodium-potassium alloy).

For the slow contacts, which undergo large current overloadings, to it is more preferable choose mercury and its alloys: possessing the increased specific gravity/weight, these liquids they contribute to the operational stability of contact with the overloadings of UM.

The greatest practical use/application obtained: mercury (for $v_к$ <50 m/s and $t_к$<200°C), alloy NaK of the eutectic or close to eutectic composition (for $v_к$ <200 m/s and $t_к$ <500°C).

Is of interest the leading work on the study of the possibilities of use/application in the contact of UM of gallium, alloys indium - gallium, mercury - indium [130].

From the point of view of electrical losses in the contact important value has value $\sigma_к = \frac{\Delta U_к}{j_к}$ of the specific skin drag of transition layer solid electrode - liquid metal. Parameter $\sigma_к$ is of the order 10^{-6} Ω·m² for the steel electrodes and the liquid metals Hg, NaK and order 10^{-9} Ω·m² for the copper electrodes and the same liquids [46]. However, the values $\sigma_к$ indicated are approximate. Precise values of parameter $\sigma_к$ taking into account a number of factors (value of current density in the contact, the cleanliness of contact pairs, temperature, etc.) at present are absent.

The use/application of alkali metals is limited to their high chemical activity. Acyclic machines with sodium - by potassium current pickup must be made by sealed/pressurized ones with the filling of the internal cavity of machine with the inert gas (dry

nitrogen, argon). To avoid the entry of surrounding air inside the machine the pressure of filler must somewhat exceed atmospheric.

The toxicity of its vapors is a deficiency/lack in mercury. Acyclic machines with the mercury contacts must be placed in the special locations, which have tributary-exhaust ventilation system. Construction/design of the UM must not allow/assume the efflux of mercury from the internal cavity and the system of contacts.

Page 128.

Chapter Six.

FUNDAMENTAL QUESTIONS OF THE CALCULATION OF ACYCLIC MACHINES.

6.1. Determination of main sizes/dimensions.

a) General operating instructions.

Engineering calculation procedure of UM is constructed on the base of the theoretical conclusions, examined in §2-2--2-4, according to which magnetic flux distribution and electric current in the solid rotor of cylindrical machine is assumed/set axial-uniform, and the distribution of magnetic induction along the working gap of disk machine is also accepted as uniform. Extending these conclusions/outputs to UM with the hollow cylindrical rotor, we consider the distribution of induction in the internal core of stator and current density in their rotor axially-uniform. The designation of basic calculated dimensions of UM of different construction/design is given in Fig. 6-1.

In the general case for cylindrical multipole UG (Fig. 6-1a, b) m_E of powered phases can be connected in series for an increase in voltage/stress U, and m_I sections - in parallel for an increase in the total current of machine I. During 100% use of active length of machine $m_E m_I = 2p$. However, a similar position exists for the disk UM.

Page 129.

b) Structural/design coefficient of UM.

Cylindrical UM with the continuous rotor. Acyclic machine with the cylindrical armature relates to the class of the electrical machines with the axial flow, whose design factor, i.e. relation $\lambda = l/D$, is rigidly determined by magnetic loads.

Let us consider the general case, when in the armature is an opening/aperture with a diameter of $d_в$ for the location of nonmagnetic shaft.

Taking into account that magnetic flux in the armature core

$$\Phi_п = \frac{\pi}{4}(D_п^2 - d_в^2) B_п = \Phi_б k_{зп} = \pi D l B_б k_{зп},$$

we will obtain the value of the design factor:

$$\lambda_ц = \frac{l}{D} = 0{,}25 \frac{\mathring{D}_п^2 - \mathring{d}_в^2}{k_{зп}} \frac{B_п}{B_б}, \qquad (6\text{-}1)$$

where $\dot{D}_p = \frac{D_p}{D}$ and $\dot{d}_s = \frac{d_s}{D}$.

In the absence of opening/aperture in the armature for nonmagnetic shaft ($\dot{d}_s = 0$), $D_p \approx D$ and $B_p/B_\delta \approx 1$, the design factor of cylindrical UM $\lambda_m = 0{,}25$.

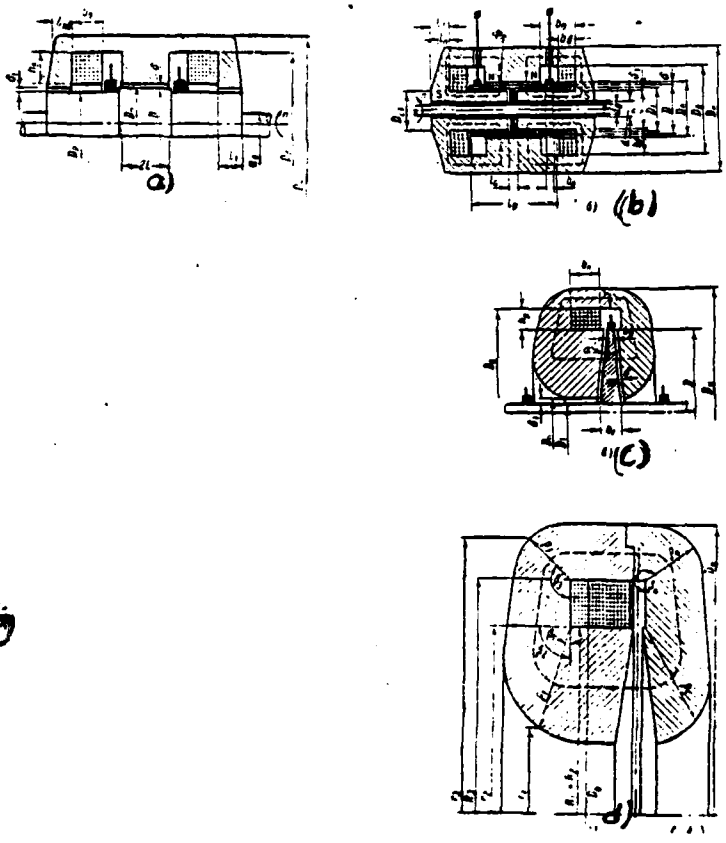

Fig. 6-1. Designation of calculated sizes/dimensions of UG. a) cylindrical with the solid rotor; b) the same with the hollow rotor; c, d) disk with the conical rotor.

Page 130.

Cylindrical UM with the hollow rotor. Using the designations, indicated in Fig. 6-1b, we will obtain analogously (with 6-1):

$$\lambda_m = 0{,}25 \frac{\tilde{D}_c^2 - \tilde{d}^2}{k_s} \frac{B_c}{B_\delta}, \qquad (6\text{-}2)$$

where

$$\mathring{D}_c = \frac{D_c}{D} \quad \text{and} \quad \mathring{d} = \frac{d}{D};$$

B_c - induction in the internal core of stator;

- k_σ - coefficient of scattering, is calculated from the formulas, given in §3-5.

Disk UM with the conical rotor (Fig. 6-1c). The design factor

$$\lambda_\delta = \frac{l}{D} = \frac{D - D_\delta}{2\cos\alpha}\frac{1}{D} = 0{,}5\frac{1-\mathring{D}_\delta}{\cos\alpha}. \qquad (6\text{-}3)$$

With flat/plane disk $\alpha = 0$, $\lambda_\delta = 0{,}5(1-\mathring{D}_\delta)$; $\mathring{D}_\delta = D_\delta/D$.

Let us note that for the disk UM is characteristic the relation

$$\lambda_{\delta 1} = \frac{b_1}{D_1} = 0{,}25\frac{j_1}{j_{p1}} \qquad (6\text{-}4)$$

during the one-sided current pickup on the shaft and

$$\lambda_{\delta 1} = 0{,}5\frac{j_1}{j_{p1}}$$

with the bilateral (j_1, j_{p1} - current density of shaft and rotor disk with $r=0.5D_1$).

C) The magnetic flux of mutual induction and emf UM.

Magnetic flux in the limits of the active length l of working gap (under one pole) and emf of multipole cylindrical corresponding to it UM comprise:

$$\Phi_\delta = S_\delta B_\delta = \pi D l B_\delta = \pi D^2 \lambda_\delta B_\delta = \frac{\lambda_\delta}{\pi} B_\delta \left(\frac{v}{n}\right)^2, \overset{(1)}{\text{об}};$$

$$E = m_E n \Phi_\delta = \pi m_E n D^2 \lambda_\delta B_\delta = \frac{m_E}{\pi}\lambda_\delta B_\delta \frac{v^2}{n}, \overset{(2)}{\text{в}}, \qquad (6\text{-}5)$$

Key: (1). Wb (2). V

where $D=\frac{v}{\pi n}$; n and v are expressed in the turns per second and meters per second.

Page 131.

Magnetic flux in active region/core and emf of disk UM is respectively equal to:

$$\left.\begin{aligned}\Phi_\delta = S_\delta B_\delta = \frac{\pi D^2}{4}\frac{1-\mathring{D}_n^2}{\cos\alpha}B_\delta = \frac{0{,}25}{\pi}\frac{1-\mathring{D}_n^2}{\cos\alpha}B_\delta\left(\frac{v}{n}\right)^2;\\ E = m_E n\Phi_\delta = \frac{0{,}25}{\pi}m_E\frac{1-\mathring{D}_n^2}{\cos\alpha}B_\delta\frac{v^2}{n} = \frac{m_E}{2\pi}\lambda_\Sigma B_\delta\frac{v^2}{n}(1+\mathring{D}_n).\end{aligned}\right\} \quad (6\text{-}6)$$

D) current and linear load UM.

Current and linear load of cylindrical UM is respectively equal to:

$$\left.\begin{aligned}I = S_p\frac{m_1}{k_I}j_p = \frac{\pi D^2}{4}(\mathring{D}_p^2-\mathring{d}_a^2)j_p = \frac{0{,}25}{\pi}\frac{m_1}{k_I}(\mathring{D}_p^2-\mathring{d}_a^2)j_p\left(\frac{v}{n}\right)^2,\ a;\\ A = \frac{I}{\pi D\mathring{D}_p}\frac{k_I}{m_1} = \frac{I_\pi}{\pi D\mathring{D}_p},\ a/м.\end{aligned}\right\} \quad (6\text{-}7)$$

During the parallel excitation of UM

$I = m_1 I_\pi - I_\delta$ and $k_I = \frac{m_1 I_\pi}{I} > 1$ - in the mode/conditions of generator;

$I = m_I I_н + I_в$ and $k_I < 1$ - in the engine operating mode.

During the independent and series excitation of UM

$$I = m_I I_н \text{ и } k_I = \frac{m_I I_в}{I} = 1.$$

Current and linear loads of disk UM are respectively equal to:

$$\left.\begin{aligned} I &= S_{p_1}\frac{m_I}{k_I} j_{p_1} = \pi D_1 b_1 \frac{m_I}{k_I} j_{p_1},\ a; \\ A &= \frac{I}{\pi D}\frac{k_I}{m_I} = \frac{I_в}{\pi D},\ a/м; \\ A_1 &= \frac{I}{\pi D_1}\frac{k_I}{m_I} = \frac{I_в}{\pi D_1},\ a/м. \end{aligned}\right\} \quad (6\text{-}8)$$

Page 132.

e) rated power of UM.

Rated power of UM is the electromagnetic power

$$P_э = E m_I I_н \cdot 10^{-3},\ \text{kW},$$

which is connected with the nominal

$$P_н = UI \cdot 10^{-3},\ \text{kW (UG)}$$

and

$$P_{\text{н}}=\frac{UI}{\eta}\cdot 10^{-3},\ \text{kW (UD)}$$

with the relationship/ratio

$$\frac{P_{\text{н}}}{P_{\text{э}}}=\frac{UI}{Em_1I_{\text{н}}\eta}=\frac{\dot{U}}{k_1\eta},$$

i.e.

$$P_{\text{н}}=P_{\text{э}}\frac{\dot{U}}{k_1\eta}.$$

In the mode/conditions of generator $P_{\text{н}}$ - nominal electrical power it is necessary to assume/set $\eta=1$; in the engine operating mode $P_{\text{н}}$ - nominal mechanical output and the efficiency $\eta<1$.

Relative voltage/stress $\left(\dot{U}=\frac{U}{E}\right)$, which characterizes a voltage drop in the effective resistance of the circuit of armature, comprises $\dot{U}<1$ in the mode/conditions of generator and $\dot{U}\geqslant 1$ in the engine operating mode; $m_1I_{\text{н}}$ - current of machine with m_1 the in parallel connected sections of armature. Rated power of UM can be also presented, using sizes/dimensions and machine parameters in the following form.

Page 133.

Cylindrical UM with solid rotor [62].

Taking into account (6-1) (6-5) and (6-7), we obtain:

$$P_э = Em_l I_л \cdot 10^{-3} = \frac{6.25 \cdot 10^{-5}}{\pi^2} m_E m_l \frac{(\mathring{D}_p^2 - \mathring{d}_в^2)_E (\mathring{D}_p^2 - \mathring{d}_в^2)_I}{k_{эм}} \times$$
$$\times B_p j_p \frac{v^4}{n^3}, \text{ kW}, \qquad (6\text{-}9)$$

where numerically equal factors $(\mathring{D}_p^2 - \mathring{d}_в^2)_E$ and $(\mathring{D}_p^2 - \mathring{d}_в^2)_I$ consider the presence in the general case of the nonmagnetic and isolated/insulated shaft respectively. If in the particular case there is a shaft isolated/insulated, but magnetic, then during the calculation only one of the factors $(\mathring{D}_p^2 - \mathring{d}_в^2)_I < 1$, is taken into consideration since in this case $(\mathring{D}_p^2 - \mathring{d}_в^2)_E = 1$.

Disk UM (with the bilateral removal/output of current from the shaft).

Taking into account (6-3) and (6-6) we find:

$$P_э = Em_l I_л 10^{-3} = \frac{12.5 \cdot 10^{-5}}{\pi^2} m_E m_l \frac{\mathring{D}_п^2 (1 - \mathring{D}_п^2)}{\cos \alpha} B_з j_1 \frac{v^4}{n^3}, \text{ kW}, \qquad (6\text{-}10)$$

where

$$\mathring{D}_ш = D_ш / D; \; D_1 \approx D_ш; \; I_л = 2\pi j_1 \frac{D_1^2}{4}.$$

f) fundamental calculated equation UM.

Let us represent fundamental calculated equation of UM in classical for the electrical machines form [105].

Diameter and length of the armature of cylindrical UM with massive rotor is respectively equal to:

$$\left.\begin{aligned} D &= \sqrt[3]{\frac{P_э}{\sigma_м \lambda_м n}}, \ м; \\ l &= \lambda_м D = 0{,}25\,\frac{\mathring{D}_р^2 - \mathring{d}_в^2}{k_{ор}} \cdot \frac{B_р}{B_б} D, \ м, \end{aligned}\right\} \qquad (6\text{-}11)$$

where

$$\sigma_м = \pi^2 \cdot 10^{-3} m_E m_l \mathring{D}_р A B_б, \ \text{kW/(m}^3 \cdot \text{rev/s)}$$

- coefficient of use of cylindrical UM, which characterizes the ratio of rated power to the sensitive volume of UM.

Page 134.

Diameter and length of the armature of cylindrical UM with the hollow rotor is respectively equal to:

$$\left.\begin{aligned} D &= \sqrt[3]{\frac{P_э}{\sigma_м \lambda_м n}}, \ м; \\ l &= \lambda_м D = 0{,}25\,\frac{\mathring{D}_с^2 - \mathring{d}^2}{k_в} \frac{B_с}{B_б} D, \ м, \end{aligned}\right\} \qquad (6\text{-}12)$$

where

$$\sigma_м = \pi^2 \cdot 10^{-3} m_E m_l A B_б, \ \text{kW/(m}^3 \cdot \text{rev/s)}.$$

Diameter and "length" of the armature of disk UM is respectively equal to:

$$\left.\begin{aligned} D &= \sqrt[3]{\frac{P_э}{\sigma_д \lambda_д n}}, \ м; \\ l &= \lambda_д D = 0{,}5\,\frac{1-\mathring{D}_в}{\cos\alpha}\,D, \ м, \end{aligned}\right\} \qquad (6\text{-}13)$$

where $\sigma_д = \frac{\pi^2}{2}\cdot 10^{-3} m_E m_l (1+\mathring{D}_в) A B_\delta$, kW/(m³·rev/s) - the coefficient of use of disk UM.

With the one-sided removal/output of current from the shaft and $D_в \approx D_1$ value $\sigma_д$ can be calculated also from the expression

$$\sigma_д = 0{,}5\cdot 10^{-3}\pi^2 m_E m_l (\mathring{D}_в + \mathring{D}_в^2) A_1 B_\delta.$$

With the bilateral removal/output of current this expression doubles.

Fundamental calculated equation of UM can be presented into a somewhat different from expressions (6-11)-(6-13) form, if we use during the conclusion/output of calculated equation electromagnetic power from expressions (6-9) and (6-10).

Cylindrical acyclic machine with the solid rotor. Air-gap diameter of UM

$$D = \sqrt[4]{\frac{P_э}{\sigma'_д n}}, \ м, \qquad (6\text{-}14)$$

where $\sigma'_д = 6{,}15\cdot 10^{-4}\frac{m_E m_l}{k_{ор}}(\mathring{D}_р^2 - \mathring{d}_в^2)_E (\mathring{D}_р^2 - \mathring{d}_в^2)_l B_р j_р$, kW/(m⁴·rev/s)

characterizes the degree of utilization of a sensitive volume of

cylindrical UM.

Page 135.

Disk acyclic machine (with the bilateral removal/output of current from the shaft). Air-gap diameter of UM

$$D=\sqrt[4]{\frac{P_э}{\sigma'_{д}n}},\ м, \qquad (6\text{-}15)$$

where

$$\sigma'_{д}=12{,}3\cdot10^{-4}m_E m_I\frac{\overset{*}{D}{}_{п}^{2}(1-\overset{*}{D}{}_{п}^{2})}{\cos\alpha}B_{\delta}j_{1},\ \text{kW/(m}^{4}\cdot\text{rev/s)}.$$

With the one-sided removal/output of current from the shaft value $\sigma'_{д}$ is reduced doubly.

Basic dimensions of UM can be also determined, on the basis of the degree of utilization of a contact surface of circular current pickup, which is characterized by linear load in the slit ring terminal

$$A_{к}=j_{к}l_{к}=\frac{I}{\pi D_{к}}\frac{k_I}{m_I}=\frac{I_{к}}{\pi D_{к}}.$$

Taking into account that presented, let us register one additional form of fundamental calculated equation.

Cylindrical UM. Air-gap diameter

$$D=\sqrt[3]{\frac{P_э}{\sigma_{к.д}\lambda_{д}n}}, \qquad (6\text{-}16)$$

where

$$\sigma_{\text{к.п}} = \pi^2 \cdot 10^{-3} m_E m_l A_{\text{к}} B_\delta D_{\text{к}}.$$

Let us note that

$$A = \frac{D_{\text{к}}}{D\mathring{D}_{\text{p}}} A_{\text{к}} = \frac{\mathring{D}_{\text{к}}}{\mathring{D}_{\text{p}}} A_{\text{к}};\ \mathring{D}_{\text{к}} = \frac{D_{\text{к}}}{D},$$

and since $\mathring{D}_{\text{к}} > \mathring{D}_{\text{p}}$, that $A > A_{\text{к}}$.

Disk UM. Air-gap diameter

$$D = \sqrt[3]{\frac{P_{\text{э}}}{\sigma_{\text{к.п}} \lambda_\delta n}}, \qquad (6\text{-}17)$$

where

$$\sigma_{\text{к.п}} = \frac{\pi^2}{2} 10^{-3} m_E m_l (1 + \mathring{D}_{\text{п}}) \mathring{D}_{\text{к}} A_{\text{к}} B_\delta$$

and

$\mathring{D}_{\text{к}} = D_{\text{к}}/D$ for the peripheral current pickup.

Page 136.

For the contact on the shaft value $\mathring{D}_{\text{к}} A_{\text{к}}$ should be replaced the expression

$$\mathring{D}_{\text{к}_1} A_{\text{к}_1};\ A_{\text{к}_1} = j_{\text{к}_1} l_{\text{к}_1} \text{ and } \mathring{D}_{\text{к}_1} = \frac{D_{\text{к}_1}}{D},$$

but during the bilateral current pickup - by expression $2\mathring{D}_{\text{к}_1} A_{\text{к}_1}$.

G) The coupling coefficients of emf and current with the

electromagnetic power of UM.

In accordance with [62], using (6-5) and (6-6), let us establish the connection/communication between E, I and $\bar{P}_э$ at given speeds n and in ratios $B_р/j_р$ and $B_э/j_э$ in the form

$$\left.\begin{aligned} K_{пE} &= \frac{E^2}{nP_э} = \frac{m_E}{m_I}\frac{B_р}{j_р}\frac{10^3}{k_{ор}}\frac{(\mathring{D}_р^2 - \mathring{d}_в^2)_E}{(\mathring{D}_р^2 - \mathring{d}_в^2)_I}, \quad в^2/(квт\cdot об/сек); \\ K_{дE} &= \frac{E^2}{nP_э} = \frac{m_E}{m_I}\frac{B_э}{j_э}\frac{1-\mathring{D}_п^2}{\mathring{D}_п^2}\frac{k\cdot 10^3}{\cos\alpha}; \end{aligned}\right\} \quad (6\text{-}18)$$

(1)

$$\left.\begin{aligned} K_{пI} &= \frac{I^2 n}{P_э} = \frac{m_I}{m_E}\frac{j_р}{B_р}\, k_{ор}\frac{(\mathring{D}_р^2 - \mathring{d}_в^2)_I}{(\mathring{D}_р^2 - \mathring{d}_в^2)_E}\, 10^3, \quad (а^2\cdot об/сек)/квт; \\ K_{дI} &= \frac{I^2 n}{P_э} = \frac{m_I}{m_E}\frac{j_э}{B_э}\frac{\mathring{D}_п^2\cos\alpha}{1-\mathring{D}_п^2}\frac{10^3}{k}, \end{aligned}\right\} \quad (6\text{-}19)$$

(2)

Key: (1). $V^2/(kW\cdot rev/s)$. (2). $(A^2\cdot rev/s)/kW$.

where $k_I = 1$; $D_э \approx D_п$;

k=1 (during the one-sided current pickup), k=0.5 (during the bilateral current pickup on the shaft).

It is easy to see, that values $K_{пE}$ and $K_{пI}$, and also $K_{дE}$ and $K_{дI}$ are inversely proportional to each other, i.e.

$$K_{пE}K_{пI} = 10^6 \quad \text{and} \quad K_{дE}K_{дI} = 10^6.$$

Page 137.

In conclusion let us register the dependence between the coefficients of "use" $\sigma'_u(\sigma'_л)$ and the coupling coefficients $K_{uE}(K_{uI})$, $K_{лE}(K_{лI})$ taking into account (6-14) and (6-15) in the form

$$\sigma'_u K_{uE} = \frac{\sigma'_u}{K_{uI}} 10^6 = 0{,}615\left[\frac{m_E(\mathring{D}_p - \mathring{d}_л^2)_E}{k_{ор}} B_p\right]^2;$$

or

$$\sigma'_л K_{лE} = \frac{\sigma'_л}{K_{лI}} 10^6 = 0{,}615\left[m_E \frac{1-\mathring{D}_л^2}{\cos\alpha} B_\delta\right]^2,$$

$$\frac{\sigma'_u}{K_{uE}} = \sigma'_u K_{uI} \cdot 10^{-6} = 6{,}15 \cdot 10^{-7}[m_I(\mathring{D}_p^2 - \mathring{d}_л^2)_I j_p]^2;$$

$$\frac{\sigma'_л}{K_{лE}} = \sigma'_л K_{лI} \cdot 10^{-6} = 24{,}6 \cdot 10^{-7}[m_I \mathring{D}_л^2 j_1]^2.$$

Latter/last expression for the disk machines corresponds to bilateral current pickup on the shaft. During the one-sided current pickup the right part is reduced four times.

H) Some special features/peculiarities of design UM.

The rigid coupling of the main sizes/dimensions of cylindrical machines, defined in assigned ratios B_p/B_δ or (B_c/B_δ) by the value of design factors λ_m, does not make it possible for an increase in the power to considerably increase length l with the constant/invariable diameter D, as this is made in the bipolar machines. However, a similar fact occurs in some types of noncontact synchronous machines.

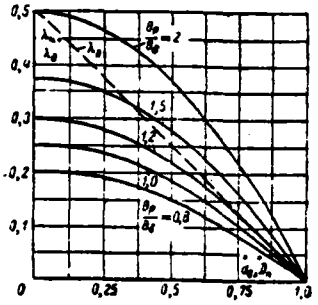

Fig. 6-2. Dependences of design factors on the relationship/ratio of the air-gap diameters and shaft $\lambda_в = f(\dot{d}_в)$ and $\lambda_к = f(\dot{D}_в)$ for the cylindrical and disk machines.

Page 138.

For an increase of the power in UM it is possible to increase a number of poles 2p. The value of induction in the gap of UM is chosen relatively greater, since value $B_з$ is not limited in this case to the saturation of toothlike layer as in the machines with the windings at the armature. Plotted functions $\lambda_в = f(\dot{d}_в)$ of $B_р/B_з$ are given in Fig. 6-2.

From expressions (6-5)-(6-10) it follows that the amounts of emf, current and power of UM are limited the permissible according to the condition strength of vorticity $v = \pi Dn$ or the permissible according to the condition efficiency of the contact with a speed of $v_к = \dot{D}_к v$, where $\dot{D}_к = D_к/D$. The values of induction $B_р$ and $B_с$ are limited to the saturation of the material of magnetic circuit, and also to

required ranges of adjustment of voltage/stress of UM. Values j_p, j_1 are chosen for reasons of the permissible heating of machines. For the ferromagnetic rotors during the approximate determination of the permissible current density it is possible to use the recommendations, indicated in §4-5. In the carried out machines values $j_p \approx (30—50) \cdot 10^4$ $a/м^2$, $A \approx (1 \div 6) 10^4$ $a/м$. are known.

At present there are no sufficient given optimum values of the coefficients of use of UM $\sigma_м$, $\sigma_п$ and $\sigma'_м$, $\sigma'_п$. The direct use/application of fundamental calculated equations will be possible on gaining of the experience of design and operation of machines. Derived relationships/ratios (6-18) (6-19) make it possible to determine main sizes/dimensions of UM variously. During the design initial data are nominal power $P_м$, voltage/stress U, speed of rotation n. On $P_м$ and U are determined rated power and emf (values $\dot{U}$ and k_I for UM are close to one and they depend on a number of poles, diagram of connection of the powered phases of armature, material and current density of conductors). Knowing $P_э$ and E, for example, for cylindrical UG, we find $K_{пЕ}$ through (6-18).

After assigning values B_p, $k_{ор}$, m_E, m_I and design concept, which is determining relation $\frac{(\mathring{D}_p^2 - \mathring{d}^2)_E}{(\mathring{D}_p^2 - \mathring{d}_в^2)_I}$, from (6-18) we find current density $I_э$. If $I_э$ is more than permitted, it is necessary to change m_E, m_I or design concept. We further find $\sigma'_м$ and air-gap diameter D through

(6-14). Value D must be checked on allowable speed v (or $v_к$) with assigned n.

If v> [v], then are changed design factors or m_E, m_I. Choosing $B_δ$ and knowing D, on (6-11) we find l, i.e., the second main size/dimension of machine. Let us note that during determination of D and l it is possible to use the coupling coefficient $K_{ДI}$, equivalent with coefficient $K_{ДE}$ in its significance.

Page 139.

Furthermore, in the beginning of calculation it is possible to assign value $j_р$ and to determine induction $B_р$. Obtained in this case the latter must not exceed the value permissible on the saturation. With assigned U, $v_м$ and m_E the size/dimension l can be determined according to the equation

$$l = \frac{U\mathring{D}_м}{m_E v_м B_δ \mathring{U}}, \text{ м.}$$

After finding then $\lambda_д$ and $D = \frac{1}{\lambda_д} l$ should be analyzed the magnetic $B_р$ and current $j_р$ charging of rotor and determined

$$n = \frac{v_м}{\pi D \mathring{D}_м}, \text{ r/s.}$$

However, for the disk UM should be applied similar ways of calculation with the use of coefficient $K_{ДE}$ or $K_{ДI}$ for determining of

diameters D, $D_в$ and length l.

Fig. 6-3 gives curves, by which it is possible to judge the effect of a change in design factors $\dot{d}_в$ and $\dot{D}_в$ to the value of coefficients $K_{вE}$, $K_{эE}$, $K_{вJ}$, $K_{эJ}$, $\bar{\sigma}_в$, $\sigma_э$. These curves it is possible to use during the calculation of main sizes/dimensions in the process of design of UM.

For determining the dimensions of armature it is possible to recommend also the practical formulas, indicated below.

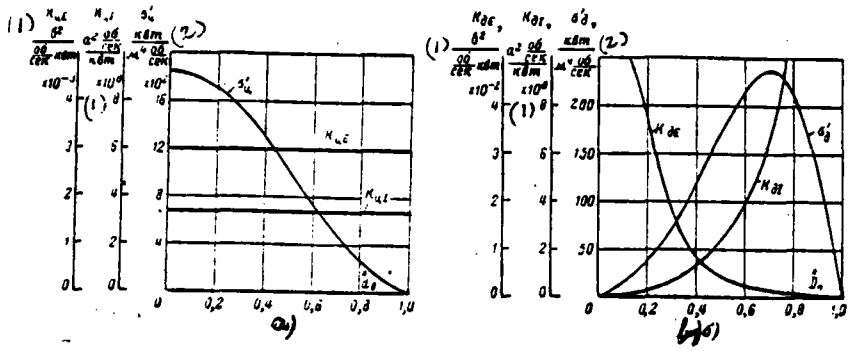

Fig. 6-3. Effect of a change in the design factors to values $K_{u.n.}$ $K'_{u.n}$ and $\sigma'_{u.n.}$ a) cylindrical UM with B_δ=1.5 T; j_n=10^6 A/m^2; m_E=2; m_I=1; $\overset{*}{D}_p$=1, k_{op}=1; b) disk UM with B_δ=1.5 T; j_1=10^6 A/m^2; m_E=1; m_I=1; cos α=1 (for the one-sided current pickup on the shaft).

Key: (1). r/s kW. (2). kW m^4 r/s.

Page 140.

The solid rotor of cylindrical UM serves simultaneously as magnetic circuit and conductor, moreover the magnetic flux of pole must wholly pass within the circle/circumference of current pickup.

Air-gap diameter on the voltage/stress with series connection of the active parts of the armature:

$$D=\sqrt{\frac{4k_{sp}U}{\pi\hat{U}(\overset{*}{D}_p^2-\overset{*}{d}_s^2)m_E B_\delta n}},\ м;$$

on the current

$$D=\sqrt{\frac{4}{\pi}\frac{k_I I}{(\overset{*}{D}_p^2-\overset{*}{d}_s^2)j_p}},\ м.$$

In this case B_p and j_p must be given to the conformity with each other.

The diameter of the hollow rotor of cylindrical UM (Fig. 6-1b) with series connection of the parts of the armature

$$D=\sqrt{D_1^2+\frac{4k_I I}{\pi j_p}},$$

where $D_1=D_c+2\delta_1$ - inner diameter of rotor.

Diameter of the internal magnetic circuit of the stator

$$D_c=\sqrt{\frac{4}{\pi \mathring{U}}\frac{k_\sigma U}{(1-\varepsilon_\text{п}^2)\,m_E B_c n}},$$

where $\varepsilon_\text{п}=d/D_c=\mathring{d}/\mathring{D}_c$.

The active diameter of disc armature of UM (Fig. 6-1c) with series connection of disks in the case of multipolar machine

$$D=\sqrt{\frac{4}{\pi}\frac{U\cos\alpha}{\mathring{U}pB_\delta n}+D_\text{в}^2},$$

where $D_\text{в}=D_1+2\delta_1$ - inner diameter of the active part of the armature.

Diameter of rotor shaft $D_1=\sqrt{\frac{4kk_I I}{\pi j_1}}$; coefficient k=1 or 0.5.

The thickness of conical disc armature at the appropriate diameter will comprise:

$$b_1=\frac{k_I I}{\pi j_{p1} D_1} \quad \text{and} \quad b_D=\frac{k_I I}{\pi j_{pD} D}=\frac{A}{j_{pD}}.$$

Page 141.

With the obtained diameters the active length of armature of UM is determined by relationship/ratio $l=\lambda_{\text{д}}\dot{D}$ or $l=\lambda_{\text{д}}D$.

Let us note that during the calculation by cylindrical UM with the hollow ferromagnetic rotor the induction in the gap δ must be determined on the relationship/ratio

$$B_{\delta}=B_{\delta 1}\frac{D_1}{D}=\dot{D}_1 B_{\delta 1},$$

moreover induction $B_{\delta 1}$ in the gap δ_1 must be chosen taking into account the permissible saturation of the material of rotor.

Examples of the calculation of the main sizes/dimensions of cylindrical and disk UM are given in the work of the authors [60].

6.2. Determination of the basic dimensions of magnetic circuit.

Cylindrical machines with the massive ferromagnetic rotor (Fig. 6-1a) will be considered.

Knowing the main size/dimension of D, for the construction-engineering reasons the approximate value of working gap

$\delta=0{,}02\div0{,}2$,cm with D=5-50 cm is chosen. After assigning the value of induction B_δ is found the drop in magnetic potential F_δ in the gaps, which corresponds to one pole pair of UM. After selecting the preliminary values of coefficients k_{cT} and $k_{p.n}$, that consider a drop in the magnetic potential in steel with the idling and the demagnetizing effect of armature with the load, is determined preliminary value of magnetizing force of excitation winding:

$$F_{в.н}=(k_{cT}+k_{p.n})k_{н}F_{\delta},$$

where $k_{cT}\approx0{,}1\div0{,}3$; $k_{p.n}\approx1{,}3\div1{,}9$ - for not compensated UM (for compensated UM also $k_{p.n}>1$); $k_{н}>1$ considers a drop in the magnetic potential in the structural/design gaps of machine.

Taking into account $F_{в.н}$ the area of window and the sizes/dimensions of the cross section of excitation winding ($b_в$ and $h_в$) are computed. The optimum relationship/ratio between $b_в$ and $h_в$ is substantiated in §6-3.

Page 142.

The diameter of the turning of stator for the excitation winding

$$D_в=D+2(h_в+\Delta h_в+\delta),$$

where $\Delta h_в$ - radial distance from the bore of stator ($D_а=D+2\delta$) to the beginning of field coil.

The outside diameter of stator (inductor)

$$D_{\text{н}} = \sqrt{D_{\text{а}}^2 + 4k_{\text{ос}}(D+\delta)\frac{lB_\delta}{B_{\text{с}}}}$$

or

$$D_{\text{н}} = D\mathring{D}_{\text{н}} = D\sqrt{\mathring{D}_{\text{а}}^2 + 4\lambda_{\text{н}}k_{\text{ос}}(1+\mathring{\delta})\frac{B_\delta}{\sigma_{\text{с}}}},$$

where $B_{\text{с}}$ - magnetic induction in the framework of inductor;

$k_{\text{ос}} = 1{,}1 \div 1{,}2$ - preliminary value of coefficient of scattering;

$$\mathring{D}_{\text{н}} = \frac{D_{\text{н}}}{D};\ \mathring{D}_{\text{а}} = \frac{D_{\text{а}}}{D};\ \mathring{\delta} = \frac{\delta}{D}.$$

For the purpose of a decrease in the weight of magnetic circuit the extreme poles of inductor are made by those chamfered. Width of pole at diameter $D_{\text{а}}$ (with the retention/preservation/maintaining of the value of induction in this section of magnetic circuit)

$$l_{\text{н.а}} = k_{\text{ос}}\frac{(D+\delta)lB_\delta}{D_{\text{а}}B_{\text{с}}} = k_{\text{ос}}\frac{1+\mathring{\delta}}{\mathring{D}_{\text{а}}}\frac{lB_\delta}{B_{\text{с}}}.$$

In the general case the induction in the gaps δ and δ_1 (Fig. 6-1a) is different. Axial length of the bore of the extreme pole

$$l_1 = \frac{D+\delta}{D_{\text{р}}+\delta_1}\frac{lB_\delta}{B_{\delta 1}} = \frac{1+\mathring{\delta}}{\mathring{D}_{\text{р}}+\mathring{\delta}_1}\frac{lB_\delta}{\sigma_{\delta 1}}.$$

The presence in stator of structural/design openings/apertures (for the current changing busbars, the conduits/manifolds of cooling system, etc.) must be considered by the corresponding increase in the sectional area of magnetic circuit. On the final outline of magnetic circuit is done verifying calculation of UM and the values of the preliminarily selected coefficients are made more precise.

During the verifying calculation by emf four-terminal UG with

the half use (Fig. 6-1a) taking into account the bulge of flow on faces of average/mean poles theoretical active length according to Richter [106] can be assumed/set by equal to $l_i=2(l+\delta)$..

Page 143.

Sizes/dimensions b_s and h_s of UM with the hollow cylindrical rotor are determined similarly to the same for the machines with the solid rotor. Some elements of sizing of magnetic circuit of UM with the hollow rotor are examined in S6-1. the determination of values D_s, D_n, l_n, l_i (Fig. 6-1b) is also similar to that presented for UM with the solid rotor.

Knowing the sizes/dimensions of disk rotor of UM and after determining the sides of the window of excitation winding, let us find the contours of profile of magnetic circuit, on the basis of the constancy of the area of its section:

$$S_c=\frac{k_s\Phi_\delta}{B_c};\ B_c=\text{const.}$$

In this case the quality of magnetic circuit will be greatest (S2-3). We assume that the surfaces of revolution, normal to flow $\Phi_c=k_s\Phi_\delta$ in the inductor, have linear generator ρ_i. The line of the outer duct of magnetic circuit will be the hodograph of radius-vector $\bar{\rho}_i$ (Fig. 6-1d). The coordinates of the points of duct/contour are connected with the relationships/ratios

$$r_i=\sqrt{R_i^2-\frac{1}{\pi}S_c\cos\beta_i};\ \rho_i=\frac{R_i-r_i}{\cos\beta_i}.$$

Necessary to consider sign β_i; angle β_i it is counted off, as shown in Fig. 6-1d.

The calculation procedures of UM of the different construction/design, which include the determination of main sizes/dimensions and sizes/dimensions of magnetic circuit, the calculation of magnetic circuit, excitation winding, voltage drop in the circuit, armature current, the calculation of current pickup, losses and efficiency of machines, and also indication according to performance calculation of UM, are published in works [63-65].

6.3. Optimum relationship/ratio of the sides of the cross section of field coil.

a) Posing of the question.

The ratio of the width of field coil $b_в$ to its height/altitude $h_в$ at the constant value of air-gap diameter D and magnetizing force of excitation $F_{в.м}$ must be chosen from the condition of minimum space (weight) of UM.

Let us find the dependence of weight or space of machine on the relation of the sides of the section of field coil $V=f\left(\frac{b_в}{h_в}\right)$ when $F_{в.н}=\text{const}$ and D=const, after assuming that the current density $j_в$, the duty factor of window $\kappa_з$ and the section of excitation winding $S_в=b_в h_в=\frac{F_{в.н}}{j_в k_з}=\text{const}$ are constant/invariable at all in practice possible values of value $b_в/h_в$.

Weight of UM in the first approximation, $G=\gamma_{ср}V$, where $\gamma_{ср}$ - average specific gravity/weight of materials in the conditional calculated space of machine V, equal to $\gamma_{ср}\approx 8\cdot 10^4$ N/m³.

B) acyclic machine with the cylindrical rotor.

Conditional calculated space of machine in accordance with Fig. 6-4a

$$V=\frac{\pi D_н^2}{4}L_в=\frac{\pi D_н^2}{4}(2l+b_з+2b_к).$$

Taking into account that

$$\frac{\pi(D_н^2-D_в^2)}{4k_{зс}}B_с=\frac{\pi(D_р^2-d_в^2)}{4k_{зр}}B_р \quad \text{and} \quad D_в=D+2(\delta+\Delta h_в+h_в)=D+2h_{в1},$$

we obtain:

$$D_н^2=D_в^2+(D_р^2-d_в^2)\frac{k_{зс}}{k_{зр}}\frac{B_р}{B_с}=4h_{в1}^2+4Dh_{в1}+D^2(1+\gamma_ш),$$

where

$$\varphi_{\text{ш}}=(\mathring{D}_{\text{п}}^2-\mathring{d}_{\text{в}}^2)\frac{k_{\text{ос}}}{k_{\text{ор}}}\frac{B_{\text{р}}}{B_{\text{с}}};\quad h_{\text{в1}}=h_{\text{в}}+\delta+\Delta h_{\text{в}};$$

and

$$L_{\text{в}}=2l+b_{\text{в}}+2b_{\text{к}}=2\lambda_{\text{ш}}D+2\lambda_{\text{к}}D+b_{\text{в}}=D(2\lambda_{\text{ш}}+2\lambda_{\text{к}})+b_{\text{в}},$$

where

$$\lambda_{\text{ш}}=\frac{l}{D}\quad\text{and.}\quad\lambda_{\text{к}}=\frac{b_{\text{к}}}{D}.$$

Page 145.

After substituting obtained values $D_{\text{в}}$ and $L_{\text{в}}$ into the expression for the space of machine, let us find:

$$V=\frac{\pi}{2}\frac{8(\lambda_{\text{ш}}+\lambda_{\text{к}})Rh_{\text{в1}}^3+2]\,8(\lambda_{\text{ш}}+\lambda_{\text{к}})R^2+}{h_{\text{в1}}}\ldots-$$

$$-\ldots\frac{+S_{\text{в1}}]h_{\text{в1}}^2+[8(\lambda_{\text{ш}}+\lambda_{\text{к}})(1+\varphi_{\text{ш}})R^2+4S_{\text{в1}}R]h_{\text{в1}}+2(1+\varphi_{\text{ш}})S_{\text{в1}}R^2}{},$$

where

$$R=0{,}5D;\ S_{\text{в1}}=h_{\text{в1}}b_{\text{в}}.$$

In accordance with the geometric relationships/ratios of cylindrical UM, that occur in practice, can be taken $\varphi_{\text{ш}}\approx 1$; $\lambda_{\text{ш}}\approx 0{,}25$; $\lambda_{\text{к}}\approx 0{,}125$. Taking into account that $\delta<<D$ and $\Delta h_{\text{в}}\ll D$, we assume/set $h_{\text{в1}}\approx h_{\text{в}}$ and $S_{\text{в1}}\approx S_{\text{в}}$.

In this case the calculated space

$$V=\frac{\pi}{2}\frac{3Rh_{\text{в}}^3+(6R^2+2S_{\text{в}})h_{\text{в}}^2+(6R^2+4RS_{\text{в}})h_{\text{в}}+4R^2S_{\text{в}}}{h_{\text{в}}}.\qquad(6\text{-}20)$$

Derivative (6-20)

$$\frac{dV}{dh_{\text{в}}}=\frac{\pi}{2}\frac{3Rh_{\text{в}}^3+(3R^2+S_{\text{в}})h_{\text{в}}^2-2R^2S_{\text{в}}}{h_{\text{в}}^2};\ h_{\text{в}}\neq 0.$$

At optimum value $h_в = h_{в0}$ we have a point of the extremum of function $V = f(h_в)$, in which

$$3Rh_в^3 + (3R^2 + S_в)h_в^2 - 2R^2S_в = 0. \qquad (6\text{-}21)$$

Checking shows that $\frac{d^2V}{dh_в^2} > 0$, at extreme point $V = V_{max}$ (and respectively $G = G_{max}$). Incomplete cubic equation (6-21) makes it possible to express size/dimension $h_{в0}$ through assigned magnitudes R and $S_в$ and to find $b_{в0} = \frac{S_в}{h_{в0}}$. Bringing (6-21) to the canonical form and its research shows that the determinant of equation is positive for all encountered in practice of relationships/ratios geometric dimensions of UM. Consequently, expression (6-21) has one real root, which can be determined according to the Cardan solution [107].

Page 146.

On the basis of the series/row of calculations curve $\frac{G}{G_{max}} = f\left(\frac{b_в}{h_в}\right)$, shown in Fig. 6-4b, is obtained. From the curve it is evident that in the range $b_в/h_в = 1{,}5 \div 3{,}5$ values G (or V) are close to G_{max} (V_{max}). UM is recommended the choosing of the relationships/ratios of the sizes/dimensions of field coil during the design from this range.

For facilitating the calculations during the determination of optimum values $h_{в0}$ and $b_{в0}$ it is possible to use the nomogram Fig. 6-5.

It makes it possible to find root $h_{в0}$ of equation (6-21) with the given ones R=0.5D and $S_в$ for the wide power range of UM. During the construction of nomogram the designations

$$\alpha = R + \frac{S_в}{3R}; \quad \beta = \frac{2}{3} RS_в.$$

are introduced. [11] The results of the solution of this problem it is possible to spread to the cylindrical UM with the hollow rotor and other electromagnetic systems [108].

C) disk acyclic machine.

Let us consider symmetrical UM with the flat/plane rotor, after taking the assumptions, analogous as that done during the solution of the previous problem in §6-3a.

In accordance with the designation of sizes/dimensions in Fig. 6-4c calculated space of the machine

$$V = \frac{\pi D_н^2}{4} L_в = \frac{\pi D_н^2}{4} (2l_н + b_в + c) =$$

where

$$= \frac{\pi D_н^2}{4} [D(2\lambda_н + \lambda_c) + b_в],$$

$$c = b_н + 2\delta; \quad \lambda_н = \frac{l_в}{D} \text{ and } \lambda_c = \frac{c}{D}.$$

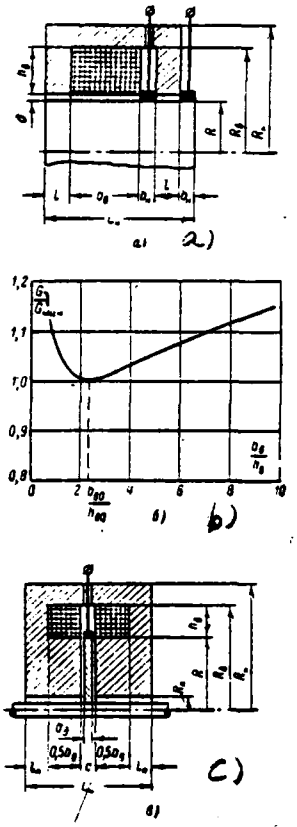

Fig. 6-4. On the calculation of UM of the smallest weight. a) the designation of the calculated sizes/dimensions of cylindrical machine; b) the same of disk; c) dependence $G/G_{min} = f(D_0/h_0)$ for the cylindrical UM with D=0.2 m and $s_0 = 6 \cdot 10^{-4}$ m^2.

Page 147.

After taking into account that $\frac{\pi}{4}(D_a^2 - D_p^2) B_c = \frac{\pi}{4}(D^2 - D_1^2) B_1 k_{oc}$

and $D_a = D + 2h_a$,

we will obtain:

$$D_{\text{в}}^2 = D_{\text{в}}^2 + D^2\varphi_{\text{д}} = 4h_{\text{в}}^2 + 4Dh_{\text{в}} + (1+\varphi_{\text{д}})D^2 \qquad \text{and} \qquad L_{\text{в}} = \varphi_{\text{д}1}D + b_{\text{в}},$$

where

$$\varphi_{\text{д}} = (1-\mathring{D}_1)\frac{B_1}{B_{\text{с}}}k_{\text{ос}};\ \mathring{D}_1 = \frac{D_1}{D};\ \varphi_{\text{д}1} = 2\lambda_{\text{в}} + \lambda_{\text{с}}.$$

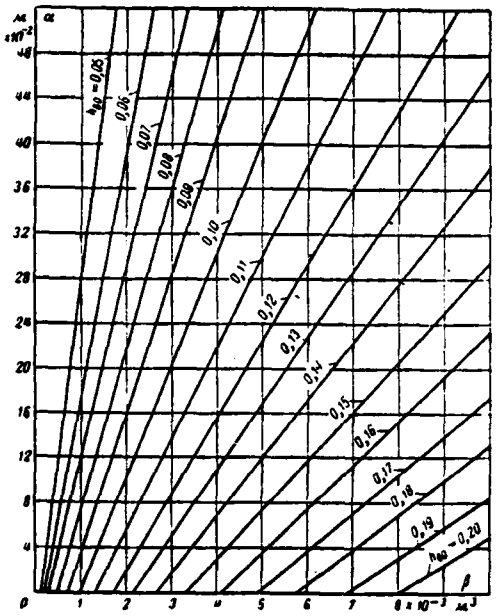

Fig. 6-5. Nomogram for determining the optimum height of the cross section of field coil.

Page 148.

Calculated space taking into account values $D_в^2$ and $L_в$

$$V = \pi \frac{D\varphi_{л1} h_в^3 + (S_в + D^2\varphi_{л1}) h_в^2 + D[S_в + 0.25D^2\varphi_{л1}(1+\varphi_л)] h_в + \ldots \rightarrow}{h_в} \ldots \rightarrow$$

$$\ldots \rightarrow \frac{+ 0.25(1+\varphi_л) D^2 S_в}{}, \qquad (6\text{-}22)$$

where

$$S_в = b_в h_в.$$

Analysis (6-22) with the help of the differentiation gives the equation of the form

$$2D\varphi_{л1} h_в^3 + (S_в + D^2\varphi_{л1}) h_в^2 - 0{,}25(1+\varphi_л) D^2 S_в = 0.$$

for obtaining the optimum value $h_в = h_{в0}$ If we take $\varphi_д \approx 1$ and $\varphi_{дI} \approx 0{,}5$, then latter/last equation will take the form:

$$Dh_в^3 + (S_в + 0{,}5D^2)h_в^2 - 0{,}5D^2S_в = 0. \qquad (6\text{-}23)$$

The incomplete equation of third power (6-23) is solved as equation (6-21), with the help of the Cardan solution. The results of the series/row of its solutions show that for obtaining the smallest weight of the magnetic circuit of disk UM with assigned magnitudes D=2R and $F_{в.н}$ (or $S_в$) it is necessary to choose the relationships/ratios of coil sides of excitation from range $b_в/h_в \approx 1{,}5 \div 3$. This range is close to the same for the cylindrical machines.

6.4. Relationships/ratios of electromagnetic loads and the appropriate relationships/ratios between the voltage/stress, the current and the power of UG.

With the given current and the voltage/stress of UG their electromagnetic loads (inductions and current density) are connected with rigid relationships/ratios. Selection of one of the loads causes the value of another. After calculating the latter, it should be compared with that permitted.

In the general case it is possible to use the following relationships/ratios respectively for the cylindrical UM with the solid rotor and the disk UM with the one-sided current pickup:

$$\frac{B_p}{j_p} = \frac{m_I k_{ep} (\mathring{D}_p^2 - \mathring{d}_в^2)_I}{\mathring{U} k_I m_E (\mathring{D}_p^2 - \mathring{d}_в^2)_E} \frac{U}{nI}$$

also, when $D_a \approx D_1$

$$\frac{B_\delta}{j_1} \approx \frac{m_1}{\mathring{U}k_1 m_E} \frac{\cos\alpha \mathring{D}_n^2}{1-\mathring{D}_n^2} \frac{U}{nl}. \qquad (6\text{-}24)$$

Page 149.

During the bilateral current pickup on the shaft of disk UM the right side of the latter/last expression increases doubly.

The connection/communication between the induction in the gap and the rotor cylindrical UG is characterized by the relationship/ratio

$$\frac{B_p}{B_\delta} = 4 \frac{\lambda_a k_{sp}}{(\mathring{D}_p^2 - \mathring{d}_a^2)_E}.$$

Connection between the linear load of armature, the current density in the rotor and in the contact of the current pickup (on the surface of rotor) of the cylindrical machine

$$\frac{A}{j_p} = \frac{(\mathring{D}_p^2 - \mathring{d}_a^2)_l}{4\mathring{D}_p} D; \quad \frac{A}{j_a} = \lambda_K D; \quad \frac{j_p}{j_a} = 4\lambda_K \frac{\mathring{D}_p}{(\mathring{D}_p^2 - \mathring{d}_a^2)_l},$$

where $\lambda_K = \frac{b_K}{D}$.

The following relationships/ratios are valid for the contacts of disk UG on the shaft and the periphery of the rotor:

$$\frac{j_1}{j_{K1}} \approx 4 \frac{\lambda_{K1}}{\mathring{D}_a} \quad \text{and} \quad \frac{j_1}{j_{KD}} \approx 4 \frac{\lambda_{KD}}{\mathring{D}_n^2},$$

where

$$\lambda_{\kappa 1}=\frac{b_{\kappa 1}}{D};\ \lambda_{\kappa D}=\frac{b_{\kappa D}}{D};\ D_{\text{н}}\approx D_1.$$

With $j_{\kappa 1}=j_{\kappa D}=j_{\kappa}$

$$\mathring{D}_{\text{н}}=\frac{D_{\text{н}}}{D}=\frac{b_{\kappa D}}{b_{\kappa 1}},$$

then

$$\frac{A_1}{j_{\kappa}}=b_{\kappa 1}=\frac{b_{\kappa D}}{\mathring{D}_{\text{н}}},$$

where A_1 - linear load of rotor shaft, determined from expressions (6-8).

Page 150.

On the basis of that presented it follows that with they are optimum for the use of active materials electromagnetic loads there exists certain range of the economically appropriate relationships/ratios between the fundamental parameters of UG: I, U, $P_{\text{э}}$.

The relationship/ratio between current and voltage/stress of cylindrical and disk machines with assigned magnitudes $B_{\text{д}}/j_{\text{д}}$, $B_{\text{д}}/j_1$ is determined by equation (6-24); U=f(I) presents linear dependence. The connection/communication between the current and the power is established/installed by formulas (6-19); dependence $P_{\text{э}}=f(I)$ -

parabolic.

Fig. 6-6 depicts the appropriate curves, calculated for 2p=2; n=50 r/s (3000 r/min); $\mathring{U}^{-1}=1{,}02$; $k_j=1{,}0$ for the cylindrical $[(\mathring{D}_p^2-\mathring{d}_p^2)_{E:I}\approx 1,\ k_{sp}\approx 1;\ B_p=B_3]$ and disk $(\mathring{D}_n=0{,}3;\ \cos\alpha\approx 0{,}99)$ machines. In this case ratios B_3/j_p and B_3/j_1 for both types of UG were changed in the range $1\cdot10^{-4}$-$3\cdot10^{-4}$ Ω·s.

6.5. Calculation of the force of unbalanced magnetic pull.

During the eccentric location of ferromagnetic rotor of UM relative to the bore of the pole of stator (Fig. 6-7), caused by inaccuracies in the working/treatment, assembly, by gap of bearings, appears electromagnetic force $T_э$ of the attraction of rotor to the stator. The direction of action $T_э$ passes through a radius with the smallest working gap.

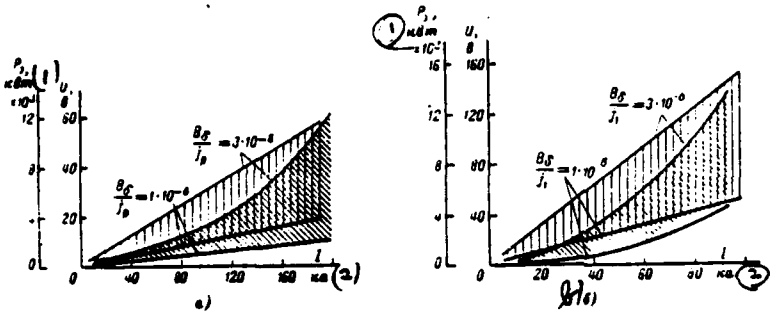

Fig. 6-6. Economically appropriate relationships/ratios U, P=f(I) with 2p=2: a) for the cylindrical ones; b) for the disk machines; U - straight line of shading; P_2 - oblique shading.

Key: (1). kW. (2). kA.

Page 151.

The calculation of force $T_э$ is necessary during the design of shafts and the selection of bearings UM. In the coaxial position of the cylinders of rotor and stator $T_э=0$, with the eccentric it can be sufficient large and theoretically $T_э \to \infty$ with the contact of cylinders. The saturation of magnetic material virtually limits value $T_э$

In accordance with the designations of sizes/dimensions in Fig. 6-7a with the relatively small gaps $\delta=R_1-R_2<<R_1$ air-gap clearance in the function of angle φ with the high accuracy obeys the law

$$\delta_\varphi = \delta(1 - \varepsilon\cos\varphi), \qquad (6\text{-}25)$$

where δ - radial clearance during the coaxial location of cylinders;

$\epsilon=e/\delta$ - relative eccentricity ($e=\epsilon\delta$).

The expression of magnetic energy in the gap for the system of cylindrical coordinates r, φ, z:

$$W_\delta=\frac{1}{2\mu_0}\int_{R_1-\delta}^{R_1}\int_0^{2\pi}\int_0^{l} B_\delta^2(\varphi)\,r\,dr\,d\varphi\,dz, \tag{6-26}$$

where l - active length in one-pole limits.

Assuming/setting a magnetic-potential difference between the surfaces, converted to the gap, by equal to F_δ, we have:

$$B_\delta(\varphi)=\frac{\mu_0 F_\delta}{\delta(1-\epsilon\cos\varphi)}. \tag{6-27}$$

After producing integration in (6-26), taking into account (6-27) we will obtain:

$$W_\delta=\frac{\pi\mu_0}{2}F_\delta^2\left[\frac{2R_1}{\delta(1-\epsilon^2)^{0.5}}-1\right]. \tag{6-28}$$

Differentiating (6-28) on the relative eccentricity and taking into account the value of the magnetic constant of $\mu_0=0.4\pi\cdot10^{-6}$ H/m, we find the force, which functions under one pole:

$$T_\delta=\lambda F_\delta^2\,k_\epsilon,\ H, \tag{6-29}$$

where

$$\lambda=\frac{l}{D_1};\ D_1=2R_1;\ k_\epsilon=1{,}97\cdot10^{-6}\left(\frac{D_1}{\delta}\right)^2\frac{\epsilon}{(1-\epsilon^2)^{3/2}}.$$

Page 152.

The values of coefficient $k_\epsilon=f(\epsilon)$ for different D_1/δ are given in Fig. 6-7c.

From (6-29) it is evident that with $\epsilon \to 0$ force $T_э$

Let us carry out replacement $F_\delta = \Phi/\Lambda_\delta$. With the known flow in the gap

$\Phi = 0{,}25\pi D_p B_p$ (D_p and B_p — diameter and induction in the middle part of the rotor) we will obtain:

$$T_э = \frac{\lambda}{\Lambda_\delta^2}\Phi^2 k_{э.} \qquad (6\text{-}30)$$

The expression of permeance of eccentric radial clearance easily is derived during the use of approximation (6-25):

$$\Lambda_\delta = \int_0^{2\pi} \frac{\mu_0 l R_1 d\varphi}{\delta(1-\varepsilon\cos\varphi)} = \frac{2\pi\mu_0 l R_1}{\delta(1-\varepsilon^2)^{0.5}} \approx$$

Key: (1). Ω·s.

$$\approx \frac{3{,}95\cdot 10^{-6}\lambda D_1^2}{\delta(1-\varepsilon^2)^{0.5}}, \text{ (1) } ом\cdot сек. \qquad (6\text{-}31).$$

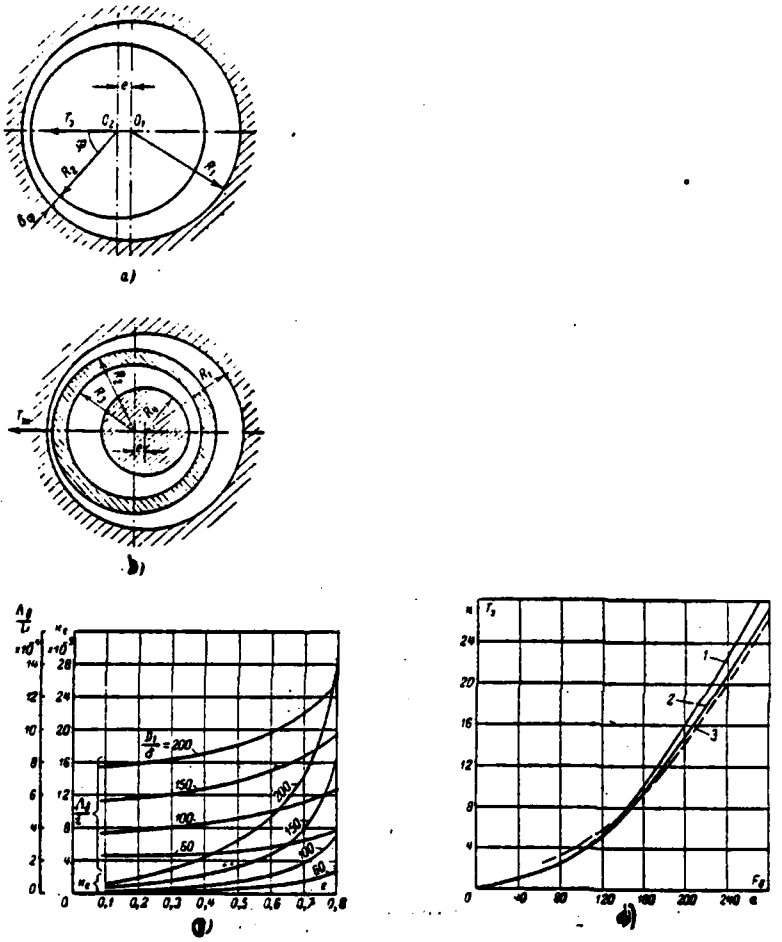

Fig. 6-7. On the calculation of the forces of the one-sided attraction of the cylindrical magnetic rotors: a) massive; b) is gentle; c) dependence κ_e and Λ_δ/τ on ϵ from parameter D_1/δ; d) the comparison of data of the calculation: 1 - according to (6-29); 2 - on (6-36) and 3 - ofexperiment with ϵ=0.5; δ_1/R_1=0.0833 for the model UM.

With the help of (6-31) it is possible to determine the force

$$T_э = \frac{1}{2} F_б^2 \frac{d\Lambda_б}{de} = \frac{1}{2} \frac{F_б^2}{\delta} \frac{d\Lambda_б}{d\varepsilon}. \quad (6\text{-}32)$$

The result of differentiation (6-31) and substitution of derivative in (6-32) coincides with (6-29).

The determination of force $T_э$ of the attraction of hollow ferromagnetic rotor (Fig. 6-7b) is reduced to two cases: determination $T_э$ for the the external δ_1 and internal δ_2 of the pole gaps of stator-rotor unit. Net force

$$T_{э.п} = T_{э1} + T_{э2},$$

moreover in accordance with Fig. 6-7b and formula (6-29)

$$T_{э1} = \lambda_1 F_{б1}^2 k_{\varepsilon 1};\ T_{э2} = \lambda_2 F_{б2}^2 k_{\varepsilon 2}. \quad (6\text{-}33)$$

In the latter/last expressions it is marked:

$F_{б1}$, $F_{б2}$ — a magnetic-potential difference between the surfaces of cylinders, converted to the external and internal gaps $\delta_1 = R_1 - R_2 = \delta_2 = R_3 - R_4$;

$$\lambda_1 = \frac{l}{D_1};\ \lambda_2 = \frac{l}{D_2};\ (D_1 = 2R_1,\ D_2 = 2R_2);\ \varepsilon_1 = \frac{e}{\delta_1};\ \varepsilon_2 = \frac{e}{\delta_2};$$

$$k_{\varepsilon 1} = 1{,}97 \cdot 10^{-6} \left(\frac{D_1}{\delta_1}\right)^2 \frac{\varepsilon_1}{(1-\varepsilon_1^2)^{3/2}};$$

$$k_{\varepsilon 2} = 1{,}97 \cdot 10^{-6} \left(\frac{D_2}{\delta_2}\right)^2 \frac{\varepsilon_2}{(1-\varepsilon_2^2)^{3/2}}.$$

In the case, when $\delta_1=\delta_2=\delta$ and $\varepsilon_1=\varepsilon_2=e/\delta$, with Φ=const taking into account the relationship/ratio

$$\frac{F_{\delta 1}}{F_{\delta 2}}=\frac{\Lambda_{\delta 1}}{\Lambda_{\delta 2}}=\frac{D_1}{D_2}=\nu$$

after the addition of expressions (6-33) we find:

$$T_{э.м}=\lambda_1 F_{\delta 1}^2 k_{\varepsilon 1}(1+\nu). \tag{6-34}$$

For the multipole UM $T_э$ increases 2p once.

Page 154.

Let us derive the formula of equivalent permeance of gaps in the system with the hollow eccentrically arranged/located ferromagnetic rotor. Applying expression (6-31) to the problem, illustrated by Fig. 6-7b, we have:

$$\Lambda_{\delta 1}=\frac{3{,}95\cdot 10^{-9}\lambda_1 D_1^2}{\delta_1(1-\varepsilon_1^2)^{0.5}};\quad \Lambda_{\delta 2}=\frac{3{,}95\cdot 10^{-9}\lambda_2 D_3^2}{\delta_2(1-\varepsilon_2^2)^{0.5}},\ \Omega\cdot s. \qquad (6\text{-}35).$$

Equivalent conductivity of two consecutive gaps

$$\Lambda_{\varepsilon n}=\frac{\Lambda_{\delta 1}\Lambda_{\delta 2}}{\Lambda_{\delta 1}+\Lambda_{\delta 2}}.$$

Differentiating $\Lambda_{\delta 1}$ and $\Lambda_{\delta 2}$ on ε_1 and ε_2, we obtain (6-33). In the case $\delta_1=\delta_2=\delta$

$$\Lambda_{\delta n}=\frac{3{,}95\cdot 10^{-9}\lambda_1 D_1^2}{\delta(1+\nu)(1-\varepsilon_1^2)^{0.5}},\ \Omega\cdot s.$$

A latter/last form of Lu can be used for determination $T_{э.м}$. On

the basis (6-32)

$$T_{э.м}=\frac{1}{2}F_{\delta n}\frac{1}{\delta}\frac{d\Lambda_{\delta n}}{de_1};\ (F_{\delta n}=F_{\delta 1}+F_{\delta 2}).$$

After the series/row of conversions taking into account the equality

$$F_{\delta n}^2=(1+\nu)^2F_{\delta i}^2$$

we obtain the result, which coincides with (6-34).

Let us note that expression (6-29) is led to the formula, obtained by A. V. Gordon [109, formula (4-43)] by other means: on the basis of simplification in G. Roters's formula [83] for permeance and subsequent differentiation of the approximate result. Let us note also that the known expression of Roter [110, formula (16a)], [83, formula (8-16a)] for calculating the electromagnetic force is registered erroneously.

Page 155.

Formula in the correct writing takes the form:

$$T_э=\frac{\pi\mu_0 lF_\delta^2}{\left\{\ln\left|1+a\left(1+\sqrt{1+\frac{2}{a}}\right)\right|\right\}^2 a\sqrt{1+\frac{2}{a}}}\frac{e}{R_1R_2},\qquad(6\text{-}36)$$

where

$$a=\frac{\delta^2-e^2}{2R_1R_2}=\frac{\delta^2(1-\varepsilon^2)}{2R_1R_2}.$$

The results of the comparison of calculated and experimental values are given in Fig. 6-7d.

The fundamental results of the calculation, examined in this paragraph, can be spread to other types of electromechanical devices/equipment with unipolar magnetization [68].

Derived formulas (6-29) (6-33) are approximate, but they ensure the accuracy of calculations. completely sufficient for the engineering practice in work [68] there are also more precise formulas for calculating the forces $T_э$, obtained during the solution of problem in the bipolar coordinates.

The effect of some factors on the amount of force $T_э$ in the disks UM with the ferromagnetic rotor was studied experimentally (see Chapter 10). The analytical solution of a question presents considerable difficulties.

Chapter Seven.

COMPARISON OF DIFFERENT ACYCLIC MACHINES.

7.1. Comparison of the coefficients of use.

For the purpose of the facilitation of the selection of construction of UM is produced below comparison of UM of different performance on their over-all payload ratios, ultimate capacities and effect of a number of poles and rotational speed by the over-all payload ratio.

With series connection of powered phases the coefficients of the use of two-pole cylindrical UM with the massive and hollow rotors × 6-1) comprise:

$$\sigma_{\text{м}} = \frac{P_{\text{э}}}{D^2 l n} = 19{,}62 \cdot 10^{-3} A_{\text{м}} B_{\delta\text{м}} \mathring{D}_{\text{р}};$$

$$\sigma_{\text{м}} = \frac{P_{\text{э}}}{D^2 l n} = 19{,}62 \cdot 10^{-3} A_{\text{м}} B_{\delta\text{м}}.$$

For the disks UM with p=1

$$\sigma_{\text{д}} = 4{,}93 \cdot 10^{-3} (\mathring{D}_{\text{н}} + \mathring{D}_{\text{в}}^{2}) A_{1\text{д}} B_{\delta\text{д}}.$$

The coefficient of the use of bipolar (collector) machines of the direct current

$$\sigma = \frac{P_э}{D^2 l n} = 9{,}86 \cdot 10^{-3} \alpha_\tau A B_\delta,$$

where $\alpha_\tau = b_\delta/\tau$ — coefficient of polar overlap.

From the given relationships/ratios it is evident that in the identical values $D^2 l$ and relations $P_э/n$ must occur the equality

$$A_\Pi B_{\delta\Pi} = \frac{1}{\mathring{D}_p} A B_{\alpha_\delta \Pi} = \frac{\alpha_\tau}{2\mathring{D}_p} A B_\delta;$$

$$A_{1\Pi} B_{\delta\Pi} = \frac{2\alpha_\tau}{\mathring{D}_\Pi + \mathring{D}_\Pi^2} A B_\delta = \frac{4\mathring{D}_p}{\mathring{D}_\Pi + \mathring{D}_\Pi^2} A_\Pi B_{\delta\Pi}.$$

Page 157.

On the average of ratio $\mathring{D}$, $\mathring{D}_\Pi$ and α_τ they are changed approximately/exemplarily within the following limits:

$$\mathring{D}_p \approx 0{,}8 \div 1{,}0, \quad \mathring{D}_\Pi = 0{,}2 \div 0{,}4, \quad \alpha_\tau \approx 0{,}63 \div 0{,}72.$$

Consequently,

$$A_\Pi B_{\delta\Pi} \approx (1{,}0 \div 1{,}25) A_\Pi B_{\delta\Pi} \approx (0{,}315 \div 0{,}45) A B_\delta;$$
$$A_{1\Pi} B_{\delta\Pi} \approx (5{,}7 \div 16{,}6) A_\Pi B_{\delta\Pi} \approx (2{,}25 \div 6{,}0) A B_\delta.$$

On the other hand, with identical $D^2 l$, $P_э/n$ and products of electromagnetic loads $A_\Pi B_{\delta\Pi} = A_{1\Pi} B_{\delta\Pi} A B_\delta$ cylindrical UM with the massive (ferromagnetic) rotor have better use of a sensitive volume, than disk UM (with the steel current carrying shaft) and bipolar machines, and disk UM have worse use than bipolar. Linear load mind with hollow ferromagnetic rotor A_Π is less than the linear load of the corresponding generators with solid rotor ($A_\Pi < A_\Pi$). Calculations are shown [60, 64] that, for example, when $P_э/n \cong 7{,}5 \cdot 10^{-4}$ kW/rev/sUM with the

hollow rotor have worse use than UM with the solid rotor, but it is better than the corresponding commutator machines.

7.2. Cylindrical machines with the massive flat rotors with the smallest number of current pickups.

A minimum number of the slide contacts of current-tap apparatus $m_к=2$ have two- and four-terminal UM with the half use of active length of armature (Fig. 7-1a, b). When $m_к=2$ is raised reliability and is simplified construction UM in comparison with the machines with a large number of current pickups.

Page 158.

Comparing the parameters of UM, carried out on structural/design given in Fig. 7-1a and b, let us take identical: 1) rated powers $P_{э1}=P_{э2}$; 2) the linear velocities on the surface of rotor $v_1=v_2$; 3) the electromagnetic loads: induction in the gap and rotor $B_{δ1}=B_{δ2}$; $B_{p1}=B_{p2}$ and current density in the contact and armature $j_{к1}=j_{к2}$; $j_{p1}=j_{p2}$. The problem of comparison consists in finding of construction/design UM, having smallest over-all payload ratio $\mathring{G}_{1(2)}=G_{1(2)}/P_{э1(2)}$, N/kW.

The average specific gravity/weight of materials is taken $\gamma_{cp1}=\gamma_{cp2}\approx 8\times 10^4$ N/m^3. In accordance with the designations of

sizes/dimensions, indicated in Fig. 7-1, with the identical design factors $\lambda_{1(2)}=l_{1(2)}/D_{1(2)}$ are obtained the following relationships/ratios of emf, currents of main sizes/dimensions and rotational speeds UM:

$$\frac{E_1}{E_2}=\frac{l_1}{2l_2}=\frac{D_1}{2D_2};\quad \frac{I_1}{I_2}=\left(\frac{D_1}{D_2}\right)^2;\quad \frac{n_1}{n_2}=\frac{D_2}{D_1};\quad \frac{P_{21}}{P_{22}}=\frac{1}{2}\left(\frac{D_1}{D_2}\right)^2=1.$$

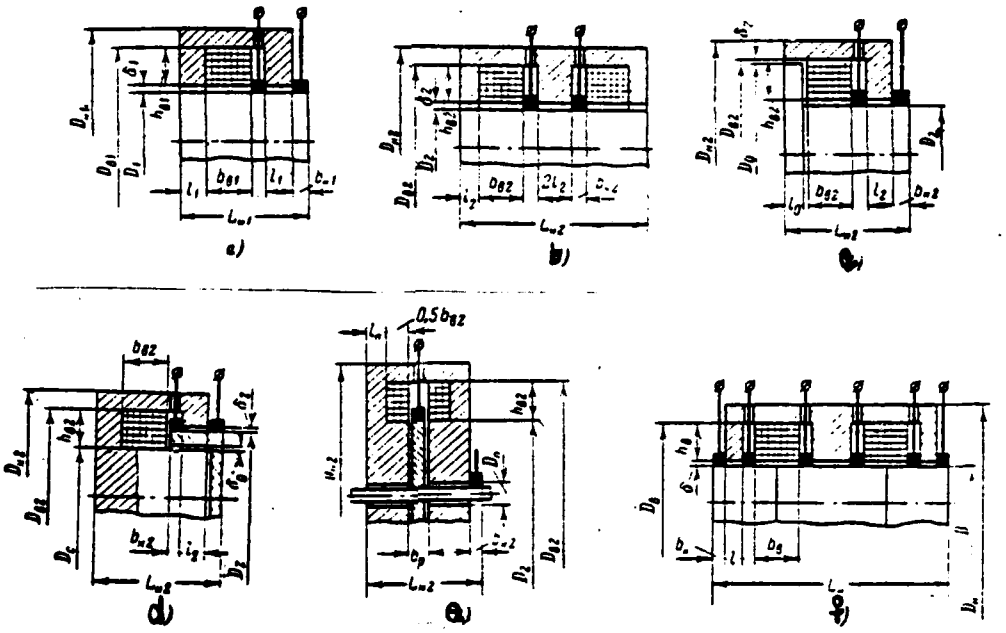

Fig. 7-1. Designation of calculated sizes/dimensions UM: a) cylindrical with solid rotor ($m_к$=2; 2p=2); b) cylindrical ($m_к$=2; 2p=4); c) with the rotor expansion; d) with the hollow rotor; e) disk; f) by multipole cylindrical (2p=4).

Page 159.

Consequently,

$$\frac{D_1}{D_2}=\frac{l_1}{l_2}=\sqrt[3]{2}=1{,}26;\ \frac{E_1}{E_2}=0{,}63;\ \ \frac{I_1}{I_2}=1{,}59;\ \ \frac{n_1}{n_2}=0{,}795.$$

Assuming/setting identical the working gaps $\delta_1=\delta_2=\delta$, n. s. (magnetizing force) of excitation to the pole pair $F_{в1}=F_{в2}=F_в$ and the sizes/dimensions of the section of field coils $b_{в1}=b_{в2}=b_в$; $h_{в1}=h_{в2}=h_в$, and

also magnetic induction in stators $B_{c1}=B_{c2}=B_c$ and disregarding leakage fluxes, we obtain the following dimensional relationships/ratios:

$$\left(\frac{D_{a1}}{D_{a2}}\right)^2=\frac{D_1^2+D_{a1}^2}{D_2^2+D_{a2}^2};$$

$$D_{a1}=D_1\left(1+2\frac{h_a}{D_1}\right);\quad D_{a2}=D_2\left(1+2\frac{h_a}{D_2}\right);$$

moreover it is taken into consideration, that

$$\delta_{1\,(2)}\ll D_{1\,(2)};\ D_2/D_1=0{,}795.$$

Consequently,

$$\left(\frac{D_{a1}}{D_{a2}}\right)^2\cong\frac{\left(\frac{h_a}{D_2}\right)^2+1{,}26\frac{h_a}{D_2}+0{,}8}{\left(\frac{h_a}{D_2}\right)^2+\frac{h_a}{D_2}+0{,}5}=f\left(\frac{h_a}{D_2}\right). \tag{7-1}$$

Similarly it is possible to show that with $l_1=1.26l_2$ and $b_{K1}/b_{K2}=$ $=D_1/D_2=1{,}26$ is correct the equality:

$$L_{a1}/L_{a2}=\frac{1{,}26+(0{,}5b_a+1{,}26b_{K2})\,l_2^{-1}}{2+(b_a+b_{K2})\,l_2^{-1}}. \tag{7-2}$$

In the general case of the ratio of weights and volumes UM when $P_{a1}=P_{a2}$ they will comprise:

$$\frac{G_1}{G_2}=\frac{V_1}{V_2}=\left(\frac{D_{a1}}{D_{a2}}\right)^2\frac{L_{a1}}{L_{a2}};\quad\frac{\mathring{G}_1}{\mathring{G}_2}=\frac{G_1P_2}{G_2P_1}=\frac{V_1}{V_2}. \tag{7-3}$$

Page 160.

Analogously for the rotors (armatures) of machines it is possible to obtain:

$$\frac{\mathring{G}_{p1}}{\mathring{G}_{p2}}=\frac{V_{p1}}{V_{p2}}=\left(\frac{D_1}{D_2}\right)^2\frac{L_{a1}}{L_{a2}}=1{,}59\frac{L_{a1}}{L_{a2}}. \tag{7-4}$$

When $B_{p1\,(2)}=B_{\delta1\,(2)}$ and $j_{K1\,(2)}=(4\div2)\,j_{p1\,(2)}$ coefficients $\lambda_{1\,(2)}=0{,}25;$

$$\lambda_{K1\,(2)}=\frac{b_{K1\,(2)}}{D_{1\,(2)}}=\frac{1}{16}\div\frac{1}{8}\quad\text{and}\quad\frac{b_{K1\,(2)}}{l_{1\,(2)}}=0{,}25\div0{,}5.$$

Taking into account latter/last relationships/ratios in the range, used for practical purposes,

$$b_a/h_a=1\div2;\ h_a/D_2=0{,}25\div0{,}75 \quad \text{and} \quad b_a/l_2=1\div6.$$

Thus, on (7-1) and (7-2)

$$\left(\frac{D_{a1}}{D_{a2}}\right)^2=1{,}44\div1{,}27;\ \frac{L_{a1}}{L_{a2}}=0{,}55\div0{,}68.$$

On the basis (7-3) and (7-4) we obtain the result

$$\frac{\mathring{G}_1}{\mathring{G}_2}=0{,}7\div0{,}98;\ \frac{\mathring{G}_{p1}}{\mathring{G}_{p1}}=0{,}88\div1{,}08.$$

The over-all payload ratio of two-pole UM when $m_к=2$ is lower than the over-all payload ratio of that corresponding to four-terminal UM. The weight of rotor per the unit of power of bipolar machine sometimes can exceed the appropriate parameter of four-terminal.

7.3. Cylindrical machines with the flat and that expanded by rotors.

During the comparison of constructions/designs UM, depicted in Fig. 7-1a and c, we assume/set by identical ones maximum linear velocities on the lateral surfaces of flat rotor and rotor expansion $v_1=v_2$, and also armature currents $I_1=I_2$. Furthermore, we assume/set by equal ones the electromagnetic loads of machines and the sizes/dimensions of the section of field coils. In this case in accordance with the designations of sizes/dimensions in Fig. 7-1 occur the expressions:

$$\frac{E_1}{E_2}=\frac{D_1 D_0}{D_2^2};\quad \frac{I_1}{I_2}=\left(\frac{D_1}{D_2}\right)^2=1;\quad \frac{P_{э1}}{P_{э2}}=\frac{n_1}{n_2}=\frac{D_0}{D_2}.$$

For identical ones $B_{\delta 1}=B_{\delta 2}$; $\delta_1=\delta_2$; $j_{к1}=j_{к2}$; $B_{c1}=B_{c2}$ we have $h_{э1}=$ $=h_{э2}=h_э$; $b_{э1}=b_{э2}=b_э$; $b_{к1}=b_{к2}=b_к$; $\lambda_1=\lambda_2$; $l_1=l_2=l$; $l_0=\frac{D_0}{D_2}l$; $D_{н1}=D_{н2}=D_н$.

Page 161.

Then when $\gamma_{ср1}=\gamma_{ср2}$ the equality is correct

$$\frac{V_1}{V_2}=\frac{D_{н1}^2 L_{д1}}{D_{н2}^2 L_{д2}}=\frac{G_1}{G_2}=\frac{2l+2b_к+b_э}{(1+D_2/D_0)l+2b_к+b_э}.$$

Since $D_2/D_0<1$, $G_1>G_2$ but $P_{э1}>P_{э2}$.

The comparison of over-all payload ratios gives:

$$\frac{\overset{*}{G}_1}{\overset{*}{G}_2}=\frac{G_1 P_2}{G_2 P_1}=\frac{(1+2\beta)D_2/D_0}{1+\beta(1+D_2/D_0)},$$

where

$$\beta=\frac{l}{2b_к+b_э}.$$

Virtually $0<\beta<1$, then

$$\lim_{\beta\to 0}\frac{\overset{*}{G}_1}{\overset{*}{G}_2}=\frac{D_2}{D_0}<1;\quad \lim_{\beta\to 1}\frac{\overset{*}{G}_1}{\overset{*}{G}_2}=\frac{3D_2/D_0}{2+D_2/D_0}<1;\quad \frac{\overset{*}{G}_1}{\overset{*}{G}_2}<1.$$

Thus, with 2p=2, $m_к=2$ and the identical armature currents and at the maximum speeds on its surface over-all payload ratio UM with the flat rotor is lower than the over-all payload ratio of machine with the rotor expansion.

7.4. Cylindrical machines with the massive and hollow rotors.

Hollow rotor is supposed ferromagnetic. Comparison UM (Fig. 7-1a and d) let us lead with identical the values of the armature currents and electromagnetic loads. Let us take the diameters of solid rotor and internal magnetic circuit of machine with the hollow rotor equal.

Page 162.

In accordance with the designations of sizes/dimensions in Fig. 7-1 with $I_1=I_2$ and $D_1=D_c$ we find

$$D_1^2=D_2^2-D_c^2=\left[1-\left(\frac{D_c}{D_2}\right)^2\right]D_2^2;\quad \frac{D_c}{D_2}=\frac{D_1}{D_2}=\frac{1}{\sqrt{2}};$$
$$\frac{E_1}{E_2}=\frac{P_{\delta 1}}{P_{\delta 2}}=\frac{n_1}{n_2}=\frac{v_1/v_2}{D_1/D_2};\quad \frac{v_1}{v_2}=\frac{D_1 n_1}{D_2 n_2}>1. \qquad (7\text{-}5)$$

When $\delta_1=\delta_2=\delta_\delta$; $l_1=l_2=l_\delta=l$; $h_{a1}=h_{a2}$; $B_{\delta 1}=B_{\delta 2}$; $j_{K1}=j_{K2}$ we have:

$$D_{a1}=D_{a2};\quad \frac{F_{\delta 1}}{F_{\delta 2}}\approx\frac{b_{\delta 1}}{b_{\delta 2}}\approx\frac{2B_{\delta 1}}{B_{\delta 1}+B_{\delta 0}}=\frac{2D_1/D_2}{1+D_1/D_2}=0{,}83;$$
$$\frac{b_{K1}}{b_{K2}}=\frac{D_2}{D_1}=\sqrt{2};\quad \frac{V_1}{V_2}=\frac{2l+b_{\delta 1}+2b_{K1}}{2l+b_{\delta 2}+2b_{K2}}=\frac{G_1}{G_2};\quad (\gamma_{cp_1}=\gamma_{cp_2}). \qquad (7\text{-}6)$$

For those examined/considered UM can be usually counted $b_{\delta 2}/l\approx 1\div 3$; $b_{\delta 2}/b_{K2}\approx 3\div 10$; the velocity ratio is taken $v_1=v_2=1.3$.

On the basis (7-5) and (7-6) in this case we obtain:

$$\frac{\dot{G}_1}{\dot{G}_2}=\frac{G_1 P_{\delta 2}}{G_2 P_{\delta 1}}\approx 0{,}5\div 0{,}6.$$

Thus, virtually machine with the hollow rotor is relatively

heavier than UM with the solid rotor.

Deficiencies/lacks UM with the hollow rotor are smaller strength and hardness of hollow cylinder in comparison with the massive cylinder or the disk, the construction-engineering complexity of centering under the conditions of the increased velocities v_2.

Slow UM with the hollow rotor are used in the bench installations; with the vertical run of shaft they have relatively simple construction/design of contact nodes.

7.5. Cylindrical and disk machines.

Let us compare the parameters of UM, depicted in Fig. 7-1a and d. For simplicity let us select disk UM with the magnetic rotor of constant thickness and flat/plane faces of stator. Let us take identical electromagnetic loads and speeds of rotation of machines as the conditions for comparison.

Page 163.

In accordance with the designations of sizes/dimensions on Fig. 7-1 we find:

$$\frac{E_{\text{п}}}{E_{\text{л}}}=\frac{E_1}{E_2}=4\left(\frac{D_1}{D_2}\right)^2\frac{\lambda}{1-\left(\frac{D_{\text{п}}}{D_2}\right)^2}\frac{B_{\delta 1}n_1}{B_{\delta 2}n_2};$$

$$\frac{v_1}{v_2}=\frac{D_1n_1}{D_2n_2}=\left(\frac{D_{\text{п}}}{D_2}\right)^2<1.$$

When

$$B_{p_1}=B_{\delta 1},\ \lambda=\frac{l}{D_1}=0{,}25;\quad \frac{D_{\text{п}}}{D_2}=0{,}3;$$

$B_{\delta 1}=B_{\delta 2}$; $n_1=n_2$; $v_2=1{,}5v_1$ (taking into account the possibility of imparting to disk the special shape); $m_{\text{к}}=2$; $j_{p_1}=j_{p_2}$ we have:

$$\frac{E_1}{E_2}=\frac{4\lambda\,(v_1/v_2)^2}{1-\left(\frac{D_{\text{п}}}{D_2}\right)^2}=0{,}488;\quad \frac{I_1}{I_2}=\left(\frac{\frac{v_1}{v_2}}{\frac{D_{\text{п}}}{D_2}}\right)^2=4{,}95;$$

$$\frac{P_1}{P_2}=\frac{4\lambda\,(v_1/v_2)^4}{(1-D_{\text{п}}^2/D_2^2)\,D_{\text{п}}^2/D_2^2}=2{,}41.$$

We assume/set $\delta_1=\delta_2$; $F_{\text{в}1}=F_{\text{в}2}$; $h_{\text{в}1}=h_{\text{в}2}=h_{\text{в}}$; $b_{\text{в}1}=b_{\text{в}2}=b_{\text{в}}$; $2b_{\text{к}}\approx\approx b_{\text{р}}+b_{\text{к}2}$; $\beta=b_{\text{в}}+2b_{\text{к}1}$; wnen $B_{c_1(2)}=B_{\delta 1(2)}$ we obtain:

$$l_{\text{п}}=\frac{1-\left(\frac{D_{\text{п}}}{D_2}\right)^2}{4}D_2;\ D_{\text{в}1}^2=2D_1^2+4D_1h_{\text{в}}+4h_{\text{в}}^2;$$

$$D_{\text{в}2}^2=\left(2-\frac{D_{\text{п}}^2}{D_2^2}\right)D_2^2+4D_2h_{\text{в}}+4h_{\text{в}}^2;$$

$$\frac{V_1}{V_2}=\frac{G_1}{G_2}=\frac{(0{,}5D_1+\beta)\,(2D_1^2+4D_1h_{\text{в}}+4h_{\text{в}}^2)}{(0{,}455D_2+\beta)\,(1{,}91D_2^2+4D_2h_{\text{в}}+4h_{\text{в}}^2)}<1,\qquad (7\text{-}7)$$

since with $v_1/v_2=0.667$ diameter $D_2=1.5D_1$.

Consequently, when $P_{\text{в}1}=2{,}41P_{\text{в}2}$

$$\frac{\dot{G}_1}{\dot{G}_2}=\frac{G_1P_{\text{в}2}}{G_2P_{\text{в}1}}<1.$$

Virtually it is possible, for example, to take $h_{\text{в}}/D_1=0{,}3$, $\beta/D_1=0{,}7$, $h_{\text{в}}/D_2=0{,}2$; $\beta/D_2=0{,}466$, then on (7-7) $\overset{*}{G}_1/\overset{*}{G}_2=0.5$ and

Thus, disk UM has considerably larger over-all payload ratio, than cylindrical.

Page 164.

7.6. Effect of a number of poles on the value of over-all payload ratio.

Let us consider cylindrical UM with the flat and solid rotors during the complete utilization of their active length. We assume/set by constant/invariable ones the diameters of rotors D, the outside diameters of stators $D_н$, the sizes/dimensions of excitation winding $h_в$ and $b_в$, and also the width of contact surfaces $b_к$ (at the identical electromagnetic loads, the rotational speeds and the linear velocities in the surface of rotor and in the contact) with a number of poles UM 2p=var. The average (equivalent) specific gravity/weight of the materials of machines is taken $\gamma_{ср} \approx 8 \cdot 10^4$ Н/м³=const. The electrical connection of the parts of the armature we choose consecutive, in this case current I=const. According to these conditions with any number of poles 2p the correctly following relationship/ratio of emf and power:

$$\frac{E_{2p}}{E_{2p+2}} = \frac{P_{2p}}{P_{в(2p+2)}} = \frac{2p}{2p+2} < 1. \qquad (7\text{-}8)$$

Space and the weight of a 2p-polar UM in accordance with the designations (Fig. 7-1f):

$$V_{2p}=\frac{\pi D_{н}^{2}}{4}(2pl+m_{в}b_{в}+m_{к}b_{к});$$

$$G_{2p}=\gamma_{ср}V_{2p},$$

where $m_{в}=p$; $m_{к}=2p+2$ - number of field coils and number of slide contacts (during 100%- use). The ratio of volumes and weights in this case is equal to:

$$\frac{V_{2p}}{V_{2p+2}}=\frac{G_{2p}}{G_{2p+2}}=\frac{1}{1+\alpha(1+\alpha p)^{-1}}<1, \qquad (7\text{-}9)$$

where

$$\alpha=1+\frac{l+0.5b_{в}}{b_{в}}>1.$$

On the basis (7-8) and (7-9) we obtain the result

$$\frac{\dot{G}_{2p}}{\dot{G}_{2p+2}}=\frac{G_{2p}}{G_{2p+2}}\frac{P_{в(2p+2)}}{P_{в2p}}=1+\frac{1}{p(1+\alpha+\alpha p)}>1.$$

Page 165.

Thus, with the increase of a number of poles over-all payload ratio UM decreases ($\dot{G}_{2p+2}<\dot{G}_{2p}$). one should take into account that in this case a number of slide contacts in the series circuit of the armature

$$\frac{m_{к(2p+2)}}{m_{к2p}}=\frac{p+2}{p+1}>1$$

respectively increases and descends reliability of UM.

Analogous result can be obtained also for the disks UM.

7.7. Comparison of one and several machines of identical power.

AD-A139 778 UNIPOLAR ELECTRIC MACHINES WITH LIQUID-METAL CURRENT PICKUP(U) FOREIGN TECHNOLOGY DIV WRIGHT-PATTERSON AFB OH A I BETTINOV ET AL. 08 MAR 84 FTD-ID(RS)T-1205-83 4/6

UNCLASSIFIED F/G 9/3 NL

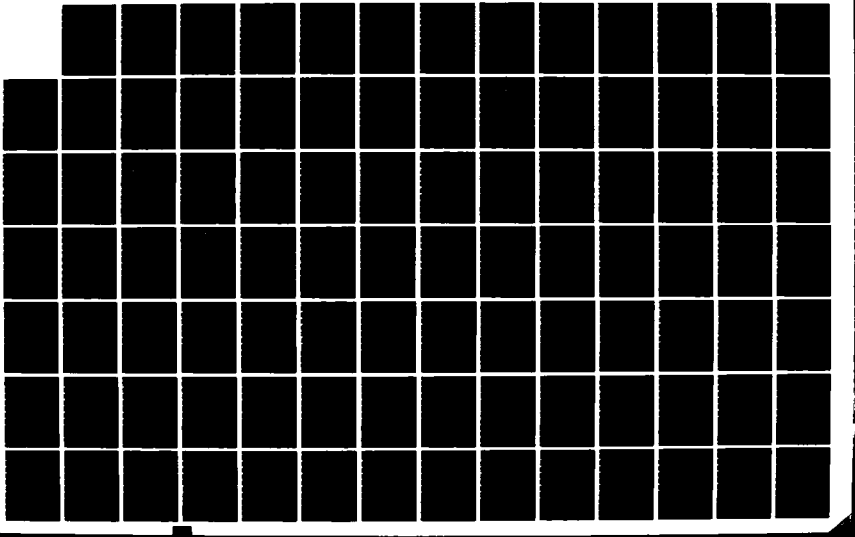

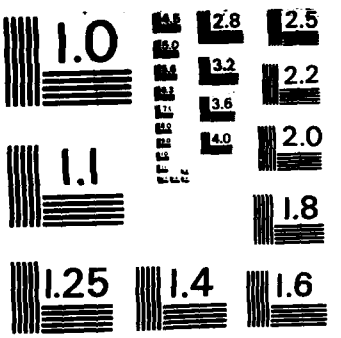

MICROCOPY RESOLUTION TEST CHART
NATIONAL BUREAU OF STANDARDS - 1963 - A

Represents interest the comparison of over-all payload ratios one UM with power $P_{э1}$ and of group of m UM with total power $mP_{э2}=P_{э1}$ ($P_{э2}$ — the power of separate machine in the group). Two-pole cylindrical machines will consider, assuming/setting by identical ones electromagnetic loads and linear velocities on the surface of rotor ($2p_1=2p_2$; $v_1=v_2$; $B_{p1}=B_{p2}$; $B_{c1}=B_{c2}$; $B_{\delta 1}=B_{\delta 2}$; $j_{p1}=j_{p2}$; $j_{к1}=j_{к2}$; $j_{в1}=j_{в2}$). without breaking generality, let us place 50% the use of active length of machine. With the equal working gaps it is possible to take the sizes/dimensions of the sides of the section of excitation windings equal. Design factor UM we choose $\lambda=0.25$.

In accordance with the designations of sizes/dimensions on fig, by 7-1 let us register expressions for the ratios of emf, currents, power, velocities and diameters:

$$\frac{E_1}{E_2}=\frac{l_1}{l_2}=\frac{D_1}{D_2};\quad \frac{I_1}{I_2}=\left(\frac{D_1}{D_2}\right)^2;$$

$$\frac{P_{э1}}{P_{э2}}=\left(\frac{D_1}{D_2}\right)^3=m;\quad \frac{n_1}{n_2}=m^{-1/3};\quad \frac{D_1}{D_2}=\frac{b_{к1}}{b_{к2}}=m^{1/3}.$$

Page 166.

Ratio of volumes and weights:

$$\frac{V_1}{V_2}=\frac{G_1}{G_2}=\frac{D_{k1}^2 L_{k1}}{D_{k2}^2 L_{k2}}=$$

$$=m^{2/3}\frac{\left[m^{1/3}+2\frac{h_k}{D_2}+2\left(\frac{h_k}{D_2}\right)^2 m^{-1/3}\right]\left[2\left(1+\frac{b_{k2}}{l_2}\right)+\frac{b_k}{l_2}m^{-1/3}\right]}{\left[1+2\frac{h_k}{D_2}+2\left(\frac{h_k}{D_2}\right)^2\right]\left[2\left(1+\frac{b_{k2}}{l_2}\right)+\frac{b_k}{l_2}\right]}>1,$$

where $m>2$, $h_{k1}=h_{k2}=h_k$ and $b_{k1}=b_{k2}=b_k$.

Let us represent the relation of over-all payload ratios taking into account the volumetric ratio in the form

$$\frac{\overset{*}{G}_1}{\overset{*}{G}_2}=\frac{G_1 P_{k2}}{G_2 P_{k1}}=\frac{G_1}{G_2 m}=$$

$$=m^{-1/3}\frac{\left[m^{1/3}+2\frac{h_k}{D_2}+2\left(\frac{h_k}{D_2}\right)^2 m^{-1/3}\right]\left[2\left(1+\frac{b_{k2}}{l_2}\right)+\frac{b_k}{l_2}m^{-1/3}\right]}{\left[1+2\frac{h_k}{D_2}+2\left(\frac{h_k}{D_2}\right)^2\right]\left[2\left(1+\frac{b_{k2}}{l_2}\right)+\frac{b_k}{l_2}\right]}<1.$$

Virtually for the wide power range UM can be taken $\frac{h_k}{D_2}\approx 0{,}25\div 1$, $\frac{b_k}{l_2}\approx 1\div 6$ and $\frac{b_{k2}}{l_2}\approx 0{,}25\div 0{,}5$. Then, for example, with m=2 and 3 we obtain $\overset{*}{G}_1/\overset{*}{G}_2=0{,}53\div 0{,}97$. If we for an example take $h_k/D_2=0{,}5$, $b_k/l_2=3$ and $b_{k2}/l_2=0{,}35$, then we will obtain dependence $\overset{*}{G}_1/\overset{*}{G}_2=f(m)$, which is registered in the form of the table:

m	2	3	4	5	6
$\overset{*}{G}_1/\overset{*}{G}_2$	0.76	0.65	0.58	0.54	0.52

Thus, the over-all payload ratio of one of more powerful/thicker UM will be less than group of m of less powerful/thick machines.

However, a similar comparison, carried out with the identical ampere-conductors per inch $A_1=A_2$, leads to the expression

$$\frac{D_1}{D_2}=\sqrt{\frac{P_{э1}}{P_{э2}}}=\sqrt{m}.$$

Page 167.

At the same time in the general case there can be $\dot{a}_1/\dot{a}_2<1$ or $\dot{a}_1/\dot{a}_2\geq 1$, and for some combinations of design factors $h_п/D_2$, $b_п/l_2$ and $b_{2к}/l_2$ over-all payload ratio $\dot{a}_1>\dot{a}_2$. For determining the concrete/specific/actual optimum version special calculations during the design are required. For the sufficiently wide power range $P_{э1}$ and $P_{э2}$ it is possible to accept $j_1=j_2$, then virtually $\dot{a}_1<\dot{a}_2$.

7.8. Effect of the rotational speed to the value of over-all payload ratio.

We assume/set with n=var by constant/invariable ones the electromagnetic loads (B_δ, B_p, B_c, j_p, $j_к$ and $j_п$), working gaps, n. s. (magnetizing force) and sizes/dimensions of the section of field coil ($b_п$ and $h_п$), and also linear velocity on the surface of rotor v and the design factors $\lambda=l/D$, $\lambda_к=b_к/D$. Let us consider for an example cylindrical UM with a number of poles 2p=2 and $m_к=2$. In accordance with the designations in Fig. 7-1 we will obtain for emf, current and power of

the expression:

$$E \equiv nB_p D^2,\ I \equiv j_p D^2 \text{ и } P_э \equiv B_p j_p n D^4.$$

In accordance with the conditions accepted the weight is UM

$$G \equiv V \equiv D_к^2 L_м = (2D^2 + 4Dh_в + 4h_в^2)(2\lambda D + 2\lambda_к D + b_в).$$

Through condition v=Dn=const we find:

$$\mathring{G} = \frac{G}{P_э} \equiv \frac{2}{B_p j_p v}\left[\alpha_1 + \beta_1\left(\frac{n}{v}\right) + \gamma_1\left(\frac{n}{v}\right)^2 + \theta_1\left(\frac{n}{v}\right)^3\right],$$

where

$$\alpha_1 = 2(\lambda + \lambda_к);\ \beta_1 = 2\alpha_1 h_в + b_в;$$
$$\gamma_1 = 2\alpha_1 h_в^2 + 2b_в h_в \text{ и } \theta_1 = 2b_в h_в^2$$

- constant values.

Thus, with an increase in the speed of rotation n and v=const over-all payload ratio will increase.

Page 168.

The analogous analysis of the value of over-all payload ratio with n=var, carried out for the constant/invariable ampere-conductors per inch A=const, gives $P_э = AB_p n D^3$ and

$$\mathring{G} \equiv \frac{2}{AB_p v}\left[\frac{\alpha_1 v}{n} + \beta_1 + \gamma_1 \frac{n}{v} + \theta_1\left(\frac{n}{v}\right)^2\right].$$

The sum, included in the brackets, is complex function f(n) from the speed of rotation n. The condition of decrease f(n) with an increase in the velocity

$$\frac{df(n)}{dn} = -\frac{\alpha_1 v}{n^2} + \frac{\gamma_1}{v} + \frac{2\theta_1}{v^2} n < 0$$

during different combinations of the parameters α_1, γ_1, θ_1, v and n

usually is satisfied in practice.

Consequently, in this case (A=const) over-all payload ratio $\dot{G}=f(n)$ is reduced with an increase in the rotational speed. However, with change n power $P_э$ varies and, as a rule, value A does not remain constant. This impedes research $\dot{G}$. At the same time the assumption about the constancy of current density in rotor j_p=const, done above, is confirmed by the analysis of the parameters of series/row of the carried out UG in the relatively wide power range.

7.9. Calculation and the comparison of cylindrical and disk non-polars dynamo of ultimate capacity.

Ultimate capacity UG is limited to permissible electromagnetic loads B_p and j_p (i.e. by the saturation of magnetic circuit and by heating) and to mechanical strength of the rotor (i.e. with the allowable voltage of material, which it is characterized by allowable speed on the periphery of rotor).

Page 169.

The maximum speed of cylindrical ferromagnetic rotor can be considered on the basis [111] according to the expression

$$v_{\text{п}} \approx 1{,}25 \cdot 10^{-2} \sqrt{\frac{[\sigma]}{1 + 0{,}212 \mathring{d}_{\text{в}}^2}}, \text{ m/s,} \qquad (7\text{-}10)$$

where $[\sigma]$ - permissible normal stress of the material of the body of rotor (steel), N/m²; $\mathring{d}_{\text{в}} = d_{\text{в}}/D$ — relation of the diameters of opening/aperture for the shaft and the outside diameter of rotor. For the solid rotors non/without- opening/aperture

$$v_{\text{п}} \approx 1{,}76 \cdot 10^{-2} \sqrt{[\sigma]}.$$

Analogously for the disk rotors of equal thickness on the basis [112] we will obtain:

$$v_{\text{п}} = 6{,}25 \sqrt{\frac{[\sigma]}{\gamma(3 + \mathring{D}_{\text{п}}^2 - \mu \mathring{D}_{\text{п}}^2 + \mu)}}, \text{ m/s,}$$

where γ, N/m³, and μ - specific gravity/weight and the Poisson ratio of the material of disk (magnetic or nonmagnetic); $\mathring{D}_{\text{п}} = D_{\text{в}}/D$ — relation of the diameters of opening/aperture for shaft and periphery of disk. For the disks of conical and hyperbolic profile/airfoil the permissible linear velocity will be above. The elements of the stress analysis of such disks are known from the specialized literature.

Allowable voltage is chosen usually equal to $[\sigma] = \sigma_{\text{т}}/n_{\text{э}}$ ($\sigma_{\text{т}}$ — yield point of material; $n_{\text{э}} > 1$ - safety factor). With the large $\sigma_{\text{т}}$ diameters of cylindrical rotors instead of $\sigma'_{\text{т}} \approx 0.7\,\sigma_{\text{т}}$ is taken since to the center of forging the mechanical properties of material deteriorate. Fig. 7-2 gives the curves

$$v_{\text{ц}} = f([\sigma]) \overset{(\text{у})}{\text{по}} \dot{d}_{\text{в}}; \quad D = f([\sigma]) \overset{\bullet}{\text{по}} \overset{(1)}{\dot{d}_{\text{в}}}, \; n \overset{(2)}{\text{и}} D = f(n) \overset{(1)}{\text{по}} \dot{d}_{\text{в}}, \; [\sigma]$$

Key: (1). per. (2). and.

for the speeds of rotation n=100-500 r/s, designed on (7-10).

At given speed of rotation n, r/s, the cut-off diameters of rotors UM are determined by expressions.

$$D_{\text{ц}} \approx \frac{4 \cdot 10^{-4}}{n} \sqrt{\frac{[\sigma]}{1 + 0{,}212 \dot{d}_{\text{в}}^2}}, \; \text{м};$$

Page 170.

$$D_{\text{ц}} \approx \frac{2}{n} \sqrt{\frac{[\sigma]}{\gamma (1 + 0{,}212 \dot{D}_{\text{п}}^2)}}; \; \mu = 0{,}3.$$

Maximum emf cylindrical UG with series connection of the active parts of the armature and 100% use comprises:

$$E_{\text{ц}} = \frac{0{,}5}{\pi} (\dot{D}_{\text{р}}^2 - \dot{d}_{\text{в}}^2)_{\text{Е}} \, p B_{\text{р}} \frac{v^2}{n}, \; \text{в}, \qquad (7\text{-}11)$$

where $B_{\text{р}}$ — saturation induction, T; v - maximum speed, m/s.

From (7-11) it is evident that for an increase in emf should be raised v and decreased n, and also increased a number of pole pairs p. Let us determine the limiting value 2p of cylindrical UG. On the basis of experiment of contemporary turbo-generator construction, we assume/set the ratio of the overall length of rotor to its diameter $L_{\text{п}}/D < 6$.

We will count $\lambda = l/D = 0.25$: $2b_к + b_в \approx 2l$, during liquid-metal current pickup $2b_к < 4pl$. In this case $L_в = p(2l + 2b_к + b_в) + 2b_к \approx 4pl < 6D$.

Thus, a maximum number of poles 2p=12. During the complete utilization a number of slide contacts $m_к = 2p + 2 = 14$, a number of insulation spacers of rotor $m_{из} = p = 6$ (rotor it is divided into $m_р = p + 1 = 7$ the isolated/insulated electrics); a number of field coils $m_в = p = 6$.

The limiting current of armature in this case

$$I_ц = \frac{0.25}{\pi}(\overset{*}{D}_р - \overset{*}{d}{}^2_в)_l\, j_р \left(\frac{v}{n}\right)^2, \qquad (7\text{-}12)$$

where $j_р$ — maximum, from the point of view of the permissible heating, current density, A/m².

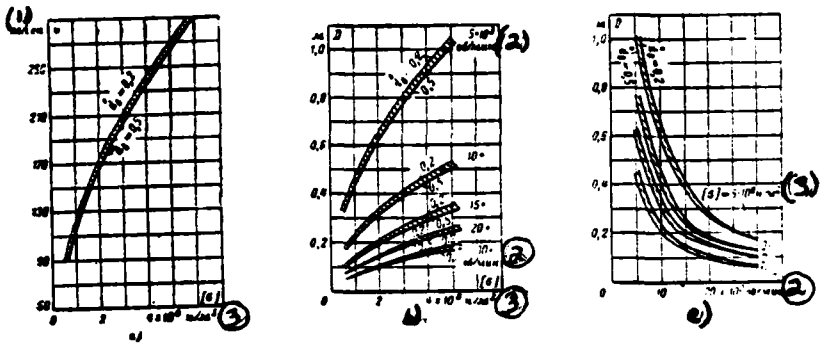

Fig. 7-2. On the calculation of the mechanical strength of ferromagnetic cylindrical armatures UM of the ultimate capacity: a) dependence v=([σ]) according to ; b) dependence D=f([σ]) on n, ; c) dependence D=f(n) on [σ],

Key: (1). m/s. (2). r/min. (3). n/m².

Page 171.

For increase l_a it is also necessary to increase v and to decrease n. Taking into account (7-11) and (7-12) we will obtain the ultimate capacity

$$P_{э.м} = EI \cdot 10^{-3} = \frac{1,25 \cdot 10^{-4}}{\pi^2}(D_p^2 - d_в^2)^2 p B_p j_p \frac{v^4}{n^3}, \quad \text{kW}, \qquad (7\text{-}13)$$

which is greater, the higher than v and lower than n, moreover tentatively it is possible to consider $B_p = 1,8$ T (18000 G); $k_{ор} \approx 1$ and

$j_p < 10^6$ A/m² (for steel). Assuming/setting v≈200 m/s, $(\dot{D}^2_p - \dot{d}^2_в)^2 \approx 1$, with the maximum ones a number of poles 2p, B_p and j_p we will obtain:

$$P_{э.ц} \approx \frac{2,18 \cdot 10^{11}}{n^3}, \quad \text{kW}.$$

In particular, for n=500 r/s we will obtain $P_{э.ц} = 1,75 \cdot 10^3$ kW.

Similarly for disk UG of the ultimate capacity (on the assumption that the greatest number of poles 2p=12) we have:

$$E_д = \frac{0,25}{\pi}(1 - \dot{D}^2_н)\, pB_з \frac{v^2}{n}, \text{ в}; \quad (7\text{-}14)$$

$$I_д = \frac{0,25}{\pi} \dot{D}^2_н j_1 \left(\frac{v}{n}\right)^2, \text{ а}; \quad (7\text{-}15)$$

$$P_{э.д} = \frac{6,25}{\pi^2} 10^{-6} (\dot{D}^2_н - \dot{D}^1_н)\, pB_з j_1 \frac{v^4}{n^3}, \text{ квт}. \quad (7\text{-}16)$$

Key: (1), V. (2). kW.

With series connection p of the disks of the armature

$$m_н = p = 6; \; m_p = m_{вз} = 0,5p - 1 = 2; \; m_в = p = 6.$$

Formulas (7-14)-(7-16) are registered for UG with the one-sided current pickup with the shaft and the disks, which have cos a=1. Since in this case $B_з \approx B_c$, and the shafts are implemented by steel ones,

$B_з < 1,8$ <1.8 T (18000 G); $j_1 < 10^6$ A/m² (100 A/cm²).

Let us compare cylindrical and disk UM of ultimate capacity under the following conditions:

$$2\rho_ц = 2\rho_д;\ n_ц = n_д;\ B_{р.ц} = B_{б.д};\ j_р = j_1;\ \mathring{D}_р = 1;\ \mathring{d}_в = 0;\ \mathring{D}_п = 0{,}25.$$

For the identical materials of cylinder and disk (steel)

$$[\sigma]_ц \approx [\sigma]_д;\ \gamma = 7{,}65 \cdot 10^4\ \text{N/m}^3,\ \mu = 0.3.$$

Taking into account the possibility of imparting to disk the special (conical) profile/airfoil we assume/set $v_ц/v_д \approx 0{,}64$.

Page 172.

Then

$$\frac{E_ц}{E_д} = 2\,\frac{\mathring{D}_р^2 - \mathring{d}_в^2}{1 - \mathring{D}_п^2}\,\frac{\rho_ц}{\rho_д}\,\frac{B_{р.ц}}{B_{б.д}}\left(\frac{c_ц}{v_д}\right)^2\frac{n_д}{n_ц} = 0{,}875;$$

$$\frac{I_ц}{I_д} = \frac{\mathring{D}_р^2 - \mathring{d}_в^2}{\mathring{D}_п^2}\,\frac{j_р}{j_1}\left(\frac{v_ц}{v_д}\right)^2\left(\frac{n_д}{n_ц}\right)^2 = 6{,}56;$$

$$\frac{P_{в.ц}}{P_{в.д}} = 2\,\frac{(\mathring{D}_р^2 - \mathring{d}_в^2)^2}{\mathring{D}_п^2 - \mathring{D}_п^4}\,\frac{\rho_ц}{\rho_д}\,\frac{B_{р.ц}}{B_{б.д}}\,\frac{j_р}{j_1}\left(\frac{v_ц}{v_д}\right)^4\left(\frac{n_д}{n_ц}\right)^3 = 5{,}72;$$

$$\frac{m_{к.ц}}{m_{к.д}} = 2{,}33;\ \frac{m_{р.ц}}{m_{р.д}} = 3{,}5;$$

$$\frac{m_{вз.ц}}{m_{вз.д}} = 3;\ \frac{m_{в.ц}}{m_{в.д}} = 1.$$

The results of calculation according to (7-11)-(7-16) the

maximum parameters UG of the compared types at different speeds of rotation of rotor for $\frac{v_2}{v_1} \approx 1,5$ are given in Table 7-1.

Table 7-1. Comparison of the approximate limiting values of the parameters UG of ultimate capacity.

(1) Параметр	(2) Тип УГ			
	(3) Цилиндрический		(4) Дисковый	
$2p$	12		12	
v, м/сек (5)	200		300	
$B_{p.b}$, тл (6)	1,8		1,8	
$j_{p.1}$, а/м²	10^6		10^6	
n, об/сек (7)	166,7	50	166,7	50
E, в (8)	412	1 370	435	1 460
I, ка (9)	115	1 270	16,1	178
$P_в$, Мвт (10)	47,3	1 740	7,0	260
D, м	0,382	1,27	0,573	1,90

Key: (1). Parameter. (2). Type UG. (3). Cylindrical. (4). Disk. (5). m/s. (6). T. (7). r/s. (8). in. (9). kA. (10). MW.

Page 173.

Is of interest obtaining the dependences of limiting values $E, I, P_в, D=f(n)$ at permissible linear velocities $v_ц \approx 200$ m/s $v_д \approx 300$ m/s for different numbers of poles 2p=2 and 2p=12 cylindrical and disk UG. It is expedient to perform generators with n≥50 r/s, i.e. according to classification [113] they will be high-speed (high-speed) machines. At the high values of n the direct drive is feasible from the gas turbine. Calculation formulas for graphing are given in Table 7-2, moreover it is assumed

$$j_p = j_1 = 10^6\ a/м^2;\ B_p = B_\delta \approx 1{,}8\ тл;\ \overset{*}{D}_p \approx 1;$$

$$\overset{*}{d}_\delta \approx 0;\ \overset{*}{D}_п \approx 0{,}25;\ \cos\alpha \approx 1;$$

$$n = 50 \div 500\ об/сек.$$

Key: (1). T. (2). r/s.

The relative values of the maximum parameters UG of cylindrical and disk types are represented in Fig. 7-3.

With n=166.7 r/s it is selected:

$$\dot{n} = 1;\ \dot{E} = 1;\ \dot{I} = 1;\ \dot{P}_э = 1;\ \dot{D} = 1.$$

In individual cases is expedient the comparison of parameters $[E/\Pi]_ц$ and $[E/\Pi]_л$ generators.

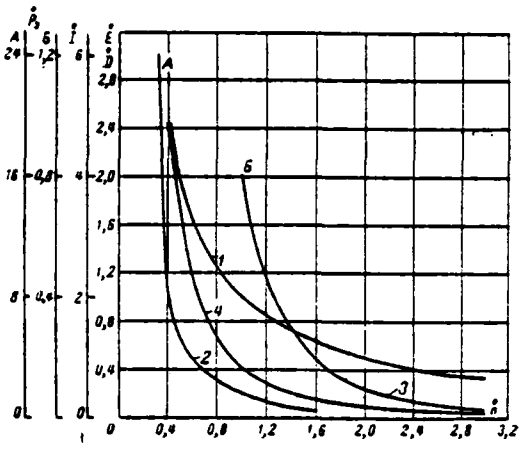

Fig. 7-3. Relative values of the maximum parameters cylindrical and disk UG when [illegible]

Page 174.

During the maximum use

$$\frac{[E/I]_a}{[E/I]_\text{ц}} \approx 0{,}133,$$

whence it follows that with the relatively larger voltages/stresses and the low currents the use/application of disk UG is more preferable. Cylindrical machine can prove to be underused on the current.

Table 7-2. Calculation formulas of the maximum parameters.

(1) Параметр	(2) Тип УГ			
	(3) Цилиндрический		(4) Дисковый	
	$p=1$	$p=6$	$p=1$	$p=6$
(5) Э. д. с. E, $в$	$\frac{1,14\cdot10^{4}}{n}$	$\frac{6,85\cdot10^{4}}{n}$	$\frac{1,21\cdot10^{4}}{n}$	$\frac{7,25\cdot10^{4}}{n}$
(6) Ток I, $а$	$\frac{3,18\cdot10^{6}}{n^{2}}$		$\frac{4,47\cdot10^{3}}{n^{2}}$	
(7) Мощность $P_в$, $квт$	$\frac{3,63\cdot10^{10}}{n^{3}}$	$\frac{2,18\cdot10^{11}}{n^{3}}$	$\frac{5,4\cdot10^{6}}{n^{3}}$	$\frac{3,24\cdot10^{10}}{n^{3}}$
(8) Диаметр D, $м$	$\frac{63,6}{n}$		$\frac{94,5}{n}$	

(1). Parameter. (2). Type UG. (3). Cylindrical. (4). Disk. (5). Emf. (6). Current. (7). Power kW. (8). Diameter D, m.

Page 175.

Chapter Eight.

MOTOR MODE OF UNIPOLAR ELECTRICAL MACHINE.

8.1. Special features/peculiarities of unipolar electric motor.

To the unipolar electrical machines let us use the reciprocity principle - they can be used in generator and motoring.

The use/application of unipolar engines (UD) is caused by the specific requirements of some installations, which acquire ever more noticeable place in the technology in connection with the development of chemical industry, metallurgy and atomic power engineering.

Unipolar motor is applied in a number of cases, enumerated below:

1) when the source of the direct current is of low voltage;

2) as the drive, which does not contribute into the system of the further pulsation of current;

3) as the engine with the sufficiently high kinetic energy of rotor, which is used in the transient modes/conditions of installation;

4) if machine must work at elevated temperatures of the environment, with the possible contact with the alkaline liquid metals or their vapors, or during the radioactive irradiation;

5) as the drive with the light over-all payload ratio and the high efficiency.

Page 176.

The use/application of UD is possible in certain cases, when the

use of a collector direct-current motor is unacceptable.

Motoring of operation of UM in the theoretical plan/layout is investigated insufficiently and it is weakly illuminated in the technical literature, although attempts at the creation of UD were done repeatedly.

By unipolar type first engine should be considered the device/equipment, known by the name "asterisks of Barlow", proposed in 1824 [3] after discovery by Faraday of the phenomenon of electromagnetic induction (1822).

The exemplary/approximate image of the "asterisk of Barlow" is represented in Fig. 8-1. Metallic asterisk 1, which fulfills the function of rotor, pivot on the axis, established/installed on iron core 2. Asterisk is contained by the poles of permanent magnet 3 and during the rotation alternately concerns by its ends/leads of the surface of mercury, which filled tray 4 in insulating plate/slab 5. To the rod and the tray direct current is fed/conducted. As a result of interaction of current, passed along the rays/beams of the "starwheel", with the magnetic field appears turning moment. Remarkable in the "starwheel of Barlow" was the use of the liquid-metal contact, to which then they returned in the process of improvement of the UM.

In [28] the disk UD with the copper-graphite brushes (Fig. 8-2) is described. The structural/design formulation of brush current pickups is the special feature/peculiarity of engine. On axis and periphery of rotor it is established/installed on eight brushes, pressure on which realized springs from the beryllium bronze (154 g/cm^3). Brushes were joined by copper ring.

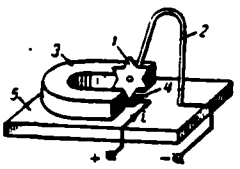

Fig. 8-1.

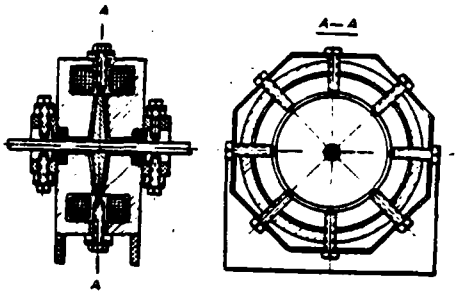

Fig. 8-2.

Fig. 8-1. Installation with UD developed by P. Barlow.

Fig. 8-2. Laboratory sample/specimen of unipolar electric motor.

Page 177.

Special feature/peculiarity of brush contact - small voltage drop and the low coefficient of friction. Rotor is made from steel with a thickness of 3.1 mm. Air gap δ=0.254 mm. The stator, which consists of two halves, is prepared from the alloy of Armco. Machine had two field coils, designed for current 6 and voltage/stress 51 V. The feed of armature was realized from the source by a voltage/stress of 2-4 V. The speed of rotation of rotor varied from 4500 to 6000 r/min. The laboratory sample/specimen of engine had an efficiency, equal to 50%.

In 1944 for the special appraratus by P. Benning [27] was planned a UD which has somewhat different design concept (Fig. 8-3). The rotor of engine 1 was assembled of two parts with outside diameter on the order 100 mm. The motionless winding of series excitation by 2 was implemented from the copper tape in the form of spiral. Current, passing through excitation winding, sliding contact 3 rotor, was abstracted/removed into external circuit through supports 4. The feed of engine was realized from the storage battery by current 100-200 A also with a voltage of 2-4 V.

With the brush current pickup the UD it has special advantages, besides the coordination of the parameters of consumed electric power with the parameters of the available sources. Transition/junction to the liquid-metal current pickups raises the possibilities of applying the UD, which in some special installations can give qualitatively new results.

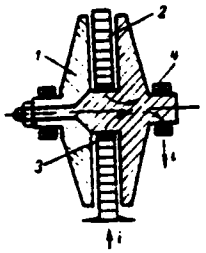

Fig. 8-3.

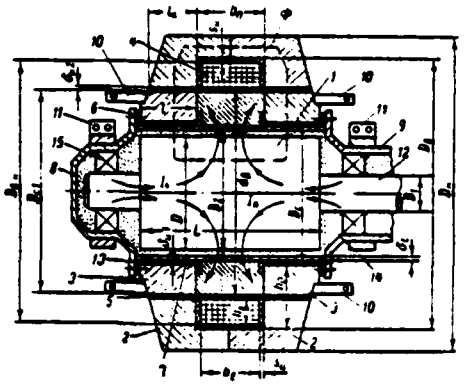

Fig. 8-4.

Fig. 8-3. The UD for the special installation of P. Benning.

Fig. 8-4. Design concept of the UD of the cylindrical type with the complete insertion/immersion of rotor into the electroconducting liquid, independent excitation and compensation bifilars.

Page 178.

One of the characteristic performances of the motor is predominantly examined below, which is an example of the economical utilization of an engine and sets the series/row of new scientific-technical problem before the latter.

Discussion deals with immersion type of UD or with the continuous liquid-metal contact, which can be used, for example, as

the drive of mechanical pump for the pumping over of electro-conductive liquids [29]. Such electro-conductive liquids, whose transportation represents complicated technical task, can be the products of the major chemical industry, molten ferrous and nonferrous metals or the widely used in atomic power engineering high-temperature liquid-metal heat-transfer agents (potassium, sodium, mercury, lithium, etc.).

Structurally/constructurally combined mechanical pump with the drive from the UD can be compared either with the electromagnetic pump or with mechanical pump, which has drive from the asynchronous the asynchronous motor; these latter/last pumps are at present the spread means of the transportation of electro-conductive liquids. Precomputations show that mechanical pumps with the drive from the UD have the substantially best indices by the weight and the efficiency, than electromagnetic ones.

Like asynchronous shielded motor, the UD with the complete insertion/immersion of rotor into the electroconducting liquid do not require the sealing devices/equipment for the distribution of the internal cavity of the motor and zone of the location impeller of mechanical pump, using the liquid enveloping in the gap for the realization of the electrical contact between stator-rotor unit.

The major advantages such a UD over the asynchronous shielded engine are the following:

1) the absence of power losses to the eddy currents in the shields and in the electro-conductive liquid, which fills the gap of machine; 2) the possibility of the execution of engine to the higher speed of rotation (speed of rotation of induction motor is limited by the frequency of feeding network; an increase in the rotational speed by increasing the frequency it conducts to the sharp decrease even without that low efficiency); 3) the possibility of work at increased ambient temperatures, since it can be carried out without the loop electro-insulation, whose thermal durability is limited to temperature of 300-500°C.

To the advantages of the shielded engine should be related the possibility of the pumping over of nonconducting liquids and the absence of the bulky electric-conductive tires, characteristic for UD, just as for the electromagnetic pumps of direct current.

Page 179.

One should also emphasize that the immersion performance of UD makes it possible to use it, also, as the drive of the controlled valve/gate or shutter/valve in the ducts/contours with the

electro-conductive liquids.

One of the possible fundamental design concepts of cylindrical type immersion engine with count poles 2p=2 it is represented in Fig. 8-4.

The rotor of motor 1 is manufactured from the magnetoconductive material (Armco, permendur, OKhNZM, and others) as single part or separately from shaft 12.

Stator 2, 3 can consist of several parts which also they are made of the magnetoconductive materials they are determined by structural/design project and larger simplicity of technology of production.

Circular poles 3 are lagged 5, 6 and are formed the compensative rings (bifilars, which are used for compensation of the armature reaction Insulation 5, 6 and 13 can be carried out in the form of coating the type Al_2O_3, B_2O and the like.

For warning/preventing the destruction of electrical insulating coatings and leaks/leakages of liquid 14 through their pores it is possible to provide thin metal shield 7 of the stainless steel (or other metals). Shield will cause certain current leak, which will be

less than analogous current leak through the walls of channels in the conductor electromagnetic pumps. The installation/setting up of shield is optional.

End shield 8 is made by dead/blind and is manufactured from the stainless steel.

Panel 9 combines the internal cavity of engine with the cavity impeller of pump without the intermediate multiplexing.

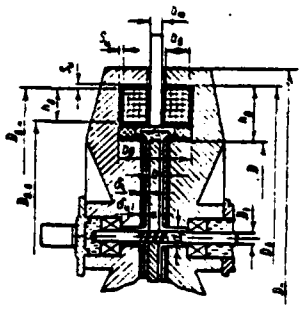

Fig. 8-5. Design concept of the UD of the disk type with the complete insertion/immersion of rotor into the electro-conductive liquid and separate excitation.

Page 180.

Bearings 15, as in the asynchronous shielded engine, they work during the complete insertion/immersion into the pumped over liquid, what is their overall deficiency/lack. They can be carried out as slide bearings, as lubricating agent of which most pumped over liquid serves. Furthermore, this there can be hydrodynamic or hydrostatic type bearings.

Excitation winding by 4 can be consecutive, parallel or independent variable, moreover a number of its turns is usually limited, which gives the possibility to fulfill the electro-insulation of wires, using thermoresistant ceramic separators, spraying/dusting/deposition or varnishes.

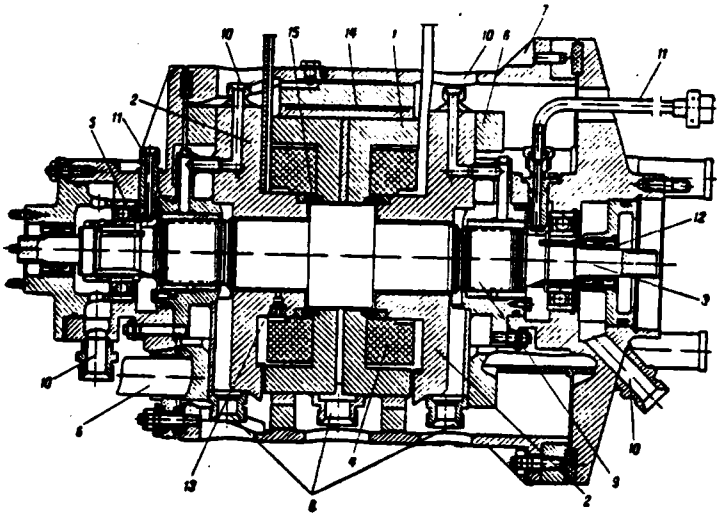

Fig. 8-6. Construction/design of the UD with the power of 30 kW. 1, 2 - poles of stator; 3 - rotor; 4 - excitation winding; 5 - bearing; 6 - current tap; 7 - housing; 8 - branch for supply and overflow of liquid metal; 9 - helical multiplexing; 10 - branch for supplying the inert gas; 11 - branch of the supply of the lubrication of bearing; 12 - multiplexing; 13 - device/equipment for the installation/setting up of level gauge last thermocouples; 14 - cooling channel; 15 - "lock".

Page 181.

The path of electric current in the rotor is shown in Fig. 8-4 by arrows/pointers, the path of magnetic flux - by dotted line. Supplying and discharge busbars 10 and 11 will have smaller weight

than in the electromagnetic pumps of identical power, since the voltage of supply of UD usually several is higher than the voltage applied to the electromagnetic pump, with the higher efficiency.

The analogous design concept disk type of UD (Fig. 8-5) is clear without the detailed description. It is profitable to combine the machine in disk variant with the pump, since the role of pumping wheel can perform disk.

The special features/peculiarities of the design concept of UD require the evaluation/estimate of the mechanical losses of friction, calculation of the electromagnetic efforts/forces, which function on the rotor, and the determination of thermal run.

Peculiar task represents setting experiment with the UD.

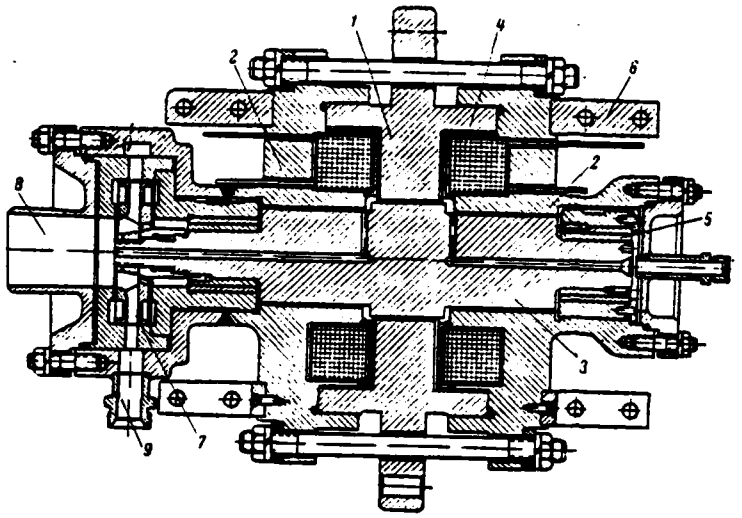

Fig. 8-7. Construction/design of UD with the power of 20 kW. 1, 2 - poles of stator; 3 - rotor; 4 - excitation winding; 5 - slide bearing; 6 - current tap; 7 - centrifugal pump impeller; 8, 9 - input and exhaust ducts of pump.

Page 182.

During the development of experimental installation first of all appear the following tasks:

1) creation of the sealing devices/equipment at output shaft butt end of engine; 2) the selection of the source of the electric power supply of high values of currents and low voltage (continuous operation from the storage batteries at the considerable power of

engine it is difficult); 3) the selection of the controllable load device for measuring the moment/torque on the shaft of engine.

Therefore during the experimental research of the UD with the complete insertion/immersion into the electro-conductive liquid can be proposed the following schematic of experimental installation. In the experiment two identical machines with separate excitation, which have general/common/total shaft and united internal cavity participate simultaneously. Machines are started in motoring in the absence of load on the shaft. The consumption of power with steady run will be caused only by internal losses of machines. Then one of the machines, changing excitation, is translated into the generator mode, presenting the controlled load of experimental engine. This schematic of bench makes it possible to avoid some technical difficulties and it is sufficiently simple to lead the distribution of the total quantity of losses.

Fig. 8-6 and 8-7 present general views of the UD, structurally/constructurally worked out [1] with the múltiplexing and without multiplexing of output shaft.

FOOTNOTE [1]. UDs are developed by S. R. Troitsky, Yu. P. Pavlov and L. Z. Kovzun in 1961. ENDFOOTNOTE.

Rated power of the first UD is below 30 kW with the voltage of supply 5.5 V and rotational speed to 24000 r/min (calculated efficiency of approximately 80%). Rated power of the second UD is 20 kW with load voltage 3.5 V and speeds of rotation 12000 r/min.

8.2. Hydrodynamic evaluation/estimate of friction moment.

Mechanical losses comprise the essential portion of the losses of the UD. Hydraulic friction, which appears in the liquid contacts during the rotation of rotor, is their fundamental source. In chapter 5 is given the calculation of hydraulic losses in the concentrated liquid contacts of the UM and the questions of magnetohydrodynamics of contact partially are touched upon.

Page 183.

The calculation of power losses to friction during the rotation of the completely immersed in the electro-conductive liquid rotor of UD is a fundamental theoretical question, since hydraulic losses will be predominant. A complicated question of hydrodynamics is complicated by the electromagnetic phenomena, whose effect can prove to be noticeable.

The design concept of liquid contact is represented in Fig. 8.8.

It is formed by the cylinder, which axisymmetrically revolves within the cylindrical jacket/case/housing. Between the cylinders the electro-conductive liquid is placed, which with $D_1=0$ completely fills end-type gaps. In the considerable ratio l/D Fig. 8-8 is the schematic device/equipment of the cylindrical UD, where the level of liquid D_1 is limited to the shaft of cylindrical rotor. With small l/D occurs the concentrated contact with a small difference in sizes/dimensions of D and D_1 or the completely immersed in the liquid rotor of UD of the disk type, when D is considerably more D_1. Values $\delta_{11}, \delta_{12}, \delta_{21}, \delta_{22}$ designated the boundary layer thicknesses of the revolving liquid on the appropriate surfaces of cylinders [1].

FOOTNOTE [1] In hydrodynamics, in order to simplify the solution of equations of motion, entire flow of the moving/driving liquid it is accepted to approximately divide into two regions: 1) the very small region, which is located on the boundaries of flow and called the boundary layer, where are considered both the inertial forces and the forces of viscosity of liquid; 2) the region of the main flow of the liquid (external flow), in which the viscosity effect is negligibly small. ENDFOOTNOTE.

Initial equations for determining the moment/torque of the hydraulic resistor/resistance of the revolving bodies are the equations of motion of the viscous incompressible fluid:

the equation of the continuity

$$\operatorname{div} v=0 \qquad (8\text{-}1)$$

and the Navier-Stokes equation, which establishes/installs the interconnection of all forces, which function on the fluid element,

$$\rho_{ж}\left[\frac{\partial v}{\partial t}+(v\nabla)v\right]=T-\nabla P_{д}+\eta_{ж}\Delta v, \qquad (8\text{-}2)$$

where v - velocity vector, been in the cylindrical coordinates three components v_r, v_φ, v_z.

$\rho_{ж}$ — density of liquid;

$\eta_{ж}$ - coefficient of viscosity/ductility/toughness;

$(v\nabla)v$ - acceleration, caused by the presence of the velocity gradient;

T - force applied from without to the volume element;

$-\nabla P_{д}$ - force directed opposite to pressure gradient;

$\eta_{ж}\Delta v$ - internal friction between the layers of liquid.

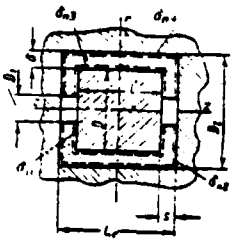

Fig. 8-8. Diagram of liquid contact.

Page 184.

In the boundary layers of liquid contacts the three-dimensional motion of liquid occurs. However, to solve three-dimensional task in general form is virtually impossible. In this case the task is facilitated by the fact that the motion is axisymmetric and, therefore, in view of symmetry depends only on two coordinates (r and z). Therefore during the deployment of equations (8-1) and (8-2) in the cylindrical coordinates it is possible to equate to all zero derivatives on φ. Furthermore, is examined steady motion, so that $\partial v/\partial t=0$. But also after these simplifications solution can be obtained, having only equated to zero velocity component along the axis z $(v_z=0)$, which to a certain degree is justified by the experiments of Schulz-Grunov, who observed the presence of the axial component of velocity only about the end/lead of the rotating disk [98].

As a result of the simplifications indicated we obtain the

following system of differential equations in the cylindrical coordinates:

$$\left.\begin{aligned} v_r\frac{\partial v_r}{\partial r}-\frac{v_\varphi^2}{r}&=\frac{T_r}{\rho_t}-\frac{1}{\rho_t}\frac{\partial P_3}{\partial r}+\nu\left[\frac{\partial^2 v_r}{\partial r^2}+\frac{\partial}{\partial r}\left(\frac{v_r}{r}\right)+\frac{\partial^2 v_r}{\partial z^2}\right];\\ v_r\frac{\partial v_\varphi}{\partial r}+\frac{v_r v_\varphi}{r}&=\frac{T_\varphi}{\rho_t}+\nu\left[\frac{\partial^2 v_\varphi}{\partial r^2}+\frac{\partial}{\partial r}\left(\frac{v_\varphi}{r}\right)+\frac{\partial^2 v_\varphi}{\partial z^2}\right];\\ 0&=T_z-\frac{\partial P_3}{\partial z};\\ \frac{\partial v_r}{\partial r}+\frac{v_r}{r}&=0, \end{aligned}\right\} \quad (8\text{-}3)$$

where $\nu=\eta/\rho_t$ - kinematic modulus of viscosity;

T_r, T_φ, T_z - components of the force applied from without.

The first three equations of system (8-3) represent the equation of a Navier-flow/discharge for the appropriate coordinates r, φ, z. In this case the left side of the equations expresses r, φ or z - to component of acceleration, obtained by fluid element as a result of the presence of the velocity gradient upon transfer from one point to another. The expressions in the brackets of the right side of the equations, multiplied by the coefficient of viscosity/ductility/toughness η, present the components of the force of internal friction between the layers of liquid. The latter/last equation of system (8-3) is obtained from the equation of the flow continuity of liquid.

The force of internal friction can be expressed also through the components of shearing stresses, which in the case of axisymmetric motion are equal to:

$$\left.\begin{aligned} \tau_{r\varphi} &= \eta_{\text{ж}}\left(\frac{\partial v_\varphi}{\partial r}-\frac{v_\varphi}{r}\right);\\ \tau_{z\varphi} &= \eta_{\text{ж}}\frac{\partial v_\varphi}{\partial z};\\ \tau_{zr} &= \eta_{\text{ж}}\frac{\partial v_r}{\partial z}. \end{aligned}\right\} \qquad (8\text{-}4)$$

The third equation of the system (8-3) serves for determining the pressure and can be excluded in the description of the motion of liquid.

System (8-3) makes it possible to obtain two integral-differential ("pulse") equations, whose solution is possible with the appropriate assumptions; it is carried out by a number of the authors with T=0 for determining the moment of resistance of those revolving in the jacket/case/housing of the disk of theoretically small thickness and cylinder [98, 99, 114-116].

The character of motion is considered by Reynolds number $Re=wD^2/4v$. With $Re<10^5$ the motion carries laminar character; with $Re>3\cdot10^5$ it is turbulent. Transition/junction from the laminar to the

turbulent flow is observed over a wide range of Reynolds numbers, which creates further difficulties in the theoretical studies, since the determination of the profile/airfoil of the distribution of rates and boundary layer thickness impedes.

With the gap smaller than the boundary layer thickness ($s<\delta_m$), the flow named the flow of Couette[1] [98] occurs.

FOOTNOTE [1]. For the laminar flow of Couette, characteristic is the linear distribution of rate according to width gap. ENDFOOTNOTE.

It serves as certain approximation/approach to a task about the boundary layer, since boundary layer can be considered as the filled with liquid gap between the bodies, in which the rate of liquid is distributed according to the linear law. The flow of bulk of liquid out of the boundary layer appears in this case as the moving/driving body. The major advantage of the task about the flow of Couette consists in the fact that the solution for it can be obtained in the final form, what is valuable for explaining the series/row of laws.

For the flow of end-type gaps, in particular when $s<\delta_m$, we will obtain expression for the moment of resistance. Since the flow of Couette is characterized by the absence of extraneous velocity components, it is possible to assume $v_r=0$.

Page 186.

Then from the second Navier-Stokes equation systems (8-3) we obtain:

$$\frac{\partial^2 v_\varphi}{\partial r^2}+\frac{\partial}{\partial r}\left(\frac{v_\varphi}{r}\right)+\frac{\partial^2 v_\varphi}{\partial z^2}=0. \qquad (8\text{-}5)$$

For the end-type gap boundary conditions will be determined by the requirements of the adhesion of liquid for solid body:

$$\left.\begin{array}{ll}\text{(1)}\ \text{при}\ z=0 & v_\varphi=r\omega;\\ \text{Ф при}\ z=s & v_\varphi=0,\end{array}\right\} \qquad (8\text{-}6)$$

Key: (1). with.

where ω - angular velocity of the revolving body.

Let us find the particular solution (8-5) from the equation, which depends only on $\left(z,\ \frac{\partial v_\varphi}{\partial z^2}=0.\right)$ It will take the form: $v_\varphi=c_1 z+c_2$. integration constant are determined with the help of boundary conditions (8-6):

$$v_\varphi=r\omega\left(1-\frac{z}{s}\right). \qquad (8\text{-}7)$$

Particular solution (8-7) will be the simultaneously unknown solution of equation (8-5).

The component of shearing stress will be expressed:

$$\tau_{z\varphi}=\tau_{1\text{в}}\frac{\partial v_\varphi}{\partial z}=-\tau_{1\text{в}}\frac{r\omega}{s}.$$

Moment of resistance for two end-type sides of the contact

$$M' = 4\pi \int_{R_1}^{R} r^2 \tau_{z\varphi} dr = -\pi \eta_э \omega R^4 \frac{1 - \bar{R}_1^4}{s}, \qquad (8\text{-}8)$$

where in accordance with Fig. 8-8: r - current radius; R=0.5D - radius of the revolving body; $R_1=0.5D_1$ - radius of the level of liquid; $\bar{h}_1=\bar{b}_1=R_1/R$ - relative radius of the level of liquid.

For studying the flow of Couette between two concentric cylinders can be also used the second Navier-Stokes equation system (8-3) for $v_r=0$ and the following boundary conditions:

$$\left.\begin{array}{ll} v_\varphi \text{ при } r=R & v_\varphi=\omega R; \\ v_\varphi \text{ при } r=R_2 & v_\varphi=0, \end{array}\right\} \qquad (8\text{-}9)$$

Key: (1). with.

where $R_2=0.5D_2$ - radius of the limiting cylinder.

Page 187.

The particular solution of the equation

$$\frac{\partial^2 v_\varphi}{\partial r^2} + \frac{\partial}{\partial r}\left(\frac{v_\varphi}{r}\right) = 0$$

takes the form:

$$v_\varphi = c_1 r + c_2/r.$$

Using boundary conditions (8-9), we obtain:

$$v_\varphi = \omega R \frac{\bar{R}_2^2}{1 - \bar{R}_2^2} \frac{\bar{r}\bar{R}_2^{-2} - 1}{\bar{r}}, \qquad (8\text{-}10)$$

where

$$\overset{*}{r}=\frac{r}{R} \text{ and } \overset{*}{R}_2=\frac{R_2}{R}.$$

It is possible to demonstrate that (8-10) it will be simultaneous the solution of equation (8-5).

In this case of the component of shearing stress and moment of resistance it is respectively equal to:

$$\left.\begin{aligned} \tau_{r\varphi} &= \eta_2\left(\frac{\partial v_\varphi}{\partial r}-\frac{v_\varphi}{r}\right)=-2\eta_2\omega R\,\frac{\overset{*}{R}_2^2}{\overset{*}{R}_2^2-1}\,\frac{1}{\overset{*}{r}}; \\ M'' &= 2\pi\int_0^l r^2\tau_{r\varphi}\,dz=-4\pi\eta_2 l\,\frac{\omega R^2}{1-\overset{*}{R}_2^{-2}}. \end{aligned}\right\} \quad (8\text{-}11)$$

When $\overset{*}{R}_1\to\infty$ we will obtain $v_\varphi=\frac{\omega R^2}{r}$ and $M''=-4\pi\eta_2 l\omega R^2$, which corresponds to the rotation of cylinder in the unlimited quiescent liquid.

Using (8-8) and (8-11), we obtain the moment of the resistor/resistance of entire cylinder in the case of the flow of Couette:

$$M=M'+M''=-\pi\eta_2\omega R^2\left[\frac{R^2}{s}(1-\overset{*}{R}_1^4)+\frac{4l}{1-\overset{*}{R}_2^{-2}}\right]. \quad (8\text{-}12)$$

It is possible to show that if the gaps are great and there are two boundary layers, each of which has a distribution of rate, characteristic for flow of Couette, and the main flow revolves with certain rate of $\beta=\omega/\omega_*$ then moment/torque is reduced

approximately/exemplarily doubly.

Page 188.

However, as numerical evaluations/estimates are shown, this result will sharply diverge from the experimental data, since the profile/airfoil of the distribution of the rates in the boundary layers both with the laminar and with the turbulent modes/conditions differs from that accepted.

The dependences given above remain indefinite, if we do not give the evaluation/estimate of boundary layer thickness. In the majority of the cases the boundary layer thickness is determined as a result of conducting of complicated designing-theoretical analysis and accepting the series/row of assumptions in the initial equations. It is known [115] that the expression for the boundary layer thickness with laminar flow takes the form:

$$\delta_{\text{п}} = \varepsilon_{\text{к}} \nu^{0,5} \omega^{-0,5}, \qquad (8\text{-}13)$$

moreover $\varepsilon_{\text{к}} < 10$. Thus, for the known task of Blasius on the flow around thin plate of parallel flow with a speed of v_∞ boundary layer thickness is equal to $\delta_{\text{п}} = 5(\nu x)^{0,5} v_\infty^{-0,5}$, where x - coordinate of flow direction.

For the infinitely thin disk, which revolves in free from the

jacket/case/housing quiescent liquid, can be accepted $c_M=2,794$ [115]. With the less exact solution $c_M=4$ [98] is obtained also.

Assuming the equality of end-type gap to the value of boundary layer ($\Delta_э=\Delta$), it is possible to express the moment of resistance of disk in accordance with (8-8) and (8-13) in the following form:

$$M' = -\frac{\pi}{c_M}\rho_1\nu^{0.5}\omega^{1.5}R^4(1-\bar{R}_1^4). \qquad (8\text{-}14)$$

The exact solution of the task of laminar boundary layer is obtained only taking into account the radial component of rate For this is used the usual reception/procedure of the hydrodynamics: composition with the help of two Navier-Stokes equations and equation of the continuity of system (8-3) of pulse equations, assignment in general form of the profile of velocities of the boundary layer, which corresponds to the results of experiment, and reducing of the integral-differential equations to algebraic, that make it possible to compute unknown coefficients.

The distribution of the rates of laminar boundary layer is assigned usually in the form of the polynomials of the second power. In this case the integration and differentiation with the substitution in the pulse equations are conducted in accordance with the propositions of Okai and Hasegawa about independence c_M from a radius and about the linear dependence on a radius of the maximum value of the radial component of rate [117].

As a result of this solution the moment of resistance of theoretically infinitely thin disk with a radius of R, which revolves in the liquid without the jacket/case/housing, can be expressed [115]:

$$M' = -1{,}69\rho_l \nu^{0{,}5}\omega^{1{,}5}R^4, \qquad (8\text{-}15)$$

where $a_M = 2{,}794$. This dependence to a certain degree will be coordinated with expression (8-14) when $\mathring{R}_1 = 0$.

Most interesting is the case, when are an external jacket/case/housing and there are two boundary layers, since to fulfill the gap, equal in magnitude to boundary layer thickness, in the UD is virtually impossible. This solution for the thin disk during the laminar flow is obtained by a number of the authors [98, 99, 114-116]:

$$M' = -3{,}3\rho_l \nu^{0{,}5}\omega^{1{,}5}R^4 \frac{\mathring{R}_2^4}{\mathring{\omega}^{1{,}5}}. \qquad (8\text{-}16)$$

Value $\mathring{\omega} = \omega/\beta$ is the function of the geometric dimensions, whose calculated dependence is given in [99]. However, for $\mathring{R}_2 \sim 1$ with a sufficient accuracy $\mathring{\omega} = 1{,}86$ can be accepted This makes it possible to express moment of resistance in the following form:

$$M' = -1{,}334\rho_l \nu^{0{,}5}\omega^{1{,}5}R^4.$$

Boundary layer thickness is computed with the help of the expression

$$\delta_{\text{п}} = 3{,}5\left(\frac{6\dot{\omega}-1}{\dot{\omega}+\frac{1}{3}}\right)^{0.5}\left(\frac{\frac{\nu}{\beta}}{2+3\dot{\omega}}\right)^{0.5}. \qquad (8\text{-}17)$$

When $\dot{\omega}=1{,}85$ we will obtain:

$$\delta_{\text{п}} = 1{,}59\nu^{0.5}\beta^{-0.5} = 2{,}17\nu^{0.5}\omega^{-0.5}.$$

In the technical literature concrete/specific/actual recommendations by choice of the boundary layer thickness of radial clearance are absent. But particular tasks with the cylinder make it possible to assume that the boundary layer thickness in the radial clearance must have the same order.

In the case of liquid contacts of UD the turbulent states of motion of liquid ($Re>3\cdot10^3$) predominantly are observed. The study of turbulent boundary layer is more complicated the laminar, although the method of solution remains the same.

Page 190.

For the turbulent mode/conditions the distribution of rates [illegible] and [illegible] is assigned usually according to power "law of 1/7". In the work of Yu. Yu. Kaunas the author considers that more matched with the experiment power "law of 1/8" [22, 100]. The dependence of its thickness on a radius is also the special feature/peculiarity of turbulent boundary layer. In the work of Okai and Hasegawa, the

authors, as many others, assumed that $\delta_n = c_n' \nu^{0,2} \omega^{-0,2} \rho^{0,6}$. In the work of Yu. Yu. Kaunas it is accepted $\delta_n = c_n' \nu^{0,133} \omega^{-0,133} \rho^{0,666}$. Furthermore, during the solution of the problem about the turbulent boundary layer are used empirical dependence for determining the value of shearing stress.

The moment/torque of resistance of the disk, which rotates in the unlimited liquid during the turbulent mode/conditions, can be determined [99] according to the equation

$$M' = -0{,}073 \rho_f \mathrm{Re}^{-0,2} \omega^2 R^5. \qquad (8\text{-}18)$$

In this case boundary layer thickness

$$\delta_n = 0{,}525 \nu^{0,2} \omega^{-0,2} R^{0,6}.$$

For the moment of resistance of theoretically infinitely thin disk in the jacket/case/housing the dependence

$$M' \approx -0{,}233 \rho_f \mathrm{Re}^{-0,2} \omega^2 R^5 \frac{\mathring{R}_2^{1,6}}{\mathring{\omega}^{1,8}}. \qquad (8\text{-}19)$$

is recommended. For the majority of the cases, which are encountered in practice, during the turbulent flow and $\mathring{R}_2 = 1$ with a sufficient accuracy it is possible to take coefficient $\mathring{\omega} = 2{,}06$. Then (8-19) it will take the form:

$$M' = -0{,}036 \rho_f \mathrm{Re}^{-0,2} \omega^2 R^5,$$

and boundary layer thickness

$$\delta_n = 0{,}097 \nu^{0,2} \omega^{-0,2} R^{0,6}.$$

Exactly as for the stream-line conditions, in the technical literature are absent concrete/specific/actual recommendations regarding the calculation of the moment of resistance and boundary

layer thickness in the radial clearance during the rotation of the extended cylindrical bodies. An exception is work [100], in which the moment of resistance of the contact, depicted in Fig. 8-8, is obtained (during the turbulent mode/conditions) and the correctness of result is confirmed experimentally.

Page 191.

The advantage of the work of kaunas consists in the experimental refinement of the series/row of the coefficients: the introduction of power "law of 1/8", a change in the empirical coefficient of 0.0225 shearing stresses on 0.0178, the establishment of fact about a decrease in the value of shearing stresses in the radial clearance by approximately 20%, and also in the analytical representation of the dependence of parameter ε on the geometric dimensions, represented usually in the form of table.

The theoretical positions of kaunas were confirmed by experiments directly with UG, which have the concentrated mercury contacts. The results of calculations and experiments did not differ to more than 2% near lgRe=7.3 $\left(\mathrm{Re}=\frac{\omega D^2}{\nu}=4\mathrm{Re}\right)$. All this makes it possible to take its work for the base during the analysis of UD.

In the work of Yu. Yu. Kaunas the author established/installed,

that the moment of resistance of the cylinder, which revolves in the jacket/case/housing, can be calculated according to the formula

$$M=-c_M\rho_f\omega^2D^5, \qquad (8\text{-}20)$$

where the moment coefficient of resistor/resistance is equal to:

$$\left.\begin{aligned} c_M &= \mathrm{Re}^{-0,182}(1-\bar{D}_1^{4,64}+3,7l/D)\,k_c;\\ k_c &= 1,25\cdot10^{-3}\,\frac{1,8\lambda^2-0,4\lambda-1}{\lambda^2+1,5\lambda-2};\\ \lambda &= \frac{\bar{D}_2^{4,64}-\bar{D}_1^{4,64}+3,7\bar{D}_2^{3,64}L/D}{1-\bar{D}_1^{4,64}+3,7l/D}. \end{aligned}\right\} \qquad (8\text{-}21)$$

Dependence k_c on the value of relation $\bar{z}=\frac{z}{r}$ is given in the form of table.

$\bar{z}$	2	2.06	2.15	2.20	2.5
k_c	$1,020\cdot10^{-3}$	$1,056\cdot10^{-3}$	$1,110\cdot10^{-3}$	$1,134\cdot10^{-3}$	$1,308\cdot10^{-3}$

In practice most frequently are encountered the cases, for which during turbulent mode/conditions $\bar{z}$ it is found in the range 2.06-2.2.

Page 192.

Consequently, if we take during the determination of moment of resistance $\bar{z}=2,15$, then error will not exceed 10%. For $\bar{z}=2,15$ we will obtain:

$$M=-1,11\cdot10^{-3}\rho_f\,\mathrm{Re}^{-0,182}(1-\bar{D}_1^{4,64}+3,7l/D)\,\omega^2D^5.$$

The obtained expression makes it possible to lead the distribution of moments/torques for the end-type gaps and to compare

with the dependences obtained previously. Thus, for the end-type gaps (l=0, D_1=0), taking into account that Re=4Re, we find:

$$M' = -8{,}65 \cdot 10^{-4} \rho_f \, \mathrm{Re}^{-0.182} \omega^2 D^5. \qquad (8\text{-}22)$$

For the gaps on the generatrices of the cylinder

$$M'' = -32 \cdot 10^{-4} \rho_f \, \mathrm{Re}^{-0.182} l \omega^2 D^4. \qquad (8\text{-}23)$$

The optimum values of boundary layer thicknesses we will obtain when $\dot{\omega} - 2$:

for the radial clearance

$$\delta_{\text{п.опт}} \approx 7 \cdot 10^{-2} \mathrm{Re}^{-0.182} D \qquad (8\text{-}24)$$

and for the end-type ones

$$\delta_{\text{п.опт}} = 4{,}57 \cdot 10^{-2} \mathrm{Re}^{-0.182} D, \qquad (8\text{-}25)$$

where

$$\mathrm{Re} = \frac{\omega D^2}{4\nu} = \frac{\omega R^2}{\nu}.$$

8.3. Effect of magnetic and electric fields to the value of friction moment.

During the calculation of the mechanical losses of engine with the complete insertion/immersion of rotor into the liquid or the concentrated liquid contact arises the question about the suitability of the dependences of usual hydrodynamics, since the motion of liquid occurs during the complicated combination of magnetic and electric fields.

The first experiments with the UM, experiment of the evaluation/estimate of hydraulic losses in the electromagnetic pumps show the permissible accuracy of calculations according to the hydrodynamic dependences.

Page 193.

Taking into account the complexity of the account of magnetic and electric fields, we carry out the analysis of physical processes in UD based on the example of the simplest flow of Couette in order to be convinced of the validity of the drawn conclusion.

Order of the research:

1. Let us establish/install the direction of magnetic and electric fields, and also appearing electromagnetic forces in the liquid, for which we will use the fundamental laws of electrodynamics.

The electromagnetic force, applied to the volume element, can be represented by vector product of the current density and magnetic induction

$$T=[j \cdot B]. \qquad (2\text{-}26)$$

Value T can be examined in the flow equation of Navier-Stokes (8-2) as external force.

For determining the current density we use a differential law of Ohm

$$j=\gamma\{-\text{grad } U^e+[v\cdot B]\}. \qquad (8\text{-}27)$$

The coupling of current density with the appearing magnetic induction is established by the equation of Maxwell

$$\text{rot } B=\mu j. \qquad (8\text{-}28)$$

Let us consider the specific cases of distributing of electromagnetic fields and forces.

In accordance with Fig. 8-8 with $l/D\to 0$ the contact represents model disk of UD with the theoretically infinitely thin disk. In actuality disk has always final thickness, especially as in UD it serves simultaneously as active conductor.

With the approach to the disk the current, consumed by engine, is distributed in certain proportion between solid body of disk and electro-conductive liquid filling gaps. A precise calculation of this distribution represents complicated mathematical problem. With motionless disk and liquid the relation of current densities will be

proportional to the relation of the specific conductivity of the materials:

$$\frac{j'_r}{j_r}=\frac{\gamma'}{\gamma}. \qquad (8\text{-}29)$$

Prime in this paragraph noted values (j'_r and γ'), which relate to solid body of rotor. Whatever there was the character of current distribution, electro-conductive liquid it will be compulsory to carry out the part of the current, which in the magnetic field of excitation will force liquid to revolve in the direction of the motion of rotor.

Page 194.

In the working zone of the disk UD, the main field of excitation in effect always will be axial and will not have others components. Its value will somewhat depend on a radius as a result of the different distance from the excitation winding, that, however, for the evaluation/estimate of the direction of electromagnetic forces does not have value. Therefore we accept $B'_{r1}=B_{r1}$, designating by index (1) field component excitations of machine or field component from the operating current in solid body of rotor.

From constrained components of primary field will exist B'_r, as the result of the armature reaction or presence of current to the loading of disk. the radial component of primary field can taken

equal to zero ($B_r^{(1)}=0$).

Recognizing the possibility of the existence of all of three components of velocity of the liquid and secondary magnetic induction (B^2 - the reaction of currents in the liquid), we express the components of current density in the liquid in accordance with (8-27):

$$\left.\begin{aligned} j_r &= \gamma(v_\varphi B_z - v_z B_\varphi) - j_0 \frac{R_1}{r}; \\ j_\varphi &= \gamma(v_z B_r - v_r B_z); \\ j_z &= \gamma(v_r B_\varphi - v_\varphi B_r). \end{aligned}\right\} \qquad (8\text{-}30)$$

We express as the gradient of the applied voltage/stress the constrained radial current density $\gamma \operatorname{grad} U^0 = j_0 \frac{R_1}{r}$, understanding by j_0 as the initial current density, which corresponds to a radius of shaft R_1. Values B_r, B_φ, B_z represent the algebraic sum of the inductions of primary and secondary fields.

From the equations of Maxwell

$$\left.\begin{aligned} -\frac{\partial B_\varphi^{(2)}}{\partial z} &= \mu j_r; \\ \frac{\partial B_r^{(2)}}{\partial z} - \frac{\partial B_z^{(2)}}{\partial r} &= \mu j_\varphi; \\ \frac{1}{r} - \frac{\partial}{\partial r}(r B_\varphi^{(2)}) &= \mu j_z. \end{aligned}\right\} \qquad (8\text{-}31)$$

Page 195.

Magnetic permeability to liquids is in effect equal to the

magnetic constant ($\mu=\mu_0$), since liquid is not magnetoconductive.

When $v_z=v_r=0$ we will obtain from (8-30) and (8-31):

$$\left.\begin{aligned} &j_\varphi=j_z=0;\ B_z^{(2)}=B_r^{(2)}=0;\\ &j_r=-j_0\frac{R_1}{r}+\gamma v_\varphi B_z^{(1)}=-\frac{1}{\mu_0}\frac{\partial B_\varphi^{(2)}}{\partial z};\\ &\frac{B_\varphi^{(2)}}{r}+\frac{\partial B_\varphi^{(2)}}{\partial r}=0. \end{aligned}\right\} \quad (8\text{-}32)$$

Thus, from the components of secondary induction is possible existence only $B_\varphi^{(2)}$.

With the help of (8-26) we express the components of the electromagnetic force

$$T_\varphi=-j_r B_z^{(1)}=j_0\frac{R_1}{r}B_0-\gamma v_\varphi B_0^2; \quad (8\text{-}33)$$

$$T_z=j_r B_\varphi=-j_0\frac{R_1}{r}B_\varphi+\gamma v_\varphi B_0 B_\varphi. \quad (8\text{-}34)$$

Force T_φ accelerates the liquid, and T_z subtends it to the disk.

In the zone of boundary layer when $v_r\neq 0$ and $v_z=0$, are valid the equalities:

$$\left.\begin{aligned} &j_r=-j_0\frac{R_1}{r}+\gamma v_\varphi B_z;\\ &j_\varphi=-\gamma v_r B_z;\\ &j_z=\gamma(v_r B_\varphi-v_\varphi B_r). \end{aligned}\right\} \quad (8\text{-}35)$$

The equations of Maxwell are represented in this case just as in the system of equations (8-31). Dependences (8-31) and (8-35) show the presence of all of three components ofinduction, current density and electromagnetic force, which complicates the solution of the

problem of boundary layer in the presence of electromagnetic fields.

For cylindrical UD the radial component of field of exictation $B_r^{(1)}=B_r$ and applied on any radius to the length l voltage/stress U are initially given ones.

Accepting in the electro-conductive liquid of gap $v_r=v_z=0$, taking into account (8-27) and (8-28) we obtain:

$$j_r=j_\varphi=0;$$

$$j_z=\gamma\left[-\frac{U}{l}+v_\varphi B_r^{(1)}\right]=\frac{1}{\mu}\frac{1}{r}\frac{\partial}{\partial r}(rB_\varphi). \qquad (8\text{-}36)$$

where magnetic permeability in the zone of the location of liquid, as earlier, it is taken as equal to μ_0.

Page 196.

Thus, in this case of no other fields, except $B_r^{(1)}$ and B_φ there exists. In this case electromagnetic force has also two components, one of which is the accelerating rotation liquid, another - subtending to the axis of the cylinder:

$$T_r=-j_zB_\varphi \text{ и } T_\varphi=j_zB_r^{(1)}. \qquad (8\text{-}37)$$

At two components of velocity in the boundary layer of the liquid of radial clearance ($v_r=0$, $v_\varphi\neq0$ and $v_r\neq0$) three components of electromagnetic force will exist, if we assume the possibility of closing/shorting the induced currents.

2. The examination of the task of laminar or turbulent boundary layer in the presence of three components of electromagnetic force make with its extremely complicated. It is at present difficult to obtain its solution in the completed form upon the complete formulation of the problem indicated. Somewhat simpler it will appear with laminar movement of liquid, especially in the presence only of magnetic field. But also in this case to obtain the expression of the value of tangential voltage/stress and boundary layer thickness is difficult due to the absence of experimental data. In this connection deserves attention the approximate computation of laminar layer according to S. M. Targ's method [118].

For the evaluation of the effect of magnetic and electric fields to the value of moment of resistance let us turn again to the flow of Couette, after taking, as before, $v_r = v_z = 0$.

Let us find the moment of the resistor/resistance of the theoretically infinitely thin disk, which revolves with the angular velocity ω and included in the jacket/case/housing with gap s smaller than the boundary layer thickness δ. We assume gap density $B_r = B_z$ of constant on any radius and current density $j_\varphi = j_0 \frac{R}{r}$ with a constrained, caused applied to radius R voltage/stress of U.

Using the second Navier-Stokes equation system (8-3) and expression for the electromagnetic force of circular direction (8-33), we obtain the following expression:

$$\frac{\partial^2 v_\varphi}{\partial r^2}+\frac{\partial}{\partial r}\left(\frac{v_\varphi}{r}\right)-\frac{\gamma}{\eta_ж}B_3^2 v_ж+j_ж\frac{B_3}{\eta_ж}\frac{R_1}{r}+\frac{\partial^2 v_\varphi}{\partial z^2}=0. \qquad (8\text{-}38)$$

Page 197.

Boundary conditions for solution (8-38) will be caused by the requirements of the adhesion of liquid for the walls of solid body:

$$\left.\begin{array}{l}\text{①при } z=0 \quad v_\varphi=r\omega;\\ \text{①при } z=s \quad v_\varphi=0.\end{array}\right\} \qquad (8\text{-}39)$$

Key: (1). with.

Particular solution (8-38) is the equation, which depends only on z:

$$\eta_ж\frac{\partial^2 v_\varphi}{\partial z^2}-\gamma B_3^2 v_\varphi+j_ж B_3\frac{R_1}{r}=0. \qquad (8\text{-}40)$$

Designating a number of Hartman $M_m=B_3 s\sqrt{\gamma/\eta_ж}$ and $c=\frac{1}{\eta_ж}j_ж B_3 R_1$, we represent (8-40) in the following form:

$$\frac{\partial^2 v_\varphi}{\partial z^2}-\frac{M_m^2}{s^2}v_\varphi+\frac{c}{r}=0,$$

general solution of whom takes the form:

$$v_\varphi=v'_\varphi+v''_\varphi=v'_\varphi+c_1e^{k_1 z}+c_2e^{k_2 z}.$$

We will obtain the particular solution, after assuming $\frac{\partial v_\varphi}{\partial z}=0$,

$$v'_\varphi=\frac{s^2}{M_m^2}\frac{c}{r}=\frac{j_ж}{\gamma B_3}\frac{R_1}{r}.$$

From the characteristic equation

$$k_{1,2}=\pm\frac{M_m}{s}.$$

Having used the boundary conditions (8-39), let us find the velocity distribution law:

$$v_\varphi = r\omega\frac{\operatorname{sh} M_m\left(1-\frac{z}{s}\right)}{\operatorname{sh} M_m}+\frac{cs^2}{rM_m^2}\times$$

$$\times\left[1-\frac{\operatorname{sh} M_m\frac{z}{s}}{\operatorname{sh} M_m}-\frac{\operatorname{sh} M_m\left(1-\frac{z}{s}\right)}{\operatorname{sh} M_m}\right]. \qquad (8\text{-}41)$$

Page 198.

It is possible to demonstrate that this result is simultaneously solution (8-38). Then the value of shearing stress

$$\tau_{z\varphi}=\eta_a\frac{\partial v_\varphi}{\partial z}=-r\omega\eta_a\frac{M_m}{s}\frac{\operatorname{ch} M_m\left(1-\frac{z}{s}\right)}{\operatorname{sh} M_m}+$$

$$+\frac{cs\eta_a}{rM_m}\left[\frac{\operatorname{ch} M_m\left(1-\frac{z}{s}\right)-\operatorname{ch} M_m\frac{z}{s}}{\operatorname{sh} M_m}\right].$$

From that obtained it is evident that value τ_m depends on z. In order to obtain the expression of moment of resistance in the final form, let us find average/mean value τ_m from the gap:

$$(\tau_{z\varphi})_{cp}=\frac{1}{s}\int_0^s\tau_{z\varphi}\,dz=-\eta_a\omega\frac{r}{s}.$$

The moment of resistance of two sides of disk will have accurately the same expression as in the absence of electromagnetic fields, i.e.

$$M'=4\pi\int_{R_1}^{R}r^2(\tau_{z\varphi})_{cp}\,dr=-\pi\eta_a\omega R^4\frac{1-\bar{R}_1^4}{s}. \qquad (8\text{-}42)$$

An analogous example with the radial clearance is not given due to the unwieldiness of expressions.

Thus, although the flow of Couette does not always reflect the true picture of the occurring phenomena, it demonstrates the insignificant effect of electromagnetic fields to the value of moment of resistance at least. To conduct accurately the evaluation of this effect under the specific conditions of immersed UD, the motion of liquid in which occurs in the environment/encirclement of the ferromagnetic bodies of complex laycut, at the present time it is difficult.

It is known that the effect of magnetic field to the value of hydraulic resistor/resistance is different for the different character of the motion of liquid and different values of ratio $(M_м/Re)_f$ or $(M_м^2/Re)_f$.

For laminar flow the value of the coefficient of hydraulic resistor/resistance ζ grows proportional to relation $(M_м/Re)_f$. index f means that as the base of calculation $M_м$ and Re the hydraulic radius of the section of the channel of liquid, equal to the ratio of the section of flow to wetted perimeter is accepted.

Page 199.

From [119] it follows that during the turbulent mode/conditions the specific resistance c_f within limits $(M_m/Re)_f=(0\div4,0)10^{-4}$ virtually is not changed. Number $(M_m/Re)_f=10^{-4}$ [120] is certain boundary, which divides the weak and essential effect of magnetic field to the value of specific resistance. When $(M^2_m/Re)_f>10^{-4}$, the empirical dependence

$$c_f=c_{f_0}+9\cdot10^{-3}\left(\frac{M_m^2}{Re}\right)_f$$

is recommended. Unfortunately, the majority of publications is devoted to the laminar or turbulent flow around bodies in the magnetic field. This carries the specific danger in the propagation of the results of these works on the UD, which has rotation of rotor and complicated distribution of magnetic fields.

Is different the effect of magnetic field also to the flow stability of liquid, since, on one hand, it decreases the extraneous agitation of flow, on the other - is changed the distribution of the rates of flow [120, 121].

Is obvious only the fact that the action of electromagnetic forces on the liquid, which fills the working gap of machine or concentrated contact, is exhibited in the acceleration of its motion in the motor mode/conditions and the delay/retarding/deceleration in the generator.

For the UD with the complete insertion/immersion of rotor into

the electro-conductive liquid the equalization of the rates of flow in the zone, adjacent to the revolving rotor, and certain increase in the velocity gradient in motionless walls is characteristic. Of this it is possible to be convinced based on the example of the flow of Couette (Fig. 8-9), although the solution conducted for it showed that the average value of the velocity gradient remains the same as in the absence of electromagnetic fields.

One should assume that electromagnetic forces to the value of moment of resistance first of all it will be determined by the relation, in which the velocity gradients are changed in the zones indicated.

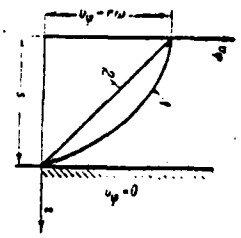

Fig. 8-9. Distribution of rate during the flow of Couette.

1 - $M_m \neq 0$; $j \neq 0$; 2 - $M_m = j_0 = 0$.

Page 200.

8.4. Internal torque of unipolar electric motor.

a). Initial equations.

Internal torque determines the main geometric dimensions of engine, since at given speed of the rotation of rotor $M_э$ its rated power characterizes.

The value of internal torque $M_э$ let us determine for the typical design concepts of UD, which can have the most diverse performance.

For determining the moment/torque usually are used the following initial equations of electrodynamics:

$$\left.\begin{aligned} \mathbf{j} &= \gamma\{-\operatorname{grad} U^* + [\mathbf{v}\cdot\mathbf{B}]\};\\ \operatorname{rot}\mathbf{B} &= \mu\mathbf{j};\\ d\mathbf{T}_э &= [\mathbf{j}\cdot\mathbf{B}]dv;\\ dM_э &= r dT_{эк}. \end{aligned}\right\} \quad (8\text{-}43)$$

However, their use in UD in this form leads to the results, which do not correspond to experimental data. The aforesaid relates

to the equation, which expresses differential Ohm's law, where value [v·B] is the function of radius ($v_\varphi = \omega r$).

The first equation of system (8-43) must be represented here just as in §2-4: $j = -\gamma \operatorname{grad} U^*$. (8-44)

Page 201.

B). Internal torque cylindrical *UD*.

Let us consider the powered phase of rotor under one pole (Fig. 8-10a), after taking the following assumptions:

1) magnetic flux over the section of cylinder it is distributed evenly to ($B_z = B_p \approx \text{const}$);

2) magnetic induction in the working gap over the entire length of pole it is constant ($B_\delta = \text{const}$) and the bulge of flow it is absent;

3) operating current over the section of rotor it is distributed evenly to ($j = j_r = j_p = \text{const}$);

4) value γ and μ at all points of cylindrical rotor they are constant, i.e. by the effect of thermal condition and saturation it

is disregarded.

Thus, in the cylindrical coordinates must be examined the following components: $j = j_z, B_r, B_z, B_\varphi$. Inductions B_r and B_z are the components of field of exictation, and induction B_φ — by result of armature reaction, i.e. the current of axial direction can be obtained in accordance with the equation of Maxwell system (8-43):

$$\frac{\partial B_\varphi}{\partial r} + \frac{B_\varphi}{r} = \mu j_z. \qquad (8\text{-}45)$$

According to the third equation of system (8-43) we are convinced, that there are two components of the electromagnetic force

$$\left.\begin{aligned} dT_{z\varphi} &= j_z B_r\, dV = 2\pi r l j_z B_r\, dr; \\ dT_{z r} &= j_z B_\varphi\, dV = 2\pi r l j_z B_\varphi\, dr. \end{aligned}\right\} \qquad (8\text{-}46)$$

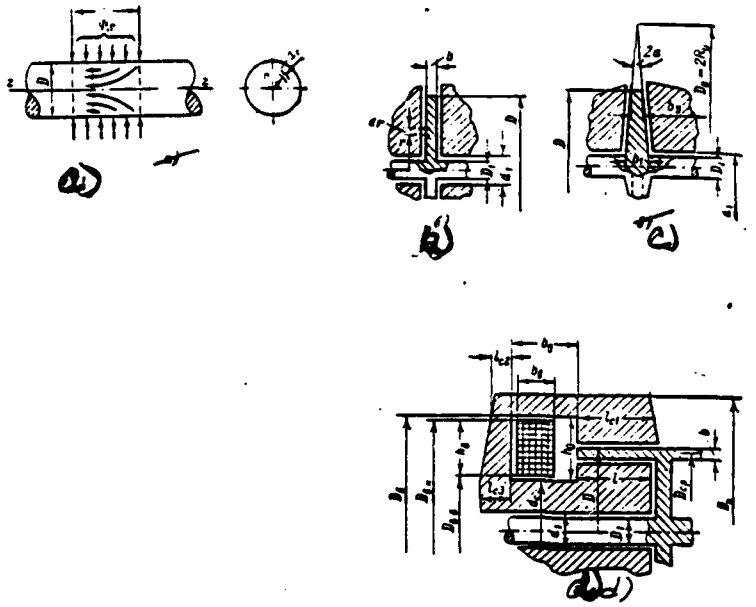

Fig. 8-10. Designations of basic geometric dimensions of UD. a) cylindrical; b) disk with the disk of equal thickness; c) with the conical disk; d) with the thin hollow rotor.

Page 202.

The radial component of electromagnetic force $dT_{эр}$ can be determined from (8-46) with the help of (8-45). This force is directed toward the axis of rotor and it will be counterbalanced by solid body of rotor, without forming torque; for this reason it is not of interest.

The tangential component of electromagnetic force $dT_{эк}$ forms turning moment, which is determined by the expression

$$M_{эк} = \int_0^R r dT_{эк} = 2\pi l j_z \int_0^R B_r r^2 dr. \qquad (8\text{-}47)$$

Problem is reduced to the definition of radial component of magnetic induction of excitation in rotor B_r, which, as is known, is the function of a radius.

Continuous cylindrical rotor. For determination $B_r=f(r)$ let us find the magnetic induction of the axial direction

$$B_z=B_p=\frac{4\Phi_\delta}{k_{\sigma p}\pi D^2}=\frac{4}{k_{\sigma p}}\frac{l}{D}B_\delta=\frac{4}{k_{\sigma p}}\lambda_1 B_\delta,$$

at first evenly distributed from the section of continuous rotor where $k_{\sigma p}$ — coefficient of scattering the powered phase of rotor.

Then magnetic induction in the radial direction of the continuous rotor

$$B_r=B_z\frac{\pi r^2}{2\pi rl}=\frac{1}{k_{\sigma p}}\frac{r}{R}B_\delta=\frac{1}{k_{\sigma p}}\overset{*}{r}B_\delta. \qquad (8\text{-}48)$$

Using (8-47) and (8-48), we determine:

$$M_{\delta 1}=\frac{2\pi}{k_{\sigma p}}lj_z B_\delta\int_0^R\frac{r^2}{R}dr=\frac{0{,}5\pi}{k_{\sigma p}}R^2lj_z B_\delta=\frac{0{,}25}{k_{\sigma p}}VDj_p B_\sigma, \qquad (8\text{-}49)$$

where $V=\pi(D^2/4)l$ - the sensitive volume of continuous rotor; the designation of moment/torque is marked by index 1, since moment/torque relates to one polar extension.

In the general case the current density and the radial component of magnetic induction can be the more complex functions of a radius, and the active length of rotor can have a value, which differs from l. Therefore solution (8-49) is approximate. However, experimental and theoretical studies (for example, see Chapter 2) showed that with

an accuracy sufficient for the practice it is possible to take even distribution j_p and B_p according to the section of cylinder, and the calculations, carried out with this assumption, they make it possible to sufficiently accurately project/design unipolar electric machines.

Page 203.

Since armature current $I_a = \pi R^2 j_p$, and the flow of excitation under one pole $\Phi_\delta = 2\pi R l B_\delta$, the expression for internal torque will take the form:

$$M_{э1} = \frac{I_a \Phi_\delta}{4\pi k_{ср}}. \qquad (8\text{-}49а)$$

After taking into account that $\Phi_\delta = \pi R^2 B_p k_{ср}$, we will obtain one additional expression for electro magnetic moment:

$$M_{э1} = \frac{j_p \Phi_\delta^2}{4\pi k_{ср}^2 B_p}. \qquad (8\text{-}49б)$$

For multipolar machine internal torque

$$M_э = m_E m_I M_{э1}, \qquad (8\text{-}50)$$

where m_E — number of powered phases of machine, connected in series (on the voltage/stress);

m_I — number of powered phases, connected in parallel (for an increase in the operating current); during 100%- use of machine $m_E m_I = 2p$.

Hollow cylindrical ferromagnetic rotor. In the case of applying

the hollow rotor, which can take place, when rotor shaft is implemented from nonmagnetoconductive material and is isolated/insulated, the radial component of the induction

$$B_r = \frac{1}{k_{sp}} B_\delta \frac{R}{r} \frac{r^2 - R_1^2}{R^2 - R_1^2} = \frac{1}{k_{sp}} B_\delta \frac{\overset{*}{r}}{1 - \overset{*2}{R_1}} \left(1 - \frac{\overset{*2}{R_1}}{\overset{*}{r^2}}\right) =$$

$$= \frac{1}{k_{sp}} B_\delta \frac{\overset{*}{d}}{1 - \overset{*2}{D_1}} \left[1 - \left(\frac{\overset{*}{D_1}}{\overset{*}{d}}\right)^2\right], \qquad (8\text{-}51)$$

where $D_1 = 2R_1$ - inner diameter of hollow rotor;

k_{sp} — coefficient of scattering;

$\overset{*}{r} = \frac{r}{R} = \frac{d}{D} = \overset{*}{d}$ and

$\overset{*}{R_1} = \frac{R_1}{R} = \frac{D_1}{D} = \overset{*}{D_1}$ — relative values.

Page 204.

Taking into account (8-47) and (8-51), we obtain expression for internal torque in the form

$$M_{e1} = \frac{2\pi}{k_{sp}} l j_p B_\delta \frac{R}{R^2 - R_1^2} \int_{R_1}^{R} r(r^2 - R_1^2)\, dr = \frac{0{,}25}{k_{sp}} V_\Sigma D j_p B_\delta, \qquad (8\text{-}52)$$

where $V_\Sigma = \pi R^2 l (1 - \overset{*2}{D_1})$ — the sensitive volume of hollow rotor.

Expressions (8-49) and (8-52) are characterized by between themselves only the value of the sensitive volume of rotor.

C). Internal torque disk *UD*.

Unipolar engine with the disk of equal thickness (b=const). Let us lead the determination of moment/torque at first for the machine of two-pole performance (Fig. 8-10b).

We accept the following assumptions:

1)magnetic induction in the working gap has only axial component $B_z = B_\delta$, constant on any radius;

2) radial current density in disk j_r evenly distributed according to thickness and in circle/circumference of disk.

After taking current density about the foundation of the disk (with $r=R_1$) of equal to j_1, we will obtain in accordance with (8-44):

$$j_r = j_1 \frac{R_1}{r}.$$

Using the third and fourth equations of system (8-43), we obtain expression for internal torque in the form

$$M_{э1} = 2\pi b B_\delta \int_{r_1=0,5d_1}^{R} j_r r^2 dr = V_\text{д} R_1 j_1 B_\delta, \qquad (8\text{-}53)$$

where $V_\text{д} = \pi(D^2 - d_1^2)\frac{b}{4} = \frac{\pi D^2}{4} b(1 - \bar{d}_1^2)$ - the sensitive volume of disk with thickness b;

$2r_1=d_1$ - bore of stator under the shaft with a radius of R_1.

Page 205.

After taking into consideration, that the current, passing through the disk, and the magnetic flux of working gap can be represented respectively

$$I_\delta=\pi D_1 b j_1 \quad \text{and} \quad \Phi_\delta=\frac{\pi D^2}{4}(1-\bar{d}_1^2)B_\delta,$$

we will obtain the following expression of moment/torque:

$$M_{э1}=\frac{D^2}{4}(1-\bar{d}_1^2)\frac{I_\delta B_\delta}{2}=\frac{I_\delta \Phi_\delta}{2\pi}. \qquad (8\text{-}53a)$$

With $D_1=d_1$

$$M_{э1}=\frac{i_\delta \Phi_\delta^2}{2\pi B_\delta}. \qquad (8\text{-}53б)$$

Internal torque of multipolar machine

$$M_э=pM_{э1}. \qquad (8\text{-}54)$$

Unipolar engine with the conical disk. During the determination of moment/torque in accordance with Fig. 8-10c the following assumptions are accepted:

1) disk is made from nonmagnetoconducting material (usual performance);

2) radial current density in disk j_r evenly distributed according to thickness and in circle/circumference of disk;

3) the gap between the disk and the stator δ is identical on any radius;

4) the axial density of field of excitation is distributed on a radius is inversely proportional to the thickness of disk; by a drop in the magnetic potential in steel is disregarded;

5) when $r=R$ $B_z=B_{\delta 1}$.

Thus, j_r, B_z and b are the functions of radius r.

From Fig. 8-10c it follows that

$$R_0=R+0{,}5\, b_D \operatorname{ctg}\alpha.$$

Thickness of disk on the arbitrary radius r

$$b(r)=2(R_0-r)\operatorname{tg}\alpha=b_D+(D-2r)\operatorname{tg}\alpha;\ b_D=2(R_0-R)\operatorname{tg}\alpha.$$

The current density, caused by the gradient of the applied voltage/stress,

$$j_r=j_1\frac{R_1}{r}\frac{b_1}{b(r)}=j_1\frac{R_1}{r}\frac{R_0-R_1}{R_0-r}, \qquad (8\text{-}55)$$

where j_1 — current density in the disk with $r=R_1$.

Magnetic induction of the working gap

$$B_z = B_{\delta 1} \frac{b_D}{b(r)} = B_{\delta 1} \frac{b_D}{2(R_e - r) \operatorname{tg} \alpha}. \qquad (8\text{-}56)$$

Page 206.

Then, taking into account (8-55) and (8-56), internal torque

$$M_{э1} = 2\pi \int_{r_1}^{R} b(r)\, j_r B_z r^2 dr = 2\pi b_D j_1 B_{\delta 1} R_1 (R_e - R_1) \int_{r_1}^{R} \frac{r}{R_e - r} dr =$$

$$= \frac{\pi}{4} D^3 b_D j_1 B_{\delta 1} \xi_D, \qquad (8\text{-}57)$$

where

$$\xi_D = \dot{D}_1 (\dot{D}_e - \dot{D}_1) \left[\dot{D}_e \ln \left| \frac{\dot{D}_e - \dot{d}_1}{\dot{D}_e - 1} \right| - (1 - \dot{d}_1) \right] = f(\dot{D}_e, \dot{D}_1, \dot{d}_1).$$

D). Internal torque UD with the thin hollow rotor.

For determining the moment/torque of bipolar machine (Fig. 8-10d) the following assumptions are accepted:

1) magnetic induction in working gap B_δ is constant along the length l and on the height/altitude of gap;

2) current density evenly distributed in circle/circumference and according to thickness of the hollow rotor b and is equal to $j_z = j_p$.

Expression for internal torque in this case takes the form:

$$M_э = 0{,}5\pi D_{ср}^2 b j_z B_\delta \int_0^l dz = 0{,}5 V_{т.р} D_{ср} j_р B_\delta, \qquad (8\text{-}58)$$

where $D_{ср} = (D - b)$ — the mean diameter of thin hollow rotor;

$V_{т.р} = \pi D_{ср} b l$ — the sensitive volume of thin hollow rotor.

Since armature current $I_я = \pi(D - b) b j_р$, and magnetic flux $\Phi_\delta = \pi(D - b) l B_\delta$, then internal torque

$$M_{э1} = 0{,}5 I_я B_\delta (D - b) = \frac{I_я \Phi_\delta}{2\pi}. \qquad (8\text{-}58а)$$

For multipolar machine with the thin hollow rotor internal torque is represented in the same form, as in the case of the disk machine:

$$M_э = m_Е m_I M_{э1}, \qquad (8\text{-}59)$$

where during 100%- use $m_Е m_I = p$.

Page 207.

In all examined in this paragraph expressions for internal torque its numerical value is obtained in the joules, the Newton meters or watt-seconds, if current density is expressed into A/m², linear dimensions - m and magnetic induction - in Wb/m².

If it is necessary to obtain moment/torque in kg·m, then it is necessary to multiply the calculated result by 0.102.

8.5. Fundamental calculated relationships/ratios of electric motor.

a). General/common/total considerations.

Let us lead the establishment of the connection/communication of initial data with geometric and electromagnetic machine parameters under the assumption of uniform magnetic flux distribution and electric current in the rotor. The target of this approach is obtaining the simple engineering dependences, which justified itself during the design of UM.

The calculated relationships/ratios of the overall dimensions of electric motor depend on the design concept. The latter is determined by the methods of excitation and compensation for armature reaction, and also by the structural/design layout of the excitation winding and compensative nodes.

In connection with that presented the given below conclusions/outputs of fundamental principles should be considered as the examples, by analogy with which can be obtained the dependences also for other performances of engine.

Initial values for the design of UD are usually: shaft horsepower of engine $P_м$, speed of rotation of rotor n, the voltage of supply of engine $U_м$ and during separate excitation - voltage of supply of excitation winding $U_в$. During the design of engine to the maximum efficiency and the minimum of weight to the assigned magnitudes should be related only $P_м$ or the moment/torque, developed with engine $M_м$. Remaining values must be determined in accordance with stated problem.

Page 208.

B). Cylindrical UD.

The constructions/designs, represented in Fig. 8-4 and 8-11, provide for separate excitation of machine. In this case if in the first case the compensation for armature reaction is realized by magnetoconductive bifilar, then the second the presence in magnetic circuit of longitudinal-radial slots for the extinguishing of the circular flow of armature reaction is assumed, and the removal/outlet (or supply) of current - by the ring busbars, which has m of the outlet ends through the framework of the stator (in Fig. 8-11b they are shown 4 outlet ends of ring busbars).

Fig. 8-12a depicts design concept with the series excitation and the compensation by bifilar. In the case of longitudinal-radial slots second insulating layer of magnetic circuit is absent ($\delta_{из}=0$); but there are output windows in the framework of stator for removing/taking the current from the consecutive excitation winding.

The overall design of excitation winding in the latter/last two cases is identical. For the uniform removal/taking (or supply) of current from the shield and its uniform distribution over the section of bifilar the construction/design of excitation winding can have complex form. From Fig. 8-12b it is evident that for the uniform removal/taking of current from the shield the contact of the first turn with the shield must be realized in several places at different length($l_к$). Analogously, can be realized the contact of latter/last turn with bifilars. This complication of the construction/design of winding ensures a good use of a machine in the circle/circumference.

For any structural/design formulation of UD during uniform magnetic flux distribution according to the section of rotor ($B_z=B_p=\text{const}$) taking into account scattering the equalities are valid:

$$l=\frac{D}{4}\frac{B_p}{B_\delta}k_{ср} \text{ и } \lambda_1=\frac{l}{D}=\frac{1}{4}\frac{B_p}{B_\delta}k_{ср}, \qquad (8\text{-}60)$$

where $k_{ср}$ — coefficient of scattering rotor.

Then, using (8-60) and an expression for internal torque (8-49), we obtain:

$$D=2\sqrt[4]{\frac{4M_{э1}}{\pi B_p j_p}}=4\sqrt{\frac{M_{э1}k_{эр}}{j_p\Phi_\delta}}. \qquad (8\text{-}61)$$

In accordance with the obtained result and (8-49b) let us find the active length of rotor under one pole:

$$l=\lambda_\delta D=\frac{B_p}{B_\delta}k_{эр}\sqrt{\frac{M_{э1}k_{эр}}{j_p\Phi_\delta}}=\frac{B_p}{B_\delta}k_{эр}\sqrt{\frac{\Phi_\delta}{4\pi k_{эр}B_p}}. \qquad (8\text{-}62)$$

Page 209.

Anti-emf of the powered phase of the rotor

$$E=lB_\delta v=\frac{\Phi_\delta v}{\pi D}=\Phi_\delta n, \qquad (8\text{-}63)$$

since $\Phi_\delta=\pi DlB_\delta$ and $v=\pi Dn$ with n expressed in r/s, then the working flow

$$\Phi_\delta=\frac{E}{n}=\dot{U}^{-1}\frac{U_д}{nm_д},$$

where $\dot{U}=U_д/E$ — coefficient of an internal voltage drops;

$m_д$ — number of powered phases of machine, connected in series.

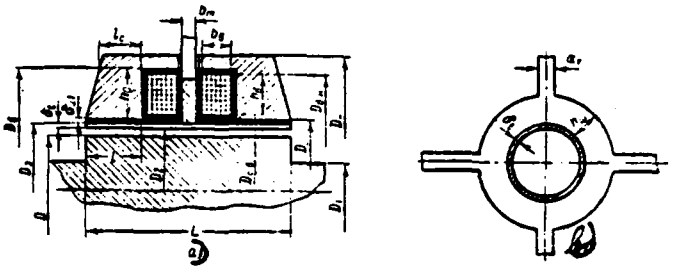

Fig. 8-11. Cylindrical UD without compensative bifilars. a) schematic device/equipment; b) the geometry of the current-carrying busbar.

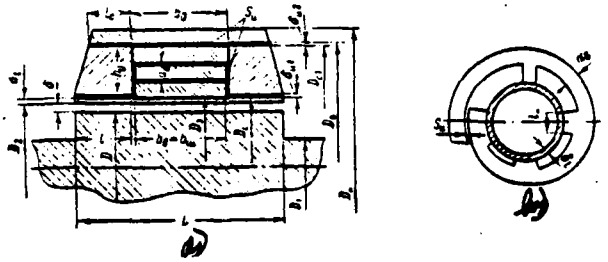

Fig. 8-12. Cylindrical UD with series excitation a) schematic device/equipment; b) the geometry of the first turn of winding.

Page 210.

In this case the diameter can be expressed through the value of assigned load voltage of the engine

$$D=2\sqrt{\frac{U_a}{\pi k_{sp} m_E \dot{U} n B_p}} \qquad (8\text{-}64)$$

or through the amount of internal torque and electromagnetic power

$$D=4\sqrt{\frac{nM_{e1}k_{sp}m_E\dot{U}}{j_p U_a}}=4\sqrt{\frac{P_{e1}}{j_p U_a}\frac{k_{sp}m_E\dot{U}}{2\pi}}, \qquad (8\text{-}64a)$$

where

$$P_{e1}=\omega M_{e1}=2\pi n M_{e1}.$$

Internal torque, developed with engine, must by the counter-balance moment of the hydraulic resistor/resistance of cylindrical rotor $M_т$ and by moment of resistance on the shaft of engine $M_в$. With the help of (8-50) we find:

$$M_{э1} = \frac{M_т + M_в}{m_E m_l}.$$

Then from (8-61) we obtain:

$$D = 2\sqrt[4]{\frac{4(M_т + M_в)}{\pi m_E m_l B_{p/p}}}. \qquad (8\text{-}65)$$

For determining the fundamental parameter D dependence (8-61) is used, where the specific electro magnetic loads of engine j_p, B_p, are initial values since value $U_в$ can be assigned insufficiently correctly. To predetermine UM and unsteady design concept of these machines with the necessary accuracy of value $\dot{U}$ and $U_в$ is difficult as a result of the low voltage.

In expression (8-65) value $M_в$ is known, since

$$M_в = \frac{P_в}{\omega} = \frac{P_в}{2\pi n}.$$

Page 211.

However, dependence (8-65) does not determine unambiguously geometric parameter D, since moment/torque $M_т$ is the complex function of the sizes/dimensions of machine. Therefore during the calculation of the basic dimensions of D and l electric motor with the rotor,

completely submerged in the liquid, it is necessary to use a method of iteration. We accept for determining the first approximation (when $k_{зр} \approx 1$)

$$M_{эл}^{(1)} \simeq \frac{1,12M_в}{m_E m_l} \text{ or } M_ц^{(1)} \approx 0,12M_в.$$

Then

$$D^{(1)} = 2\sqrt[4]{\frac{4,48}{\pi m_E m_l}\frac{M_в}{j_р B_в}} \text{ and } l^{(1)} = \frac{D^{(1)}}{4}\frac{B_р}{B_б}. \quad (8\text{-}66)$$

The coefficient, equal to 1.12, can be refined in the process of gaining of the experience of the design of similar machines.

For the determination of the second approximation/approach of the basic dimensions of D^2 and l^2 is necessary the refinement of value $M_в$, the search for the first approximation of the overall length of rotor L^1.

In accordance with Fig. 8-4, 8-11 and 8-12

$$L^{(1)} = p(2l^{(1)} + b_0). \quad (8\text{-}67)$$

Size/dimension b_0 depends on the method of excitation, compensation for the armature reaction and layout of excitation winding.

For the design concept, shown in Fig. 8-4,

$$b_0=b_в+2s_к, \tag{8-68}$$

where $s_к$ — size/dimension of insulation or structural/design gap of window for positioning/arranging the excitation winding.

The axial size/dimension of excitation winding $b_в$ in principle can be accepted arbitrarily. However, for each concrete/specific/actual machine there is an optimum value $b_в$, which can be found by the multiple repetition of the calculation of machine. With an increase in size/dimension $b_в$ it increases the overall length of rotor and, consequently, also the hydraulic losses of machine. With small size/dimension $b_в$ the relation of the sizes/dimensions of the window of magnetic circuit can prove to be considerably greater than one, which is undesirable due to the increase of the magnetic leakage fluxes and gain in weight of the machine (see Chapter 6).

Page 212.

Axial size/dimension $b_в$ in the first approximation, can be found from the expression

$$b_в=\sqrt{\frac{Q_в}{k_в}}, \tag{8-69}$$

where $k_в=h_в/b_в$ — preliminarily taken relation of the sizes/dimensions of the sides of winding.

The section of winding $Q_в$ is determined from the expression

$$Q_в = b_в h_в = \frac{F_в}{k_{3в} j_в}, \qquad (8\text{-}70)$$

where $F_в$ — magnetizing force of excitation winding;

$j_в$ — the taken or allowable current density in the winding;

$k_з$ — the duty factor of the window of winding with wire.

With the dense coil/winding of conductors by strict series/rows the duty factor can be calculated:

$$\left.\begin{aligned} k_з &= \frac{\pi}{4}\left(\frac{d_{0в}}{d_{из}}\right)^2 \text{ для (1) круглого провода;} \\ k_з &= \frac{a_{0в} b_{0в}}{a_{из} b_{из}} \text{ для (2) прямоугольного провода.} \end{aligned}\right\} \qquad (8\text{-}71)$$

Key: (1). for the round conductor; (2). for the rectangular wire.

In expressions (8-71) it is accepted:

$d_{0в}$ — the diameter of bare conductor;

$d_{из}$ — the diameter of the isolated/insulated conductor;

$a_{0в}$ and $b_{0в}$ — side of rectangular skinned wire;

$a_{0м}$ and $b_{0м}$ — the same with the insulation.

However, in the beginning of sizing of conductor occur unknown. Therefore in the precomputations it is possible to take k_3=0.40-060 for the circular conductor and $^{\prime}k_3$=0.50-0.70 for the rectangular conductor. The ranges of a change in the duty factor can be refined in the process of designing the concrete/specific/actual machines.

Magnetizing force of excitation winding

$$F_в = F_\delta k_{ст} k_{р.в} = \frac{2k_{ст}k_{р.в}}{\mu_0}[\delta' k_\delta B_\delta + \delta_{м2} B_с], \qquad (8\text{-}72)$$

where F_δ — magnetizing force, which corresponds to nonmagnetic "gaps";

$\delta' = \delta + \delta_г + \delta_{м1}$ — nonmagnetic "gap";

$k_\delta > 1$ — coefficient of air gap;

$B_с$ — magnetic induction in steel of rotor;

$k_{р.в}$ — coefficient, which considers the saturation of steel from the cross flow of armature reaction (see recommendations in Chapter 4);

$k_{ст}$ — coefficient of magnetic circuit, defined as relation of total magnetizing force to magnetizing force of nonmagnetoconducting sections, i.e.

$$k_{c\tau}=1+\frac{F_{c\tau}}{F_\delta}.$$

Page 213.

Usually $k_{c\tau}=1,05\div1,5$. For determining the basic dimensions in the first approximation, it is possible to take $k_{c\tau}^{(1)}\approx1,2$. Value $k_{c\tau}$ must be made more precise after conducting of the detailed calculation of the magnetic circuit of engine.

Radial clearance between stator-rotor unit δ can be accepted as minimally permitted for structural/design and technological reasons taking into account (8-24):

$$\delta>2\delta_{\text{п.опт}}\approx0,14\text{Re}^{-0,103}D^{(1)}. \quad (8\text{-}73)$$

Thus, for preliminarily selected coefficient $k_в$ we find values $b_в$ and $h_в$.

Outer diameter of compensative bifilar is determined, being assigned by current density in compensators j_c:

$$D_{c_1}=2\sqrt{\frac{I_c}{\pi j_c}+\left(\frac{D_c}{2}\right)^2}. \quad (8\text{-}74)$$

Diameter of the internal bore of the magnetic circuit of stator (compensators)

$$D_c=D^{(1)}+2(\delta+\delta_t+\delta_{в1}). \quad (8\text{-}75)$$

The current, which passes from the compensator, approximately is computed:

$$I_c\approx\pi(0.5\ D_c-\delta_{в1})^2 j_p \quad (8\text{-}76)$$

After determining D_{c1}, we calculate internal and outer diameters of excitation winding ($D_{в.в}$ and $D_{в.н}$). consequently, also ratio $h_в$ / $b_в$, which must be close to unity. If necessary the calculation must be repeated at other given value of coefficient $k_в$.

After determining in the first approximation, the overall length of rotor, it is possible to begin the refinement of the value of the moment/torque of hydraulic resistor/resistance $M_т$ with $l=L^1$ on (8-20) and (8-21). In this case to the termination of complete rational design they take zero diameter of output shaft ($D_1=0$) as equal to, since losses to hydraulic friction of shaft are approximately/exemplarily equal to the losses of face of cylinder with a similar diameter. The refinement of value will make it possible already in the second approximation/approach to obtain completely satisfactory results.

After obtaining the final values of D_1, D_2, l, L and some other values, it is possible to determine entire geometry of the magnetic circuit of engine and excitation winding.

The section of the conductor of excitation winding with the assigned voltage of the supply $U_в$ and the geometry of the coil

$$q_{пр}=\frac{\pi(D_{в.с}+k_в b_в)}{U_в \gamma_в} F_в, \qquad (8\text{-}77)$$

accepted, where $\gamma_в$ — the specific conductivity of the material of conductor.

In accordance with $q_{пр}$ the geometry of conductor ($d_{0п}$, $d_{0в}$ or $a_{0п}$, $b_{0п}$ and $a_{0в}$, $b_{0в}$), is chosen, the discreteness of a number of turns in the layer at length $b_в$ is checked and the duty factor of winding is made more precise.

Number of turns of excitation winding

$$w=\frac{F_в}{I_в}=\frac{F_в}{q_{пр} j_в}. \qquad (8\text{-}78)$$

Bore diameter of window under the excitation winding

$$D_в=D_с+2h_0. \qquad (8\text{-}79)$$

Outer diameter of stator with the magnetic induction in steel $B_с$

$$D_н=D\sqrt{\frac{B_р}{B_с}k_в+\left(\frac{D_в}{D}\right)^2}, \qquad (8\text{-}80)$$

where $k_в$ — coefficient of scattering the magnetic system of engine.

For the calculations of first approximation $k_в=1{,}1\div1{,}2$. The thickness of magnetic circuit at diameter $D_в$

$$L_с=0{,}25\frac{D^2}{D_в}\frac{B_г}{B_с}k_{зп}, \qquad (8\text{-}81)$$

where the coefficient of scattering for this section of magnetic circuit $k_{зп}$ is accepted somewhat smaller $k_з$.

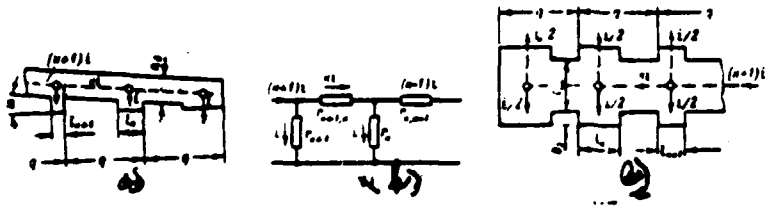

Fig. 8-13. Excitation winding of cylindrical UD. a) scanning/sweep of the first turn of series winding; b) the equivalent schematic of the first turn of winding; c) scanning/sweep of the latter/last turn of series winding with the uniform bilateral of the removals/takings of current.

Page 215.

For the design concept of winding, represented in Fig. 8-11a, difference from expression (8-68)

$$b_0 = 2b_з + 4s_и + b_ш. \qquad (8\text{-}82)$$

In this case it is implied that the excitation winding consists of two coils with a length of $b_з$ each with the voltage/stress on each $U_з$. Coils can be combined between themselves consecutively/serially and in parallel.

The size/dimension of busbar $b_ш$ (see Fig. 8-11b) can be determined, if we assign current density $j_ш$ in the place of its direct contact with the shield:

$$b_m = \frac{m_1 l_c}{\pi D_a j_m}, \qquad (8\text{-}83)$$

where

$$D_a = D + 2(\delta + \delta_t).$$

Inner diameter of field coils

$$D_{a.a} = D_a + 2s_u. \qquad (8\text{-}84)$$

Magnetizing force of each coil

$$F_a = F_\delta \frac{k_{c\tau} k_{p.a}}{2} = \frac{k_{c\tau} k_{p.a}}{\mu_0} \delta' k_\delta B_\delta. \qquad (8\text{-}85)$$

Outer diameter of stator D_a is determined on (8-80). However, it is necessary to have in mind that the magnetic induction for the section in the point of emergence of the discharge busbars will be somewhat more than B_c:

$$B'_c = \frac{D^2}{D_a - D_a} \frac{k_\sigma B_\tau}{D_a + D_a - \frac{2}{\pi} m a'_m}, \qquad (8\text{-}86)$$

where m - number of outlets in the magnetic circuit;

a'_m — width of outlet under the busbar.

Remaining machine parameters will be defined just as for the previous design concept.

The determination of fundamental machine parameters, whose design concept is depicted in Fig. 8-12a, is conducted also on the analogous dependences. Certain special feature/peculiarity appears only in the determination magnitude D_a and b_a in connection with the

new method of the contact of consecutive excitation winding with the shield and the compensators (or by the outgoing through the framework of stator busbars).

Page 216.

Scanning/sweep of the first turn of winding is represented in Fig. 8-13a. It is assumed that the busbar has an inclination/slope toward the level of the contacted surfaces at angle α for the transition/junction of busbar without the sharp curvatures to the second (normal) turn of winding. This complicated profile/airfoil of turn can be made from the materials of both the busbar and the shield. We accept below, that the specific conductivity of its material is equal to specific electric conductivity of the material of coil busbars of excitation ($\gamma_в$).

Fig. 8-13b depicts the equivalent diagram of profile/airfoil. Slope angle can be calculated according to the formula

$$\operatorname{tg}\alpha = \frac{a'_в}{\pi D_в}, \qquad (8\text{-}87)$$

where $a'_в$ — thickness of busbar with the one-sided layer of insulation.

Height/altitude of k and (k+1) "teeth":

$$h_{вk} = \operatorname{tg}\alpha\,[0{,}5l_k + (k-1)\,q] + 0{,}5a_в \sec\alpha;$$

$$h_{вk+1} = \operatorname{tg}\alpha\,[0{,}5l_{k+1} + kq] + 0{,}5a_в \sec\alpha.$$

Toothlike division $q=\frac{\pi D_0}{m}$, $a_ш$ — the thickness of busbar; m - number of sections of separation.

The resistors/resistances of the equivalent diagram:

$$r_k=\frac{h_{ш k}}{\gamma_ш l_k b_ш};\quad r_{k+1}=\frac{h_{ш k+1}}{\gamma_ш l_{k+1} b_ш};$$

$$r_{k+1,k}=\frac{0.5l_{k+1}+(q-0.5l_k)}{\gamma_ш a_ш b_ш \cos\alpha},$$

where $b_ш$ —width of busbar.

Then on the basis of Kirchhoff's law it is possible to register the equality

$$r_k+kr_{k+1,k}=r_{k+1},$$

from which we find:

$$l_{k+1}=\left(-A_1+\sqrt{A_1^2+2A_2\frac{k}{a_ш}}\right)\frac{a_ш}{k}, \qquad (8\text{-}88)$$

where

$$A_1=\frac{q(k-1)\sin\alpha}{l_k}+\frac{a_ш}{2l_k}+\frac{k(q-0.5l_k)}{a_ш};$$

$$A_2=qk\sin\alpha+0{,}5a_ш.$$

Page 217.

According to expression (8-88), being assigned by the length of one contacted section $l_{k=1}$, it is possible to determine the length of the subsequent sections.

Magnetizing force of the first turn of excitation winding can be calculated as follows:

$$F_{s1}=\sum_{k=1}^{m}\frac{k}{m}i=I_s\sum_{k=1}^{m}\frac{k}{m^2}, \qquad (8\text{-}89)$$

where i - current, passing through one contacted surface;

I_s — the full current of excitation winding.

With m≥6 the effect of discreteness is reduced, and with a sufficient accuracy it is possible to consider that value $\sum_{k=1}^{m}\frac{k}{m^2}$ is equal to half of turn.

Voltage drop across the first turn

$$U_{s1}=\sum_{k=1}^{m}\frac{kiq}{\gamma_s a_s b_m\cos\alpha}=\sum_{k=1}^{m}\frac{kql_s}{\gamma_s a_s b_m m\cos\alpha}. \qquad (8\text{-}90)$$

Analogously must be designed the latter/last turn of excitation winding, if its output from the stator is not produced by the entire busbar through one slot.

If latter/last turn evenly distributes current to bivilar, then in accordance with Fig. 8-13c it can be found

$$l_{k+1}=\left[\sqrt{A_1^2+4A_2\frac{k}{b_m}}-A_1\right]\frac{b_m}{2k}, \qquad (8\text{-}91)$$

where

$$A_1=2\left(\frac{b_3+0,5b_m}{2l_s}+\frac{k}{b_m}(q-0,5l_s)\right);$$

$A_2=b_3+0,5b_m$; $q=\frac{\pi D_{ext}}{m}$ — toothlike division; b_3 — size/dimension of "tooth".

During the design of the engine of smallest possible weight the tendency toward an increase in the speed of rotation of rotor is natural. For the engine with the complete insertion/immersion of rotor into the liquid the rotational speed determines the efficiency of machine, since hydraulic losses with the constant geometry of rotor increase proportionally $n^{2,8 \div 3}$. However, in UD with the increase of velocity the geometric dimensions of rotor will be sharply reduced.

Page 218.

It induces this at the assumption that there is a value of velocity, at which hydraulic losses are minimum. But this assumption is inaccurate, since with E=const (assigned voltage) the value of hydraulic losses P_{mn} with an increase in the velocity will be approximately/exemplarily proportional $\sqrt{n}$. This coupling of the parameters must be taken into consideration at the selection of the optimum rotational speed, which corresponds to the rational weight ratio and efficiency.

C). Disk UD.

The conclusion/output of fundamental calculated relationships/ratios for disk UD with b=const will be carried out less in detail, taking into account possible analogy with the cylindrical machine.

The design concept of disk UD, given in Fig. 8-5, provides for separate excitation with the decrease of the effect of the field of armature reaction with the help of the radial gashes in the magnetic circuit. However, as in the cylindrical machine, the use of consecutive excitation winding and compensators (see Fig. 4-5), is possible.

From the expression for internal torque (8-53) it follows:

$$D=\sqrt{\frac{8M_{\text{эл}}}{\pi b D_1 j_1 B_\delta}+d_1^2}, \qquad (8\text{-}92)$$

where d_1 - bore diameter of magnetic circuit for the fitting/sowing to the shaft.

From the expression for the magnetic flux in the working gap

$$D=\sqrt{\frac{4\Phi_\delta}{\pi B_\delta}+d_1^2}. \qquad (8\text{-}92a)$$

The value of the diameter of shaft D_1 must be chosen both on the mechanical strength and on the permissible current density of shaft j_p:

$$D_1=2\sqrt{\frac{I_a k}{\pi j_p}}, \qquad (8\text{-}93)$$

where k=0.5 during the bilateral supply of current to the disk and

k=1 - with the one-sided, and armature current (disk) is determined on (8-53a):

$$I_{\text{я}} = \frac{2\pi M_{\text{в1}}}{\Phi_{\delta}}.$$

Page 219.

Thus, current is the function of magnetic flux and, consequently, also the geometric dimensions of machine.

Expression D_1 through D can be obtained in the form of the solution of the equation of high degree. For this reason for simplification in the calculation should be recommended the method of iteration, after taking for (8-92) certain value of D_1, which corresponds to the expected order of the consumed current, and after leading the refinement of this value subsequently according to expression (8-93).

Expression for anti-emf of machine can be represented in the form

$$E = B_{\delta} v_{\text{ср}} \frac{D - d_1}{2} = B_{\delta} \omega \frac{D^2 - d_1^2}{8} = \Phi_{\delta} n, \qquad (8\text{-}94)$$

where B_{δ} — average, constant in any radius value of magnetic induction in the working gap, and n - rotational speed, expressed in r/s.

With the help of (8-94) working magnetic flux we will obtain in the previous form:

$$\Phi_{\delta} = \frac{U_{\text{в}}}{\dot{U} m_E n}.$$

Then on (8-92a)

$$D=\sqrt{\frac{4U_{\text{д}}}{\pi m_E \hat{U} n B_\delta}+d_1^2}. \qquad (8\text{-}95)$$

Dependence (8-95) serves for checking the conformity of parameter D the value of the assigned voltage.

Internal torque is expressed through the sum of the moments/torques

$$M_{\text{эл}}=\frac{M_{\text{х}}+M_{\text{д}}}{m_E m_l}=\frac{M_{\text{х}}+M_{\text{д}}}{p},$$

where $M_{\text{д}}$ — moment/torque of the hydraulic resistor/resistance of entire multipole system.

Since $M_{\text{х}}$ is the function of the basic dimensions of machine and essential value in UD with the complete insertion/immersion of rotor into the liquid, then for precision determination of D it is used, as before the method of iteration. For the calculations of first approximations it is possible to take $M_{\text{х}}^{(1)}=0{,}1\ M_{\text{д}}$.

Page 220.

The size/dimension of disk actually does not depend on the geometry of winding; therefore the refinement of value with the help of expressions (8-20) and (8-21) can be carried out sufficiently

AD-A139 778 UNIPOLAR ELECTRIC MACHINES WITH LIQUID-METAL CURRENT PICKUP(U) FOREIGN TECHNOLOGY DIV WRIGHT-PATTERSON AFB OH A I BETTINOV ET AL. 08 MAR 84 FTD-ID(RS)T-1205-83 5/6

UNCLASSIFIED F/G 9/3 NL

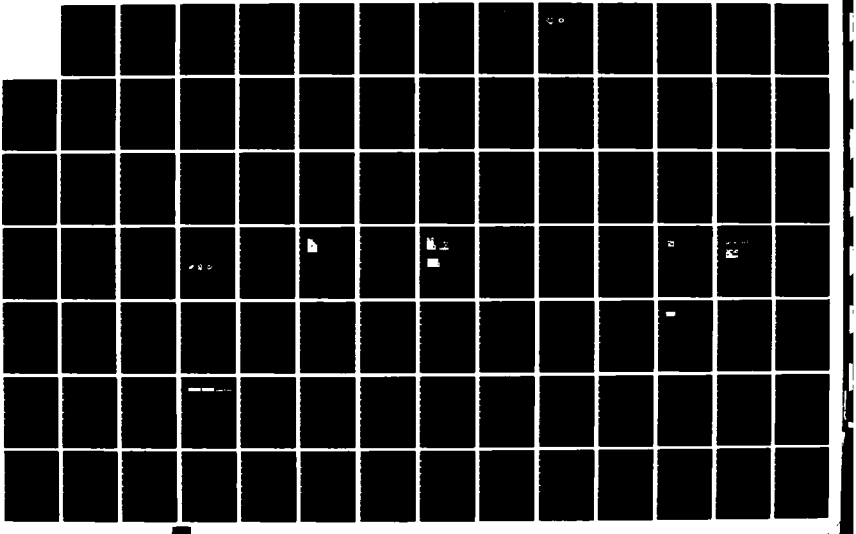

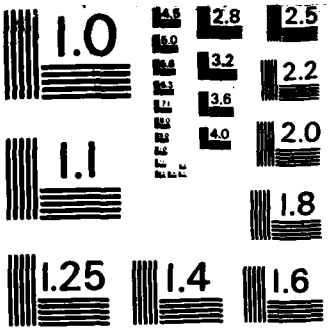

MICROCOPY RESOLUTION TEST CHART
NATIONAL BUREAU OF STANDARDS-1963-A

rapidly, if we assume l=b and $L_c = b + 2\delta$. In this case one should take into account that the effect of the thickness of disk b on value $\dot{M}_{\text{д}}$ will be insignificant. Therefore for the calculations of first approximations it is possible to take:

$$b^{(1)} = \frac{D_1^{(1)}}{4k} \frac{j_p}{j_1}.$$

Air-gap clearance δ between stator-rotor unit they accept that minimally permitted for structural/design and technological reasons taking into account (8-25):

$$\delta \geqslant 2\delta_{\text{п.опт}} \approx 0{,}1 D \mathrm{Re}^{-0{,}182}. \qquad (8\text{-}96)$$

Determining the dimensions of coils, window for positioning/arranging the excitation winding and geometry of magnetic system does not present difficulty and can be carried out according to the expressions, analogous to those, which were given for the cylindrical machine and in this case they are not repeated.

D). Unipolar engine with the hollow rotor.

The examination of fundamental dependences is carried out in connection with the design concept, depicted in Fig. 8-10d, implying if necessary the presence of insulating layers, protective shields, and also contact shields, busbars and bifilars - compensators or longitudinal-radial gashes.

From the equation for internal torque (8-58) it follows:

$$D=b+\sqrt{\frac{2M_{31}}{\pi b l j_p B_\delta}}. \qquad (8\text{-}97)$$

In this case, as during the conclusion/output of expression for internal torque, we assume that the magnetic induction in working gap/interval B_δ is constant over a radius and the active length of machine.

In (8-97) remain unknown values not only M_{31}, but also b and l, which themselves are the functions of the mean diameter of hollow rotor.

Page 221.

The value of internal torque M_{31} can be represented in general form through net torque and moment/torque of the hydraulic resistor/resistance of entire machine, just as for the disk machine. However, in the case of the complete insertion/immersion of rotor into the liquid the moment/torque of hydraulic resistor/resistance can here comprise considerably larger portion $M_м$ even in the comparison with cylindrical UD, since the friction surface grows approximately/exemplarily doubly. The fundamental method of evaluation/estimate M_{31} it remains as before the method of successive approximation.

The thickness of hollow rotor can be expressed:

$$b=\frac{I_{\text{я}}}{\pi D_{\text{ср}} j_{\text{р}}}=\frac{I_{\text{я}}}{\pi(D-b) j_{\text{р}}}. \qquad (8\text{-}98$$

The approximate estimate of the magnitude of current in rotor $I_{\text{я}}$ can be produced as follows:

$$I_{\text{я}}^{(1)}=\frac{m_E P_{\text{я}}}{p\eta^{(1)} U_{\text{я}}}, \qquad (8\text{-}99)$$

where η^1 - preliminarily given value efficiency of two-pole engine, which corresponds to the speed of rotation of rotor (η^1=0.6-0.7) accepted.

Then from (8-97) and (8-98)

$$D=b+\frac{2M_{\text{э1}}}{lI_{\text{я}}B_{\delta}}. \qquad (8\text{-}100)$$

After taking the equality of magnetic flux in the working gap/interval (at the mean diameter of hollow rotor $D_{\text{ср}}$) and in the section of magnetic circuit with a diameter of $d_{\text{с}}$, we will obtain:

$$l=\frac{D-b}{4}\frac{B_{\delta}}{B_{\text{с}}}\zeta^2-\frac{d_1^2}{4(D-b)}\frac{B_{\text{с}}}{B_{\delta}}, \qquad (8\text{-}101)$$

where $\zeta=\frac{d_{\text{с}}}{D-b}$ — coefficient, selected from the considerations of the minimum scattering of magnetic flux through the window for positioning/arranging the excitation winding;

$B_{\text{с}}$ — magnetic induction in steel of stator;

$d_1=D_1+2\delta_1$ - bore diameter of internal magnetic circuit for the shaft of engine.

Joint solution (8-100) and (8-101) relative to D gives:

$$D=b+\frac{1}{\zeta}\sqrt{\frac{8M_{s1}}{l_a B_\delta}+d_1^2}. \qquad (8\text{-}102)$$

the diameter of shaft D_1 is determined with the help of expression (8-93).

Page 222.

Since the value of anti-emf of machine is equal to:

$$E=0{,}5D_{cp}l_\delta B_\delta=n\Phi_\delta=\frac{U_a}{\dot{U}m_E} \qquad (8\text{-}103)$$

and

$$M_{s1}=\frac{\Phi_\delta I_a}{2\pi}.$$

that is not difficult to establish/install conformity to the geometry of machine to the assigned magnitude of the voltage/stress

$$D=b+\frac{1}{\zeta}\sqrt{\frac{4U_a}{\pi m_E\dot{U}B_\delta n}+d_1^2}. \qquad (8\text{-}104)$$

The gaps between the stator and the hollow rotor, necessary for calculating the moment/torque of hydraulic resistor/resistance, are chosen just as in cylindrical UD.

The establishment of the complete coupling of all fundamental parameters is carried out by iterative method.

The geometric dimensions of the excitation winding and magnetic circuit are defined just as for other UD.

Chapter Nine.

BASES OF THEORY AND CALCULATION OF NONPOLAR DYNAMOS WITHOUT FERROMAGNETIC CIRCUIT.

9.1. General information about acyclic machines without the ferromagnetic inductor.

Nonpolar dynamos without the ferromagnetic magnetic circuit-inductor and with the nonmagnetic rotor (armature) are used in the technology of charged particle accelerators for the creation of strong magnetic fields. With inductions on the order of 10 T (10^5 G) the accelerators do not also have the ferromagnetic circuit, the field of accelerator can simultaneously serve as the field of exictation of generator. Nonpolar dynamos are implemented with the consecutive or with the compound excitation (when starting winding of separate excitation is present). Cylindrical [122] and disk [95] machines with the liquid-metal current pickup are used. Obtain the strong fields (~10 T) due to the short-term current pulses of order

(0.5-3)10³ A with the duration of 0.1-0.5 s, which are generated by UG. The use/application of latter/last magnetic cores is inexpedient: in the overall field of exictation UG and accelerator the induction considerably exceeds the saturation induction of the material of magnetic circuit. However, the induction of field of exictation UG on the order of 0.5-1 T comparatively simply is achieved due to the high current density in the winding of series connection for a period of time of the work of impulse/momentum/pulse.

Page 224.

Rotors UG are used as the flywheels, which reserve kinetic energy. Dispersal/acceleration of UG is produced by the special drive motors of low power or with the help of air jets [95]. In the latter case on the rotor there are openings/apertures, which perform the role of the turbine blades. Dispersal/acceleration of UG in motoring with the feed from the source of direct current is feasible. Fig. 9-1 presents construction/design of UG, investigated experimentally in [95].

During the pulsed mode with the short duration and the relatively larger porosity of impulses/momenta/pulses, characteristic for the accelerators, the sizes/dimensions of excitation winding of UG do not reach excessive value, even if we do not take special

measures for its cooling. For the continuous duty represents interest the development of UG without the ferromagnetic circuit with the excitation winding, cooled by liquified helium, by hydrogen or by another gas. For the field coils, made from hollow tubular conductors, on which the cooling fluid circulates, it is proposed to apply molybdenum or hafnium alloys [123].

The elements/cells of theory pulse disk UG are examined in [95]. Equations of the equilibrium of emf in the circuit of armature and conservation of energy with the attenuation of angular velocity during the work of impulse/momentum/pulse are given.

The designing-theoretical research of UG without ferromagnetic circuits at the constant velocity of the rotation of rotor up to now were not conducted. The results of this research can prove to be useful during the evaluation/estimate of the efficiency/cost-effectiveness of UG without ferromagnetic inductor, intended for the continuous duty (with the superconducting excitation windings or with a deep cooling).

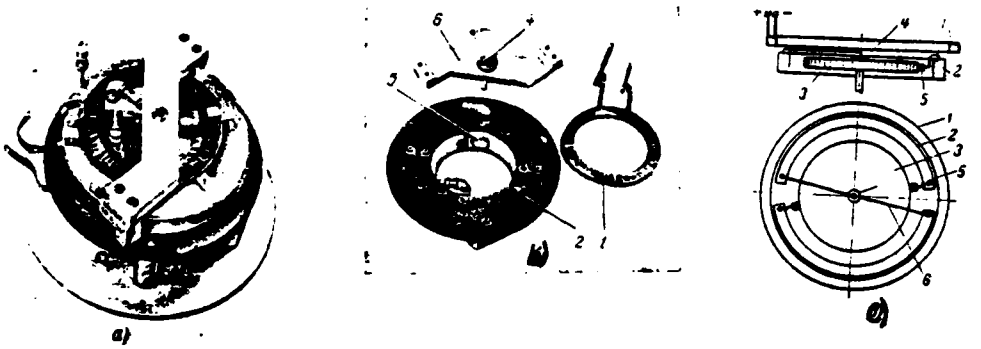

Fig. 9-1. Non-polar dynamo without the ferromagnetic circuit for the feed of betatron. a) general view; b) individual parts of UG; c) the connection diagram; 1 - coil of separate excitation; 2 - series winding; 3 - disc armature; 4, 5 - mercury "brush" (jet-edge contacts); 6 - short-circuiting busbar (field of exictation of UG serves as simultaneously accelerating field of betatron).

Page 225.

Let us note that to the use of superconductivity for increasing the efficiency of electrical equipment is at present paid the attention both in the Soviet Union [1] and abroad [124].

FOOTNOTE [1]. Acad. V. I. Wexler's article in the newspaper "Pravda" from 31 Mar. 1962. ENDFOOTNOTE.

The result of calculation of emf in UG it is possible to use, also,

during the design of electrical measuring equipment, for example for the absolute determination of one resistors/resistances (ohm) and the dielectric constant, where disk UG without the ferromagnetic circuit [40, page 279] is applied.

In contrast to UG with the magnetic circuit from the ferromagnetic material in those examined/considered UM especially should be analyzed a question about the self-excitation.

In nonpolar dynamos with the ferromagnetic circuit the nonlinearity of no-load characteristic (with the linear volt-ampere characteristic of energizing circuit) and the presence of residual magnetization of inductor, as a rule, ensure reliable self-excitation and stable work of machine at the selected point of characteristic. Acyclic machine without the ferromagnetic core has linear no-loads characteristic and energizing circuit, which usually can intersect only in the beginning of coordinates. Consequently, a similar generator is not self-excited. To ensure initial voltage/stress is possible either with the help of the special winding of separate excitation or with the use/application of a permanent magnet. Stable operation it is possible to attain by the use/application of a nonlinear element/cell either in the magnetic or in electrical energizing circuit, and also by the selection of the value of the resistor/resistance of energizing circuit. The exemplary/approximate

form of characteristics is given in Fig. 9-2.

Page 226.

9.2. The magnetic field of machines without the ferromagnetic circuit.

During the calculation of magnetic fields cylindrical and disk UG, depicted in Fig. 9-3a, b, let us take the following assumptions:

1. Non-polars dynamo work in the steady-state mode/conditions; field coils are connected in series in the circuit of armature or are fed from the independent source.

2. The sizes/dimensions of the cross section of field coil are considerably lower than its mean radius; we examine the magnetic field of excitation at the points, arranged/located from the winding on the distances, which considerably exceed the sizes/dimensions of its section.

3. The effect of the devices/equipment, which ensure self-excitation of UG, we do not consider.

Distribution in the space of induction B of field of exictation can be found, after using relationship/ratio B= rot A (A - the vector potentia' of e' :tromagnetic field).

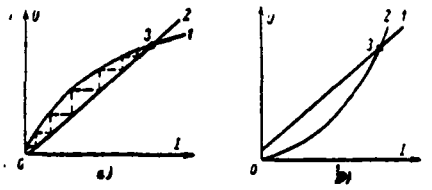

Fig. 9-2. To a question about the self-excitation of UG without the ferromagnetic circuit. a) the characteristic of machine with the nonlinear element/cell in the magnetic circuit; b) the same with nonlinear element in the electrical circuit; 1 - no-load characteristic of UM; 2 - volt-ampere characteristics of energizing circuit; 3 - stable operating point.

Page 227.

As is known [125], with the adopted assumptions

$$A = \frac{\mu_0}{4\pi}\oint_l \frac{F_s dl}{|\rho|}, \text{ V·s/m},$$

where $F_{в.о}$ —the full current (magnetizing force) of field coil;

$\mu_0 = 4\pi \cdot 10^{-7}$, H/m - magnetic permeability of vacuum;

ρ, m - distance from the element of length dl of field coil to the point of field in question.

As a result of the meridional symmetry in the cylindrical coordinate system r, φ, z vetor-potential A has only azimuth component.

After the series/row of conversions it is possible to obtain:

$$A_\varphi = \frac{\mu_0 F_s}{\pi} \sqrt{\frac{R_s}{r}} \frac{1}{k} \left[\left(1 - \frac{k^2}{2}\right) K(k) - E(k) \right], \qquad (9\text{-}1)$$

moreover

$K(k) = \int_0^{\pi/2} \frac{d\alpha}{\sqrt{1-(k\sin\alpha)^2}}$; $E(k) = \int_0^{\pi/2} \sqrt{1-(k\sin\alpha)^2}\, d\alpha$ — complete elliptic integrals respectively of the 1st and 2nd kind;

$k = \sqrt{\frac{4R_s r}{(R_s+r)^2+z^2}}$ — modulus/module of elliptical integrals ($0 \leqslant k \leqslant 1$);

R_s and $\alpha = \pi - \varphi/2$ - the mean radius of circular field coil and calculated angle.

After developing expression rot A in the cylindrical coordinates and after taking into account that $A_r = A_z = 0$, we will obtain for the field of exictation:

$$B_r(r, z) = \mathrm{rot}_r A = -\frac{\partial A_\varphi}{\partial z}; \qquad (9\text{-}2)$$

$$B_\varphi(r, z) = \mathrm{rot}_\varphi A = 0; \qquad (9\text{-}3)$$

$$B_z(r, z) = \mathrm{rot}_z A = \frac{A_\varphi}{r} + \frac{\partial A_\varphi}{\partial r}. \qquad (9\text{-}4)$$

Page 228.

The components of vector of magnetic induction (9-2) and (9-4) let us find by differentiation (9-1) taking into account relationships/ratios [126]:

$$\frac{dK(k)}{dk}=\frac{E(k)}{k(1-k^2)}-\frac{K(k)}{k};\quad \frac{dE(k)}{dk}=\frac{E(k)-K(k)}{k};$$

$$\frac{\partial k}{\partial r}=\frac{k}{2r}-\frac{k^3(R_0+r)}{4R_0r};\quad \frac{\partial k}{\partial z}=-\frac{k^3z}{4R_0r}.$$

After the series/row of conversions we have:

$$B_r(r,\ z)=\frac{\mu_0F_0}{4\pi}\cdot\frac{z}{R_0r}\sqrt{\frac{R_0}{r}}\left[E(k)\frac{k(2-k^2)}{2(1-k^2)}-K(k)k\right]=$$

$$=\frac{\mu_0F_0}{2\pi}\left[E(k)\frac{R_0^2+r^2+z^2}{(R_0-r)^2+z^2}-K(k)\right]\frac{z}{r\sqrt{(R_0+r)^2+z^2}},\ \overset{(1)}{m\Lambda};\qquad (9\text{-}5)$$

$$B_z(r,\ z)=\frac{\mu_0F_0}{4\pi}\cdot\frac{1}{R}\sqrt{\frac{R_0}{r}}\left[E(k)\frac{(R_0+r)k^2-2rk}{2r(1-k^2)}+K(k)k\right]=$$

$$=\frac{\mu_0F_0}{2\pi}\left[E(k)\frac{R_0^2-r^2-z^2}{(R_0-r)^2+z^2}+K(k)\right]\frac{1}{\sqrt{(R_0+r)^2+z^2}},\ \textcircled{D}\ m\Lambda.\qquad (9\text{-}6)$$

Key: (1). T.

The manifestation of armature reaction in UG without the ferromagnetic circuit is unique. Transverse (azimuth) armature field

causes the distortion of field of exictation, but longitudinal-demagnetizing effect of transverse armature reaction cannot be exhibited, since the magnetic core is absent and normal to the surface of armature the components of magnetic induction B_δ or B_{δ_0} are not changed in the value. The pattern of lines of the magnetic induction of the resulting magnetic field is interesting. The latter has three-dimensional/space spiral character and cannot be represented as plane-parallel.

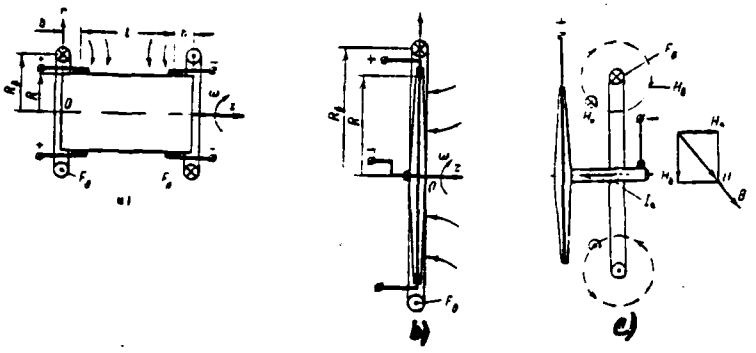

Fig. 9-3. Illustrations to the calculation of UG without the ferromagnetic circuit. a) network of cylindrical generator with the designation of sizes/dimensions; b) the same of disk generator; c) to the explanation of the resulting magnetic field of UG with the load (armature reaction).

Page 229.

The analogy of the resulting field of UM with the field of the system of rectilinear and circular currents, examined in S1-5, is clarified by Fig. 9-3c. Let us note that the nonplanarity (three-dimensional nature) and multipoint nature of the lines of magnetic field are observed also in the synchronous machines with claw-shaped poles [80] and in some other magnetic systems moreover here this is caused not by the presence by the specific form of the oriented currents, but by the peculiarity of the form of magnetic circuit.

9.3. Electromotive forces of cylindrical and disc armature.

Knowing the magnetic field of excitation, it is possible to find emf of armature UG. The material of armature (rotor) is taken nonmagnetic.

For the subsequent integration it is necessary to represent complete elliptic integrals in expressions (9-5) and (9-6) in the form of series/rows [126]:

$$E(k)=\frac{\pi}{2}\left\{1-\frac{1}{2^2}k^2-\frac{1^2\cdot 3}{2^2\cdot 4^2}k^4-\ldots-\left[\frac{(2m-1)!!}{2^m m!}\right]^2\frac{k^{2m}}{2m-1}-\ldots\right\};$$

$$K(k)=\frac{\pi}{2}\left\{1+\left(\frac{1}{2}\right)^2k^2+\left(\frac{1\cdot 3}{2\cdot 4}\right)^2k^4+\ldots+\left[\frac{(2m-1)!!}{2^m m!}\right]^2k^{2m}+\ldots\right\},$$

where (2m-1) !!=1·3·5 ... (2m-1). Rejection in these series/rows of terms is older than the second even at the values of modulus/module k, close to one, as calculations showed, does not lead to the large error during the subsequent determination of emf in cases $R_a>r$. In this case after conversions we obtain expressions for the components of magnetic induction in the form

$$B_r(r,\ z)=\frac{3\mu_0 F_a R_a^2 rz}{2[(R_a-r)^2+z^2]\left[\sqrt{(R_a+r)^2+z^2}\right]^5},\ \frac{(1)}{m.a.}; \qquad (9\text{-}7)$$

$$B_z(r,\ z)=\frac{\mu_0 F_a R_a^2}{2}\left\{\frac{1}{\left[\sqrt{(R_a+r)^2+z^2}\right]^3}+\right.$$

$$\left.+\frac{3(R_a-r)r}{[(R_a-r)^2+z^2]\left[\sqrt{(R_a+r)^2+z^2}\right]^3}\right\},\ \frac{(1)}{m.a.} \qquad (9\text{-}8)$$

Key: (1). T.

Page 230.

In the linear medium of emf of cylindrical UG, depicted in Fig. 9-3a, it is determined according to the principle of the superposition of the fields, created by each field coil (it is considered normal to the surface of armature the component of magnetic induction):

$$e_{\text{ц}} = 2\int_{b}^{l+b} \omega R B_r(r, z)\, dz, \qquad (9\text{-}9)$$

where in accordance with the designations in Fig. 9-3 l, R and b, m - active length and outside radius of armature and distance from the plane of field coil to the current pickup;

ω, rad/s - angular velocity of armature. Substituting in (9-9) expression (9-7) and producing integration [66], we obtain:

$$e_{\text{ц}} = 3\mu_0 F_{\text{в}} \omega R_{\text{в}}^2 R^2 \left\{ \frac{1}{[(R_{\text{в}}-R)^2+b^2]\sqrt{(R_{\text{в}}+R)^2+b^2}} - \right.$$

$$- \frac{1}{(R_{\text{в}}-R)^2+(l+b)^2]\sqrt{(R_{\text{в}}+R)^2+(l+b)^2}} -$$

$$- \frac{1}{4R_{\text{в}}R}\left[\frac{\sqrt{(R_{\text{в}}+R)^2+b^2}}{(R_{\text{в}}-R)^2+b^2} - \frac{\sqrt{(R_{\text{в}}+R)^2+(l+b)^2}}{(R_{\text{в}}-R)^2+(l+b)^2}\right] +$$

$$\left. + \frac{1}{16R_{\text{в}}R\sqrt{R_{\text{в}}R}} \ln \frac{[\sqrt{(R_{\text{в}}+R)^2+b^2}+2\sqrt{R_{\text{в}}R}][\sqrt{(R_{\text{в}}+R)^2+(l+b)^2}-2\sqrt{R_{\text{в}}R}]}{[\sqrt{(R_{\text{в}}+R)^2+b^2}-2\sqrt{R_{\text{в}}R}][\sqrt{(R_{\text{в}}+R)^2+(l+b)^2}+2\sqrt{R_{\text{в}}R}]} \right\}. \qquad (9\text{-}10)$$

For disk UG without the ferromagnetic circuit the calculation of emf in the case of the location of the disk of armature and field

coil in one plane z=0 (Fig. 9-3b) in effect is of greatest interest. In this case greatest will be emf, developed with the armature:

$$e_{\Sigma}=\int_0^R \omega B_z(r,\ z)\,r\,dr. \qquad (9\text{-}11)$$

Page 231.

Substituting (9-8) in (9-11) and producing integration in the limits of disk, we find:

$$e_{\Sigma}=\frac{1}{16}\mu_0 F_0 \omega R_0\left[3\ln\frac{R_0+R}{R_0-R}-6\frac{R}{R_0+R}-2\left(\frac{R}{R_0+R}\right)^2\right]. \qquad (9\text{-}12)$$

Let us note that expressions (9-10) and (9-12) can be represented in the form of the relative parameters.

For example,

$$\mathring{e}_{\Sigma}=\frac{1}{16}\mu_0 v \mathring{R}_0\left[3\ln\frac{\mathring{R}_0+1}{\mathring{R}_0-1}-\frac{6}{\mathring{R}_0+1}-2\left(\frac{1}{\mathring{R}_0+1}\right)^2\right],$$

where

$$\mathring{e}_{\Sigma}=\frac{e_{\Sigma}}{F_0};\ v=\omega R;\ \mathring{R}_0=\frac{R_0}{R}.$$

According to derived formulas (9-10) and (9-12) it is possible to produce verifying calculation of UG with intended sizes of armature. For the purpose of checking the accuracy of the obtained formulas verifying calculation of emf of disk UG [66] is carried out. The initial data of the parameters of UG, investigated experimentally in work [95] were undertaken. The disagreement between calculation and experimental data composed about 12%, that it is possible to consider it acceptable in the engineering practice with the

assumptions pointed out above.

9.4. Calculation method by emf according to the mutual inductance of the excitation windings and armature.

a). Formulation of the problem.

When the sizes/dimensions of the cross section of field coils (independent variable, consecutive or parallel) are relatively small and coils can be represented as single-turn, calculation of emf of cylindrical and disk UM without the ferromagnetic circuit can be carried out also, using a concept of the mutual inductance of thin annuluses. This calculation method is convenient when the tables of complete elliptic integrals are present. In particular, taking into account unwieldiness of expression (9-10), during the calculation of cylindrical machines the method in question should be given the preference.

Page 232.

The electromotive force for any construction/design of UM without the ferromagnetic circuit

$$e=\frac{\omega\Phi_\delta}{2\pi}=\frac{\omega MF_\delta}{2\pi},\ \text{V},$$

where $\Phi_\delta=MF_\delta$ — working magnetic flux, engaged with the armature,

i.e., passing through the surface of the armature between the circles/circumferences of current pickups, Wb;

F_0 - magnetizing force of coil, which creates the flow of excitation Φ_{0a};

M - calculated mutual inductance, H.

We consider values F_0 and ω given. Consequently, for determining emf it is necessary to find value M.

b). Cylindrical is mind.

Is placed conditionally on the surface of the armature of cylindrical UM (Fig. 9-3a) in the circles/circumferences of circular current pickups thin single-turn ducts/contours. By considering field coils as thin rings, let us find the mutual inductance of each of the field coils with ducts/contours 1 (nearest to the coil) and 2. Using [127], we obtain respectively:

$$M_{21}=\mu_0\sqrt{R_2R}\left[\left(\frac{2}{k_{21}}-k_{21}\right)K(k_{21})-\frac{2}{k_{21}}E(k_{21})\right]; \quad (9\text{-}13)$$

$$M_{22}=\mu_0\sqrt{R_2R}\left[\left(\frac{2}{k_{22}}-k_{22}\right)K(k_{22})-\frac{2}{k_{22}}E(k_{22})\right], \quad (9\text{-}14)$$

where the moduli/modules

$$k_{21}=\sqrt{\frac{4R_2R}{(R_2+R)^2+b^2}} \text{ и } k_{22}=\sqrt{\frac{4R_2R}{(R_2+R)^2+(l+b)^2}}.$$

Calculated mutual inductance of field coil with the cylindrical

armature of the machine

$$M_{\text{д}}=M_{\text{в1}}-M_{\text{в2}}.$$

In the cylindrical UM the field coils are placed symmetrically relative to the equator of armature (Fig. 9-3a).

Page 233.

According to the principle of the superposition of the flows of mutual induction from two coils of emf of the machine

$$e_{\text{д}}=\frac{\omega M_{\text{д}}F_{\text{в}}}{\pi}=\frac{\mu_0\omega F_{\text{в}}\sqrt{R_{\text{в}}R}}{\pi}\left[2\left(\frac{K(k_{\text{в1}})-E(k_{\text{в1}})}{k_{\text{в1}}}-\frac{K(k_{\text{в2}})-E(k_{\text{в2}})}{k_{\text{в2}}}\right)-\right.$$

$$\left.-k_{\text{в1}}K(k_{\text{в1}})+k_{\text{в2}}K(k_{\text{в2}})\right]. \qquad (9\text{-}15)$$

Let us introduce the relative parameters

$$\mathring{R}_{\text{в}}=\frac{R_{\text{в}}}{R} \text{ и } \mathring{e}_{\text{д}}=\frac{e_{\text{д}}}{F_{\text{в}}},$$

of the showing respectively difference in the air-gap diameters and field coil and value of emf with value magnetizing force/ $F_{\text{в}}=I\omega$. Then

$$\mathring{e}_{\text{д}}=\frac{\mu_0 v\sqrt{\mathring{R}_{\text{в}}}}{\pi}\left[2\left(\frac{K(k_{\text{в1}})-E(k_{\text{в1}})}{k_{\text{в1}}}-\frac{K(k_{\text{в2}})-E(k_{\text{в2}})}{k_{\text{в2}}}\right)-\right.$$

$$\left.-k_{\text{в1}}K(k_{\text{в1}})+k_{\text{в2}}K(k_{\text{в2}})\right], \qquad (9\text{-}15\text{a})$$

where $v=\omega R$ - linear velocity of the lateral surface of armature, m/s;

$$k_{\text{в1}}=\sqrt{\frac{4\mathring{R}_{\text{в}}}{(\mathring{R}_{\text{в}}+1)^2+\mathring{b}^2}};\ k_{\text{в2}}=\sqrt{\frac{4\mathring{R}_{\text{в}}}{(\mathring{R}_{\text{в}}+1)^2+(\mathring{l}+\mathring{b})^2}},$$

$$\mathring{b}=\frac{b}{R};\ \mathring{l}=\frac{l}{R}.$$

Latter/last expression makes it possible to construct the dependence of the relative values of emf from velocity v from parameter $\mathring{R}_{\text{в}}$ (Fig. 9-4a).

With the value of parameter k_{n} close to one, modulus/module also approaches one, since usually $k<1$. In this case the calculation of emf according to formula (9-15), in which expression M_{n1} in the form (9-13) is used, becomes difficult. Difficulties appear because the tabular values of elliptical integrals $K(k_{n1})$, which correspond to the adjacent values of modulus/module k_{n1}, strongly differ from each other and any precise interpolation between them is virtually impossible.

Page 234.

In this case it is expedient for the purpose of an increase in the accuracy to use for the substitution into the calculated expression of emf another formula of mutual inductance [127], obtained from (9-13) with the help of the conversion of Landen, which reduces modulus/module k_{n1}:

$$M_{n1}=\frac{2\mu_0\sqrt{R_nR}}{\sqrt{k_{n11}}}[K(k_{n11})-E(k_{n11})], \tag{9-16}$$

where

$$k_{n11}=\frac{1-\sqrt{1-k_{n1}^2}}{1+\sqrt{1-k_{n1}^2}}.$$

If necessary it is possible to obtain also value

$$M_{n2}=\frac{2\mu_0\sqrt{R_nR}}{\sqrt{k_{n21}}}[K(k_{n21})-E(k_{n21})], \tag{9-17}$$

analogously, moreover

$$k_{n21}=\frac{1-\sqrt{1-k_{n2}^2}}{1+\sqrt{1-k_{n2}^2}}.$$

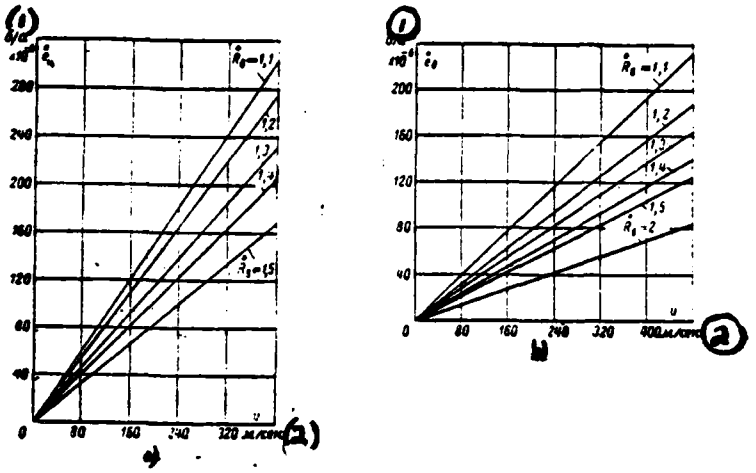

Fig. 9-4. Dependence of emf of armature with the single field current on the velocity. a) cylindrical UG $vr\ \dot{e}_{\text{ц}} = f(v)$ on $\dot{R}_{\text{в}}$; b) disk UG $vr\ \dot{e}_{\text{д}} = f(v)$ on $\dot{R}_{\text{в}}$.

Key: (1). V/A. (2). m/s.

Page 235.

But if value $k_{\text{в}11}$ from (9-16) proves to be insufficiently small, then, by applying repeatedly the conversion of Landen [127], it is possible to obtain:

$$M_{\text{в}1} = \frac{4\mu_0 \sqrt{R_{\text{в}} R}}{\sqrt{2(1+k_{\text{в}12})}\sqrt[4]{k_{\text{в}12}}}\left[(1+k_{\text{в}12})K(k_{\text{в}12}) - E(k_{\text{в}12})\right], \quad (9\text{-}18)$$

where

$$k_{\text{в}12} = \left(\frac{1-\sqrt[4]{1-k_{\text{в}1}^2}}{1+\sqrt[4]{1-k_{\text{в}1}^2}}\right)^2 \text{ — new modulus}$$

Calculations according to (9-15) become irrational and with

relatively larger values $l>1$. In this case modulus/module k_{12} is small and formula (9-14) for M_{12} contains a difference in the values close to each other, which decreases the accuracy of calculations emf. In this case it is expedient to use inverse transformation of Landen [127], which increases modulus/module k_{12}. For mutual inductance M_{12} we obtain the calculated expression

$$M_{12}=\mu_0\sqrt{R_1R}\left[\frac{K(k_{120})}{k_{12}(1+k_{12})}-\frac{1+k_{12}}{k_{12}}E(k_{120})\right], \qquad (9\text{-}19)$$

where new modulus/module $k_{120}=\frac{2\sqrt{k_{12}}}{1+k_{12}}$.

The calculation method presented is valid also for the cylindrical UM with the hollow rotor.

C). Disk UM.

We will assume/set the disk of armature relatively thin. It is placed single-turn ducts/contours in the plane of armature on the circles/circumferences of the circular current pickups: on the periphery of disk (1) and in center (2) in accordance with Fig. 9-3b.

In the general case the field coil with disk UM can be placed not in one plane with the disk, but at certain distance of z=b from it.

It is analogous with previous the calculated mutual inductance of the field coil and armature

$$M_{\text{я}}=M_{\text{в1}}-M_{\text{в2}},$$

moreover

$$M_{\text{в1}}=\mu_0\sqrt{R_{\text{в}}R}\left[\left(\frac{2}{k_{\text{в1}}}-k_{\text{в1}}\right)K(k_{\text{в1}})-\frac{2}{k_{\text{в1}}}E(k_{\text{в1}})\right]; \quad (9\text{-}20)$$

$$M_{\text{в2}}=\mu_0\sqrt{R_{\text{в}}R_0}\left[\left(\frac{2}{k_{\text{в2}}}-k_{\text{в2}}\right)K(k_{\text{в2}})-\frac{2}{k_{\text{в2}}}E(k_{\text{в2}})\right], \quad (9\text{-}21)$$

where

$$k_{\text{в1}}=\sqrt{\frac{4R_{\text{в}}R}{(R_{\text{в}}+R)^2+b^2}}, \quad k_{\text{в2}}=\sqrt{\frac{4R_{\text{в}}R_0}{(R_{\text{в}}+R_0)^2+b^2}};$$

R_0 - radius of a circle of current pickup in the center of disk.

The electromotive force of disk machine is expressed by the formula, analogous (9-15):

$$e_{\text{я}}=\frac{\omega}{2\pi}M_{\text{я}}F_{\text{в}}. \quad (9\text{-}22)$$

With two field coils, symmetrically arranged/located on distances $z=\pm b$, according to the principle of the superposition of emf $e_{\text{я}}$ it doubles in comparison with the value in (9-22).

With respect to calculation $M_{\text{в1}}$ and $M_{\text{в2}}$ for the disk machines are valid the same observations, that for the appropriate values of cylindrical machines.

The in practice most important case for the calculation of disk

UM with disk (z=0). Current pickup in the center of disk is supposed concentrated, and by its radius-relatively small ($R_0 \ll R$). In this case $M_{\text{зр}} < M_{\text{в1}}$ and value $M_{\text{в2}}$ can be disregarded/neglected.

Then for the calculation of emf of disk UM we obtain the formula

$$e_{\text{д}} = \frac{\mu_0 \omega F_{\text{в}} \sqrt{R_{\text{в}} R}}{2\pi} \left[\left(\frac{2}{k} - k \right) K(k) - \frac{2}{k} E(k) \right], \qquad (9\text{-}23)$$

where $k = \sqrt{\frac{4R_{\text{в}}R}{(R_{\text{в}}+R)^2}}$.

With $\mathring{R}_{\text{в}} = R_{\text{в}}/R$, the close ones to one, for the calculation by emf is recommended the formula

$$e_{\text{д}} = \frac{\mu_0 \omega F_{\text{в}} \sqrt{R_{\text{в}} R}}{\pi \sqrt{k_1}} [K(k_1) - E(k_1)], \qquad (9\text{-}24)$$

where $k_1 = \frac{1-\sqrt{1-k^2}}{1+\sqrt{1-k^2}}$.

Page 237.

If modulus/module k_1 also proves to be close to one, should be used the formula

$$e_{\text{д}} = \frac{2\mu_0 \omega F_{\text{в}} \sqrt{R_{\text{в}} R}}{\pi \sqrt{2(1+k_2)} \sqrt[4]{k_2}} [(1+k_2) K(k_2) - E(k_2)], \qquad (9\text{-}25)$$

moreover

$$k_2 = \frac{1-\sqrt{1-k_1^2}}{1+\sqrt{1-k_1^2}} = \left(\frac{1-\sqrt[4]{1-k^2}}{1+\sqrt[4]{1-k^2}} \right)^2.$$

Expression (9-23) it is possible to reduce to the form

$$\mathring{e}_{\text{д}} = \frac{\mu_0 v \sqrt{\mathring{R}_{\text{в}}}}{2\pi} \left[\left(\frac{2}{k} - k \right) K(k) - \frac{2}{k} E(k) \right], \ \mathbf{V}, \qquad (9\text{-}26)$$

where $v = \omega R$ - linear velocity on the periphery of disk, m/s;

$$\mathring{e}_{\text{д}} = \frac{e_{\text{д}}}{F_{\text{в}}}; \ k = \sqrt{\frac{4\mathring{R}_{\text{в}}}{(\mathring{R}_{\text{в}}+1)^2}}; \ \mathring{R}_{\text{в}} = \frac{R_{\text{в}}}{R}.$$

On the basis (9-26) are designed graphs $\dot{d}_a = f(v)$ on R_m represented in Fig. 9-4b.

9.5. Some special features/peculiarities of the design of generators.

Let us consider the specific character of determination of the basic dimensions of cylindrical and disk UG without the ferromagnetic circuit.

The diameter of the external surface of cylindrical armature is found during the calculation according to assigned current I_a of the machine:

$$D = 2R = \sqrt{\frac{4I_a}{\pi(1-\dot{d}_0^2) j_p}}, \text{ м},$$

where $\dot{d}_a = d_a/D$ - is considered the presence of the isolated/insulated rotor shaft (d_a - diameter of opening/aperture for the shaft);

j_p, $a/м^2$ - current density in the rotor, taken to uniform in accordance with the engineering procedure of calculation (see §2-4).

Page 238.

The value of the design factor of cylindrical machine $\lambda = 0.5$ should be taken:

$$\lambda = \frac{l}{D} = \frac{l}{2R} = 1{,}25 \div 1{,}5; \; \dot{l} = \frac{l}{R}.$$

Calculations show that the active length (distances between the current pickups), which exceeds $l \approx 1.5\ D$, is not appropriate, since in this case emf virtually does not increase, but losses and weight of armature grow. Fig. 9-5 gives the appropriate curves

$$\dot{e}_a = f(\lambda) \text{ (1) по } \dot{R}_в \text{ (2) при } v = \text{const.}$$

Key: (1). on. (2). with.

The optimum value of relative value of the mean radius of the field coil of cylindrical machine comprises:

$$\dot{R}_в = \frac{R_в}{R} \approx 1.$$

Differentiation of value $\dot{e}_a$ from (9-15a) for the purpose of research for the maximum of function $\dot{e}_a(\dot{R}_в)$ gives, in particular, for determining the optimum radius (when $d\dot{e}_a/d\dot{R}_в = 0$) expression $\dot{R}_в = (1 - \dot{b}')^{0.5}$. Usually $\dot{b}' < 1$, therefore should be taken value $\dot{R}_в \approx 1$.

As calculations confirm, function $\dot{e}_a = f(\dot{R}_в)$ reaches maximum when $\dot{R}_в \approx 1$ (see Fig. 9-5).

A change in parameter $\dot{\delta} = \delta/R$ insignificantly affects the value of emf $\dot{e}_a$. According to the design considerations one should tentatively choose $\dot{\delta} \approx 0{,}15 \div 0{,}25$.

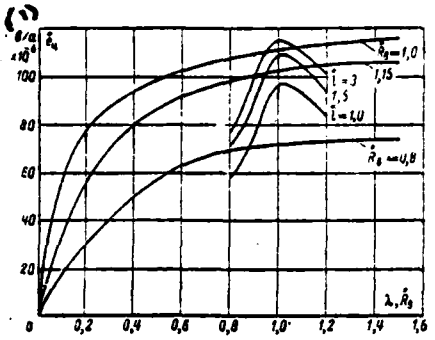

Fig. 9-5. Calculated dependences $\dot{e}_{\text{ц}} = f(\lambda)$ on $\dot{R}_{\text{в}}$ and $\dot{e}_{\text{ц}} = f(\dot{R}_{\text{в}})$ on $\dot{I}_{\text{J}}$ when $\delta = 0{,}15$; v=150 m/s for the cylindrical generator.

Key: (1)/ V/A.

Page 239.

Thus, the rational schematic of cylindrical generator must correspond to Fig. 9-6. Value of magnetizing force of field coil $F_{\text{в}}$ and the sizes/dimensions of the cross section of coil are determined by the given voltage of generator $U_{\text{ц}} = \dot{U}_{\text{ц}} e_{\text{ц}} \left(\dot{U}_{\text{ц}} = \frac{U_{\text{ц}}}{e_{\text{ц}}} < 1;\ F_{\text{в}} = I_{\text{в}} w_{\text{в}} \right)$ and permissible for reasons heat emission by the current density $j_{\text{в}}$ in the field coil.

With those selected a number of turns $w_{\text{в}}$ and main sizes/dimensions D and l their conformity with the assigned voltage is established/installed by verifying calculation according to

formulas (9-15)-(9-19). For convenience in the approximate computations in the curves, depicted Fig. 9-7, gives the values of the elliptical integrals E=f(k) and K=f (k). During the refined calculations it should be used appropriate tables [126].

The calculation of resistor/resistance and electrical losses of the armature of cylindrical machine taking into account the nonuniformity of current distribution is produced in accordance with the conclusions/outputs, given in §2-5.

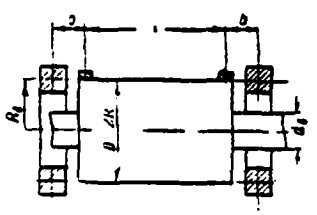

Fig. 9-6.

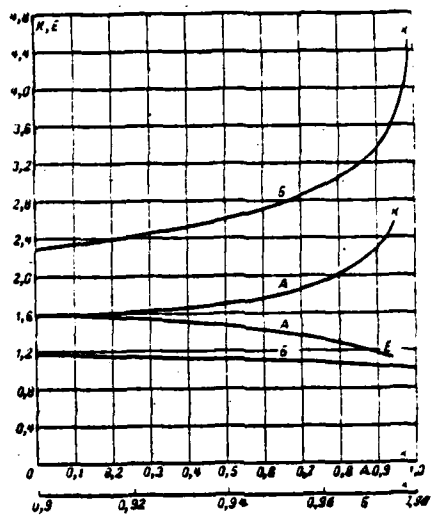

Fig. 9-7.

Fig. 9-6. Schematic device/equipment of cylindrical generator.

Fig. 9-7. Values of the elliptical integrals E=f(k) and K=f(k).

Diameter D=2R of armature disk UG without the ferromagnetic circuit with assigned voltage $U_a = \dot{U}_a \sigma_a \left(\dot{U}_a = \frac{U_a}{\sigma_a} < 1\right)$ is determined by verifying calculation according to formulas (9-23)-(9-25). Value $\dot{R}_a$ is chosen according to the design considerations.

During the location of the field coil and disk of armature in

the different planes one should accept $\dot{R}_*=1$ during their location in one plane (z=0) $\dot{R}_*>1$. The thickness of disk with assigned current I_* of armature is calculated from the appropriate expressions, given in §6-1. Electrical losses in the disk are determined from the formulas, examined in §2-6.

With the efficiency selected according to the conditions of contact or strength of the disk of the linear velocity v on the periphery of rotor value magnetizing force F_* of field coil disk UG depends on the assigned voltage. The sizes/dimensions of cross section and the permissible current density in the excitation winding are determined by heat emission conditions.

Examples of verifying calculations cylindrical and disk UG are given in [66]. They show that with the identical air-gap diameters D=2R, magnetizing force of field coils and at the rotational speeds the cylindrical generator (with two field coils) develops voltage/stress, is approximately/exemplarily 1.7 times less than disk UG. Calculations in examples [66] were performed through formulas (9-10) and (9-12).

For the comparison of these formulas with the formulas of the method of mutual inductance the calculations of emf of disk and cylindrical UG with different values $\dot{R}_*$ were performed. The method of

mutual inductance is in principle more precise, since it does not require resolution in the series/rows of elliptical integrals.

During comparative calculations it was explained that for the cylindrical machines the method of mutual inductance gives the somewhat smaller values of emf, than formula (9-10). The difference as results of calculation becomes greater, the nearer the parameter R_* to one, and it reaches to 30%. This is explained by the weakened convergence of series of the resolution of elliptical integrals with modulus/module k→1. For disk machines both calculation methods give close results. In particular, during the verifying calculation of disk UG, indicated in §9-4, the disagreement between data of calculation (9-23) and experiment [95] was about 9%. Disagreement in the calculations according to (9-12) and (9-23) in this case composed approximately/exemplarily 3.5%.

Page 241.

It is possible to show that the over-all payload ratio of the armature of cylindrical generator

$$\dot{G}_a \equiv \frac{\lambda + \lambda_\sigma}{j_p B_p} \cdot \frac{\gamma}{\omega R} \quad (\omega R = v),$$

where $\lambda = 0.5\lambda' = l/2R$; $\lambda_\sigma = b_\sigma/2R$ - design factors; j_p, B_p - current density and induction in the rotor, accepted by uniform ones to; γ - the specific gravity/weight of material. From the expression for $\dot{G}_a$ it is evident

that with the constant/invariable electromagnetic loads and the design factors, and also at the constant linear velocity v on the surface of armature its over-all payload ratio remains constant with ω=var. It is possible to also show that with the constant ampere-conductors per inch, $A = I_a/2\pi R$ over-all payload ratio $\dot{q}_a = 1/\omega$, i.e. is reduced with the increase of angular velocity $\omega = 2\pi n$.

However, similar conclusions can be drawn, also, for disk UG without the ferromagnetic circuit.

9.6. Elements/cells of the theory of the pulsed mode of generators without the ferromagnetic circuit.

Let us consider the diagram of UG with the compound (independent variable and consecutive) excitation, shown in Fig. 9-8. Let us carry out the theoretical analysis of the pulsed mode of the generator, with which the load suddenly varies from 0 to 100% and vice versa. This mode/conditions is feasible with the work of UG on the winding of particle accelerator. Connection of UG with the load is produced with the help of disconnector K (Fig. 9-8), which can be liquid-metal.

Fundamental assumptions during the research of problem are enumerated below:

1) generator drive powerful/thick, angular velocity does not vary with a change in load (ω=const); 2) the supply of power of excitation winding powerful/thick; voltage on this winding does not vary during the transient processes in generator ($U_в$=const); 3) pulse repetition period it is such, that for the time between rise/drop and load dropping electromagnetic processes in the generator manage to be established/installed; 4) its own inductance of massive armature is negligible; load circuit does not have inductive coupling with the windings of generator; 5) the nonlinearity of system, possible in the general case for guaranteeing the stable work of generator, we do not consider.

Page 242.

Let us note that in UG without the ferromagnetic circuit the analysis is facilitated by the absence of pole face winding in the series circuit of armature.

Let us compose the initial equations:

1. The loop equation of the load

$$u = R_н i + L_н \frac{di}{dt}, \qquad (9\text{-}27)$$

where u, i - voltage/stress and the current of generator (instantaneous values);

$R_{\text{н}}$, $L_{\text{н}}$ - resistor/resistance and the inductance (coefficient of self-induction) of load.

2. The equation of internal circuit of the generator

$$u = \omega M_{\text{п.я}} i + \omega M_{\text{в.я}} i_{\text{в}} + R'_{\text{я}} i + L_{\text{п}} \frac{di}{dt} + M_{\text{в.п}} \frac{di_{\text{в}}}{dt}, \quad (9\text{-}28)$$

where $M_{\text{п.я}}$, $M_{\text{в.я}}$, $M_{\text{в.п}}$ - calculated mutual inductance (coefficients of mutual inductance) of the windings of series excitation and armature, separate excitation and armature, independent and series excitation; $L_{\text{п}} \approx L_{\text{я}}$ - inductance of the winding of series excitation (equal to inductance internal circuit of armature); $R'_{\text{я}} \approx R'_{\text{р}} + R'_{\text{п}} + R'_{\text{п}}$ - resistor/resistance of internal circuit of armature taking into account the attenuating action of eddy currents in solid rotor $(R'_{\text{р}})$, consecutive busbar/tire winding $(R'_{\text{п}})$, with liquid-metal current pickup $(R'_{\text{п}})$; $\omega = 2\pi n$.

3. The loop equation of separate excitation

$$u_{\text{в}} = R_{\text{н.в}} i_{\text{в}} + L_{\text{в}} \frac{di_{\text{в}}}{dt} + M_{\text{п.в}} \frac{di}{dt}, \quad (9\text{-}29)$$

where $u_{\text{в}} = U_{\text{в}}$; $i_{\text{в}}$ - voltage/stress and current; $R_{\text{н.в}}$, $L_{\text{в}}$ - resistor/resistance and the inductance of the winding of separate excitation; $M_{\text{п.в}}$ - coefficient of mutual induction of the windings of the independent and series excitation.

The parameters of analyzed circuit (R, L, M) can be determined by calculation or it is experimental. In particular, the mutual inductance of excitation windings with the armature can be obtained on the basis of the corresponding formulas, given in S9-4.

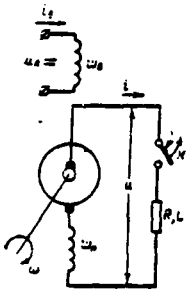

Fig. 9-8. On the calculation of pulsed operation of UG with the compound (independent variable and consecutive) excitation.

Page 243.

Let us register the initial conditions for the modes/conditions of load change, necessary during the solution of system of equations (9-27)-(9-29).

a). Rise/drop of the load

$$u(t)|_{t=0}=\omega M_{в.в}\frac{U_в}{R_{в.в}};\ i(t)|_{t=0}=0;\ i_в(t)|_{t=0}=\frac{U_в}{R_{в.в}}.$$

b). Load dropping

$$u(t)|_{t=0}=U;\ i(t)|_{t=0}=\frac{U}{R_н};\ i_в(t)|_{t=0}=\frac{U_в}{R_{в.в}}.$$

The system of equations of circuits UG we solve by operational method on the basis of the transform of Laplace [81]. Taking into account initial conditions after the series/row of conversions we find the functional dependence of circuital current of armature on the time with the rise/drop of the load

$$i(t)=\frac{dU_{\text{в}}}{a}\left[\frac{T_{\text{в}}p_1+1}{p_1(p_2-p_1)}(e^{p_1t}-e^{p_2t})-\frac{1}{p_1p_2}\right], \qquad (9\text{-}30)$$

where

$$a=\omega M_{\text{в.я}};\ T_{\text{в}}=\frac{L_{\text{в}}}{R_{\text{в.в}}};\ a=M_{\text{д.в}}M_{\text{в.д}}+(L_{\text{д}}-L_{\text{д}})L_{\text{в}};$$

$$p_{1,2}=\frac{-\beta\pm\sqrt{\beta^2+4av}}{2a};\ \beta=\omega M_{\text{д.в}}M_{\text{в.я}}+R_{\text{д.в}}(L_{\text{д}}-L_{\text{д}})+$$
$$+\omega L_{\text{в}}M_{\text{д.я}}-R'_{\text{я}}L_{\text{в}}-R_{\text{д}}L_{\text{в}};$$
$$v=\omega R_{\text{д.в}}M_{\text{д.я}}-R_{\text{д.в}}R'_{\text{я}}-R_{\text{д.в}}R_{\text{д}}.$$

Form of process (9-30) is determined by the values of roots of p_1 and p_2, that depend on the relationship/ratio of the parameters of real system UG.

With load dropping, disregarding processes in the arc, we will obtain instantaneous reduction in current of armature from value $U/R_{\text{в}}$ to zero (circuit break).

Thus, the form of current pulse will will be represent curve with the obtained functional build-up/growth of current (9-30) to the steady (by hypothesis) value with the subsequent steep/abrupt drop up to zero, after which the impulse/momentum/pulse is repeated. Between the impulses/momenta/pulses is possible certain pause, during which the current-carrying parts of UG cool off.

Page 244.

Chapter Ten.

EXPERIMENTAL STUDY OF ACYCLIC MACHINES WITH LIQUID-METAL CURRENT PICKUP.

10.1. Problems and the means of experimental research of acyclic machines with the liquid contacts.

During the development the mind with the liquid contacts of current-tap apparatus appears the need for the experimental check of the series/row of designing-theoretical positions, efficiency of contact nodes, study of magnetic system and characteristics of the prepared machines. These questions can be studied both in the experimental models of machines and on the special models.

Questions of experimental research of the mercury contacts of different types are examined in the works of B. I. Ugrimov [6], Yu. Yu. Kaunas [22], D. A. Vatt [47 and 48], P. Klaudi [49], B. G. Karasev and G. T. Semikov [129].

Research of characteristics mind with brush current pickup is carried out by I. P. Ivanov and B. V. Kostin [10], characteristics of UG with the mercury contacts - D. A. Vatt [14]. However, many questions are experimentally studied insufficiently.

In the process of the scientific research work on UM, conducted in the Moscow Aviation Institute named Sergo Ordzhonikidze, came to light some general principles of experimental research mind, the procedure of the tests of machines, approved in practice, was worked out.

Experimentally were studied: characteristics of UG with the circular liquid-metal contacts, magnetic leakage and armature reaction mind; hydrodynamics of contacts, the one-sided attraction of the rotors of cylindrical and disk UM. For the tests special accessory equipment, in particular water-cooled main-line tubular busbars and load rheostat, argon-mercury system of contacts was worked out.

Page 245.

Research was conducted on one of the experimental models of UG,

model of high-speed/high-velocity liquid-metal contact, static electromagnetic devices/equipment, which simulated scattering, armature reaction and the one-sided attraction of machines, and also on the electrolytic models of the distribution of magnetic induction and current density in the cylindrical rotor.

The short description of the subjects of experimental research is given below, the special features/peculiarities of the experimental proceedure with the mind are stated, are given the results of experiments, and also their discussion and comparison with the calculation [1].

FOOTNOTE [1]. The results of the comparison of the theoretical value of emf of UG without the ferromagnetic circuit with experimental data are indicated in chapter 9. ENDFOOTNOTE.

10.2. Subjects of experimental research.

a). Non-polar dynamo ~~May~~ MAI [2].

FOOTNOTE [2]. Generator was demonstrated on VDNKh [Exhibition of Achievements of the National Economy of the USSR in the pavilion "higher education in the USSR" in 1964. ENDFOOTNOTE.

The experimental model of UG with rated power of 10 kW is the cylindrical uncompensated machine of four-terminal performance with the half use on the voltage/stress with two slide contacts of liquid-metal (mercury) current-tap apparatus. Excitation of UG is independent. Magnetic circuit is made from magnetically soft steel (rotor - from st. 10, stator - made of armco steel). As the liquid current pickup floating slit ring terminal is selected, since it provides the symmetry of current distribution and does not require special pump.

Current tap into the external target is produced by two series/rows of the radially arranged/located copper plugs, forced against positive and negative stationary circular electrodes with the help of the pin connections.

Page 246.

Contact liquid from the special reservoirs is supplied into the interelectrode space under the effect of pressure of argon through branch, the located in the lower part of housing of UG. For the creation in the internal cavity of the machine of the atmosphere of the inert gas through the openings/apertures in the panels argon is fed/conducted. In the upper part of the housing are control branches, which are communicated with the contacts. They serve for the gas supply with the purging of machine in the process of cleaning/ purification.

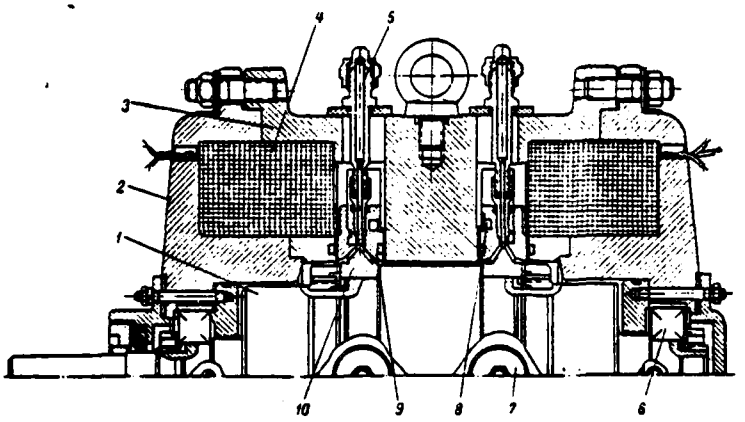

Fig. 10-1. The longitudinal section of experimental generator. 1 - rotor; 2 - panel of stator; 3 - stator; 4 - field coil (n=950); 5 - control branch; 6 - ball bearing; 7 - current-deflecting plug; 8 - channel of water cooling; 10 - rotating electrode.

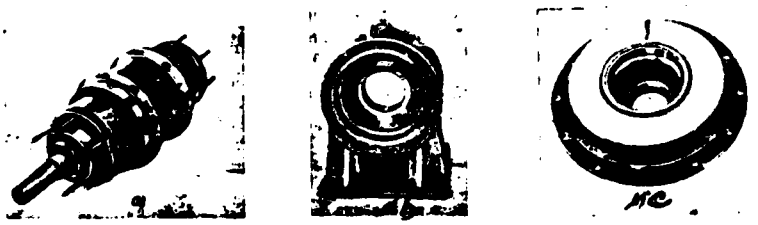

Fig. 10-2. Structural/design device/equipment of generator MAI; a) rotor; b) stator; c) panel with the field coil.

Page 247.

The elements of the construction/design of experimental model of UG are clarified by the drawing of its longitudinal section (Fig. 10-1), appearance of UG is shown in Fig. 1-12. Flat solid rotor with the

copper nickle-plated slip rings, stator of generator and panel with the field coil are shown in Fig. 10-2a, b, c. Connection of UG with the load was realized by a set of the copper lamellar busbars, which exit from each plug of current tap, and by the main-line copper tubular busbars, water-cooled. Fig. 10-3 shows the connections of the packets of lamellar busbars with UG and tubular busbars. In the foreground Fig. 10-3 the reservoirs for the contact liquid with the control gashes for the reading of the necessary level of mercury are shown.

The contacts of current-tap apparatus UG have water cooling with the help of the annular channels on the stationary electrodes. Supply and derivation are performed through branch in the lower machine part.

The need for cooling channels for the removal/outlet of losses is caused by the fact that the maximum relative rate of the electrodes of contact reaches 56.5 m/s, also, during the mercury current pickup of loss to friction, rates proportional to cube, they are great (up to now similar contacts they were applied for rates on the order of 30 m/s).

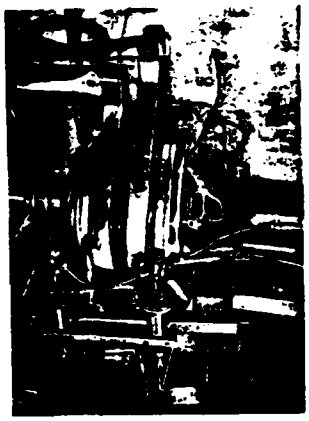

Fig. 10-3. Connection of UG with the discharge busbars.

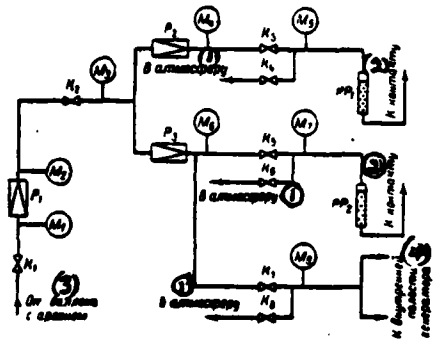

Fig. 10-4. Schematic of argon-mercury system. K_1 - tap/crane of tank/balloon; K_2, K_3, K_5, K_7 - main-line taps/cranes; K_4, K_6, K_8 - taps/cranes of letting out; M_1, M_2 - manometers of tank/balloon; M_3-M_8 - main-line manometers; P_1 - reducer of tank/balloon; P_2, P_3 - main-line reducers PP_1, PP_2 - mercury reservoirs.

Page 248.

The schematic of the argon-mercury system UG, which ensures

supply and issue of contact liquid and the creation of the atmosphere of inert gas, is shown in Fig. 10-4.

As the load device/equipment of UG the planned and prepared in the MAI tubular rheostat (Fig. 10-5a) was used. Tubes made of the stainless steel, which has the increased specific resistor/resistance, cooled by water. The assigned combination of the series-parallel connections of the tubes of rheostat for the creation of the necessary load of UG was realized with the help of the set of the aluminum and copper busbars of special construction/design.

For interrupting power circuit of UG the disconnector of the type P-5 with handwheel drive (Fig. 10-5b) was used.

The general view of experimental installation UG is represented in Fig. 10-6. In the foreground instrument table is visible, in the background (after the Plexiglas window of box) is arranged/located UG together with the drive motor and by discharge busbars.

In the box the suction and exhaust ventilation in accordance with the requirements of safety engineering was equipped.

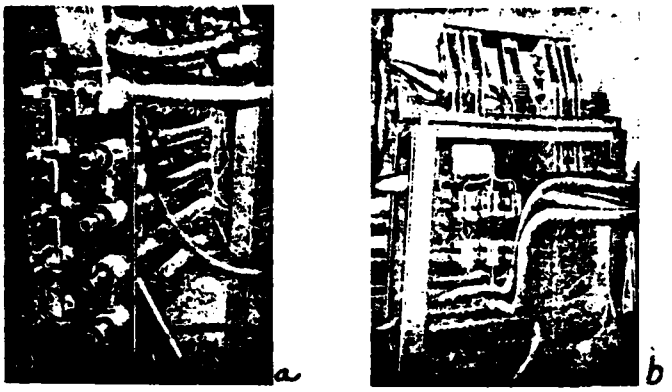

Fig. 10-5. Load device/equipment of non-polar dynamo of the MAI. a) tubular rheostat with the water cooling; b) disconnector with the steering-wheel drive.



Fig. 10-6. The general view of experimental installation.

Page 249.

1в). Model of high-speed/high-velocity liquid-metal contact.

For the preliminary final adjustment of the argon-mercury system of UG and the research of hydrodynamics of liquid contact was used the special disk model, whose longitudinal section was represented in Fig. 10-7. The contact device of model does not have fundamental design differences from the contacts of UG.

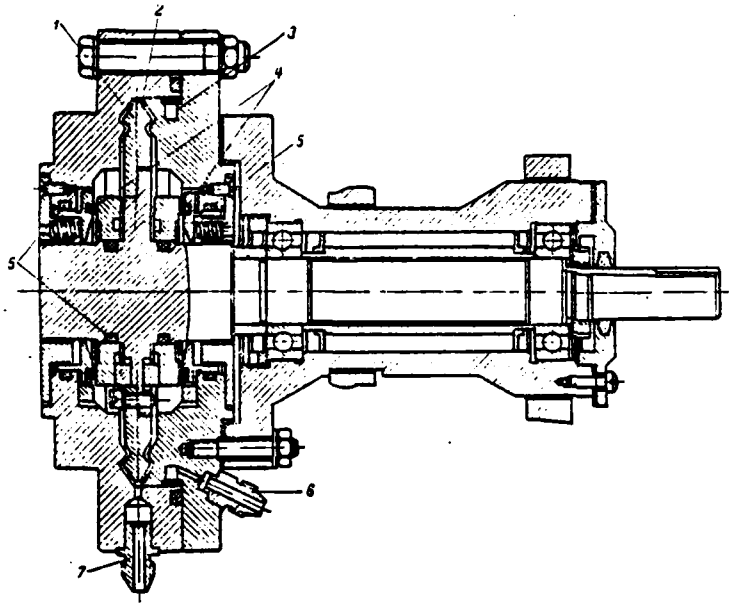

Fig. 10-7. Construction/design of the model of circular liquid-metal contact. 1 - disk rotor; 2 - liquid metal; 3 - water cooling channel; 4 - graphite multiplexing; 5 - rubber packing ring; 6 - branch for the water supply; 7 - branch for the supply of metal.

Page 250.

The maximum relative rate in the circular mercury contact of model is 90 m/s. For the removal/outlet of the losses of friction is used water channel, which has input and output branch. The fundamental parts of model are made from the stainless steel of the brand 1X18H9T. In the model there are a lower branch for supply and output of liquid metal, upper branch for the control/checking and the

blowing through, lateral of branch for the supply of argon into the internal cavity of model. Together with the motionless rubber O-ring seals in the model high-speed/high-velocity graphite multiplexing is used. The appearance of the model of contact is shown in Fig. 10-8.

The schematic of the argon-mercury system of model is similar to the diagram, represented in Fig. 10-4, moreover only the one branch of diagram is used and respectively one mercury reservoir.

e f). Model for the study of armature reaction.

The special static model of two-pole cylindrical UM in the dismantled/selected form is represented in Fig. 10-9a. Current to faces of the "rotor" of model was fed/conducted from the independent source with the help of the copper busbars, which are screwed into the "rotor". The latter did not revolve during the supplying of coil current of excitation, since turning moments under unlike poles of model average out. Magnetic flux in the model with the "idling" and in the presence of current in the "rotor" was measured with the help of the special coil, and also by means of the sensor of Hall's emf. On the model were investigated physics of the phenomenon of armature reaction, were checked the methods of the quantitative account of its demagnetizing effect, the rationality of the use/application of nonmagnetic radial separators (sections/cuts) for preventing the

saturation by the field of armature current (Fig. 10-9b). Model is designed for the work with the maximum current of "rotor" 500 A. The general view of experimental installation is given in Fig. 10-9c.

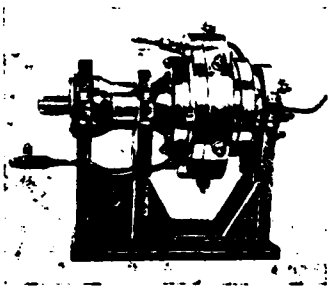

Fig. 10-8. The general view of the experimental model of contact.

Page 251.

д). Devices/equipment for measuring the forces of unbalanced magnetic pull.

For checking the derived calculation formulas of the electromagnetic forces of one-sided attraction was applied the model of the magnetic system of four-terminal cylindrical UM. The schematic of measuring unit is given in Fig. 10-10a. The results of experiment are given in S6-5 (Fig. 6-7g).

Was undertaken an attempt at the study of the electromagnetic forces of the one-sided attraction of disk UM with the ferromagnetic rotor.

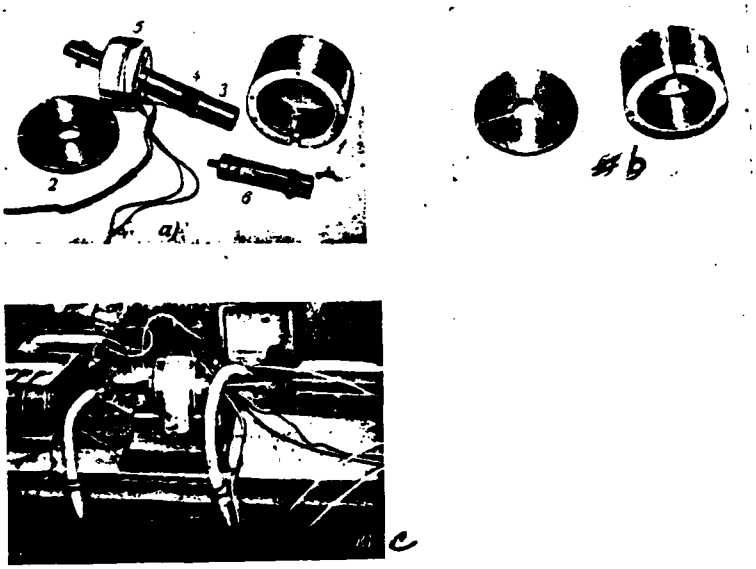

Fig. 10-9. Model for the study of armature reaction. a) model in dismantled form: 1 - stator; 2 - cover/cap of stator; 3 - "rotor"; 4 - search coil on the "rotor"; 5 - excitation winding; 6 - current-conducting busbar; b) stator and cover/cap with the radial gashes; c) the general view of experimental installation.

Page 252.

Experimentally was checked effect relative to the axial shift of the "rotor" of the model of magnetic system (Fig. 10-10b) and value of a drop in the magnetic potential in the gaps on the value of electromagnetic effort/force.

е). Electrolytic baths, which simulate the distribution of magnetic induction and current density in the cylindrical rotor.

Models are the Plexiglas cylinders with the covers/caps, filled with electrolyte - by the dilute solution in the water of copper sulfate. To the inner cylinder face copper circular electrodes are fastened/strengthened, to which the voltage/stress from the source of alternating current is fed/conducted. In the cylinders there are openings/apertures for the insertion of feeler gage, which measures a change of the potential of the internal points of cylinder in the function of their axial and radial coordinates.

Model for studying the distribution of magnetic induction (Fig. 10-11a) is geometrically similar to the part of the rotor, which corresponds to one pair of polar extensions. The width of circular electrodes is proportional to the axial length l of pole. Electrodes border on faces of cylinder.

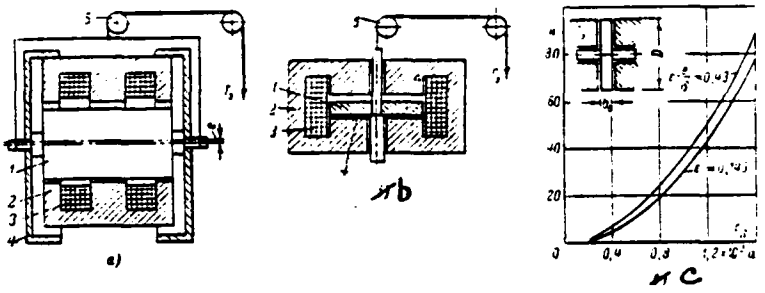

Fig. 10-10. Installation diagrams for measuring the forces of one-sided attraction of UM. a) cylindrical; b) disk; 1 - rotor; 2 - stator; 3 - excitation winding; 4 - device/equipment for the installation of eccentricity or axial shift; 5 - unit of the counterbalancing device; c) experimental dependences $f_1=f(F_1)$ for the disk UM, $S\delta=\pi D^2/4=80$ cm^2; $b_1/D=0.11$.

Page 253.

Model for the research of density distribution of current (Fig. 10-11b) is geometrically similar to the rotor of four-terminal machine with the half use according to the voltage/stress (with two slit ring terminals).

Measuring circuit is given in Fig. 10-11.

10.3. Special features/peculiarities of the methodology of experiments.

With the high currents, characteristic to UG with the liquid-metal contacts, load devices/equipment (experimental rheostats) usually allow/assume only discrete/digital changes in the resistor/resistance during switching of their sections.

Smooth control is hindered/hampered by the effect of the instability of contact resistance in the connections. In this case virtually it cannot be supported $I_г$=const during the removal/taking of full-load saturation curves of UG and vary smoothly $I_г$ during the removal/taking of external and self-regulation. For obtaining the "working" characteristics should be used the artificial reception/procedure: to remove/take sets of "load" characteristics $U=f(I_в)$ on $R_г$=const and $I_г=f(I_в)$ from $R_г$=const and by geometric construction (Fig. 10-12) found the characteristics of the generator: load $U=f(I_в)$, $I_г$=const external $U=f(I_г)$, $I_в$=const and regulating $I_в=f(I_г)$, U=const. This method was used with testing of sample/specimen UG.

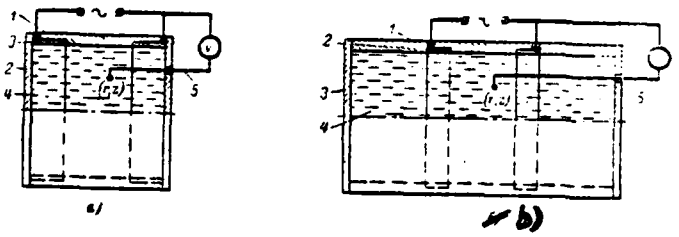

Fig. 10-11. The schematics of the models of electrolytic baths for the research of distribution; a) magnetic induction; b) current density; 1 - Plexiglas cylinder; 2 - cover/cap; 3 - copper electrode; 4 - electrolyte; 5 - point feeler gage.

Page 254.

Research of power losses of UG should be followed method of their distribution during the rotation of generator the engine, which has considerably smaller than UG, power. Are determined mechanical losses in the bearings of UG, then loss in the contacts during the successive supply in them of liquid metal, supplementary no-load losses after the excitation (independent variable) of machine. The corresponding losses compose a difference in the powers required by engine in two subsequent experiments (taking into account losses in the engine itself). A contact voltage drop and losses in the circuit of armature with the load are determined with the feed unexcited UG from the independent source. Since UG with the slit ring terminals allows/assumes the filling with contact liquid only in motion, to

measure a voltage drop is possible only with the revolving rotor. To avoid errors from emf, caused by residual/remanent magnetic flux, the magnetic circuit of machine must be thoroughly demagnetized.

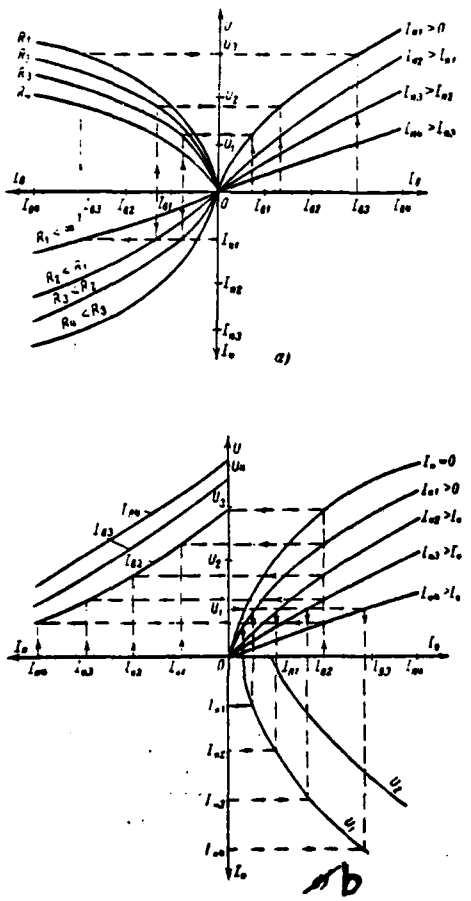

Fig. 10-12. Construction of the characteristics of generator. a) load; b) external and regulating.

Page 255.

The temperature of contact UG was measured with the help of the placed thermocouples, the temperature of excitation winding - according to the impedance method, ambient temperature was monitored

by mercury thermometer.

The magnetic leakage fluxes of excitation winding in UG and on the model were measured by fluxmeter with the help of the search coils, arranged/located in the lower and upper layers of excitation winding.

Leakage flux was determined on a difference in the readings on the fluxmeter, joined alternately to the search coils. Before the reading the magnetic circuit was demagnetized with variable field, reading was produced after the commutation of coil current of excitation. Leakage flux between faces of rotor and stator was determined on the model Fig. 10-9 during the removal/distance from the plane of the foundation of the search coil, arranged/located coaxially with the rotor.

The phenomenon of armature reaction on the model was investigated by different methods. Longitudinal magnetic flux was measured by fluxmeter with the help of the search coil on the "rotor" with the commutation of field current and different strengths of current, which passes according to the "rotor". Were taken/removed the following characteristics of model: magnetic $\Phi_в=f(I_в)$, $I_я=0$; external $\Phi_в=f(I_я)$, $I_в=$const; load $\Phi_в=f(I_в)$, $I_я=$ const and regulating $I_в=f(I_я)$, $\Phi_в=$const. During the tests before each reading the magneti-

circuit was demagnetized with variable field to avoid the effect of residual magnetization on the saturation.

Characteristics were plotted also with the help of the film gauge of Hall's emf from mercury selenide. Gap density was measured by sensor. Diagram with the compensation for the nonequipotentiality of Hall electrodes (Fig. 10-13) was used. Furthermore, the longitudinal flow of static model was oscillogramed with the connection/attachment of radiator/resonator/element to the search coil and the commutation of current $I_в$ at different values $I_в$ (initial values of field current were identical).

The effect of armature field of UG was evaluated in the usual way according to a change in the voltage/stress of machine with the load.

Transient processes of UG were studied via the oscillography of voltages/stresses and circuital currents of excitation and armature with an abrupt change in the modes/conditions of these circuits.

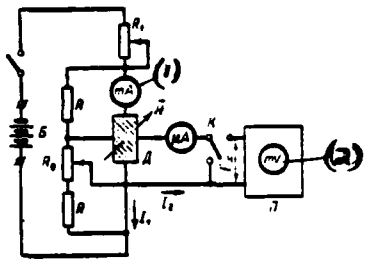

Fig. 10-13. Circuit diagram of the tape/film (HgSe) sensor D emf Hall E_x for measuring the magnetic field H with the compensation for the nonequipotentiality of Hall electrodes (R=12 kiloohm; R_0=0-2 kiloohm, it is tuned with H=0 to current I_2=0 in the lower position of switch K); R_1 limits current I_1; Б - dc power supply; П - potentiometer for measurement $\overline{E_x}$ (in the upper position of switch K).

Page 256.

With the commutation in the circuit of excitation winding the latter was fed from the storage battery, which has negligible internal resistor/resistance in order to avoid its effect on the parameters of the system being investigated.

The fact was the special feature/peculiarity of model tests of contact that the work of this contact at the relative rate of more than 80 m/s (at the rotational speed to 9000 r/min) for the first time was investigated. Mercury and water served as working fluids.

The latter, as noted in §5-3, simulated sodium and alloy NaK (on the technical reasons). On the water the starting and the stop of the model were mastered: liquid into contact gap was supplied during the rotation of rotor and was issued before its retardation; it was produced checking the correctness of the designed space of liquid in the contact (with the help of the control upper branches). However, similar operations were produced with UG.

During model tests of contact the dependences of the losses of friction on the rate for the water and mercury were removed/taken; was measured the pressure of argon, under action of which the liquid entered contact; was checked the efficiency of cooling channel.

In the model for measuring the force of the one-sided attraction of cylindrical UM the value of relative eccentricity was established/installed with the help of the attached to faces of rotor rings, the bore of rim of which along the line came into contact with the external surface of the stator of model. A change in the eccentricity was achieved by the variation of the bore diameter of rings. In the model of disk UM with the ferromagnetic rotor the assigned magnitude of relative axial pull-over was established/installed by means of the calibrated nonmagnetic separators, screwed on to face of the pole of stator.

During the supplying of coil current of the excitation of models appeared the one-sided attraction of the "rotor", whose force was counterbalanced by laboratory set of weights.

The models of the electrolytic analogs of rotor were used only for the qualitative checking (without taking into account the scales of simulation) of the derived calculation formulas of the distribution of induction and current density in the rotor. According to the results of value measurement of potentials U=f(r, z) the derivatives

$\left.\frac{\partial U}{\partial r}\right|_{z=\text{const}}$ and $\left.\frac{\partial U}{\partial z}\right|_{r=\text{const}}$ were considered. The latter made it possible to judge the distribution of values B_r, B_z, j_r, j_z proportional to them (in accordance with the problems, examined in Chapter 2).

Page 257.

During the simulation it was assumed that electrical conductivity of electrolyte was constant and does not depend on the coordinates of the points of internal cylinder capacity and on the voltage/stress applied to the electrodes. This corresponds to the assumptions adopted relative to rotor about the constancy of magnetic permeability and electrical conductivity.

10.4. Fundamental results of experiment and their discussion.

1. Oscillograms (Fig. 10-14a) demonstrate flux exclusion $\Phi_в$ of model for the study of armature reaction with increase of current in the "rotor" and constant quantity of magnetizing force of excitation $F_в$. Fig. 10-14b shows external characteristics of model in the relative units, obtained by the methods of fluxmeter and sensor of Hall's emf. Absolute values $\Phi_в$ in the measurements the Hall pickup were less than measured by fluxmeter for 10-15%. This is explained by the nonuniform distribution of induction through the area of the sensor, whose width is commensurated with the axial length of pole. The decrease of slope/transconductance $\Delta\dot{\Phi}_в/\Delta\dot{I}_я$ of the characteristic of model with the radial section in the stator is caused by a decrease in the saturation of magnetic circuit by cross field. Calculations showed that drops in the magnetic potential for the longitudinal flow in the stator to the section/cut are virtually identical with idling ($I_я$=0) and with the load ($I_я$=500 A). Primary meaning has a saturation of rotor by the field of armature reaction as in UG.

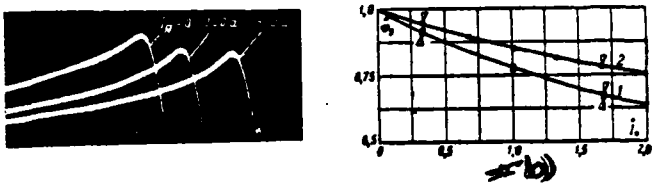

Fig. 10-14. Results of experiments. a) the oscillogram of magnetic flux Φ_δ in the model for the study of armature reaction when I_a = var; b) external characteristics of models $U_a = f(I_a)$ in the relative units with I_a = const U_a=1 with I_a=300 a); 1 - model without the section/cut (∇ - method of fluxmeter; Δ - method of the sensor of Hall's emf); 2 - model with the radial section in the stator.

Page 258.

2. The calculated and experimental dependences of losses to friction in the model of liquid-metal contact on the linear velocity in the slit ring terminal are represented in Fig. 10-15. From the curves the resemblance of the properties of water and alkali metals is evident. More heavy metals (mercury, gallium) cause the considerable increase of mechanical losses. Function $P_{к.т}=f(v_к)$ is close to cubic parabola. Curves show that for the purpose of increase of efficiency of UG with speed contacts to rationally apply alloy NaK of eutectic composition as the working fluid.

Temperature excess of the external surface of the model of

contact on the side, where the water cooling channel is passed, was about 40°C with the work with mercury for $v_к$=80 m/s. From opposite side of slit ring terminal temperature excess was more than 70°C. This fact came to light/detected/exposed the advisability of applying the cooling liquid channels along both sides of similar high-speed/high-velocity contacts.

3. The tests of UG were conducted in the range of the speeds of rotation n=50-150 r/s (3000-9000 r/min). Experimental and design characteristics of machine are represented in Fig. 10-16. Since the measured voltage drop in the mercury current pickup and the rotor composed value on the order of 10^2 V, decrease in the voltages/stresses of UG with an increase in the load is caused in essence by the effect of transverse armature reaction. Value of magnetizing force F_{qd} is commensurated with value of magnetizing force of excitation with the idling and is caused to a considerable degree by the saturation of rotor with the load.

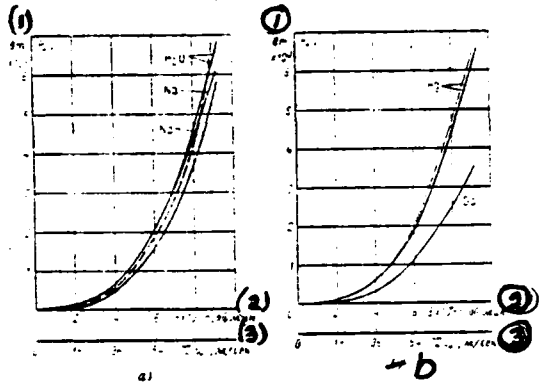

Fig. 10-15. Dependence of the losses of friction on the speed in the model of contact. a) for the alkali metals; b) for mercury and gallium; calculation - solid lines; experiment - dotted lines.

Key: (1). W. (2). r/min. (3). m/s.

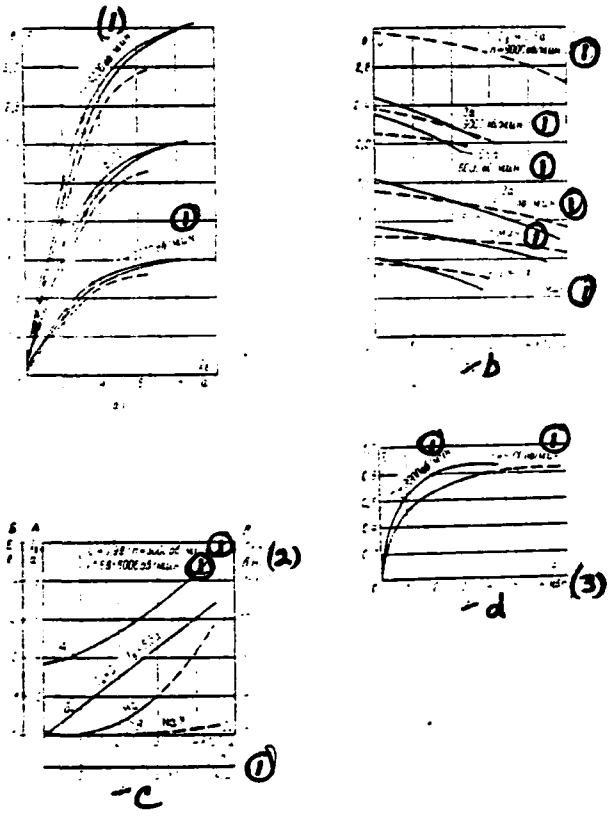

Fig. 10-16. Experimental and design characteristics of UG. a) idling $E=f(I_0)$ on n; b) external $U=f(I_0)$ on n; c) regulating high-speed/high-velocity E=f(n) and the dependence of losses to friction on speed f(n) for mercury and eutectics NaK; d) the dependence efficiency on the power η=f(P); calculation - dotted lines; experiment - solid lines.

Key: (1). r/min. (2). kW.

Page 260.

During the tests of UG is discovered the phenomenon of the pumping over of contact liquid of one reservoir of system in another through air gap under the effect of the pumping action of the revolving rotor, which is caused by the nonidentity technological fulfilling of contacts. For mercury "pumping effect" was observed with $n \geqslant 7000$ r/min ($v_к \geqslant 44$ m/s). Argon overpressure in the reservoirs with the contact liquid was not equal. In particular, for mercury with n=3000 r/min it was 0.4 atm(tech) for one contact and 0.15 atm(tech) for another. With n=9000 r/min the pressure grows to 0.8-1.2 atm(tech).

The entry/incidence of contact liquid was a deficiency/lack in the argon-mercury system into the internal cavity of UG with hitch (emergency, with the break of feed) of drive motor. Without being counterbalanced by centrifugal force, mercury under the action of argon pressure flowed/occurred/lasted inside the generator and partially it settled on the machine parts. With relief its basic part was returned to the contact system on the chutes in the lower part of the bore of stator.

In the subsequent rational designs it is necessary to provide the release of contacts and the automatic protection, which

removes/takes pressure with the stop of machine. Possibly also the use/application of systems UG with the complete insertion/immersion of rotor into the liquid metal. These systems do not have the deficiencies/lacks indicated; however, it is more complicated by the construction/design, mainly due to the problem of multiplexing.

At the speed of rotation n=7000 r/min UG gave power of approximately 10 kW with U=2.1 into, $I_н$ =4700 A. The maximum current, obtained prolongedly in the process of tests from UG, was 5400 A.

The structure of power losses of UG is the following.

Losses to friction in each of the mercury contacts of current pickup with n=3000 r/min according to the measurement data are 60 W (which coincides with the calculation). With n=9000 r/min these losses are 1120 W.



Fig. 10-17. Oscillograms of transient processes of UG with n=50 r/s (3000 r/min). a) for =f(t) with the idling UG; b) =f(t) when =const; c) g for =f(t) with rise/drop and load dropping =2300 a; =8 a.

Page 261.

Electrical losses in the rotor and contact resistance of contacts when $I_н$=4000 A are approximately 50 W, losses in the thoroughly heated field coils with rated current $I_{в.н}$=6.5 A are equal to 170 W. Mechanical losses in the bearings with n=3000 r/min are 150 W. Incremental losses in the first approximation, can be disregarded/neglected. With rated current $I_н$=4000 A also voltage/stress U=0.835 V for n=3000 r/min efficiency of generator it composed 87% (at the power P=3.33 kW). Let us note that the efficiency of the collector direct-current generators of low voltage on current $I_н$=5000 a even with P=60 kW composes 69% (according to GOST 1651-54).

After 4.5 h of work in the mode/conditions P=3.6 kW; U=0.9 v ; $I_н$ = 4000 A; $I_в$=9 A; n=3000 r/min temperature excess of the

water-cooled contacts was approximately 40°C, temperature excess of excitation winding reached 70°C. This testifies about the possibility to allow during the nominal rating high current density in the excitation winding, than accepted in the sample/specimen UG.

4. Fig. 10-17 depicts the oscillograms of transient processes in UG. In the upper part of the oscillograms the scale of the time marker, whose period is 0.1 s, is indicated. Processes in energizing circuit are finished approximately/exemplarily during 1.8 s. Slanting sections curved $i_в = f(t)$ (in contrast to the exponential curve) are caused by the attenuating action of eddy currents in the massive parts of the magnetic circuit. Processes in the circuit of armature with the rise/drop and load dropping are finished approximately/exemplarily after 0.1-0.12 s and have the rapidly attenuating aperiodic character. The serration of curves $i_я=f(t)$ is explained by the frequency properties of radiator/resonator/element, which is confirmed by the serration of zero flow line. Fig. 10.17c, g does not show the zero line of the voltage/stress of armature. The given oscillograms demonstrate also a decrease in conservative values of voltage/stress under the effect of the armature reaction (in comparison with the floating voltage).

As a result of the inspection of that dismantled/selected after the termination of the tests of UG is discovered (for 130 h of work) the decomposition of nickel coating in some places of the circular electrode of rotor and the formation/education of fine/small sinks. Electrodes were covered with the black coating of mercury oxides. This testifies about the need for the periodic cleaning/purification of contacts (approximately/exemplarily for every 100 h of work) even in the presence of argon medium. Protective coatings from the rhodium are more reliable; however, their operating checking is necessary.

5. Fig. 10-10c gives the results of measuring the force of the one-sided attraction of the magnetic "rotor" of the model of disk UM. It is experimentally established/installed, that the value of relative axial shift little affects the amount of force. The latter depending on the value of a drop in the magnetic potential in the gaps is changed approximately/exemplarily according to the quadratic law. For obtaining the calculated dependences is necessary a strict study of magnetic fields of scattering of disk UM. (See also Fig. 6-7d).

6. The tests of the electrolytic models of rotor showed that in the zone between the electrodes the potential is changed along the axis according to the linear law and virtually does not depend on the radial coordinate:

$$U(z)|_{r=\text{const}} \approx U_0 + kz;\ U(r)|_{z=\text{const}} \approx \text{const},$$

where U_0 - electrode potential. Differentiating expression U(z) and U(r), we see that

$$\frac{\partial U}{\partial z} \approx k = \text{const};\ \frac{\partial U}{\partial r} \approx 0.$$

Consequently, in the zone between the poles the magnetic induction of rotor $B_p \approx B_z = \text{const}$; $B_r = 0$, and current density in the zone between contacts $j_p \approx j_z = \text{const}$; $j_r = 0$.

In the extreme zones, which adjoin faces of model (Fig. 10-11b), it is discovered, that the derivatives $\partial U/\partial z$ and $\partial U/\partial r$ have very low values, i.e., the branching of current into these zones of rotor UM is small.

10.5. Comparison of fundamental calculated and experimental data.

Basic dimensions, parameters and characteristics of UG and special models were calculated from the methods, presented in the previous chapters of this book. For the purpose of checking the methods of quantitative account of magnetizing force F_{qd} the generator was specially carried out uncompensated. Design characteristics of UG were obtained by the following path.

On the experimental taken/removed in the toroidal samples/specimens curves of the magnetization of the materials of magnetic circuit the family of curves of simultaneous magnetization and dependence $\mu_a = f(H)$ were constructed. With the help of these data was calculated the reactive/jet triangle UG for different currents of load (by methods, examined in §4-3), which was used during the construction of the family of full-load saturation curves $U = f(I_в)$ on $I_в$. on this family other characteristics UG were constructed. Performance calculation of idling is carried out taking into account the recommendations, given in Chapter 3. As can be seen from those given in Fig. 10-16 curved difference in the calculated and experimental data do not exceed 10%.

However, a similar comparison is carried out for the model of cylindrical machine. A difference in the data composed 6-8%.

The calculated and experimental data of hydrodynamic losses in the liquid contact (Fig. 10-15) are distinguished not more than to 8%.

The comparison of data of calculation and measurement of the leakage fluxes of field coil and between the surfaces of magnetic circuit, carried out for the model and the sample/specimen UG, difference to 20% showed.

Table 10-1.
Summary of the parameters of UG with the mercury contacts.

Параметр (2)	Скорость вращения, *n об/мин* (1)		
	3 000	6 000	9 000
1. Мощность *P*, *квт*	3,33	6,66	10
2. Напряжение *U*, *в*	0,835	1,67	2,5
3. Ток якоря $I_я$, *а*	4 000	4 000	4 000
4. Ток возбуждения $I_в$, *а*	6,5	6,5	6,5
5. Скорость в контактах $v_к$, *м/сек*	18,8	37,6	56,5
6. Потери в контактах $P_{кт}$, *вт*	118	820	2 240
7. Мощность возбуждения $P_в$, *вт*	170	170	170
8. [redacted] η, %	87	83,5	78
9. Размеры статора, *мм*	$D_я = 246$;	$D_я = 220$;	$L_я = 250$ ($\delta = 0,6$)
10. Размеры ротора, *мм*	$D = 106$;	$D_р = 86$;	$l = 22$;
11. Магнитная индукция, *тл*	$B_р = 1,4$;	$B_\delta = 1,1$;	$B_с = 1,1$
12. Вес ротора, статора, катушек возбуждения и общий вес УГ, *кГ*	$G_р = 10$;	$G_с = 82$; $G = 107$	$G_в = 15$;

Over-all payload ratio of UG (with n=9000 r/min) composes G=G/P=10.7 kg/kW, the overall dimensions 355×320×385 mm.

Key: (1). Speed of rotation, n r/min. (2). Parameter. (3). Power P, kW. (4). Voltage/stress U, V. (5). Armature current A. (6). Field current A. (7). Speed in contacts m/s. (8). Losses in contacts W. (9). Power of excitation W. (10). Efficiencies η, %. (11). Sizes/dimensions of stator, mm. (12). Sizes/dimensions of rotor, mm. (13). Magnetic induction, T. (14). Weight of rotor, stator, field coils and total weight of UG, kgf.

This testifies about the insufficient accuracy of calculation formulas. However, since the leakage fluxes are relatively small, it is possible to use formulas for the engineering calculations of magnetic circuit.

The experimental check to electrolytic models qualitatively confirmed the obtained theoretical outputs about the approximate uniformity of magnetic flux distribution in the middle part of the rotor and the electric current in the zone between the slit ring terminals of armature UM.

Thus, checking designing-theoretical methods shows their practical suitability during the design of unipolar electric generators with the liquid-metal current pickup.

The fundamental parameters of the experimental models of UG of MAI are given in Table 10-1.

Page 265.

~~Application.~~ appendix.

CALCULATION OF ACYCLIC MACHINES.

P. 1. Example of the calculation of non-polar dynamo with the massive cylindrical armature.

A. Assignment

1. Initial data. The power of generator $P_г$=120 kW; voltage/stress U=6 c; the speed of rotation n=100 r/s (6000 r/min); the mode of operation - prolonged; cooling generator is natural air; current pickup circular liquid-metal on the base of eutectic NaK, cooling current pickup forced liquid.

2. Structural/design and electrical oscillator circuit. Let us select the compensated machine with the complete utilization of active length of armature and the total voltage (Fig. 1-16e), that

has pole face winding from the magnetic-conducting material and separate excitation. A number of poles 2p=2, a number of powered phases of armature, connected in series, $m_E=2$, a number of powered phases, connected in parallel, $m_I=2p/m_E=1$ (during 100%- use); a number of slide contacts $m_к=2p+2=4$ (with series connection of powered phases); a number of electrically isolated/insulated parts of rotor $m_p=p+1=2$ (rotor shaft we assume/set by that isolated/insulated, magnetic); a number of insulating radial separators in rotor $m_{пр}=p=1$; a number of induction coils, the designed for complete n. s. (magnetizing force) of excitation $m_в=p=1$ (sometimes coil it can be divided structurally/constructurally into two parts, as shown in Fig. 1-16e).

Coefficient, which considers the branching of current into parallel circuits of armature, $k_I=m_I I_в/I=1$; $I=I_в$ (during separate excitation).

Page 266.

B. Determination of main sizes/dimensions.

3. Current of the generator:

$$I=\frac{P_в\cdot 10^3}{U}=\frac{120\cdot 10^3}{6}=20\cdot 10^3\ a;$$

$$I_в=\frac{k_I}{m_I}I=20\,000\ a.$$

4. Electromotive force of the armature:

$$E=\frac{U}{\dot{U}}=\frac{6}{0,98}\approx 6,1 \text{ V},$$

where $\dot{U}\approx 0,98$ — tentative value of relative voltage/stress, a voltage drop in internal circuit of the armature (it is made more precise after the calculation of the resistor/resistance of armature and collector shoe gears), characterizes.

5. Calculated (electromagnetic) power:

$$P_э=m_1 E I_я\cdot 10^{-3}=6,1\cdot 20\,000\cdot 10^{-3}=122 \text{ kW}.$$

6. Coupling coefficient of emf with the electromagnetic power:

$$K_{uE}=\frac{E^2}{nP_э}=\frac{6,2^2}{100\cdot 122}=3,15\cdot 10^{-3} \text{ V}^2/(\text{kW}\cdot\text{rev/s}).$$

7. Current density in the rotor (armature). On the basis of expression (6-18)

$$j_p=\frac{m_E}{m_I}\frac{B_p}{K_{uE}}\frac{10^3}{k_{sp}}\frac{\left(\dot{D}_p^2-\dot{d}_в^2\right)_E}{\left(\dot{D}_p^2-\dot{d}_в^2\right)_I}=\frac{2\cdot 1,5\cdot 10^3\cdot 0,9}{3,15\cdot 10^{-3}\cdot 1,05\cdot 0,837}=10^6 \text{ a/m}^2,$$

where

$B_p=1,5$ T - selected value of magnetic induction in the rotor;

$k_{sp}\approx 1,05$ — approximate value of coefficient of scattering between the surfaces of the magnetic circuit (it is made more precise after

determining of the dimensions of magnetic circuit);

$\mathring{D}_p = D_p/D \approx 0{,}95$; $\mathring{d}_в = d_в/D \approx 0{,}25$ - tentative values of the design factors (they are made more precise in the process of design);

$(\mathring{D}_p^2 - \mathring{d}_в^2)_l \approx 0{,}95^2 - 0{,}25^2 = 0{,}837$ (for the isolated/insulated shaft);

$(\mathring{D}_p^2 - \mathring{d}_в^2)_E \approx 0{,}95^2 = 0{,}9$ (for the magnetic-conducting shaft).

Page 267.

8. Main sizes/dimensions of machine.

a). Air-gap diameter (armature diameter).

On the basis (6-14)

$$D = \sqrt[4]{\frac{P_в}{c'_п n}} = \sqrt[4]{\frac{124}{1{,}33 \cdot 10^3 \cdot 100}} = 0{,}175 \text{ м},$$

where the coefficient

$$c'_п = 6{,}15 \cdot 10^{-4} \frac{m_E m_l}{k_{эф}} (\mathring{D}_p^2 - \mathring{d}_в^2)_E (\mathring{D}_p^2 - \mathring{d}_в^2)_l B_p i_p =$$

$$= 6{,}15 \cdot 10^{-4} \frac{2 \cdot 0{,}9 \cdot 0{,}837}{1{,}05} 1{,}5 \cdot 10^6 = 1{,}33 \cdot 10^3 \quad \text{kW/m}^4 \cdot \text{rev/s}$$ characterizes the degree of utilization of a sensitive volume of machine.

b). The active length, which corresponds to one pole,

$$l = \lambda_п D = 0{,}233 \cdot 0{,}175 = 0{,}039 \text{ м},$$

moreover the design factor of the machine

$$\lambda_{\text{п}} = 0{,}25 \cdot \frac{(\tilde{D}_{\text{р}}^2 - \tilde{d}_{\text{в}}^{2})_E}{k_{\sigma p}} \cdot \frac{B_{\text{р}}}{B_{\delta}} = 0{,}25 \cdot \frac{0{,}9}{1{,}04} \cdot \frac{1{,}5}{1{,}45} = 0{,}233,$$

where $B_{\delta} = 1{,}45$ T - selected value of magnetic induction in the working gap.

C. Determination of the basic dimensions of magnetic circuit.

9. Air gap between rotor and surface of the bore of inductor. For construction-engineering reasons for the machine of average/mean power we accept:

$$\delta = 0{,}5(D_{\text{п}} - D) = 1{,}5 \cdot 10^{-3} \text{ м},$$

where the bore diameter of the pole

$$D_{\text{п}} = D + 2\delta = 0{,}175 + 2 \cdot 1{,}5 \cdot 10^{-3} = 0{,}178 \text{ м}.$$

Page 268.

10. Sizes/dimensions of the cross section of field coil. a). Area of the cross section of the coil

$$S_{\text{в}} = b_{\text{в}} h_{\text{в}} = \frac{F'_{\text{в.п}}}{k_{\text{з}} j'_{\text{в}}} = \frac{8\,300}{0{,}35 \cdot 3{,}65 \cdot 10^{6}} = 65 \cdot 10^{-4} \text{ м}^2,$$

moreover the approximate value n. s. (magnetizing force) of field coil with the nominal load of the machine

$$F'_{\text{в.н}} = (k_{\text{ст}} + k_{\text{р.п}})\ k_{\text{п}} F_{\delta} = (0{,}25 + 1{,}65)\, 1{,}25 \cdot 3\,500 = 8\,300 \text{ а}.$$

where $k_{ст}=0,25$; $k_{р.я}=1,65$ and $k_в=1,25$ — selected values of the coefficients, which consider respectively a drop in the magnetic potential in steel of magnetic circuit with the idling; the demagnetizing effect of transverse armature reaction (in the rotor) and a drop in the magnetic potential in the structural/design gaps of the magnetic circuit (they are made more precise during the verifying calculation after the determination of basic dimensions and construction of magnetic circuit);

$$F_\delta=\frac{2\delta B_\delta}{\mu_0}=\frac{2\cdot 1,5\cdot 10^{-3}\cdot 1,45}{4\cdot 3,14\cdot 10^{-7}}=3\,500\ a$$

- drop in the magnetic potential in two working gaps;

$j'_в=3,65\cdot 10^6$ $a/м^2$; $k_з=0,35$ - selected values of the current density and duty factor of window with copper of field coil.

b). Height/altitude of the section of field coil. In accordance with Sect. 6-3 we find the parameters of the nomogram:

$$\alpha=R+\frac{S_в}{3R}=0,0875+\frac{65\cdot 10^{-4}}{3\cdot 0,0875}=11,2\cdot 10^{-2}\ м;$$

$$\beta=\frac{2}{3}RS_в=\frac{2}{3}0,0875\cdot 65\cdot 10^{-4}=380\cdot 10^{-6}\ м^2,$$

where R=0.5D=0.5·0.175=0.0875 m - radius of armature.

Through the nomogram (Fig. 6-5) we find the optimum height:

$$h_в=h_{в.о}\approx 5\cdot 10^{-2}\ м.$$

c). Width of field coil:

$$b_в=b_{в.о}=\frac{S_в}{h_{в.о}}=\frac{65\cdot 10^{-4}}{5\cdot 10^{-2}}=13\cdot 10^{-2}\ м,$$

moreover the relationship/ratio of the sides of the section

$$\frac{b_п}{h_п}=\frac{13\cdot10^{-3}}{5\cdot10^{-3}}=2{,}6.$$

For technical-design reasons it is expedient to place analogously the coil between the current pickups within the stator with the design concept of one pair of polar extensions, shown in Fig. 1-16h (without the distribution of coil into two parts).

Page 269.

In this case the construction/design of the current-deflecting devices/equipment is simplified and electrical losses in the armature in comparison with the schematic of the machine, given in Fig. 1-16e, are reduced.

11. Basic dimensions of magnetic circuit.

a). The diameter of the turning of the stator:

$$D_в=D+2(h_в+\Delta h_в+\delta)=0{,}175+2(0{,}05+0{,}01+1{,}5\cdot10^{-3})=0{,}298\ м,$$

where $\Delta h_в\approx0{,}01$ m - radial distance from the surface of armature to the internal surface of field coil.

b). The calculated outside diameter of stator (inductor)

$$D_н=k_0D\sqrt{\dot{D}_в^2+4\lambda_н k_{ос}\left(1+\frac{\delta}{D}\right)\frac{B_з}{B_c}}=$$

$$=1{,}04\cdot0{,}175\sqrt{1{,}7^2+4\cdot0{,}223\cdot1{,}1\left(1+\frac{1{,}5\cdot10^{-3}}{0{,}175}\right)\frac{1{,}45}{1{,}45}}=0{,}36\ м,$$

where $\mathring{D}_в = D_в/D = 0{,}298/0{,}175 = 1{,}7$ — relative diameter of the turning of stator for positioning/arranging the excitation winding;

$k_в \approx 1.04$ - coefficient, which considers the presence in stator of the openings/apertures, which can lead to the inadmissible local increase in the induction;

$k_{вс} \approx 1{,}1$ — approximate value of the coefficient of scattering the inductor (it is made more precise after determining of the dimensions of magnetic circuit);

$B_c = 1{,}45$ T - selected value of magnetic core induction of stator.

c). Width of pole at diameter $D_в$ of the stator:

$$l_{п.в} = k_{вс} \frac{1 + \frac{\delta}{D}}{\mathring{D}_в} \cdot \frac{lB_в}{B_c} = 1{,}1 \frac{1 + 1{,}5 \cdot 10^{-3}/0{,}175}{1{,}7} \cdot \frac{0{,}039 \cdot 1{,}45}{1{,}45} = 0{,}0252 \text{ м}.$$

Pole they are selected with the chamfered external (end-type) surfaces for the purpose of the reduction of the weight of magnetic circuit.

d). The calculated axial length of the generator:

$$L_в = c_0 [2(l + 2b_к) + b_в] = 1{,}06 [2(0{,}039 + 2 \cdot 0{,}02) + 0{,}13] = 0{,}31 \text{ м},$$

moreover in accordance with Sect. 5-3 the width of the electrode of contact on the surface of the rotor

$$b_к \approx \frac{I_в}{\pi \mathring{D}_{р.в} D j_{р.в}} = \frac{20 \cdot 10^3}{3{,}14 \cdot 0{,}95 \cdot 0{,}175 \cdot 1{,}9 \cdot 10^6} = 0{,}02 \text{ м},$$

where $\mathring{D}_{p.к} \approx D_p = 0{,}95$ — approximate value of design factor;

$j_{p.к} = 1{,}9 \cdot 10^6$ A/m² - selected value of current density in the zone of the pressing of electrode;

$c_0 = 1.06$ - coefficient, which considers a structural/design increase in the axial length of machine.

Page 270.

D. Calculation of magnetic circuit.

12. Coefficients of scattering for stator-rotor unit.

a). Relative permeance of scattering.

On the basis of expression for Λ_δ and formula (3-9)

$$\mathring{\Lambda}_1 = \frac{\Lambda_1}{\Lambda_\delta} = \frac{\mathring{D}^2_{\delta.н} k_\varphi(\xi)\,\delta}{4\lambda_н b} = \frac{1{,}7^2 \cdot 0{,}26 \cdot 1{,}5 \cdot 10^{-3}}{4 \cdot 0{,}233 \cdot 0{,}18} = 6{,}7 \cdot 10^{-3},$$

where $b \approx c_0(b_з + 2b_к) = 1{,}06 \cdot (0{,}13 + 2 \cdot 0{,}02) = 0{,}18$ m - width of the turning of stator;

$\mathring{D}_{з.н} = D_{з.н}/D \approx \mathring{D}_з = 1{,}7$ — relative diameter of the external surface of field coil;

$$\xi = \frac{D_{з.з}}{D_{з.н}} \approx \frac{D_з + 2\Delta h_з}{D_з} = \frac{0{,}178 + 2 \cdot 0{,}01}{0{,}298} = 0{,}667;$$

$k_\varphi(\xi)=0{,}26$ (on the curve, given in Fig. 3-2d).

On the basis of expression (3-5)

$$\mathring{\Lambda}_2=\frac{\Lambda_2}{\Lambda_\delta}=\frac{\mathring{D}^2_{\text{в.ш}}(\xi^2-x^2)\delta}{4\lambda_\text{ш}b}=\frac{1{,}7^2(0{,}667^2-0{,}6^2)1{,}5\cdot10^{-3}}{4\cdot0{,}233\cdot0{,}18}=2{,}2\cdot10^{-3},$$

where $x=D_\text{ш}/D_{\text{в.ш}}=0{,}178/0{,}298=0{,}6.$

In accordance with the sizes/dimensions of the magnetic circuit

$$\frac{D_\text{в}-D_\text{ш}}{2\cos\theta}=\frac{0{,}36-0{,}178}{2\cdot0{,}974}=0{,}0935>\frac{D}{2}=\frac{0{,}175}{2}=0{,}0875,$$

where $\theta=\operatorname{arctg}\frac{l-l_{\text{в.з}}}{0{,}5(D_\text{в}-D_\text{ш})}=13^\circ$ or $\theta=0{,}227$ rad;

$$\operatorname{tg}\theta=0{,}23;\ \cos\theta=0{,}974.$$

Page 271.

On the basis of expression (3-11)

$$\Lambda_\delta\approx(D+\delta)\left[10^{-6}+\frac{\pi b_\text{э}}{\pi+\theta}\ln\left(1+\frac{D}{\delta}\right)\right]=$$

$$=(0{,}175+1{,}5\cdot10^{-3})\left[10^{-6}+\frac{4\cdot10^{-6}}{3{,}14+0{,}227}\ln\left(1+\frac{0{,}175}{1{,}5\cdot10^{-3}}\right)\right]=$$

$$=1{,}17\cdot10^{-6}\ \text{ом}\cdot\text{сек};\ (1)$$

$$\mathring{\Lambda}_\delta=\frac{\Lambda_\delta}{\Lambda_\delta}=\frac{\Lambda_\delta\delta}{4\cdot10^{-6}Dl}=\frac{1{,}17\cdot10^{-6}\cdot1{,}5\cdot10^{-3}}{4\cdot10^{-6}\cdot0{,}175\cdot0{,}039}=64\cdot10^{-3},$$

Key: (1). Ω·s.

where permeance of working gap under one pole

$$\Lambda_\delta\approx\frac{4\cdot10^{-6}Dl}{\delta}=\frac{4\cdot10^{-6}\cdot0{,}175\cdot0{,}039}{1{,}5\cdot10^{-3}}=18{,}2\cdot10^{-6}\quad\Omega\cdot\text{s}.$$

b). Coefficient of scattering for the inductor.

With the odd number of pole pairs

$$k_{\sigma c}=1+\sigma_c=1+2(\mathring{\Lambda}_1+\mathring{\Lambda}_2)+\mathring{\Lambda}_3=1+2(6{,}7+2{,}2)\cdot 10^{-3}+64\cdot 10^{-3}=1{,}074.$$

c). Coefficient of scattering for the rotor (with p=1):

$$k_{\sigma p}=1+\mathring{\Lambda}_s=1+0{,}064=1{,}064.$$

The designed values of coefficients of scattering are close to those preliminarily selected.

13. Drop in the magnetic potential in the rotor (with the idling). On the basis of expressions (3-25) and 3-27)

$$F_p=\zeta_p k_{\sigma p} H_p (L_\delta - l + 0{,}5D)\approx 0{,}9\cdot 1{,}06\cdot 1\,700\times$$
$$\times (0{,}31-0{,}039+0{,}5\cdot 0{,}175)=580\,a,$$

where $H_p=f(B_p)=1\,700$ `a - magnetic intensity in the rotor, are determined on the curve of magnetization of the material of the rotor (for the selected magnetically soft material of the type of Armco H_p it is found at $B_p=1{,}5$ T from with curve $H_q=0$, given in Fig. 4-4a);

$\zeta_p\approx 0{,}9$ — coefficient, which considers the nonuniformity of the distribution of magnetic induction in the rotor (for relatively long rotor ζ_p it is close to one).

Page 272.

14. Drop in the magnetic potential in the magnetic circuit of stator (with the idling).

а). Drop in the magnetic potential in the pole

$$F_п = H_{расч} l_{ср} = 1\,320 \cdot 0{,}076 = 100\ а,$$

where in accordance with the formula of parabolas with m=4 (Sect. 3-8)

$$H_{расч} = \frac{1}{12}(H_0 + 4H_1 + 2H_2 + 4H_3 + H_4) =$$

$$= \frac{10^3}{12}(15 + 4 \cdot 13 + 2 \cdot 12 + 4 \cdot 12{,}5 + 17{,}5) = 1\,320\ а/м.$$

During determination of H_0 ... H_4 from the curve of magnetization B=f(H) for selected magnetically soft steel (Fig. 4-4a, curve H_q=0) are taken into consideration the following relationships/ratios, which cause the corresponding inductions B_0 ... B_4:

$$r_0 = 0{,}5D_{\text{п}} = 0{,}5 \cdot 0{,}178 = 0{,}089 \text{ м};$$

$$r_m = 0{,}25\,(D_{\text{в}} + D_{\text{п}}) = 0{,}25\,(0{,}298 + 0{,}36) = 0{,}165 \text{ м};$$

$$r_i = r_0 + i\frac{r_m - r_0}{m};\ r_1 = 0{,}108 \text{ м};\ r_2 = 0{,}127;\ r_3 = 0{,}146 \text{ м};$$

$$l_i = l - (r_i - 0{,}5D_{\text{п}})\operatorname{tg}\theta;$$

$$l_1 = 0{,}0346 \text{ м};\ l_2 = 0{,}0303 \text{ м};\ l_3 = 0{,}0259 \text{ м};\ l_4 = l_m = 0{,}0215 \text{ м};$$

$$S_i = 2\pi r_i l_i;\ S_1 = 0{,}0234 \text{ м}^2;\ S_2 = 0{,}0242 \text{ м}^2;$$

$$S_3 = 0{,}0238 \text{ м}^2;\ S_4 = S_m = 0{,}0223 \text{ м}^2;$$

$$B_i = \frac{\Phi_\delta}{S_i} = \frac{\Phi_\delta k_{\text{ос}}}{S_i} = \frac{\pi D l B_\delta k_{\text{ос}}}{S_i} =$$

$$= \frac{3{,}14 \cdot 0{,}175 \cdot 0{,}039 \cdot 1{,}45 \cdot 1{,}074}{S_i} = \frac{3{,}33 \cdot 10^{-2}}{S_i};$$

$$B_0 \approx B_\delta = 1{,}45 \text{ тл (1)};\ B_1 = 1{,}42 \text{ тл (1)};\ B_2 = 1{,}38 \text{ тл (1)};$$

$$B_3 = 1{,}4 \text{ тл (1)};\ B_4 = 1{,}48 \text{ тл (1)}.$$

Key: (1). T.

Page 273.

Calculated length of unit magnetic flux in the pole:

$$l_{\text{ср}} = r_m - r_0 = 0{,}165 - 0{,}089 = 0{,}076 \text{ м}.$$

b). A drop in the magnetic potential in the core (framework) of the stator:

$$F_{\text{сс.}} = H_{\text{с}}(b + l_m) = 1\,500(0{,}18 + 0{,}0215) = 300 \text{ а},$$

where $H_{\text{с}}$ is determined on the curve of magnetization $H_q = 0$ (Fig. 4-4a) with $B_{\text{с}} = 1{,}45$ T.

During the selection for the magnetic circuit of other brands of magnetic materials should be used their curve magnetization B=f(H), known from the standards/normals or the literature.

c). Drop in the magnetic potential in the magnetic circuit of the stator:

$$F_c = 2F_z + F_{c.c} = 2 \cdot 100 + 300 = 500 \ a.$$

d). The refined value of the coefficient, which considers the incidence/drop in magnetic potential in the magnetic circuit with the idling

$$k_{c\tau} = \frac{F_p + F_c}{k_\delta F_\delta} = \frac{580 + 500}{1,25 \cdot 3500} = 0,243,$$

which is close to that preliminarily selected.

15. Magnetizing force of field coil with the idling:

$$F_в = k_\delta F_\delta + F_p + F_c = 1,25 \cdot 3500 + 580 + 500 = 5450 \ a.$$

The value of coefficient k_δ can be refined after the development of the construction/design of generator.

16. Calculation n. s. (magnetizing force) of excitation winding with the load. The approximate account of armature reaction is produced only in the active region/cores of rotor, since armature field in the appropriate zones of stator is compensated.

a). Drop in the magnetic potential in the inactive zone of the

rotor

$$F_{p1} \approx k_{ср} H_p (b_з + b_к) c_е = 1{,}064 \cdot 1\,700\,(0{,}13 + 0{,}02)\,1{,}06 = 290\ а.$$

b). Drop in the magnetic potential in the active region/core of rotor (between the planes, passing through the middles of current pickups)

$$F_{p2} \approx k_{ср} \zeta_p H_{р.з} (l + b_к) c_е =$$
$$= 1{,}064 \cdot 0{,}9 \cdot 25 \cdot 10^3\,(0{,}039 + 0{,}02)\,1{,}06 = 1\,500\ а.$$

Page 274.

The average value of the intensity/strength of field of exictation $H_{р.з}$ in the mode/conditions of nominal load is determined with $B_p = 1{,}5$ T on the curve of simultaneous magnetization, for which

$$H_q = H_{я.ср} = \frac{I_я}{\pi D_{ср}} \cdot \frac{D_{ср}^2 - d_в^2}{D^2 - d_в^2} = \frac{I_я}{2\pi D} \cdot \frac{1 + 3\mathring{d}_в}{(1 + \mathring{d}_в)^2} =$$

$$= \frac{20 \cdot 10^3}{2 \cdot 3{,}14 \cdot 0{,}175} \frac{1 + 3 \cdot 0{,}25}{(1 + 0{,}25)^2} \approx 20 \cdot 10^3\ а/м,$$

where $H_{я.ср}$ — intensity/strength of armature field in the rotor at diameter $D_{ср} = 0{,}5(D + d_в)$.

This curve is constructed according to the same rules, according to which are constructed graphs $B_d = f(H_d)$ on H_q, those represented in Fig. 4-4a.

Let us clarify construction. After assigning, for example, by value $H_d = 25 \cdot 10^3$ a/m, we compute

$$H = \sqrt{H_d^2 + H_q^2} = \sqrt{(25 \cdot 10^3)^2 + (20 \cdot 10^3)^2} = 32 \cdot 10^3\ а/м.$$

On the curve of magnetization of material $B_d=f(H_d)$ when $H_q=0$ we find induction of the resulting field B=1.92 T, appropriate $H=32\cdot10^3$ a/m.

We calculate the induction

$$B_d=B\frac{H_d}{H}=1{,}92\frac{25\cdot10^3}{32\cdot10^3}=1{,}5 \text{ T}.$$

Thus, with $B_d=B_p=1{,}5$ T and $H_q=H_{\text{д.ср}}$ we obtain $H_{\text{р.д}}=H_d=25\cdot10^3$ a/m. Analogously are computed other points of the curve of simultaneous magnetization.

c). Drop in the magnetic potential in the rotor:

$$F_{\text{р.д}}=F_{\text{р1}}+2F_{\text{р2}}=290+2\cdot1\,500=3\,290 \text{ а}.$$

d). Magnetizing force of field coil:

$$F_{\text{в.д}}=F_{\text{с}}+F_{\text{р.д}}+k_{\text{д}}F_{\delta}=500+3\,290+1{,}25\cdot3\,500=8\,160 \text{ а}.$$

e). The refined value of the coefficient, which considers armature reaction

$$k_{\text{р.д}}=\frac{F_{\text{в.д}}}{k_{\text{д}}F_{\delta}}-k_{\text{с.т}}=\frac{8\,160}{1{,}25\cdot3\,500}-0{,}243=1{,}63,$$

which is close to the preliminary value.

Page 275.

E. Calculation of pole face winding.

17. Outside diameter and the thickness of compensative cylinder ($D_{н.к}$ and $h_{к.о}$):

$$D_{н.к}=\sqrt{D_{в.к}^2+\frac{4I_н}{\pi j_{к.о}}}=\sqrt{0{,}178^2+\frac{4\cdot 20\cdot 10^3}{3{,}14\cdot 1{,}5\cdot 10^6}}=0{,}22\ м,$$

where $D_{в.к}=D_ц=0{,}178$ m - cylinder bore;

$j_{к.о}=1{,}5\cdot 10^6$ a/m - current density in the winding;

$$h_{к.о}=0{,}5(D_{н.к}-D_{в.к})=0{,}5(0{,}22-0{,}178)=0{,}021\ м.$$

18. The electrical resistance of pole face winding (under one pole):

$$R_{к\,о}\approx\frac{4\rho_{ct}c_o l}{\pi(D_{н.к}^2-D_{в.к}^2)}=\frac{4\cdot 0{,}0196\cdot 10^{-6}\cdot 1{,}06\cdot 0{,}039}{3{,}14(0{,}22^2-0{,}178^2)}=6{,}12\cdot 10^{-8}\ \text{ohm},$$

where $\rho_{ct}\approx 0{,}011(1+\alpha_c t)\cdot 10^{-6}=0{,}011\cdot(1+0.006\cdot 130)\cdot 10^{-6}=0{,}0196\cdot 10^{-6}$ Ω·m - specific resistor/resistance of steel at an approximate temperature t=130°C;

$\alpha_c=0{,}006$ 1/deg - temperature specific resistance of steel.

F. Calculation of excitation winding.

19. Average/mean length of the turn of the coil:

$$L_в = 0{,}5\pi(1+\xi)D_{в.н} = 0{,}5 \cdot 3{,}14 \cdot (1+0{,}667) \cdot 0{,}298 = 0{,}78 \text{ м}.$$

20. The cross-sectional area of the wire:

$$q_в = \frac{F_{в.н}}{U_в}\rho_{мt}L_в = \frac{8\,160}{115}0{,}0258 \cdot 10^{-6} \cdot 0{,}78 = 1{,}43 \cdot 10^{-6} \text{ м}^2,$$

$$\rho_{мt} \approx 0{,}017(1+\alpha_м t) \cdot 10^{-6} = 0{,}0258 \cdot 10^{-6}$$

where $\rho_{мt}$ Ω·m - resistivity of copper wire at expected operating temperature of coil t=130°C; $\alpha_м$=0,004 1/deg - temperature specific resistance of copper; $U_в$ =115 C - the voltage/stress of separate excitation. The wire with a diameter of 1.35 mm (without the insulation) corresponds to this section.

21. Field current with the load;

$$I_{в.н} = j_в q_в = 3{,}6 \cdot 10^6 \cdot 1{,}43 \cdot 10^{-6} = 5{,}14 \text{ а},$$

where

$$j_в = j'_в \frac{F_{в.н}}{F'_{в.н}} = 3{,}65 \cdot 10^6 \frac{8\,160}{8\,300} = 3{,}6 \cdot 10^6 \text{ а/м}^2$$

- real current density in the coil.

Page 276.

22. Number of turns of the coil:

$$w_в = \frac{F_{в.н}}{I_{в.н}} = \frac{8\,160}{5{,}14} = 1\,600.$$

23. Field current with the idling:

$$I_в = \frac{F_в}{w_в} = \frac{5\,450}{1\,600} = 3{,}4 \text{ а}.$$

24. Resistor of the excitation:

AD-A139 778 UNIPOLAR ELECTRIC MACHINES WITH LIQUID-METAL CURRENT PICKUP(U) FOREIGN TECHNOLOGY DIV WRIGHT-PATTERSON AFB OH A I BETTINOV ET AL. 08 MAR 84 FTD-ID(RS)T-1205-83 6/6

UNCLASSIFIED F/G 9/3 NL

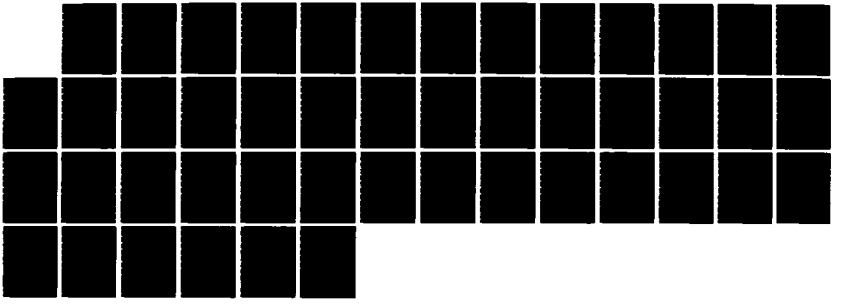

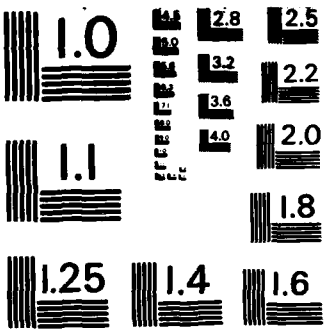

MICROCOPY RESOLUTION TEST CHART
NATIONAL BUREAU OF STANDARDS - 1963 - A

$$R_{в.э}=w_в\cdot\frac{\rho_{м.т}L_в}{q_в}=\frac{U_в}{I_{в.н}}=\frac{115}{5,14}=22,5 \text{ ohm}.$$

25. Power of excitation winding:

$$P_{в.н}=I^2_{в.н}R_{в.э}=U_вI_{в.н}=115\cdot5,14=590 \text{ W}.$$

G. Calculation of current-tap apparatus.

In accordance with the assignment we choose as the contact medium alloy NaK, we assume/set electrodes by copper ones with the protective coating. Operating temperature of contact we tentatively accept t=100°C. Calculation is conducted according to the diagram, presented into Sect. 5-3.

26. Linear relative velocity on the surface of the armature:

$$v=\pi Dn=3,14\cdot0,175\cdot100=55 \text{ m/s}.$$

27. The outside diameter of the rotating electrode:

where $v_к=\mathring{D}_кv=1,2\cdot55=66$ m/s - relative velocity of electrodes;

$\mathring{D}_к=D_к/D\approx1,2$ — design factor (relative diameter).

28. The width of the sharpening of the electrode:

$$l_к \approx \frac{I_к}{3\pi D_к j_к} = \frac{20 \cdot 10^3}{3 \cdot 3,14 \cdot 0,21 \cdot 10^7} = 1 \cdot 10^{-3} \text{ м},$$

where $j_к = 10^7$ A/m^2 - current density in the contact.

29. Diameter of the insertion/immersion of the rotating electrode:

$$D_{1к} \approx D_к - 2l_к \cos \alpha_к = 0,21 - 2 \cdot 10^{-3} \cdot 0,819 = 0,2084 \text{ м}.$$

30. Width and the diameter of the turning:

$$L_к = l_к + 0,3 D_к \mathrm{Re}^{-0,182} = 1 \cdot 10^{-3} + 0,3 \cdot 0,21 \cdot 0,041 = 3,58 \cdot 10^{-3} \text{ м};$$

$$D_{2к} = D_к (1 + 0,32 \mathrm{Re}^{-0,182}) = 0,21 (1 + 0,32 \cdot 0,041) = 0,2128 \text{ м},$$

where $\mathrm{Re}^{0,182} = 24.5$ is determined on curve (Fig. 5-6a) when

$$\mathrm{Re} = \frac{2 D_к v_к}{\nu_t} = \frac{2 \cdot 0,21 \cdot 66}{60 \cdot 10^{-6}} = 4,62 \cdot 10^7;$$

$\nu_t = 60 \cdot 10^{-6}$ m/s - kinematic viscosity NaK (Table 5-1).

31. determination of the losses of friction in the contact.

a). Coefficient of friction:

$$c = \frac{D_к - D_{1к} + 0,8 l_к}{l_к \mathrm{Re}^{0,182}} \varphi_к(\lambda) =$$

$$= \frac{0,21 - 0,2084 + 0,8 \cdot 10^{-3}}{24,5 \cdot 10^{-3}} 7,2 \cdot 10^{-3} = 0,7 \cdot 10^{-3},$$

where

$$\lambda = \frac{D_{2к} - D_{1к} + 0,84 L_к}{D_к - D_{1к} + 0,8 l_к} =$$

$$= \frac{0,2128 - 0,2084 + 0,84 \cdot 3,58 \cdot 10^{-3}}{0,21 - 0,2084 + 0,8 \cdot 10^{-3}} = 3,1;$$

$\varphi_{\text{к}}(\lambda) \approx 7.2 \cdot 10^{-3}$ (Fig. 5-6b).

b). The losses of friction (in one contact):

$$P_{\text{к.т}} = 8 c \rho_t l_{\text{к}} D_{\text{к}} v_{\text{к}}^3 = 8 \cdot 0{,}7 \cdot 10^{-3} \cdot 850 \cdot 10^{-3} \cdot 0{,}21 \cdot 66^3 = 287 \text{ W},$$

where $\rho_t \approx 850$ kg/m³ - density NaK (Table 5-1).

Page 278.

32. Determination of electrical losses.

a). The electrical resistance of the layer of the liquid metal:

$$R_{\text{ж}} \approx \frac{1}{3\pi\gamma_t (L_{\text{ж}} + l_{\text{к}})} \ln \frac{D_{2\text{к}}}{D_{1\text{к}}} =$$

$$= \frac{1}{3 \cdot 3{,}14 \cdot 2{,}38 \cdot 10^6 (3{,}58 + 1) 10^{-3}} \ln \frac{0{,}2128}{0{,}2084} \approx 2 \cdot 10^{-7} \ \Omega$$

$\gamma_t \approx \frac{1}{0{,}42 \cdot 10^{-6}} = 2{,}38 \cdot 10^6$

where ^ $1/\Omega \cdot \text{m}$ - electrical conductivity NaK (Table 5-1).

б). Electrical losses (in one contact):

$$P_{\text{к.э}} = I_{\text{к}} \Delta U_{\text{к}} + I_{\text{к}}^2 R_{\text{ж}} = 20 \cdot 10^3 \cdot 0{,}02 + (20 \cdot 10^3)^2 \, 2 \cdot 10^{-7} =$$

$$= 400 + 80 = 480 \text{ (1)}$$

Key: (1). W.

where $\Delta U_{\text{к}} \approx 2\sigma_{\text{к}} j_{\text{к}} = 2 \cdot 10^{-9} \cdot 10^7 = 0{,}02$ C - a voltage drop across contact resistance between the liquid metal and the solid electrodes;

$\sigma_к = R_{к.п} S_к \approx 10^{-9}$ $\Omega \cdot м^2$ - approximate value of the specific skin drag of make-before-break contact ($R_{к.п}$; $S_к$ — contact resistance and the area of contact surface).

H. Calculation of losses and efficiency.

33. The electrical resistance of armature, which corresponds to one,

$$R_я = \frac{4 k_R c_0 (l + b_я) \rho_{ст}}{\pi D^2 (1 - d_я^2)} =$$

$$= \frac{4 \cdot 2 \cdot 1{,}06 \, (0{,}039 + 0{,}02) \, 0{,}0196 \cdot 10^{-6}}{3{,}14 \cdot 0{,}175^2 \, (1 - 0{,}25^2)} = 9{,}5 \cdot 10^{-6} \ \Omega$$

moreover in this case it is accepted $k_R = f(L'_я / R) \approx 2$ with

$$\frac{L'_я}{R} \approx \frac{c_0 (l + 2 b_я)}{0{,}5 D} = \frac{1{,}06 \, (0{,}039 + 2 \cdot 0{,}02)}{0{,}5 \cdot 0{,}175} = 0{,}95.$$

34. Electrical losses in the armature:

$$P_я = 2 p I_я^2 R_я = 2 \cdot 20^2 \cdot 10^6 \cdot 9{,}5 \cdot 10^{-6} = 76 \ \text{W}.$$

Page 279.

35. Electrical losses in pole face winding:

$$P_{к.о} = 2 p I_я^2 R_{к.о} = 2 \cdot 20^2 \cdot 10^6 \cdot 6{,}12 \cdot 10^{-6} = 49 \ \text{W}.$$

36. Power losses in the contacts:

$$P_к = m_к (P_{к.т} + P_{к.э}) = 2(287 + 480) = 1530 \quad W.$$

37. The power losses of the generator:

$$\Sigma P = k_ш (P_в + P_{к.о}) + P_к + P_д + P_м = \\ = 2(76 + 49) + 1530 + 590 + 2400 = 4770 \quad W,$$

where $P_м \approx 0{,}02 P_в \cdot 10^3 = 0{,}02 \cdot 120 \cdot 10^3 = 2400$ W - approximate value of mechanical losses (in the bearings, also, for friction of rotating parts against the filler of the internal cavity of generator);

$k_m \approx 2$ — approximate value of the coefficient, which considers electrical losses in the internal coupling busbars (it is made more precise after the study of the construction/design of busbars).

38. Efficiency of the generator

$$\eta = \frac{P_в}{P_в + \Sigma P \cdot 10^{-3}} = \frac{120}{120 + 4{,}77} \approx 0{,}96.$$

I. On performance calculation of generator.

39. No-load characteristic. Is been given the series/row of the values of emf in the range E_i =1-8 in. Flow in working gap $\Phi_{в.} = E_i/n$;

n=100 r/s and corresponding inductions are determined B_a, B_p, B_c. In this case the coefficients of scattering assume/set by those not changing. For each value Φ_{bi} is carried out the calculation of magnetic circuit and they determine value F_{zi}. According to obtained data characteristic is constructed $E=f(F_z)$.

40. Full-load saturation curves.

From the calculation of magnetic circuit with load I_a=const the series/row of values n. s. (magnetizing force) of the longitudinally demagnetizing effect of transverse armature reaction $F_{qd}=F_{a.a}-F_a$, which correspond to different values of emf is found E_i.

From the calculation of electrical circuit the internal incidence/drop in voltage of the generator

$$\Delta U=m_g I_a(R_a+R_{a.c})+m_a(I_a R_m+\Delta U_a)+I_a R_m,$$

is found where R_m — resistor/resistance of coupling busbars within the machine.

Page 280.

From parameters F_{qd}=var and ΔU=const (with E=var and I_a=const) is constructed rad of the reactive/jet triangles, with the help of which according to no-load characteristic full-load saturation curve

when $U=f(F_в)$ is determined $I_я=\text{const.}$

After performing such operations for several fixed values of current $I_я$, the family of full-load saturation curves is obtained. With its aid it is possible to construct the families of external and self-regulation of machine.

Voltage drop in internal circuit of armature (with the nominal load):

$$\Delta U=2\cdot 20\cdot 10^3(9{,}5\cdot 10^{-6}+6{,}12\cdot 10^{-6})+2(20\cdot 10^3\cdot 2\cdot 10^{-7}+0{,}02)+$$
$$+20\cdot 10^3\cdot 31{,}2\cdot 10^{-6}\approx 0{,}061 \text{ в},$$

where tentatively

$$R_щ=\frac{P_щ}{I_я^2}\approx\frac{P_я+P_{я.о}}{I_я^2}=\frac{125}{20^2\cdot 10^3}=31{,}2\cdot 10^{-6} \text{ ohm.}$$

In this case the refined value

$$\mathring{U}=\frac{U}{U+\Delta U}=\frac{6}{6+0{,}061}=0{,}985,$$

which is close to the preliminarily selected (p. 4) value.

P. 2. Example of the determination of the main sizes/dimensions of disk non-polar dynamo.

A. Assignment.

1. Initial data. Power $p_н=15$ kW; voltage/stress U=5 in; the speed of rotation n=150 r/s (9000 r/min); the operating mode is prolonged; cooling natural air; current pickup circular liquid-metal on base of NaK (with the forced liquid cooling).

Page 281.

2. Structural and electrical diagram. Let us select the uncompensated machine with the nonmagnetic conical rotor disk, prepared from the copper-beryllium alloy. Current pickup on the shaft is one-sided. Excitation independent. Number of poles 2p=2, moreover $m_1=m_2=1$. Number of slide contacts $m_к=2$. Number of field coils $m_в=2$. Coefficients $k_I=1$ and k=1 (one-sided current pickup on the shaft).

B. Determination of the main sizes/dimensions of

3. Current of the generator:

$$I=\frac{P_н\cdot 10^3}{U}=\frac{15\cdot 10^3}{5}=3\cdot 10^3\ a;$$

$$I_я=\frac{k_I}{m_1}I=3000\ a.$$

4. The electromotive force of the armature:

$$E=\frac{U}{\hat{U}}=\frac{5}{0,98}=5,1\ в,$$

where it is tentatively accepted $\mathring{U}=0{,}98$.

5. Calculated (electromagnetic) power:

$$P_э = m_l E I_л \cdot 10^{-3} = 5{,}1 \cdot 3000 \cdot 10^{-3} = 15{,}3 \text{ kW}.$$

6. Coupling coefficient of emf with the power

$$K_{лE} = \frac{E^2}{nP_э} = \frac{5.1^2}{150 \cdot 15{,}3} = 11{,}3 \cdot 10^{-3} \text{ V}^2/(\text{kW} \cdot \text{rev/s}).$$

7. Current density in the shaft. On the basis (6-18) when $D_1 \approx D_ш$ the preliminary value

$$j'_1 \approx \frac{m_E}{m_l} \frac{B_\delta}{K_{лE}} \cdot \frac{1-\mathring{D}_ш^2}{\mathring{D}_ш^2} \cdot \frac{10^3 k}{\cos\alpha} = \frac{1{,}2}{11{,}3 \cdot 10^{-3}} \times$$

$$\times \frac{1-0{,}3^2}{0{,}3^2} \cdot \frac{10^3}{0{,}99} = 1{,}1 \cdot 10^6 \text{ a/м}^2,$$

where $B_\delta = 1{,}2$ T (for the machines with the nonmagnetic disk);

$$\mathring{D}_ш = D_ш/D \approx 0{,}3; \quad \cos\alpha \approx 0{,}99.$$

Page 282.

8. Main sizes/dimensions of machine.

a). Air-gap diameter On the basis of (6-15)

$$D = \sqrt[4]{\frac{P_э}{\sigma' \lambda n}} = \sqrt[4]{\frac{15{,}3}{67{,}8 \cdot 150}} = 0{,}197 \text{ м},$$

where during the one-sided current pickup on the shaft

$$s'_{\text{д}} = 6{,}15 \cdot 10^{-4} \cdot m_g m_l \frac{\mathring{D}_{\text{д}}^2 (1 - \mathring{D}_{\text{д}}^2)}{\cos \alpha} B_t j_1 =$$

$$= 6{,}15 \cdot 10^{-4} \frac{0{,}3^2 (1 - 0{,}3^2)}{0{,}99} 1{,}2 \cdot 1{,}1 \cdot 10^{-6} = 67{,}8 \text{ kW/(m}^2 \cdot \text{rev/s)}.$$

b). Active length:

$$l = \lambda_{\text{д}} D = 0{,}354 \cdot 0{,}197 \approx 0{,}07 \text{ м},$$

where the design factor

$$\lambda_{\text{д}} = 0{,}5 \frac{1 - \mathring{D}_{\text{д}}}{\cos \alpha} = 0{,}5 \frac{1 - 0{,}3}{0{,}99} = 0{,}354.$$

C. Some sizes/dimensions of stator.

9. The diameter of the current carrying shaft:

$$D_1 = D_{\text{д}} - 2\delta_1 = 0{,}059 - 2 \cdot 1{,}5 \cdot 10^{-3} = 0{,}055 \text{ м},$$

where $D_{\text{д}} = \mathring{D}_{\text{д}} D = 0{,}3 \cdot 0{,}197 = 0{,}059$ m - diameter of opening/aperture in the magnetic circuit for the shaft.

In this case real current density in the steel shaft

$$j_1 = \frac{4}{\pi} \cdot \frac{I_{\text{п}}}{D_1^2} = \frac{4 \cdot 3\,000^{\text{тк}}}{3{,}14 \cdot 0{,}055^2} = 1{,}26 \cdot 10^6 \text{ а/м}^2.$$

10. Contours of profile of disk.

a). Calculated thickness on the surface of shaft on (6-4)

$$b_1 = \lambda_{\text{д}1} D_1 = 0{,}15 \cdot 0{,}055 = 8{,}25 \cdot 10^{-3} \text{ м},$$

where $\lambda_{\pi_1} = 0{,}25 k_{p_1} \frac{j_1}{j_{p1}} = 0{,}25 \cdot 0{,}95 \cdot \frac{1{,}26 \cdot 10^6}{2 \cdot 10^6} = 0{,}15$ — design factor;

$j_{p_1} \approx 2 \cdot 10^6$ $a/м^2$ - current density in the disk from the nonmagnetic material;

$k_{p_1} = 0{,}95$ - coefficient, which considers the decrease of the diameter of shaft after treatment in the zone of the pressing of disk.

Page 283.

b). The thickness of disk at the active diameter

$$b_D = \frac{I_\pi}{\pi j_D D} = \frac{3\,000}{3{,}14 \cdot 2 \cdot 10^3 \cdot 0{,}197} = 2{,}4 \cdot 10^{-3}\ м,$$

where $j_D \approx j_{p_1} \approx 2 \cdot 10^6$ A/m² - current density in the disk.

In this case the refined value

$$\cos z = \cos\left(\operatorname{arctg} \frac{b_1 - b_D}{D - D_1 k_{p1}}\right) \approx 0{,}999,$$

which is close to the preliminarily selected value.

Further calculation is conducted similarly to that presented for the cylindrical machines in the previous example (taking into account specific character disk (UG).

P. 3. Example of the determination of the main sizes/dimensions of non-polar dynamo with the hollow rotor.

A. Assignment.

1. Initial data. Power $P_г$=20 kW voltage/stress U=5 in; the speed of rotation n=50 r/s (3000 r/min); the operating mode is prolonged; cooling natural air; current pickup circular liquid-metal (with the forced cooling).

2. Structural and electrical diagram. Let us select the compensated machine with the ferromagnetic cylinder of rotor during the half use. Number of poles 2p=4, a number of powered phases of armature, connected in series, $m_г$=2, in parallel - m_1=1. Number of slide contacts

Excitation independent, a number of field coils $m_в$=2; coefficient k_1=1. The location of rotor shaft is horizontal (Fig. 6-1b).

Page 284.

B. Determination of main sizes/dimensions.

3. Current of the generator:

$$I=\frac{P_г\cdot 10^3}{U}=\frac{20\cdot 10^3}{5}=4\cdot 10^3\ a;$$

$$I_я=\frac{k_1}{m_1}I=4000\ a.$$

4. Electromotive force of the armature:

$$E=\frac{U}{\mathring{U}}=\frac{5}{0,98}=5,1 \text{ V},$$

where tentatively $\mathring{U}=0,98$.

5. Calculated (electromagnetic) power:

$$P_э=m_1EI_a\cdot10^{-3}=5,1\cdot4000\cdot10^{-3}=20,4 \text{ KVM}.$$

6. The coefficient of use in (6-12):

$$\sigma_м=\pi^2\cdot10^{-3}m_Bm_1AB_\delta=$$
$$=3,14^2\cdot10^{-3}\cdot2\cdot5500\cdot1,4=1,52\cdot10^2 \text{ kW/(m}^3\cdot\text{rev/s)},$$

where ampere-conductors per inch and induction in the working gap is tentatively accepted A=5500 by a/m; $B_\delta=1,4$ T.

7. Main sizes/dimensions.

a). Air-gap diameter In accordance with (6-12)

$$D=\sqrt[3]{\frac{P_э}{\sigma_м\lambda_{вл}n}}=\sqrt[3]{\frac{20,4}{1,52\cdot10^2\cdot0,195\cdot50}}=0,24 \text{ м},$$

where the design factor:

$$\lambda_{\text{п}} = 0{,}25\,\frac{\overset{*}{D}{}_c^2 - \overset{*}{d}{}^2}{k_\sigma}\cdot\frac{B_c}{B_\delta} = 0{,}25\,\frac{0{,}94^2 - 0{,}235^2}{1{,}1}\cdot\frac{1{,}45}{1{,}4} = 0{,}195;$$

$k_\sigma = 1{,}1$ — coefficient of scattering;

$B_c = 1{,}45$ T - magnetic induction in the internal magnetic circuit of stator;

$\overset{*}{D}_c = D_c/D = 0{,}94;$

$\overset{*}{d} = d/D \approx 0{,}235$ - approximate values of relative diameters (Fig. 6-1b).

b). Active length, which corresponds to one pole:

$$l = \lambda_{\text{п}} D = 0{,}195\cdot 0{,}24 = 0{,}0468\ \text{м}.$$

Page 285.

C. Some sizes/dimensions of rotor.

8. The inner diameter:

$$D_1 = D_c + 2\delta_1 = 0{,}226 + 2\cdot 1{,}5\cdot 10^{-3} = 0{,}229\ \text{м},$$

where $D_c = \overset{*}{D}_c D = 0{,}94\cdot 0{,}24 = 0{,}226$ m - diameter of internal magnetic circuit; $\delta_1 = 1.5\cdot 10^{-3}$ m - auxiliary gap.

In this case current density in the rotor:

$$j_p = \frac{4I_\text{п}}{\pi(1-\overset{*}{D}{}_1^2)D^2} = \frac{4\cdot 4\,000}{3{,}14(1-0{,}955^2)\cdot 0{,}24^2} = 0{,}985\cdot 10^6\ \text{а/м}^2,$$

where the relative diameter:

$$\mathring{D}_1 = D_1/D = 0{,}229/0{,}24 = 0{,}955.$$

9. The calculated axial length of the rotor:

$$l_p = c_{o.p}(2l + l_e + 2b_k) = 1{,}05(2 \cdot 0{,}0468 + 0{,}01 + 2 \cdot 0{,}0265) = 0{,}165 \text{ м},$$

where the width of the electrode of the contact:

$$b_k = \frac{I_k}{\pi \mathring{D}_p D j_{p.k}} = \frac{4\,000}{3{,}14 \cdot 0{,}95 \cdot 0{,}24 \cdot 2{,}1 \cdot 10^6} = 0{,}0265 \text{ м};$$

$j_{p.k} \approx 2{,}1 \cdot 10^6$ A/m² - current density in the zone of the pressing of electrode;

$c_{o.p} \approx 1{,}05$ and $\mathring{D}_p \approx 0{,}95$ - design factors;

l_e=0.01 m - width of slot in the internal magnetic circuit (Fig. 6-1b).

Further calculation is performed similarly to that presented in the first example for the cylindrical generators with the solid rotor taking into account the specific character of machines with the hollow rotor.

Page 286.

P.4. EXAMPLE OF THE CALCULATION OF UNIPOLAR ELECTRIC MOTOR WITH MASSIVE FERROMAGNETIC CYLINDRICAL ARMATURE COMPLETELY IMMERSED IN LIQUID METAL.

Let us consider the determination of the basic dimensions of engine only; the detailed calculation of engine is analogous to the calculation of generator, presented in the P 1.

A. Assignment.

1. Initial data. $P_в = 5 \cdot 10^3$ W (n·m/s); n=100 r/s (6000 r/min); $U_в$ — arbitrary; the operating mode prolonged; contact liquid - eutectic alloy NaK; expected operating temperature of the liquid metal T=573°K (300°C).

Parameters of the contact liquid:

$$\rho_t = 838 \ кг/м^3 \ (н \cdot сек^2/м^4);$$

$$\eta_{вт} = 2{,}99 \cdot 10^{-4} \ н \cdot сек/м^2;$$

$$\nu_t = \frac{\eta_{вт}}{\rho_t} = 35{,}65 \cdot 10^{-8} \ м^2/сек;$$

$$\gamma = 1{,}84 \cdot 10^6 \ 1/ом \cdot м.$$

Key: (1). N·s²/m⁴. (2). N·s/m². (3). m²/s. (4). 1/ohm·m.

2. Structural and electrical diagram. Machine is compensated with the help of bifilar, excitation independent $2p=2$; $m_I=2$; $m_E=1$; $k_I=1$.

B. Determination of the basic dimensions and parameters.

In accordance with Chapter 8 we calculate the values of first approximation.

1. Net torque on the shaft of the engine:

$$M_в = \frac{P_в}{\omega} = \frac{P_в}{2\pi n} = \frac{5 \cdot 10^3}{2 \cdot 3{,}14 \cdot 100} = 7{,}96 \ \text{N·m}.$$

Page 287.

2. The first approximation of the value of the electromagnetic moment developed under one pole:

$$M_{s1}^{(1)}=\frac{1,12M_{\text{н}}}{m_E m_l}=\frac{1,12\cdot 7,96}{2}=4,46 \quad \text{N}\cdot\text{m}.$$

3. Electromagnetic loads:

$$j_{\text{p}}=1\cdot 10^6\ A/м^2;\ B_{\text{p}}=1,0 \quad \text{T}.$$

4. Diameter of rotor in accordance with formula (8-61):

$$D^{(1)}=2\sqrt[4]{\frac{4M_{s1}^{(1)}}{\pi j_{\text{p}} B_{\text{p}}}}=2\sqrt[4]{\frac{4\cdot 4,46}{3,14\cdot 1\cdot 10^3\cdot 1,0}}=97,5\cdot 10^{-3}\ м.$$

5. The active length of rotor under one pole as per (8-60):

$$l^{(1)}=\frac{D^{(1)}}{4}\frac{B_{\text{p}}}{B_{\delta}}k_{\text{ср}}=\frac{97,5\cdot 10^{-3}}{4}\cdot\frac{1,0}{0,7}\cdot 1,1=38,3\cdot 10^{-3}\ м,$$

where it is accepted $B_{\delta}=0,7$ T, $k_{\text{ср}}=1,1$.

6. Reynolds number:

$$\text{Re}^{(1)}=\frac{\omega(D^{(1)})^2}{4\nu}=\frac{2\pi n(D^{(1)})^2}{4\nu}=\frac{2\cdot 3,14\cdot 100\cdot(97,5\cdot 10^{-3})^2}{4\cdot 35,65\cdot 10^{-6}}=418\cdot 10^3.$$

7. Values of radial clearance in accordance with (8-73):

$$\delta\geqslant 0,14\cdot(\text{Re}^{(1)})^{-0,182}\cdot D^{(1)}=0,14(418\cdot 10^3)^{-0,182}\cdot 97,5\cdot 10^{-3}=$$
$$=0,56\cdot 10^{-3}\ м.$$

We accept $\delta=1\cdot 10^{-3}$ m.

8. Thickness of metal shield and layer of the electro-insulation:

$$\delta_l=0,3\cdot 10^{-3}\ м,\quad \delta_{\text{из}}=0,3\cdot 10^{-3}\ м.$$

9. Bore diameter of the magnetic circuit of stator on (8-75):

$$D_c^{(1)} = D^{(1)} + 2(\delta + \delta_t + \delta_{\text{кл}1}) =$$
$$= 97{,}5 \cdot 10^{-3} + 2(1 + 0{,}3 + 0{,}3) \cdot 10^{-3} = 100{,}7 \cdot 10^{-3} \text{ м}.$$

10. Current in the compensator on (8-76):

$$I_c^{(1)} \approx \pi (0{,}5 D_c^{(1)} - \delta_{\text{кл}1})^2 j_p =$$
$$= 3{,}14 (0{,}5 \cdot 100{,}7 \cdot 10^{-3} - 0{,}3 \cdot 10^{-3})^2 \cdot 1 \cdot 10^6 = 7\,850 \text{ А}.$$

Page 288.

11. Outer diameter of compensative bifilar as per (8-74):

$$D_{c1}^{(1)} = 2\sqrt{\frac{I_c^{(1)}}{\pi j_c} + \frac{(D_c^{(1)})^2}{4}} = 2\sqrt{\frac{7\,850}{3{,}14 \cdot 0{,}5 \cdot 10^6} + \frac{(100{,}7 \cdot 10^{-3})^2}{4}} = 174 \cdot 10^{-3} \text{ м},$$

where it is accepted $j_c = 0{,}5 \cdot 10^6$ A/м^2.

12. Magnetizing force of excitation winding on (8-72):

$$F_в = \frac{2 k_{ст} k_{р.п}}{\mu_0} (\delta' k_\delta B_\delta + \delta_{\text{кл}2} B_c) =$$

$$= \frac{2 \cdot 1{,}2 \cdot 1{,}05}{4\pi \cdot 10^{-7}} (1{,}6 \cdot 10^{-3} \cdot 1{,}001 \cdot 0{,}7 + 0{,}3 \cdot 10^{-3} \cdot 1{,}2) = 2\,970 \text{ А},$$

where $\delta' = \delta + \delta_t + \delta_{\text{кл}1} = 1 \cdot 10^{-3} + 0{,}3 \cdot 10^{-3} = 1{,}6 \cdot 10^{-3}$ м, moreover it is accepted:

$$k_\delta = 1{,}001; \quad k_{ст} = 1{,}2; \quad k_{р.п} = 1{,}05; \quad \delta_{\text{кл}2} = 0{,}3 \cdot 10^{-3} \text{ м}.$$

13. Section of winding on (8-70):

$$Q_в = \frac{F_в}{k_з j_в} = \frac{2\,970}{0{,}7 \cdot 2{,}5 \cdot 10^6} = 16{,}6 \cdot 10^{-4} \text{ м}^2.$$

Duty factor and current density in the winding respectively $k_з = 0.7$ and $j_в = 2.5 \cdot 10^6$ A/м^2.

14. Axial size/dimension of coil in the first approximation, on (8-69):

$$b_{\text{к}}=\sqrt{\frac{Q_{\text{к}}}{k_{\text{к}}}}=\sqrt{\frac{16{,}6\cdot10^{-4}}{0{,}5}}=57{,}5\cdot10^{-3}\ м,$$

where the preliminarily taken relation of coil sides $k_{\text{к}}=\frac{h_{\text{к}}}{b_{\text{к}}}=0{,}5$.

The height/altitude of the window of magnetic circuit in this case comprises:

$$h_{\text{к}}\approx 0{,}5\,(D_{c1}^{(1)}-D_{c}^{(1)})+h_{\text{к}}+2s_{\text{к}}=$$

$$=0{,}5(174\cdot10^{-3}-100{,}7\cdot10^{-3})+0{,}5\cdot57{,}5\cdot10^{-3}+2\cdot1{,}5\cdot10^{-3}=68{,}4\cdot10^{-3}\ м.$$

Axial size/dimension of winding on (8-68):

$$l_{\text{о}}=b_{\text{к}}+2s_{\text{к}}=57{,}5\cdot10^{-3}+2\cdot1{,}5\cdot10^{-3}=60{,}5\cdot10^{-3}\ м;$$

$$\frac{h_{\text{о}}}{l_{\text{о}}}=\frac{68{,}4\cdot10^{-3}}{60{,}5\cdot10^{-3}}=1{,}13.$$

Page 289.

For the purpose of the decrease of scattering we make more precise the geometry of winding, after taking $k_{\text{к}}=0{,}4$. In this case

$$b_0^{(1)}=\sqrt{\frac{Q_0}{k_0}}=\sqrt{\frac{16,6\cdot10^{-4}}{0,4}}=64,4\cdot10^{-3}\ м,$$

$$h_0^{(1)}=0,5\,(D_{c1}^{(1)}-D_c^{(1)})+k_0b_0^{(1)}+2s_{\text{ш}}=$$
$$=0,5\,(174\cdot10^{-3}-100,7\cdot10^{-3})+0,4\cdot64,4\cdot10^{-3}+$$
$$+2\cdot1,5\cdot10^{-3}=57,2\cdot10^{-3}\ м;$$

$$l_0^{(1)}=b_0^{(1)}+2s_{\text{ш}}=64,4\cdot10^{-3}+2\cdot1,5\cdot10^{-3}=67,4\cdot10^{-3}\ м;$$

$$\frac{h_0^{(1)}}{l_0^{(1)}}=\frac{57,2\cdot10^{-3}}{67,4\cdot10^{-3}}<1.$$

15. Overall length of rotor on (8-67):

$$L^{(1)}=p\,[2l^{(1)}+l_0^{(1)}]=1\cdot[2\cdot38,3\cdot10^{-3}+67,4\cdot10^{-3}]=144\cdot10^{-3}\ м.$$

Let us calculate the values of the second approximation/approach.

16. Simplified expression of moment/torque. After replacing in formulas (8-20) and (8-21) the parameter l on L^1, it is possible to make more precise the value of the moment/torque of hydraulic resistor/resistance in the second approximation/approach. To more simply use not (8-20) and (8-21), but the expression

$$M_{\text{т}}^{(2)}=1,11\cdot10^{-8}\rho_t\,\mathrm{Re}^{-0,182}\,(1-\bar{D}_1^{4,64}+3,7\,L^{(1)}/D^{(1)})\,\omega^2D^{(1)5}=$$
$$=8,65\cdot10^{-4}\,\rho_t\,(\mathrm{Re}^{(1)})^{-0,182}\,(1-\bar{D}_1^{4,64}+3,7L^{(1)}/D^{(1)})\,(2\pi n)^2\,D^{(1)5}=$$
$$=8,65\cdot10^{-4}\cdot838\,(418\cdot10^3)^{-0,182}\left(1-3,7\cdot\frac{144\cdot10^{-3}}{97,5\cdot10^{-3}}\right)\times$$
$$\times(2\cdot3,14\cdot100)^2\cdot(97,5\cdot10^{-3})^5=0,672\ \text{(1)}\cdot м,$$

Key: (1). N·m.

where we accept at first, that friction on faces of cylinder at diameter D_1 is approximately/exemplarily equal to friction of shaft; therefore we assume/set $\dot{D}_1 = 0$.

17. Refined value of numerical coefficient (p. 2). In this case

$$\frac{M_{\text{ц}}^{(2)}}{M_{\text{п}}} = \frac{0,672}{7,96} = 0,0845.$$

Page 290.

Taking into account bearing friction, coefficient can be taken as equal to 1.09.

18. Internal torque:

$$M_{\text{э}1}^{(2)} = \frac{1,09 M_{\text{п}}}{m_E m_I} = \frac{1,09 \cdot 7,96}{2} = 4,33 \text{ N} \cdot \text{m}.$$

19. Second approximation/approach of the value of the diameter of the rotor

$$D^{(2)} = 2\sqrt[4]{\frac{4M_{\text{э}1}^{(2)}}{\pi j_{\text{р}} \cdot B_{\text{р}}}} = 2\sqrt[4]{\frac{4 \cdot 4.33}{3,14 \cdot 1 \cdot 10^{6} \cdot 1,0}} = 97 \cdot 10^{-3} \text{ м}.$$

Being congruent/equating the results, obtained in paragraphs 19 and 4, we see that the disagreement between the value of the second and first approximation is insignificant. This makes it possible to take already second approximation/approach for the final result.

The values of coefficients $k_{\text{э.р}}, k_{\text{э}}, k_{\text{ст}}, k_{\text{р.п}}$ are made more precise

after the calculation of magnetic circuit in accordance with the indications, led in Chapter 3 and 4.

Coefficient k_* is made more precise with the help of expressions (8-71), (8-77) and (8-78).

The overall dimensions of machine are determined on the basis (8-79)-(8-81) and are made more precise after the study of construction/design.

20. The nominal voltage/stress of the machine

$$U_н = m_г E + \Sigma\Delta U = m_г n \Phi_\delta + \Sigma\Delta U,$$

where $\Sigma\Delta U$ – voltage drop in internal circuit of armature.

Let us calculate the main things of electric motor with assigned magnitude $U_н = 2$ V.

With the help of dependence (8-64a) is determined the first approximation of the value of the diameter:

$$D^{(1)} = 4\sqrt{\frac{nM_{эл}^{(1)}}{j_э U_н} k_{ср} m_г \dot{U}^{(1)}} =$$

$$= 4\sqrt{\frac{100 \cdot 4{,}46}{0{,}5 \cdot 10^6 \cdot 2} \cdot 1{,}1 \cdot 1 \cdot 1{,}06} = 91 \cdot 10^{-3} \text{ м},$$

where the relative voltage/stress is preliminarily accepted $\dot{U}^{(1)} = 1{,}06$; furthermore, it is accepted $j_э = 0{,}5 \cdot 10^6$ а/м^2; $k_{ср} = 1{,}1$.

Active length of the rotor

$$l^{(1)}=\frac{D^{(1)}}{4}\frac{B_p}{B_\delta}k_{ср}=\frac{91\cdot10^{-3}}{4}\cdot\frac{1,0}{0,7}1,1=35,7\cdot10^{-3}\ м.$$

During the refined calculation the refinement of the quantity

$$\dot{U}=\frac{U_в}{m_E E}=\frac{m_E E+\Sigma\Delta U}{m_E E}.$$

plays the determining role. In other respects the calculation is analogous presented above.

P.5. Example of the calculation of the fundamental parameters of unipolar engine with the disk rotor.

A. Assignment.

1. Initial data. $P_н$ =2·10³ W; n=50 r/s (3000 r/min); $U_в$ - arbitrary; the operating mode prolonged; contact liquid - alloy NaK, the parameters of alloy are analogous to those given in the example P-1.

2. Structural and electrical diagram. Let us consider the uncompensated machine with the circular (concentrated) contacts and the rotor disk of constant thickness; m_l=1; m_E=1; k_l=1; excitation independent.

B. Determination of the basic dimensions and parameters.

Let us calculate the values of first approximation.

1. Net torque on the shaft of the engine:

$$M_в = \frac{P_в}{\omega} = \frac{P_в}{2\pi n} = \frac{2 \cdot 10^3}{2 \cdot 3,14 \cdot 50} = 6,37 \text{ N} \cdot \text{m}.$$

2. Internal torque:

$$M_{в1}^{(1)} \approx \frac{1,03 M_в}{m_g m_l} = \frac{1,03 \cdot 6,37}{1} = 6,57 \text{ N} \cdot \text{m}.$$

Page 292.

Numerical coefficient is selected as being equal to 1.03, since circular current pickups on the shaft and the periphery serve as the source of mechanical losses mainly, in this case the moment/torque of hydraulic resistor/resistance will be less than in the case of the complete insertion/immersion of rotor into the liquid.

3. The diameter of the shaft:

$$D_в^{(1)} = 4kb^{(1)} \frac{f_l^{(1)}}{f_p^{(1)}} = 4 \cdot 0,5 \cdot 4 \cdot 10^{-3} \frac{4 \cdot 10^6}{1,5 \cdot 10^6} = 21,3 \cdot 10^{-3} \text{ м} \approx 22 \cdot 10^{-3} \text{ м},$$

where it is selected with $b^{(1)} = 4 \cdot 10^{-3}$ m;

$k = 0{,}5$ (при двустороннем (1) токосъеме);

$j_1^{(1)} = 4 \cdot 10^6$ $a/м^2$;

$j_p^{(1)} = 1{,}5 \cdot 10^6$ $a/м^2$.

Key: (1). during the bilateral current pickup.

4. Consumed current:

$$I_a^{(1)} = \pi b^{(1)} D_1^{(1)} j_1^{(1)} = 3{,}14 \cdot 4 \cdot 10^{-3} \cdot 22 \cdot 10^{-3} \cdot 4 \cdot 10^6 = 1\,105 \text{ } a.$$

5. The diameter of disk in accordance with (8-92):

$$D^{(1)} = \sqrt{\frac{8M_{31}^{(1)}}{\pi b^{(1)} D_1^{(1)} j_1^{(1)} B_\delta} + (d_1^{(1)})^2} = \sqrt{\frac{8M_{31}^{(1)}}{I_a^{(1)} B_\delta} + (d_1^{(1)})^2} =$$

$$= \sqrt{\frac{8 \cdot 6{,}57}{1\,105 \cdot 0{,}5} + (24 \cdot 10^{-3})} = 309 \cdot 10^{-3} \text{ } м,$$

where it is accepted $B_\delta = 0{,}5$ T;

$$d_1^{(1)} = D_1^{(1)} + 2\delta_1 = 22 \cdot 10^{-3} + 2 \cdot 1 \cdot 10^{-3} = 24 \cdot 10^{-3} \text{ } м.$$

Let us calculate the values of the second approximation/approach, after taking $b^{(2)} = 5 \cdot 10^{-3}$ m; B=0.7 T.

6. Diameter of the shaft:

$$D_1^{(2)} = 4kb^{(2)} \frac{j_1^{(1)}}{j_p^{(1)}} = 4 \cdot 0{,}5 \cdot 5 \cdot 10^{-3} \cdot \frac{3 \cdot 10^6}{1{,}5 \cdot 10^6} = 26{,}7 \cdot 10^{-3} \text{ } м.$$

We accept $D^{(2)}_1 = 27 \cdot 10^{-3}$ m.

7. Consumed current:

$$I_a^{(2)} = \pi b^{(2)} D_1^{(2)} j_1^{(1)} = 3{,}14 \cdot 5 \cdot 10^{-3} \cdot 27 \cdot 10^{-3} \cdot 4 \cdot 10^6 = 1\,695 \text{ } a.$$

Page 293.

8. Diameter of the disk:

$$D^{(2)}=\sqrt{\frac{8M_{31}^{(1)}}{l_{\pi}^{(2)}B_{\delta}}+(d_1^{(2)})^2}=\sqrt{\frac{8\cdot 6,57}{1\,695\cdot 0,7}+(29\cdot 10^{-3})^2}=212\cdot 10^{-3}\ м,$$

where $d_1^{(2)}=D_1^{(2)}+2\delta_1=27\cdot 10^{-3}+2\cdot 1\cdot 10^{-3}=29\cdot 10^{-3}$ м.

9. Linear velocity on the periphery of rotor disk:

$$v=\pi D^{(2)}n=3,14\cdot 212\cdot 10^{-3}\cdot 50=334\ \text{m/s}.$$

10. Current density of shaft in accordance with expression (8-93):

$$j_p^{(2)}=4k\frac{I_{\pi}^{(2)}}{\pi D_1^{(2)}}=4\cdot 0,5\cdot\frac{1\,695}{3,14\,(27\cdot 10^{-3})^2}=1,48\cdot 10^6\ а/м^2.$$

11. counter-emf of engine as per (8-94)

$$E=\omega B_{\delta}\frac{(D^{(2)})^2-(d_1^{(2)})^2}{8}=2\cdot 3,14\cdot 50\cdot 0,7\cdot\frac{(212\cdot 10^{-3})^2-(29\cdot 10^{-3})^2}{8}=1,2\ \text{V}.$$

To further refinement is subject numerical coefficient (p. 2) by calculating the mechanical losses of machine.

With the assigned magnitude of voltage/stress U_* for calculating the basic dimensions it is necessary to select preliminarily relative voltage/stress $\dot{U}^{(1)}$ and to use expression (8-95) it is analogous how this was done during the calculation of cylindrical engine.

P.6. EXAMPLE OF THE CALCULATION OF THE MAIN DIMENSIONS OF ENGINE WITH A HOLLOW ROTOR.

A. Assignment.

1. Initial data. $P_м=2\cdot10^3$ W; n=50 r/s; $U_0\leq2$ V; the current pickup of circular liquid-metal on base of NaK (parameters of alloy they are analogous to those given in the previous examples).

2. Structural and electrical diagram. Excitation independent; $m_1=1$; $m_2=1$.

Page 294.

B. Determination of main sizes/dimensions.

Let us calculate the values of first approximation.

1. Net torque of the engine:

$$M_м=\frac{P_м}{2\pi n}=\frac{2\cdot10^3}{2\cdot3,14\cdot50}=6,37\ \text{N}\cdot\text{m}.$$

2. Internal torque:

$$M_{s1}^{(1)} \approx \frac{1,03M_{\text{н}}}{m_E m_f} = \frac{1,03 \cdot 6,37}{1,1} = 6,57 \text{ N·m.}$$

3. Armature current

$$I_{\text{я}}^{(1)} = 1\,800\,a. \qquad (a=A)$$

4. Diameter of shaft in accordance with (8-93)

$$D_1^{(1)} = 2\sqrt{\frac{kI_{\text{я}}^{(1)}}{\pi f_{\text{ps}}^{(1)}}} = 2\sqrt{\frac{0,5 \cdot 1\,800}{3,14 \cdot 1,5 \cdot 10^6}} = 27,6 \cdot 10^{-3} \text{ м,}$$

where k=0.5; $f_{\text{ps}}^{(1)} = 1,5 \cdot 10^6$ $a/м^2$.

5. Diameter of opening/aperture for the shaft:

$$d_1^{(1)} = D_1^{(1)} + 2\delta_1 = 27,6 \cdot 10^{-3} + 2 \cdot 0,7 \cdot 10^{-3} = 29 \cdot 10^{-3} \text{ м.}$$

6. The diameter of the hollow cylinder of rotor on (8-102)

$$D^{(1)} = b + \frac{1}{\xi^{(1)}}\sqrt{\frac{8M_{s1}^{(1)}}{I_{\text{я}}^{(1)}B_c} + (d_1^{(1)})^2} = 2 \cdot 10^{-3} +$$

$$+ \frac{1}{0,85}\sqrt{\frac{8 \cdot 6,57}{1\,800 \cdot 1,2} + (29 \cdot 10^{-3})^2} = 188 \cdot 10^{-3} \text{ м,}$$

where it is accepted [redacted]=1.2 by T; $\xi^{(1)}$=0.85.

7. Linear velocity on the surface of the rotor:

$$v = \pi D^{(1)} n = 3,14 \cdot 188 \cdot 10^{-3} \cdot 50 = 295 \text{ m/s.}$$

Page 295.

8. The active length of rotor on (8-101):

$$l^{(1)}=\frac{D^{(1)}-b}{4}\cdot\frac{B_c}{B_\delta}(\xi^{(1)})^2-\frac{(d_1^{(1)})^2}{4(D^{(1)}-b)}\cdot\frac{B_c}{B_\delta}=$$

$$=\frac{188\cdot10^{-3}-2\cdot10^{-3}}{4}\cdot\frac{1,2}{0,7}\cdot0,85^2-\frac{(29\cdot10^{-3})^2}{4(188\cdot10^{-3}-2\cdot10^{-3})}\cdot\frac{1,2}{0,7}=56\cdot10^{-3}\ м,$$

where it is accepted $B_\delta=0,7$ T.

9. Against emf of machine on (8-103):

$$E^{(1)}=0,5D_{cp}^{(1)}\,l^{(1)}\omega B_\delta=(D^{(1)}-b)\,l^{(1)}\pi nB_\delta=$$

$$=(188\cdot10^{-3}-2\cdot10^{-3})\cdot56\cdot10^{-3}\cdot3,14\cdot50\cdot0,7=1,1\ V.$$

10. Current density in the rotor:

$$j_p^{(1)}=\frac{I_я^{(1)}}{\pi D_{cp}^{(1)}b}=\frac{1\,800}{3,14\cdot186\cdot10^{-3}\cdot2\cdot10^{-3}}=1,54\cdot10^8\ а/м^2.$$

Further refinement is conducted analogously with that presented in the previous examples.

P.7. EXAMPLE OF THE CALCULATION OF THE FUNDAMENTAL PARAMETERS OF CYLINDRICAL NON-POLAR DYNAMO WITHOUT THE FERROMAGNETIC CIRCUIT.

A. Assignment.

1. Initial data. Power $P_н=50$ kW; voltage/stress $U_н=1$ V; linear velocity on the surface of rotor v=200 m/s. The operating mode is short-term; current pickup is liquid-metal.

2. Structural and electrical diagram. Let us select machine with the combined (parallel and independent variable) excitation.

Page 296.

The winding of separate excitation is intended only for guaranteeing the relatively small of initial emf, which causes self-excitation. The location of the spools of parallel excitation corresponds to the diagram, given in Fig. 9-6. The coils of parallel excitation single-turn (busbar/tire); between themselves are connected in series and contrarily.

Relative geometric sizes/dimensions we accept the following (S 9-5):

$$\mathring{b}=0{,}25;\ \mathring{R}_в=\sqrt{1-\mathring{b}^2}=\sqrt{1-0{,}25^2}=0{,}97;\ \mathring{l}=3.$$

In this case the moduli/modules of the elliptical integrals:

$$k_{в1}=\sqrt{\frac{4\mathring{R}_в}{(\mathring{R}_в+1)^2+\mathring{b}^2}}=\sqrt{\frac{4\cdot 0{,}97}{(0{,}97+1)^2+0{,}25^2}}=0{,}992;$$

$$k_{в2}=\sqrt{\frac{4\mathring{R}_в}{(\mathring{R}_в+1)^2+(\mathring{b}+\mathring{l})^2}}=\sqrt{\frac{4\cdot 0.97}{(0{,}97+1)^2+(0{,}25+3)^2}}=0{,}5225.$$

Elliptical integrals in the function of moduli/modules are determined on tables [82] or approximately on the curves, given in Fig. 9-7.

B. Determination of main sizes/dimensions.

3. Current of the generator:

$$I=\frac{P_{\text{г}}\cdot 10^3}{U}=\frac{50\cdot 10^3}{1}=50\cdot 10^3\ a.$$

4. Air-gap diameter (S 9-5):

$$D=\sqrt{\frac{4Ik_I}{\pi(1-\hat{d}_{\text{в}}^2)j_{\text{в}}}}=\sqrt{\frac{4\cdot 50\cdot 10^3\cdot 1,2}{(1-0,25^2)\,4,8\cdot 10^6}}=0,13\ м,$$

where $\hat{d}_{\text{в}}=d_{\text{в}}/D=0,25$ — relative diameter of opening/aperture for the shaft;

$j_{\text{в}}=4,8\cdot 10^6$ A/m² - current density in the armature;

$k_I=1,2$ (it considers field current).

5. The active length of the armature:

$$l=\lambda D=1,5\cdot 0,13=0,195\ м,$$

where $\lambda=0,5\hat{l}=1,5$ — design factor.

Page 297.

C. Verifying calculation by emf of generator.

6. Relative emf of armature on (9-15a):

$$\dot{e}_{\text{п}} = \frac{\mu_0 v \sqrt{R_0}}{\pi}\left[2\left(\frac{K(k_{01}) - E(k_{01})}{k_{01}} - \frac{K(k_{02}) - E(k_{02})}{k_{02}}\right) - \right.$$

$$\left. - k_{01}K(k_{01}) + k_{02}K(k_{02})\right] = \frac{4\pi \cdot 10^{-7} \cdot 200\sqrt{0,97}}{\pi} \times$$

$$\times\left[2\left(\frac{3,47 - 1,023}{0,992} - \frac{1,695 - 1,456}{0,5225}\right) - 0,992 \cdot 3,47 + 0,5225 \cdot 1,695\right] =$$

$$= 1,17 \cdot 10^{-4} \text{ в/а.}$$

Key: (1). V/A.

7. Refined value emf.

On the basis (9-14) and (9-16)

$$\dot{e}_{\text{п}} = \frac{\omega(M_{01} - M_{02})}{\pi} = \frac{\mu_0 v \sqrt{R_0}}{\pi}\left[2\left(\frac{K(k_{011}) - E(k_{011})}{\sqrt{k_{011}}} - \right.\right.$$

$$\left.\left. - \frac{K(k_{02}) - E(k_{02})}{k_{02}}\right) + k_{02}K(k_{02})\right] = \frac{4\pi \cdot 10^{-7} \cdot 200 \cdot \sqrt{0,97}}{\pi} \times$$

$$\times\left[2\left(\frac{1,975 - 1,28}{\sqrt{0,79}} - \frac{1,695 - 1,456}{0,5225}\right) + 0,5225 \cdot 1,695\right] = 1,2 \cdot 10^{-4} \text{ V/A,}$$

where

$$k_{011} = \frac{1 - \sqrt{1 - k_{01}^2}}{1 + \sqrt{1 - k_{01}^2}} = \frac{1 - \sqrt{1 - 0,992^2}}{1 + \sqrt{1 - 0,992^2}} = 0,79.$$

We accept $\dot{e}_{\text{п}} = 1,2 \cdot 10^{-4}$ V/A.

D. Calculation of the coils of parallel excitation.

8. Magnetizing force of coil and field current:

$$F_в = \frac{U}{\dot{e}_в \dot{U}} = \frac{1}{1{,}2 \cdot 10^{-4} \cdot 0{,}95} \approx 8{,}8 \cdot 10^3 \ a,$$

where $\dot{U} = U/e_в \approx 0{,}95$ (is considered a voltage drop in internal circuit of armature);

$$I_в = \frac{F_в}{w_в} = 8\,800 \ a; \quad w_в = 1.$$

Page 298.

9. Sizes/dimensions of coil. a). The mean diameter of the busbar:

$$D_в = 2R_в = \dot{R}_в D = 0{,}97 \cdot 0{,}13 = 0{,}126 \ м;$$

b). The cross-sectional area of the busbar:

$$S_в = \frac{F_в}{j_в} = \frac{8.8 \cdot 10^3}{30 \cdot 10^6} = 2{,}93 \cdot 10^{-4} \ м^2,$$

where $j_в = 30 \cdot 10^6$ A/m² - current density in the busbar (during the short-term mode/conditions).

c). Width and the height/altitude of section. The section of busbar we assume/set by square, then

$$b_в = h_в = \sqrt{S_в} = \sqrt{2{,}93 \cdot 10^{-4}} = 1{,}71 \cdot 10^{-2} \ м.$$

10. Resistor:

$$R_{в.э} = \frac{\pi \rho_{м.t} D_в}{S_в} = \frac{3{,}14 \cdot 0.0422 \cdot 10^{-6} \cdot 0.126}{2{,}93 \cdot 10^{-4}} = 5{,}7 \cdot 10^{-5} \ \Omega$$

where the specific resistor/resistance of copper at an expected temperature t=370°C

$$\rho_{м.t} = 0{,}017 \cdot 10^{-6}(1+\alpha_м t) = 0{,}017 \cdot 10^{-6}(1+0{,}004 \cdot 370) = \\ = 0{,}0422 \cdot 10^{-6}\ \Omega \cdot м$$

$\alpha_м = 0{,}004$ 1/deg - temperature specific resistance of copper.

11. Checking the value of field current:

$$I_в = \frac{U}{2R_{вв}} = \frac{1}{2 \cdot 5{,}7 \cdot 10^{-5}} = 8{,}78 \cdot 10^3\ а.$$

In this case

$$k_I = \frac{I + I_в}{I} = \frac{(50 + 8{,}78) \cdot 10^3}{50 \cdot 10^3} \approx 1{,}18,$$

which is close to preliminarily given one (p. 4).

12. Checking the value of relative size/dimension $\bar{b}$:

$$\bar{b} = \frac{b}{R} = \frac{0{,}5(b_{р.п} + b_ш)c_б}{0{,}5D} = \frac{(1{,}53 + 1{,}71) \cdot 10^{-2} \cdot 1{,}05}{0{,}13} = 0{,}26,$$

where the width of the electrode of contact on the surface of the rotor

$$b_{р.п} = \frac{I_я}{\pi D j_{р.п}} = \frac{59 \cdot 10^3}{3{,}14 \cdot 0{,}13 \cdot 9{,}4 \cdot 10^6} = 1{,}53 \cdot 10^{-2}\ м;$$

$j_{вп} = 9.4 \cdot 10^6$ A/m² - current density;

$c_б = 1.05$ - design factor;

$I_я = k_I I = 1{,}18 \cdot 50 = 59 \cdot 10^3$ A - armature current

Page 299.

Consequently, calculated value $\bar{b}$ is close to that preliminarily

selected.

13. Angular velocity of the rotor:

$$\omega=\frac{v}{0,5D}=\frac{200}{0,5\cdot 0,13}=3080 \text{ rad/s.}$$

14. Speed of rotation of the generator

$$n=\frac{\omega}{2\pi}=\frac{3080}{2\cdot 3,14}\approx 500 \text{ r/s } (30\cdot 10^3 \text{ r/min}).$$

P.8. EXAMPLE OF THE CALCULATION OF THE FUNDAMENTAL PARAMETERS OF DISK NON-POLAR DYNAMO WITHOUT THE FERROMAGNETIC CIRCUIT.

A. Assignment.

1. Initial. Power $P_н$=12 kW; voltage/stress U=1 V.; linear velocity on the periphery of rotor v=300 m/s; the speed of rotation of generator n=500 r/s.

The operating mode is intermittent, current pickup liquid-metal.

2. Structural and electrical diagram. Let us select machine with the combined (consecutive and independent variable) excitation, k_I=1. The winding of separate excitation is intended for the creation by

relatively small initial emf (in comparison with the voltage of the generator), which causes self-excitation. Field coils and the disk of armature we place in one plane. Current pickup in the center of disk is supposed concentrated.

Page 300.

B. Determination of the fundamental parameters.

3. Current of the armature:

$$I_n = \frac{P_n \cdot 10^3}{U} = \frac{12 \cdot 10^3}{1} = 1{,}2 \cdot 10^4 \ a.$$

4. Diameter and the calculated thickness of disk on the periphery

$$D = \frac{v}{\pi n} = \frac{300}{3{,}14 \cdot 500} = 0{,}19 \ м;$$

$$b_D = \frac{I_n}{\pi D j_D} = \frac{1{,}2 \cdot 10^4}{3{,}14 \cdot 0{,}19 \cdot 4 \cdot 10^6} = 0{,}005 \ м,$$

where $j_D = 4 \cdot 10^6$ – current density in the disk.

5. Relative emf of generator on (9-26):

$$e_n^* = \frac{\mu_0 v \sqrt{R_\delta^*}}{2\pi} \left[\left(\frac{2}{k} - k \right) K(k) - \frac{2}{k} E(k) \right] =$$

$$= \frac{4\pi \cdot 10^{-7} \cdot 300 \cdot 1{,}25}{2\pi} \left[\left(\frac{2}{0{,}992} - 0{,}992 \right) \cdot 3{,}47 - \frac{2}{0{,}992} \cdot 1{,}023 \right] \approx 10^{-4} \ в/а.$$ (1)

Key: (1). V/A.

where the modulus/module of the elliptical integrals

$$k=\sqrt{\frac{4\mathring{R}_\delta}{(\mathring{R}_\delta+1)^2}}=\sqrt{\frac{4\cdot 1,25}{(1,25+1)^2}}=0,992;$$

$\mathring{R}_\delta \approx 1,25$ - a relative radius.

6. Refined value of relative emf. On the basis of expression (9-24)

$$\mathring{e}_{\text{д}}=\frac{\mu_0 v\sqrt{\mathring{R}_\delta}}{\pi\sqrt{k_1}}[K(k_1)-E(k_1)]=$$

$$=\frac{4\pi\cdot 10^{-7}\cdot 300\cdot\sqrt{1,25}}{\pi\sqrt{0,79}}(1,975-1,28)=1,07\cdot 10^{-4}\ \text{в/а}.$$ (1)

Key: (1). V/A.

where the modulus/module

$$k_1=\frac{1-\sqrt{1-k^2}}{1+\sqrt{1-k^2}}=\frac{1-\sqrt{1-0,99^2}}{1+\sqrt{1-0,99^2}}=0,79.$$

We accept $\mathring{e}_{\text{д}}=1.07\cdot 10^{-4}$ V/A.

Page 301.

7. Magnetizing force and the current of the coil of the series excitation:

$$F_\delta=\frac{U}{\mathring{e}_{\text{д}}\mathring{U}}=\frac{1}{1,07\cdot 10^{-4}\cdot 0,78}=12\cdot 10^3\ a,$$

(a=A)

where $\mathring{U}=U/e_{\text{д}}\approx 0,78$ (for the series-wound dynamo);

$$I_\delta=\frac{F_\delta}{w_\delta}=12000\ a;\quad w_\delta=1.$$

8. Sizes/dimensions of coil. a). The mean diameter of the busbar:

$$D_ш = \mathring{R}_ш D = 1{,}25 \cdot 0{,}19 = 0{,}237 \text{ м}.$$

b). The sectional area of the busbar:

$$S_ш = \frac{F_ш}{j_ш} = \frac{12\,000}{13 \cdot 10^6} = 9{,}23 \cdot 10^{-4} \text{ м}^2;$$

where $j_ш = 13 \cdot 10^6$ A/m² - current density of excitation.

c). Sizes/dimensions of section (widths and heights/altitudes):

$$b_ш = h_ш = \sqrt{S_ш} = \sqrt{8{,}9 \cdot 10^{-4}} = 0{,}0304 \text{ м}.$$

In this case the calculated value

$$\mathring{R}_ш = \frac{R_ш}{R} = \frac{0{,}5\,(D + h_ш)\,k_0}{0{,}5D} = \frac{(0{,}19 + 0.0304)\,1{,}08}{0{,}19} = 1{,}255,$$

where $k_0 = 1.08$ - the design factor, which considers the height/altitude of collector shoe gear. Consequently, calculated value $\mathring{R}_0$ is close to the preliminarily selected value of a relative radius (p. 5).

Page 302.

9. Resistor of the series excitation:

$$R_{ш.з} = \frac{\pi \rho_{м.t} D_ш}{S_ш} = \frac{3{,}14 \cdot 0{,}0272 \cdot 10^{-6} \cdot 0{,}237}{9{,}23 \cdot 10^{-4}} = 2{,}2 \cdot 10^{-4} \text{ ohm}$$

where the specific resistor/resistance of copper at an expected temperature t=150°C:

$$\rho_{M\,t} = 0{,}017 \cdot 10^{-6}(1 + \alpha_M t) = 0{,}017\,(1 + 0{,}004 \cdot 150) =$$
$$= 0{,}0272 \cdot 10^{-6}\ \Omega \cdot m;$$

$\alpha_M = 0{,}004$

Λ 1/deg - temperature specific resistance of copper.

10. Voltage drop in the coil of series excitation.

$$\Delta U_s = I_s R_{s.s} = 12 \cdot 10^3 \cdot 2{,}2 \cdot 10^{-6} = 0{,}264\ V.$$

11. Angular velocity of the rotor

$$\omega = 2\pi n = 2 \cdot 3{,}14 \cdot 500 = 3140\ \text{rad/s}.$$

Pages 303-308.

REFERENCES

1. Ефремов Д. В., Радовский М. И., Динамомашина в ее историческом развитии, Изд-во АН СССР, 1934.
2. Ефремов Д. В., Радовский М. И., Электродвигатель в его историческом развитии, Изд-во АН СССР, 1936.
3. Гусев С. А., Очерки по истории развития электрических машин, Госэнергоиздат, 1955.
4. Справочная книга для электротехников (СЭТ), т. V, изд. КУБУЧ, 1934.
5. Арнольд Э., Лакур И. Л., Машины постоянного тока, т. I, ГНТИ, 1931.
6. Ugrimoff B., Die unipolare Gleichstrommaschine, Dissertation, Berlin, 1910.
7. Петров Г. Н., Электрические машины, ч. II, Госэнергоиздат, 1947.
8. Костенко М. П., Электрические машины, часть общая, Госэнергоиздат, 1944.
9. Myers E. H., Homopolar generator, «Westinghouse Engineering», 1956, v. 16, № 2.
10. Униполярные машины и применение постоянных магнитов в электромашиностроении, под ред. К. И. Шенфера, Изд-во АН СССР, 1940.
11. Андреев П. А., Канаев А. А., Федорович Е. Д., Жидкометаллические теплоносители ядерных реакторов, Судпромгиз, 1959.
12. Эрвин А. Ф., Насосы для ядерных энергетических установок, «Атомная техника за рубежом», 1958, № 1.
13. Gigot E. N., Applying unipolar generators, «Allis Chalmers Electrical Review», 1962, v. 27, № 2.
14. Watt D. A., The development and operation of a 10 kW homopolar generator with mercury brushes, «Proceeding IEE», A, 1958, v. 105, № 21.
15. Жидкометаллические теплоносители, под ред. А. Е. Шейндлина, Издательство иностранной литературы, 1958.

16. Direct current without commutation, «Steel», 1961, v. 149, № 24.
17. Liquid metal turns the tide to high d. c. generation, «The Iron Age», 1961, v. 188, № 21.
18. 150 000 continuous d-c amperes easy for acyclic generator, «Power Engineering», 1962, v. 66, № 1.
19. Oliphant M. L., The acceleration of protons to energies above 10 GeV, «Proceedings of the royal Society», A, 1956, v. 234, № 1199.
20. Blamy J. W., Carden P. O., Hibbard L. U., Inall E. K., Marshall R. A., sir M. L. Oliphant, The large homopolar generator, «Nature», 1962, v. 195, № 4837.
21. Homopolar generator, «Electrical Engineering», 1962, v. 39, № 6.
22. Каунас Ю. Ю., Исследование ртутного контакта для униполярной машины, Автореферат кандидатской диссертации, Каунас, 1954.
23. Униполярная машина, Французский патент № 1204301, класс 12, 5, 25/1 1960.
24. Алиевский Б. Л., Современные конструкции и области применения униполярных электрических машин, Научные доклады высшей школы, серия «Электромеханика и автоматика», 1959, № 2.
25. Алиевский Б. Л., Униполярные электрические машины, ЦБТИ ЭП, Информационно-технический сборник, 1959, № 10.
26. Алиевский Б. Л., Современные униполярные генераторы, ГОСИНТИ, Сб. статей № 20-63-526/13, 1963.
27. Böning P., Unipolarmotor, «Elektrotechnische Zeitschrift» (ETZ), A, 1952, № 3.
28. Ku J. H., Kamal A., A new homopolar motor, «Journal of the Franklin Institute», 1954, v. 258, № 1.
29. Троицкий С. Р., Электропривод насоса, Авторское свидетельство СССР № 144093, Бюллетень изобретений, 1962, № 1.
30. Ходоров Т. Я., Униполярная машина переменного тока, Авторское свидетельство СССР № 67095, Бюллетень изобретений, 1946, № 9.
31. Лившиц А. Л., Рогчев И. С., Генераторы периодических импульсов сильного тока, Госэнергоиздат, 1959.
32. Михайлов-Микулинский М. С., Петров Г. Н., Алексеев-Мохов С. Н., Преобразователь переменного тока в постоянный, Авторское свидетельство СССР № 124513, Бюллетень изобретений, 1959, № 23.
33. Никулин М. А., Униполярный электромашинный усилитель, Авторское свидетельство СССР № 114953, 1958.
34. Тихомиров В. А., Лавровский В. А., Униполярный генератор электрического тока, Авторское свидетельство СССР № 140480, 1961.
35. Klaudy P., Unipolarmaschine für Wechselstrom, Австрийский патент № 211514, класс 21d, 85, 10/VIII 1960.
36. Lee W. H., Homopolar generator, Патент США № 2990485, класс 310-178, 27/VI 1961.
37. Долина В. И., Применение униполярной машины для измерения скорости вращения, «Электричество», 1957, № 2.
38. Цирлин Ю. Л., Тахогенератор типа униполярной машины, Авторское свидетельство СССР № 137574, Бюллетень изобретений, 1961, № 8.
39. Кулебакин В. С., Испытание электромашин и трансформаторов, ОНТИ, 1935.
40. Физические основы электротехники, под ред. К. М. Поливанова, Госэнергоиздат, 1960.
41. Электрическая муфта с плавным регулированием скорости, «Промышленная энергетика», 1960, № 1.
42. Klaudy P., Unipolarmaschine, Патент ФРГ № 1121711, класс 21d^1, 6, 19/VII 1962.

43 Mayr O., Elektromechanischer Energiespeicher, Патент ФРГ № 1116810, класс 21d³, 3/01, 30/V 1962.

44. Алексеев Г. Н., Непосредственное превращение различных видов энергии в электрическую и механическую, Госэнергоиздат, 1963.

45. Acyclic unit generates direct current directly, «Chemical Engineering», 1961, v. 68, № 24.

46. Poulain J., Récents développements des machines acycliques à courant continu, «Bulletin de la société franc. des électriciens», 1961, v. 2, № 23.

47. Watt D. A., Liquid metal brushes, AERE, Report CE/R № 820, 1956.

48. Watt D. A., A homopolar generator for high current low voltage D. C. supply, AERE, Report ED/R № 1843, 1956.

49. Klaudy P., Eigenschaften und Anwendungsmöglichkeiten vor Flüssigkeitskontakten, «Elektrotechnische Zeitschrift» (ETZ), A, 1955, Bd 76, № 15.

50. Klaudy P., Schnellaufende Unipolarmaschinen — der zeitige und in Zukunft zu erwartende Anwendungsmöglichkeiten, «Österreichische Ingen. Zeitschrift», 1963, Bd 6, № 5.

51. Salagean T., Demensionarea generatoarelor unipolare cu rotor bobinat, «Electrotechnica», 1955, № 2—3.

52. Bonnefille R., Poulain J., Sur la realisation d'une machine acyclique à balais liquides, «Comptes rendus Académie des sciences», 1961, v. 252, № 25.

53. Комар Е. Г., Униполярная машина с цилиндрическим якорем, «Электротехнический сборник», 1931, № 2.

54. Костин Б. В., Новый униполярный генератор, «Электричество», 1939, № 2.

55. Мозжерин В. Г., Низковольтные униполярные генераторы малой мощности, Труды Ивановского энергетического института, 1940, т. II, III.

56. Мозжерин В. Г., Машинная постоянная низковольтных униполярных генераторов, Труды Ивановского энергетического института, 1958, т. VIII.

57. Мозжерин В. Г., Униполярная машина с водяным охлаждением токосъемного устройства, «Вестник электропромышленности», 1960, № 9.

58. Хлусевич Б. С., Реакция якоря в униполярных генераторах, Труды ЛОЛКВАИУ, 1957, т. I.

59. Хлусевич Б. С., Униполярная машина переменного тока и некоторые вопросы ее конструирования, Труды ЛОЛКВАИУ, 1958, т. III.

60. Бертинов А. И., Алиевский Б. Л., Троицкий С. Р., Определение главных размеров и коэффициенты использования униполярных машин цилиндрического и дискового типов, ГОСИНТИ, сб. статей № 20-63-526/13, 1963.

61. Алиевский Б. Л., Бертинов А. И., Калугин В. Н., Хан В. Х., Униполярные генераторы постоянного тока для питания кондукционных насосов, сб. «Вопросы магнитной гидродинамики», Изд. АН Латв. ССР, 1963.

62. Алиевский Б. Л., Бертинов А. И., Троицкий С. Р., Основные расчетные соотношения униполярных электрических машин, Изв. АН СССР, серия «Энергетика и транспорт», 1964, № 1.

63. Бертинов А. И., Алиевский Б. Л., Схема расчета цилиндрических униполярных генераторов постоянного тока, ГОСИНТИ, сб. статей № 20-63-526/13, 1963.

64. Алиевский Б. Л., Бертинов А. И., К расчету униполярных генераторов с полным ротором, ГОСИНТИ, сб. статей № 20-63-526/13, 1963.

65. Бертинов А. И., Алиевский Б. Л., Хан В. Х., Схема расчета дисковых униполярных генераторов постоянного тока, ГОСИНТИ, сб. статей № 20-63-526/13, 1963.

66. Алиевский Б. Л., Хан В. Х., Основы расчета униполярных генераторов без ферромагнитного магнитопровода, ГОСИНТИ, сб. статей № 20-63-526/13, 1963.

67. Алиевский Б. Л., Бертинов А. И., Результаты экспериментального исследования униполярного генератора низкого напряжения для питания кондукционных насосов постоянного тока, Доклад на IV Рижском совещании по магнитной гидродинамике, «Магнитная гидродинамика», 1965, № 4.

68. Алиевский Б. Л., Бертинов А. И., Варлей В. В., Расчет силы одностороннего магнитного притяжения некоаксиальных цилиндров при униполярном намагничивании, «Электричество», 1964, № 2.

69. Кочин Н. Е., Векторное исчисление и начала тензорного исчисления, Изд-во АН СССР, 1961.

70. Миткевич В. Ф., Магнитный поток и его преобразования, Изд-во АН СССР, 1946.

71. Moon P., Spencer D. E., Some electromagnetic paradoxes, «Journal of the Franklin Institute», 1955, v. 260, № 5.

72. Погожев С. А., К вопросу об униполярных машинах, Труды Ивановского энергетического института, 1957, т. VII.

73. Reulos R., Courant magnetique et relativite. Nouvelle théorie des machines unipolaires, «Archives des sciences», 1957, v. 10, № 4.

74. Тамм И. Е., Основы теории электричества, ГИТТЛ, 1956.

75. Полотовский Л. С., Емкостные машины постоянного тока высокого напряжения, Госэнергоиздат, 1960.

76. Бертинов А. И., Алиевский Б. Л., Миронов О. М., Калугин В. Н., Хан В. Х., Униполярная машина, Авторское свидетельство СССР № 154316, Бюллетень изобретений, 1963, № 9.

77. Толвинский В. А., Электрические машины постоянного тока, Госэнергоиздат, 1956.

78. Нетушил А. В., Поливанов К. М., Основы электротехники, часть III, Госэнергоиздат, 1956.

79. Смирнов В. И., Курс высшей математики, т. II, Физматгиз, 1961.

80. Апсит В. В., Синхронные машины с когтеобразными полюсами, Изд. АН Латв. ССР, 1959.

81. Атабеков Г. И., Теория линейных электрических цепей, изд-во «Советское радио», 1960.

82. Янке Е., Эмде Ф., Таблицы функций, Физматгиз, 1959.

83. Ротерс Г. К., Электромагнитные механизмы, Госэнергоиздат, 1949.

84. Бессонов Л. А., Электрические цепи со сталью, Госэнергоиздат, 1948.

85. Крылов А. Н., Лекции о приближенных вычислениях, ГИТТЛ, 1950.

86. Мелентьев П. В., Приближенные вычисления, Физматгиз, 1962.

87. Das-Gupta A. K., Design of self-compensated high-current comparatively higher voltage homopolar generators, «Power Apparatus and Systems», 1961, № 56.

88. Бертинов А. И., Алиевский Б. Л., Калугин В. Н., Хан В. Х., Униполярный генератор, Авторское свидетельство СССР № 156219, Бюллетень изобретений, 1963, № 15.

89. Алиевский Б. Л., Калугин В. Н., Хан В. Х., Униполярная машина, Авторское свидетельство СССР № 160742, Бюллетень изобретений, 1964, № 5.

90. Акимов-Перетц Г. А., Проблема бесколлекторной машины постоянного тока, «Электричество», 1924, № 8.

91. Homopolar generator to exite synchrocyclotron at Carnegie tech, «Power Generation», 1949, v. 53, № 11.

92. Хольм Р., Электрические контакты, перевод под ред. Д. Э. Брускина и А. А. Рудницкого, Издательство иностранной литературы, 1961.

93. Мерл В., Электрический контакт, Госэнергоиздат, 1962.

94. Silvermen J., Ionic brush, Патент США № 2978600, класс 310-232, 4/IV 1961.

95. Strough R. L., Shrader E. F., Pulsed air core series disk generator for production of high magnetic fieldes, «The Review of Scientific Instruments», 1951, v. 22, p. 578—582.

96. Klaudy P., Fortschritte in Bau von Unipolarmaschinen durch Anwendung von Flüssigkeitskontakten, «Elektrotechnik und Maschinenbau» (E u M), 1961, Bd 78, № 3.

97. Schwab A., Flussigkeitsgleitkontakt, Патент ФРГ № 1094354, класс 21d, 64/01, 8/VI 1961.

98. Шлихтинг Г., Теория пограничного слоя, Издательство иностранной литературы, 1956.

99. Дорфман Л. А., Гидродинамическое сопротивление и теплоотдача вращающихся тел, Физматгиз, 1960.

100. Kaunas J., Сопротивление трения цилиндрических тел, вращающихся в жидкости, KPI Darbai, 1957, т. VI (на литовском языке).

101. Тютин И. А., Электромагнитные насосы для жидких металлов, Изд. АН Латв. ССР, 1959.

102. Брановер Г. Г., Кирко И. М., Лиелаусис О. А., Экспериментальное изучение влияния поперечного магнитного поля на распределение скоростей в потоке ртути, Труды института физики АН Латв. ССР, 1961, вып. XII.

103. Дукуре Р. К., Упит Г. П., Некоторые вопросы контактных свойств металлических поверхностей, Труды института физики АН Латв. ССР, 1961, вып. XII.

104. Баландин Ю. Ф., Марков В. Г., Конструкционные материалы для установок с жидкометаллическими теплоносителями, Судпромгиз, 1961.

105. Бертинов А. И., Проектирование самолетных электрических машин. Выбор главных размеров, Оборонгиз, 1953.

106. Рихтер Р., Электрические машины, том. I, ОНТИ, 1935.

107. Курош А. Г., Курс высшей алгебры, Физматгиз, 1962.

108. Алиевский Б. Л., Бертинов А. И., К расчету магнитной системы цилиндрического спирального насоса постоянного тока наименьшего веса, Доклад на IV Рижском совещании по магнитной гидродинамике, «Магнитная гидродинамика», 1966, № 1.

109. Гордон А. В., Сливинская А. Г., Электромагниты постоянного тока, Госэнергоиздат, 1960.

110. Roters H. C., Electromagnetic devices, New York — London, 1944.

111. Красовский Б. Н., Вопросы прочности электрических машин., Изд-во АН СССР, 1951.

112. Кожешник Я., Механика вращающихся электрических машин, Госэнергоиздат, 1958.

113. Алексеев А. Е., Конструкция электрических машин, Госэнергоиздат, 1958.

114. Лойцянский Л. Г., Аэродинамика пограничного слоя, ОГИЗ, 1941.

115. Лойцянский Л. Г., Ламинарный пограничный слой, Физматгиз, 1962.

116. Кочин Н. Е., Кибель И. А., Розе Н. В., Теоретическая гидродинамика, ГИТТЛ, 1948.

117. Okaya T., Hasegawa M., «Jap. Journal of Physics», 1939, v. 13, № 1.

118. Тарг С. М., Основные задачи теории ламинарных течений, ГИТТЛ, 1951.

119. Брановер Г. Г., Лиелаусис О. А., Об особенностях влияния поперечного магнитного поля на турбулентные течения жидкого металла при различных числах Рейнольдса, «Вопросы магнитной гидродинамики», Рига, 1963.

120. Кирко И. М., Особенности магнитогидродинамических явлений в жидких металлах и электролитах. Труды института физики АН Латв. ССР, 1961, вып. XII.

121. Кирко И. М., Жидкий металл в электромагнитном поле, «Энергия», 1964.
122. Rioux C., Sur un nouveau modèle de dynamo-unipolaire autoexcitée, «Comptes rendus Académie des sciences», 1962, v. 255, № 7.
123. Janiczek S., Нормальная машина, Польский патент № 44923, класс 21d¹, 6, 21/IX 1961.
124. Сверхпроводимость и ее применение в электротехнике, «Энергия», 1964.
125. Нейман Л. Р., Калантаров П. Л., Теоретические основы электротехники, ч. III, Госэнергоиздат, 1959.
126. Градштейн И. С., Рыжик И. М., Таблицы интегралов, сумм, рядов и произведений, Физматгиз, 1962.
127. Цейтлин Л. А., Индуктивности проводов и шинопроводов, Госэнергоиздат, 1950.
128. Суханов Л. А., Сафиуллин Р. Х., Вобков Ю. А., Электрические униполярные машины, ОНТИ ВНИИЭМ, 1964.
129. Карасев В. Г., Семенов Г. Т., Униполярный генератор для экспериментального стенда, сб. статей «Электрофизическая аппаратура», вып. 2, Атомиздат, 1964.
130. Годжелло А. Г., Вопросы устойчивости и стабильности индукционно-динамического токосъемного устройства, Диссертация, МЭИ, 1965.

Pages 309-311.

No typing.

END

FILMED

5-84

DTIC